Evolution and functional characterisation of uncoupling proteins in vertebrates

Department of Animal Physiology
Faculty of Biology
Philipps-Universität Marburg

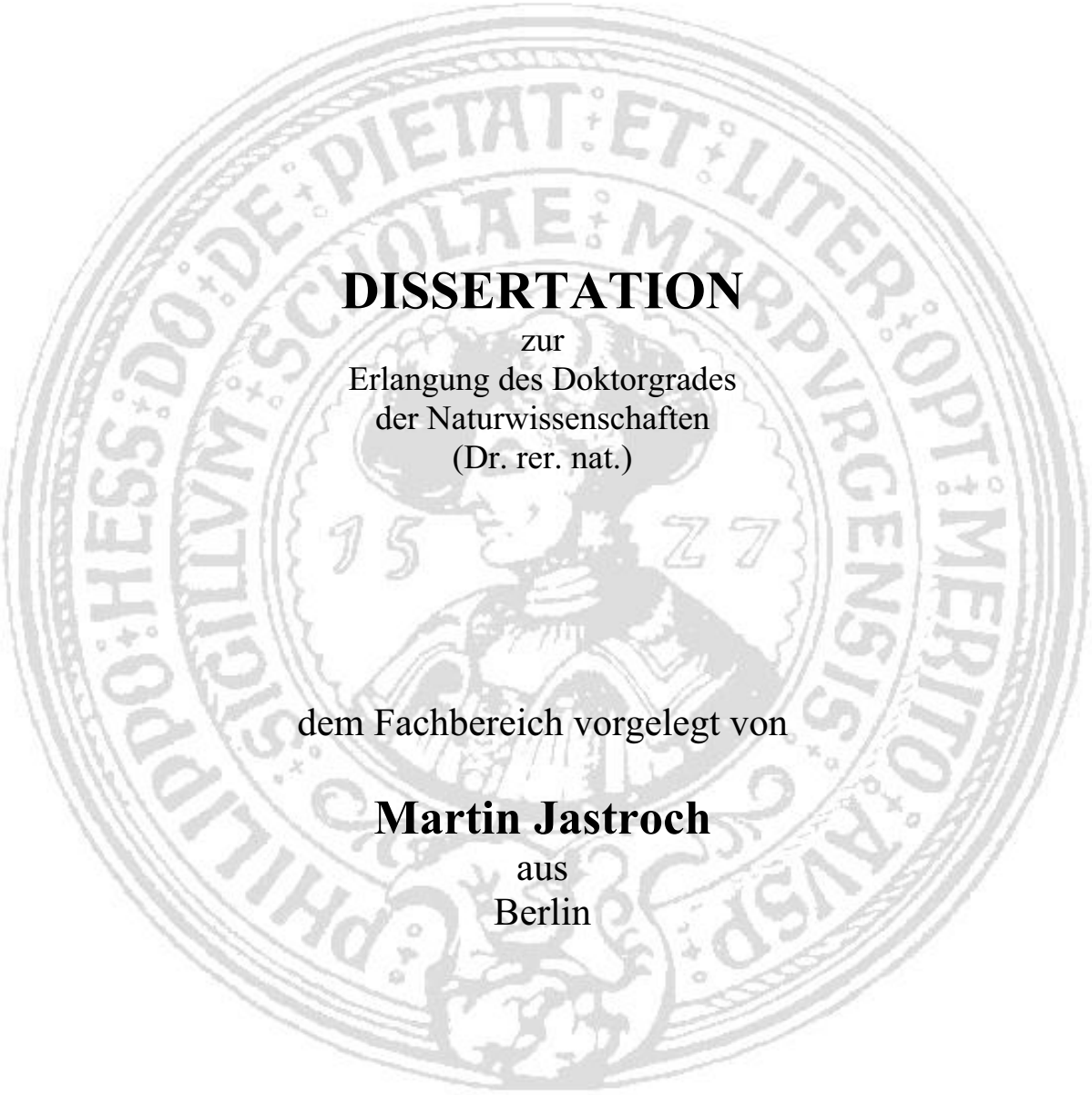

DISSERTATION

zur
Erlangung des Doktorgrades
der Naturwissenschaften
(Dr. rer. nat.)

dem Fachbereich vorgelegt von

Martin Jastroch
aus
Berlin

Marburg/ Lahn 2007

Vom Fachbereich Biologie der Philipps-Universität Marburg als Dissertation am

_____ angenommen.

Erstgutachter _____

Zweitgutachter _____

Tag der mündlichen Prüfung _____

CONTENTS

GLOSSARY OF TERMS

Glossary of terms

ADP	adenosine-diphosphate
ATP	adenosie-triphosphate
ANT	adenine nucleotide translocase
ATP	adenosie-triphosphate
BAT	brown adipose tissue
BSA	bovine serum albumine
CAT	carboxyatractylate
COX	cytochrome c oxidase
GDP	guanosine-diphosphate
HNE	4-hydroxy-2-nonenal
Jo	rate of oxygen consumption
MYA	million years ago
NST	nonshivering thermogenesis
PDK-4	pyruvate dehydrogenase kinase
RCR	respiratory control ratio
ST	shivering thermogenesis
$TPMP^+$	triphenylmethylphosphonium
T_a	ambient temperature
T_b	body temperature
UCP	uncoupling protein; “protein” or transcript
UCP	uncoupling protein gene

Introduction

The physiological role of uncoupling protein 1 (UCP1) in adaptive nonshivering thermogenesis (NST)

Mammals defend their high body temperature (T_b) against lower ambient temperatures (T_a) by biochemical, morphological and behavioural adaptation. High body temperature precludes the need for homeothermic mammals to be sensitive to ambient temperature because they can maintain physiological function despite fluctuations in ambient temperature (1). It has been suggested that evolution of high aerobic capacity and high mitochondrial basal proton conductance facilitated the development of endogenous heat production (1,2). Resting metabolic rates of all organs contribute to basal heat production but adaptive thermogenic mechanisms are required to defend T_b when T_a decreases. Two mechanisms have evolved in eutherian mammals to increase endogenous heat production during cold stress: shivering (ST) and nonshivering thermogenesis (NST). ST liberates heat by mechanic non-coordinated muscle contractions (3). In small mammals ST generates insufficient amounts of heat in the cold (4), because they expose a larger surface area relative to their volume and consequently lose more heat (5). Supplementary thermogenic mechanisms are also required in some mammalian species, which have the ability to enter hypometabolic states (torpor or hibernation) to save energy. They need additional heat production to rewarm to normal body temperature during arousal.

Small mammals including newborn and hibernators, compensate for a higher demand of heat production using adaptive NST (6-8). Brown adipose tissue (BAT) contributes significantly to adaptive NST, giving small mammals the advantage to survive the cold (9). UCP1, belonging to the mitochondrial carrier proteins, is located in the inner membrane of BAT mitochondria and provides the molecular basis for NST (10). UCP1 increases proton conductance and uncouples oxidative phosphorylation from ATP synthesis by dissipating proton motive force as heat.

UCP1-knockout mice are unable to defend their body temperature when exposed to the cold, confirming that UCP1 is crucial for NST (11). Furthermore, a naturally disrupted *UCP1* gene in pigs results in poor thermoregulation and sensitivity to cold exposure (12).

Regulation and biochemistry of UCP1

Sympathetic neuronal control activates BAT in the cold by noradrenaline release. This leads to immediate triglyceride breakdown, recruitment of mitochondrial oxidative capacity, and transcription and activation of uncoupling protein 1 (UCP1) (13). The free fatty acids, which are released from triglycerides, are activated with coenzyme A and metabolised but also activate UCP1 directly. The mechanism of fatty acid activation remains unclear and there are three competing models: (a) fatty acids are required cofactors, facilitating transport of protons (14); (b) cycling of fatty acids is required for proton transport (UCP1 transports fatty acid anions from the matrix to the intermembrane space, and this is followed by protonation and flip-flop of the acids back to the matrix) (15) or (c) there is no mechanistic requirement for fatty acids but they overcome nucleotide inhibition by simple competitive kinetics (16,17). Proton transport of UCP1 can be potently inhibited with purine nucleoside di- and triphosphates, including ADP, GDP, ATP and GTP. For biochemical experiments, activation and inhibition of uncoupling activity are used to demonstrate presence and native function of UCP1.

Evolution of BAT and UCP1

The high interest in the genetics, biochemistry and physiology of BAT and UCP1 is reflected in numerous studies, mostly conducted in rodents. However, little effort has been invested to clarify the distribution of BAT and UCP1 in the animal kingdom. This is surprising as the question when vertebrates gained adaptive NST to maintain physiological function in the cold may be answered by uncovering the evolution of BAT and UCP1. So far, BAT and UCP1 have only been identified and studied in modern eutherian mammals, including humans. In a

comprehensive review on the physiological significance of BAT and UCP1 it has been stated that "*brown adipose tissue with its new protein, uncoupling protein-1 (UCP1, thermogenin), may have been the one development that gave us as mammals our evolutionary advantage, i.e., to survive and especially to be active during periods of nocturnal or hibernal cold, to survive the cold stress of birth, and probably also by promoting our survival on diets low in essential macronutrients, especially protein*." (9). Brown adipose tissue is regarded as a mammalian prerogative but intriguingly, some attempts to identify BAT and UCP1 in marsupials, the next relatives of eutherian mammals, have failed so far.

The controversy about the presence of NST, BAT and UCP1 in marsupials

Marsupials diverged from eutherian mammals about 150 MYA (18). Extant species can be found on the American and Australian continent but fossils have also been excavated on the Eurasian continent (19). Marsupials are endothermic like eutherians, defending body temperature well over a wide range of ambient temperature (20,21) - but apparently lack BAT (22,23). Together with the absence of BAT, the presence of adaptive NST in marsupials has been controversially discussed in the past. In macropods the injection of noradrenaline leads to an increase of metabolic rate (24,25), a response attributed to skeletal muscle by others (26,27). Non-macropodid marsupials show no or minor response to noradrenaline (28-30). Notably, albeit some evidence for NST in marsupials, no study demonstrates that NST is adaptive in the cold. Studies on the kowari (*Dasyuroides byrney*) for example provide indirect indication of adaptive NST replacing shivering thermogenesis (31). Cold-acclimated compared to warm-acclimated individuals show a decrease in shivering tremor during cold exposure.

Previous studies directly investigating the presence of BAT have used morphological characteristics (22,24) and showed UCP1-like immunoreactivity in the interscapular fat deposit of *Sminthopsis crassicaudata* (32) but these experiments are regarded as insufficient to prove the presence of BAT and UCP1 (22,33-35).

Unequivocal detection of UCP1 in marsupials requires genomic or gene transcript data but several attempts to identify the nucleotide sequence have failed so far (36-38). Therefore, BAT and UCP1 are regarded as monophyletic traits of eutherian mammals. However, the identification of UCP1 in marsupials would provide the molecular base for further investigations on adaptive NST.

The controversy about marsupial adaptive thermogenesis led to the search for alternative thermogenic mechanisms and organs. The discovery of the UCP1-paralogues UCP2 and UCP3 expanded the range of potential proteins that might be involved in thermogenesis in mammals.

The paralogous proteins of UCP1

Based on structural and sequence similarities, two paralogous proteins have been identified in eutherian mammals, exhibiting tissue specificity different from UCP1. While UCP2 is ubiquitously expressed (39), the expression of UCP3 is restricted to skeletal muscle, heart and BAT (40). The physiological function of these novel UCPs is still matter of debate. The close relationship to UCP1 implies a thermogenic function. Indeed, UCP3 knockout mice have a diminished thermogenic response to the drug MDMA (3,4-methylenedi-oxymethamphetamine) in skeletal muscle (41). In contrast, noradrenaline-stimulated NST in UCP1 knockout mice is absent demonstrating that UCP2 and UCP3 cannot compensate adaptive NST (11). Results from further efforts to unravel the physiological roles of UCP2 and UCP3 suggest that the function is not thermogenic. Regulation of UCP3 expression hints a role in lipid metabolism. An upregulation of UCP3 expression has been observed in physiological states of increased free fatty acid levels like food deprivation, cold exposure, and acute exercise (42,43).

Functional evidence for fatty acid transport (UCP3), neuroprotection (UCP2) and modulation of the immune system (UCP2) is discussed (44), whereas the function of UCP2 in pancreatic insulin secretion has been intensively investigated and described using UCP2 knockout mice (45). In pancreatic β-islets, UCP2 controls insulin secretion by decreasing the cellular ATP/ADP

ratio. This observation can be explained with an uncoupling function of UCP2. Biochemical studies proposed that all UCPs prevent superoxide production. Superoxide is highly reactive towards lipid membranes and proteins, causing mitochondrial dysfunction (46) but its generation is highly sensitive to the uncoupling of oxidative phosphorylation (47). In the proposed model, superoxide activates mild uncoupling by UCP2 and UCP3, and therefore decreases in a negative feedback loop the de novo production (48). The peroxidation of membrane phospholipids by superoxide generates carbon-centred radicals, in particular 4-hydroxynonenal (HNE). HNE also activates mild uncoupling mediated by UCPs or the adenine nucleotide translocase (ANT) (49).

Outside the mammalian class, further uncoupling proteins have been found in birds (50), plants (51) and fish (52). Studies in the king penguin suggest a thermogenic role for avian UCP (53), while plant UCP might be involved to maintain the mitochondrial redox poise facilitating photosynthesis (54). A UCP2 orthologue in zebrafish and carp has only been identified but not further characterized (52).

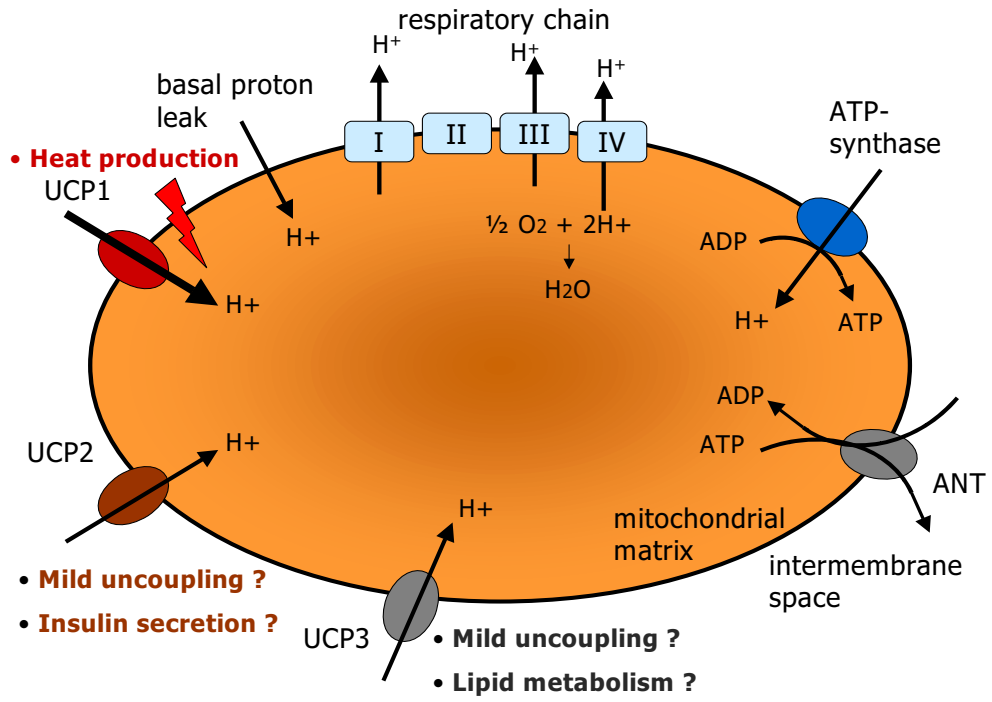

Fig. 1 Simplified scheme of components regulating mitochondrial bioenergetics. Electrons are donated to complex I or II and transported to a lower energy level until they finally reduce oxygen to water at complex IV. The energy released is used to transport protons from the matrix to the intermembrane space thereby creating proton motive force. The electrochemical gradient is used to drive the ATP-synthase converting ADP into ATP. The ANT (adenine nucleotide transporter) exchanges mitochondrial ATP with cytosolic ADP thus supplying the cell with energy equivalents. Protons also return to the matrix via so far unknown pathways (basal proton leak) or UCP1. High leakage of UCP1, inducible by fatty acids, dissipates proton motive force as heat. The function of UCP2 and UCP3 is unresolved. UCP2 might catalyse mild uncoupling, either for general protection from superoxide production or specialized in pancreatic beta-cells to regulate insulin secretion. Uncoupling activity of UCP3 has been demonstrated, but, others address the function to fatty acid export from the matrix.

Animal models used during the PhD project

In order to answer the question when UCP1 emerged during evolution, my approach was to search for UCPs in representative members of different vertebrate groups (Fig. 2). The teleost fish separated from the mammalian lineage about 420 MYA ago. The common carp, *Cyprinus carpio*, was used for studies on UCP gene expression and mitochondrial function. The marsupial lineage developed independently of eutherian mammals around 150 MYA. Within the marsupials, continental drift separated South American and Australian species about 80 MYA. We started a breeding colony of the gray short-tailed opossum, *Monodelphis domestica*, as a

representative species of South American marsupials. To investigate Australian marsupials, I collected road kills of different marsupial species in Queensland, Australia, and trapped the yellow-footed Antechinus, *Antechinus flavipes*, in the subtropical rainforest of the Darling Downs area in Queensland, Australia. Two additional Australian marsupial species, the fat-tailed dunnart, *Sminthopsis crassicaudata*, and the striped-face dunnart, *Sminthopsis macroura*, were provided by Dr. P. Frappell, La Trobe University, Melbourne, Victoria, Australia and Dr. B. McAllan, University of New England, New South Wales, Australia, respectively. Afrotherian mammals, a phylogenetically ancient eutherian group, remained endemic to Africa while modern mammals migrated to other continents about 100 MYA. A recent study on the rock-elephant shrew, *Elephantulus myurus*, found evidence for noradrenaline-mediated NST (55). Therefore, we investigated whether this thermogenic response is mediated by UCP1 and BAT in this species.

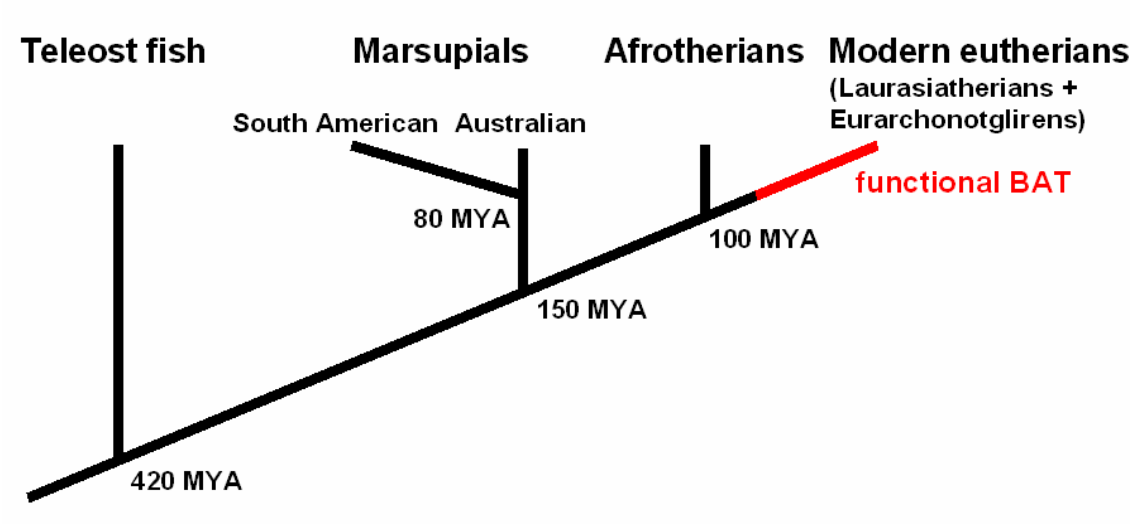

Fig. 2 Simplified phylogeny of vertebrates on a timescale, illustrating the divergence of the species used in this thesis.

Aim of the PhD project

The goal of the thesis was to identify UCPs, in particular UCP1, in different vertebrate groups and to examine the phylogenetic relationships of the novel UCPs within the core UCP protein family. Furthermore, I studied UCP gene regulation in different species and used functional assays to characterise the novel UCPs. The evolution of UCP1 may uncover the evolutionary history of molecular mechanisms leading to NST in modern eutherian mammals while cross-species comparisons of UCP2 and UCP3 orthologues will assist in the annotation of their physiological function.

During my PhD thesis, I aimed to answer the following questions:

1. Can I use standard molecular techniques to identify UCP1 or other UCPs in marsupials, the closest relatives of eutherian mammals?
2. Are further UCP family members present in lower vertebrates like fish and can we use upcoming genome projects to identify them?
3. If so, what is the function of the fish UCPs?
4. Will the presence of *UCPs* in fish genomes facilitate the identification of *UCP1* in the genome of the marsupial *M. domestica* or is the gene absent as hypothesised by others?
5. Are BAT and UCP1 present and functional in an Afrotherian species, the rock elephant shrew, *E. myurus*?
6. Do UCP2 and UCP3 play any role in adaptive NST of marsupials in the absence of UCP1? Can I measure UCP1-like uncoupling activity in tissues expressing marsupial UCP3 as hypothesised by other studies?
7. Functional comparisons of different UCPs are hampered by different mitochondrial and genetical background. In a mammalian cell system ectopically expressing UCPs, can we measure native function allowing direct comparisons of UCP orthologues and paralogues?

Methods

In this thesis, standard molecular methods were used and are briefly summarised in this section. The methodology of measuring proton leak kinetics is described in detail as it represents the core technique in this thesis. I learned this biochemical technique in the group of Dr. Martin Brand at the MRC Dunn Nutrition Unit, Cambridge University, Cambridge, and established the methodology for my studies in the laboratories of the Philipps-Universität Marburg and of the University of Southern Queensland, Toowomba, Australia.

Animal experiments:

Animal experiments were approved by the Animal Ethics Committee of the University of Southern Queensland, Queensland Environmental Protection Agency, and Environment Australia. Animal experiments at the Philipps-Universität Marburg, Germany and at Leibniz-Institute of Freshwater Ecology and Inland Fisheries, Berlin, Germany were performed in accordance with the German Animal Welfare Laws. Common carps at Cambridge University, Cambridge, UK were killed within UK Home Office rules.

Molecular techniques:

- Nucleotide fragments (e.g. DNA, RNA and cDNA) were analysed using **standard cloning techniques, Southern and Northern blot analysis, and reverse transcriptase-polymerase chain reaction**
- **Construction and screening of cDNA libraries** for the identification of full length cDNAs. Furthermore, **RACE-PCR experiments** were deployed to identify the 5'- and 3'-UTR of the UCP1 transcript in *Sminthopsis crassicaudata*.
- UCP protein concentrations in crude tissue homogenates were determined using **standard immunoblotting techniques**.

- **In situ hybridisation** with radio-labelled riboprobes allowed detection of mRNA with anatomical precision. Sagittal and coronal cryo-brain sections of the common carp were analysed for neuroanatomical distribution of carp UCP1 mRNA. Sagittal and coronal whole body-sections of *M. domestica* embryos were analysed for the expression of *M. domestica* UCP1 and UCP2. Complementary sense riboprobes were used as a control.
- **Cell culture techniques** were learnt to grow, maintain and harvest HEK293 cells.

Bioinformatical analysis:

- In silico search for UCPs in public databases was performed using the BLAST algorithm. **Gene analysis and genomic mapping** served for the annotation of the identified *UCP* genes. *ClustalX* and *genedoc* were used to align sequence data which were subjected to **phylogenetic inference**. Evolutionary trees were constructed using the neighbor joining approach in the *phylip package* or alternatively, Bayesian statistics were employed using *Mrbayes*.

Biochemistry:

- **Polarographic measurements of cytochrome c oxidase activity** in tissue homogenates to analyse changes in oxidative capacity
- **Isolation of mitochondria** by differential centrifugation
- **Simultaneous measurements of mitochondrial oxygen consumption and membrane potential** of isolated mitochondria to determine the kinetics of the proton leak. This methodology is described in detail in the following section:

Simultaneous measurements of mitochondrial oxygen consumption and membrane potential

Mitochondrial oxygen consumption

Respiration of isolated mitochondria is measured in a temperature-regulated chamber, with a Clark-type electrode in the base. The electrode is separated from the measuring chamber by a thin Teflon membrane which is permeable to molecular oxygen. A platinum cathode is polarized negatively with respect to a silver anode. Both electrodes are electrochemically connected with a saturated potassiumchloride solution. Molecular oxygen is reduced to water at the cathode (equation 1) and the anode becomes oxidised (equation 2). The electrical current is directly related to the partial oxygen pressure of the medium. This allows the measurement of oxygen uptake by mitochondria. The electrodes are calibrated with air-saturated medium (100%) assuming oxygen concentration as reported previously (56). Electrode currents are amplified using an oxygen analyser (polarisation and amplifying unit, OXY 030A, Rank Brothers, Cambridge, UK), processed using a Powerlab device and downloaded to a laptop using the *Chart5* program (ADInstruments). Oxygen consumption (J_0) can be calculated from the slope of the oxygen traces (equation 3; oxygen traces are introduced in Fig. 3).

(1) $O_2 + 2\ H_2O + 4\ e \rightarrow 4\ OH^-$

(2) $4\ Ag + 4\ Cl^- - 4\ e \rightarrow 4\ AgCl$

(3) $$J_o = \frac{(x\ \%\ min^{-1}) * (\text{saturated nmol O } ml^{-1})}{(100 * \text{mg mito.protein } *ml^{-1})}$$

Firstly, different mitochondrial respiration rates are measured to determine the integrity of the mitochondrial inner membrane (Fig. 3). The reaction starts with the addition of a substrate (e.g. succinate) to establish state 2 respiration, ADP is then added to stimulate ATP-synthase activtiy (state 3). Oligomycin inhibits the ATP-synthase and the residual respiration represents oxygen consumption driving proton leak (state 4) which is caused by either proteins embedded in the

mitochondrial inner membrane or by leakiness of the lipid bilayer. In the end of the run, administration of the artificial protonophore FCCP completely dissipates proton motive force and is a measure for maximal respiration. The coupling state of the mitochondria is determined by the ratio of state 3 respiration divided by state 4 (respiratory control ratio).

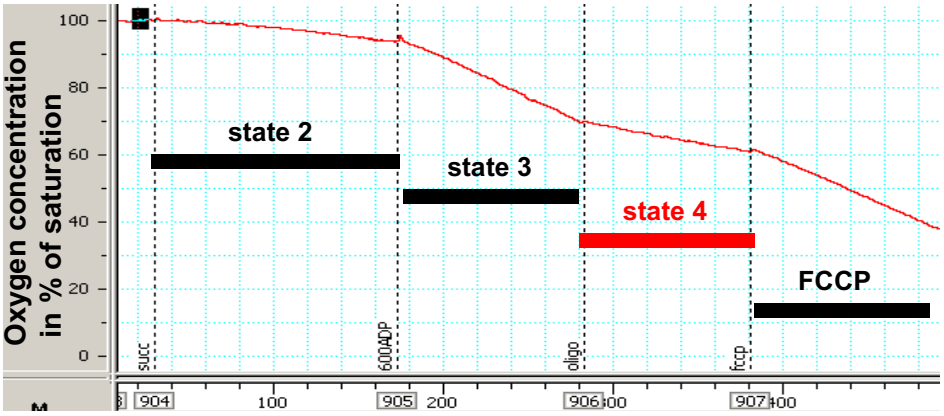

Fig. 3 A representative mitochondrial oxygen consumption trace recorded with *Chart5*. The y-axis shows oxygen concentration of the medium in percent of saturation and the x-axis shows the time (in seconds). Oxygen consumption rate can be calculated using the slope of the trace according to equation 3.

Mitochondrial membrane potential

For the measurement of proton conductance membrane potential is measured simultaneously with oxygen consumption, using a lipophylic cation which distributes across the mitochondrial inner membrane according to the Nernst equation (equation 4), relating membrane potential to the concentration gradient (C^+_{in}; C^+_{out}). I determined the membrane potential by measuring the concentration gradient for the cation $TPMP^+$. A $TPMP^+$ sensitive electrode and a reference electrode are inserted into the measuring chamber and register the concentration of $TPMP^+$ outside the mitochondrial matrix ($TPMP^+_{out}$). The concentration of $TPMP^+$ inside the mitochondrial matrix is simply the concentration of $TPMP^+$ added minus $TPMP^+_{out}$. The potential charge between $TPMP^+$ sensitive and reference electrode is amplified (ph Amplifier, ADInstruments) and processed in parallel to the oxygen consumption measurements in the Powerlab device.

Values for mitochondrial volume (v) and $TPMP^+$ binding (b) are taken from (57) allowing the calculation of mitochondrial membrane potential (equation 5).

(4) $$\Delta\psi = \left(\frac{RT}{F}\right) * \ln\left(\frac{[C^+_{in}]}{[C^+_{out}]}\right)$$

(5) $$\Delta\psi\ (mV) = \left(\frac{RT}{F}\right) \frac{\log (TPMP^+_{added} - TPMP^+_{out}) * b_{TPMP+}}{(v) * mg\ protein\ ml^{-1} * TPMP^+_{out})}$$

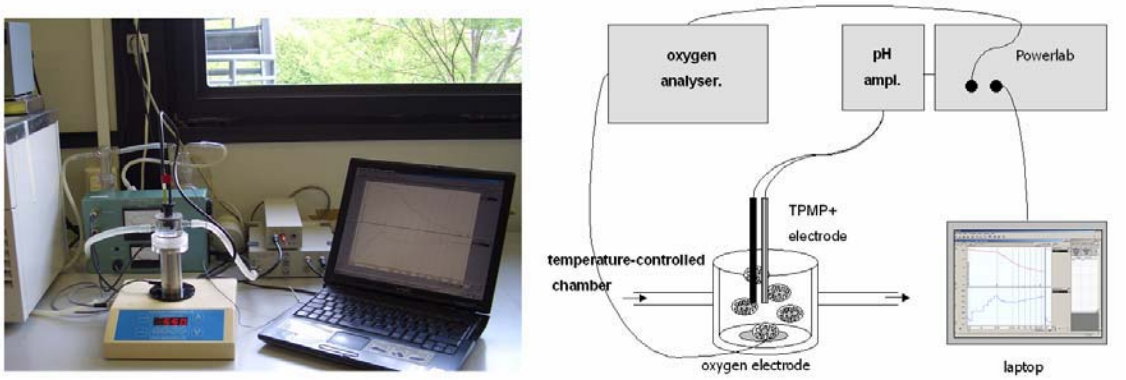

Fig. 4 Photograph and schematic drawing of the apparatus for measurements of proton leak kinetics. Mitochondrial respiration and membrane potential are simultaneously recorded in a temperature controlled chamber. Oxygen electrode signals are amplified in an oxygen analyser and $TPMP^+$ sensitive electrode signals are amplified in a pH-amplifier. Both signals are processed in the Powerlab and downloaded to a laptop for further analysis.

Proton leak kinetics

The full kinetic response of proton leak (monitored as state 4 oxygen consumption rate) to stepwise changes in its driving force, membrane potential, is measured. The protonmotive force consists of the membrane potential (about 150 mV) and a pH gradient (equivalent to about 30 mV). In the experiments proton motive force is entirely converted to membrane potential (about 180 mV) by addition of the potassium-proton exchanging ionophore nigericin. The addition of rotenone inhibits complex I of the respiratory chain to prevent oxidation of endogenous substrates. The $TPMP^+$ sensitive electrode is calibrated by sequential additions of $TPMP^+$ into the medium (Fig. 5; 1) followed by addition of the substrate (succinate, a complex II substrate in

our experiments) to start the reaction (Fig. 5; 2). The upper trace registers oxygen consumption simultaneously with $TPMP^+$ uptake of the mitochondria in the lower trace. To determine the kinetics of proton leak, proton motive force is changed by stepwise inhibition of substrate oxidation with malonate, a competitive inhibitor of the succinate dehydrogenase (Fig. 5;3). At the end of each run, addition of FCCP completely dissipates proton motive force and releases $TPMP^+$ to correct for the drift of the $TPMP^+$ electrode during the run. The drift for any point during the run (x) can be calculated using equation 6, where A. and B. represent time points in the beginning and at the end of the run (see Fig. 5).

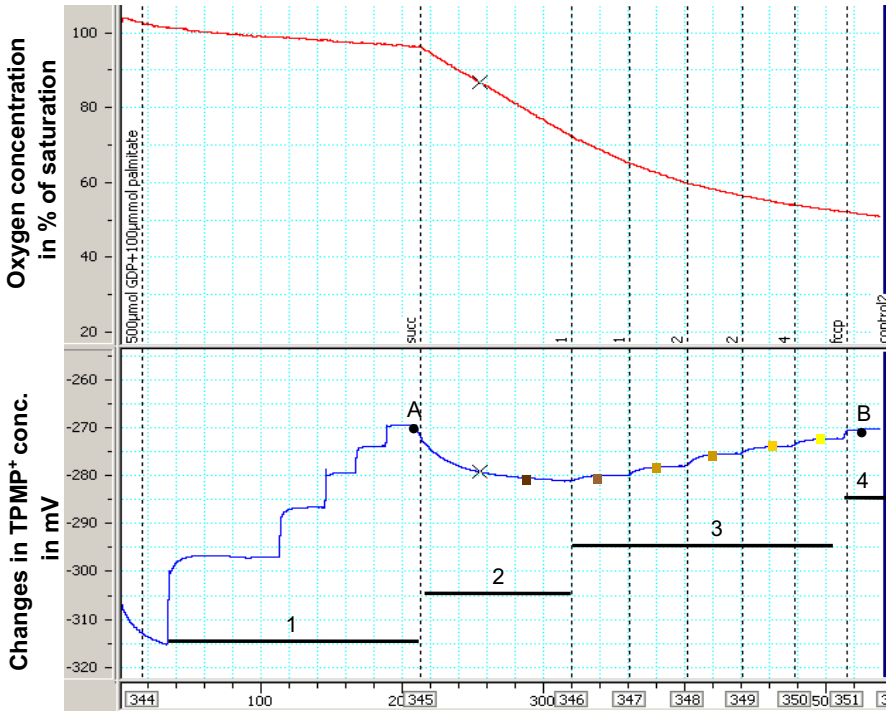

Fig. 5 A representative proton leak measurement. The upper trace shows oxygen consumption, the lower trace shows the recording of membrane potential. In phase 1, the $TPMP^+$ sensitive electrode is calibrated with sequential additions of $TPMP^+$. In phase 2, substrate is added, the mitochondria start respiring (upper trace), build up membrane potential and take up $TPMP^+$ (lower trace). In phase 3, stepwise inhibition of mitochondrial respiration reduces membrane potential. After reaching steady state conditions, further inhibitor is sequentially added to determine the kinetics of the proton leak. In phase 4, FCCP releases all exchangeable $TPMP^+$. Drift can be calculated by comparing the $TPMP^+$ sensitive electrode potential in the beginning of the run (A) with the end (B). The coloured dots in the $TPMP^+$ trace represent selected membrane potentials with corresponding oxygen consumption that is used to describe the kinetics of proton leak (see Fig. 6)

$$\text{(6)} \qquad \text{correction for drift} = \frac{(mV_A - mV_B)*(t_A - t_x)}{(t_A - t_B)}$$

Comparing proton leak kinetics

Plotting oxygen consumption against its corresponding membrane potential illustrates the kinetics of proton leak (Fig. 6). As proton leak is a nonlinear function of membrane potential, different leak curves are compared by analysing the oxygen consumption driving proton leak at a common membrane potential (dotted lines).

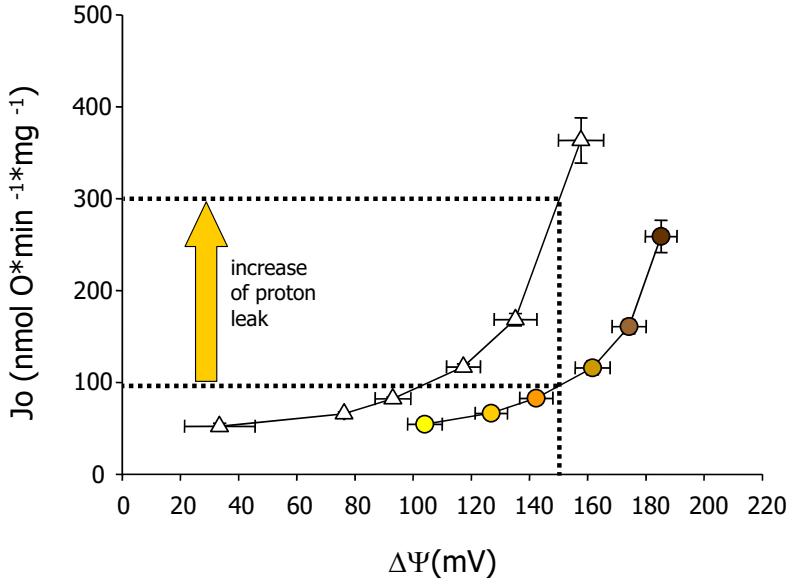

Fig. 6 Two proton leak curves are plotted. To compare the different curves, oxygen consumption driving proton leak has to be compared at a certain membrane potential. In this example, proton leak is three times increased. Notably, if only state 4 respiration is compared as a measure for proton leak (the highest point of the curve), one is falsely estimating proton leak to be just 1.5 times greater.

Results and Discussion

The evolution of UCP1 in vertebrates – a summary

This thesis unravels the evolution of UCP1, a crucial protein for heat generation recruited during adaptive NST. In eutherian mammals UCP1 uncouples the respiratory chain from ATP synthesis to dissipate proton motive force as heat but the question of when the protein emerged during evolution and what its original function was, has not been resolved.

In the initial studies we show that standard molecular techniques are insufficient to detect UCP1 (Jastroch et al. 2004a, Chapter I) but the phylogeny of UCPs suggests an ancient origin of UCP1 (Jastroch et al. 2004b, Chapter II). The presence of UCP1 in fish demonstrates the emergence of UCP1 before the divergence of ray-finned and lobe-finned vertebrate lineages 420 MYA (Jastroch et al. 2005, Chapter III). UCP1 gene regulation in the common carp, *Cyprinus carpio*, indicates a physiological role other than heat production but biochemical studies suggests that carp UCP1 is a functional uncoupling protein with broadly the same activatory and inhibitory characteristics as eutherian UCP1 (Jastroch et al. 2007, Chapter IV). Studies in marsupials, which separated from eutherians 150 MYA, demonstrate that in these species transcriptional control targets UCP1 expression to adipose tissue (Jastroch et al. in preparation, Chapter V). In the gray short-tailed opossum, *Monodelphis domestica*, UCP1 is transiently expressed and restricted to the early development, similar to observations in larger eutherian neonates. In the fat-tailed dunnart, *Sminthopsis crassicaudata*, UCP1 is expressed during adulthood and is elevated in response to cold exposure. Although these experiments suggest the presence of UCP1-mediated NST, UCP1-dependent thermogenesis in the animal has yet to be shown in marsupials. However, the identification of a BAT-like tissue provides the molecular basis to reinvestigate adaptive NST in marsupials. In the phylogenetically ancient afrotherian rock elephant shrew, *Elephantulus myurus*, a species that diverged from modern eutherians about 100 MYA, we demonstrate the presence of functional BAT (Mzilikazi, Jastroch, Meyer, and

Klingenspor, submitted, Chapter VI). Although NST, BAT and UCP1 are found in *E. myurus*, NST does not appear to be adaptive as demonstrated in modern eutherians. While adaptivity of NST seems not to be required in our experiments, the significance of NST during the seasons of the mild natural habitats of South Africa remains to be investigated in further studies.

The focus of the thesis is the evolution of UCP1 but I also investigated if UCP3 might have a thermogenic role in the yellow-footed Antechinus, *Antechinus flavipes*, a marsupial lacking BAT (Jastroch et al., in preparation, Chapter VII). A thermogenic function of UCP3, as found for UCP1, can be excluded by measurements of uncoupling activity in myotubular mitochondria. However, I found evidence that mild uncoupling mediated by the ANT (adenine nucleotide translocase) occurs in myotubular mitochondria of cold-acclimated *A. flavipes* and may play a role in protection from oxidative stress during cold exposure.

The search for UCPs in vertebrates has resulted in the identification of UCP2 and UCP3 in different vertebrate groups and might assist to resolve their physiological roles. By comparing phylogenetic branch lengths and gene regulation, I suggest that in contrast to UCP1, the function of UCP2 and UCP3 may be well conserved in all vertebrates.

Finally, in order to compare different UCP orthologues and paralogues, we have established cell lines ectopically expressing mouse UCP1. In isolated mitochondria of this cell system, we demonstrate native function of mouse UCP1 (Jastroch et al. 2007, BBA, Chapter VIII and Results and Discussion). This cell system will serve in future studies to compare different UCPs in the presence of an identical mitochondrial and genetical background.

The following paragraphs will give further details on my studies, elucidate the approaches and achievements, discuss the results and give an outlook for future studies.

Molecular techniques identify UCP2 and UCP3 but not UCP1 in marsupials

Initially, we searched for the presence of UCP1 in marsupials, the closest endotherm relative of the eutherian trait (Jastroch et al. 2004b). It has been suggested that adaptive NST may be of major importance in Australian Dasyurids since they belong to the smallest marsupials. Therefore, we used the dasyurid *Antechinus flavi*pes in our studies. We identified UCP2 and UCP3 but not UCP1 mRNA, using heterologous rodent probes and consensus primers derived from eutherian UCP1 sequences. UCP2 and UCP3 may compensate for the lack of UCP1 but UCP2 and UCP3 gene expression was not upregulated in the cold. Instead, UCP3 mRNA levels increased in response to fasting, hinting at a role in lipid metabolism as found for eutherians (42). Our suggestion was corroborated by a parallel upregulation of PDK-4 (pyruvate dehydrogenase kinase-4) as an index for the switch from carbohydrate to lipid metabolism. We also concluded in this study that molecular techniques were not appropriate to identify UCP1 in distantly related mammalian species.

Phylogenetic inference suggests an ancient origin of UCP1 in vertebrates

Surprisingly, we found in our phylogenetic tree of the UCP core family, that UCP1 was the first protein diverging from the UCP1-UCP2-UCP3 branch, before UCP2 and UCP3 separated from each other. Therefore, the presence of UCP2 orthologues in fish (52) suggests that UCP1 could have evolved independently at the evolutionary stage of the teleost fish (Fig. 7). Furthermore, we found in our tree, that elongated branch lengths within the UCP1 group most likely hampered the use of heterologous probing in marsupials (Jastroch et al. 2004b).

As phylogenetic inference of all UCP sequences known so far indicated that UCP1 has already evolved at the evolutionary stage of the teleost fish, we did not categorically exclude the presence of UCP1 in marsupials.

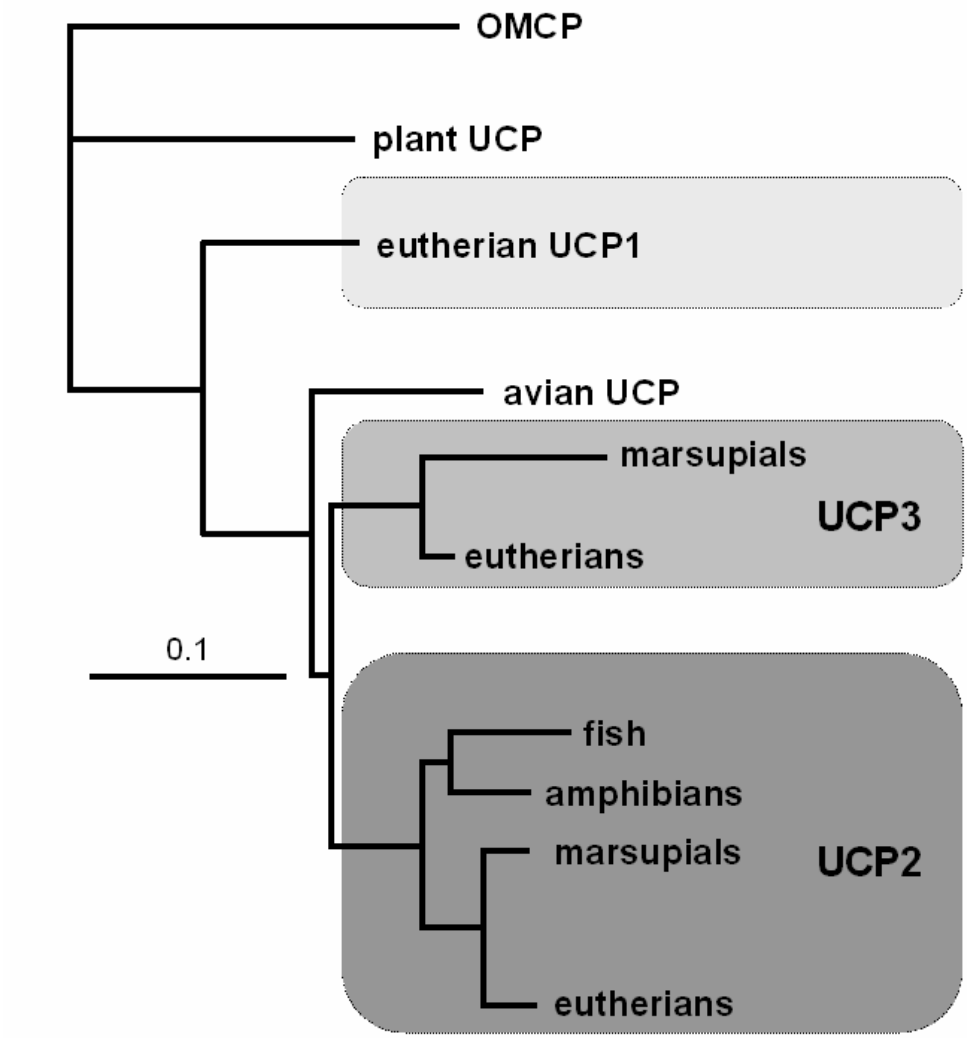

Fig. 7 Evolutionary tree of the core UCP family using the neighbor-joining approach. This tree is a simplified version of the evolutionary tree that can be found in Jastroch et al. 2004a, Chapter I.

The evolution of UCP1 in vertebrates traces back to teleost fish

Standard molecular methods failed to identify UCP1 in marsupials but our phylogenetic studies indicated the presence in fish. This finding prompted us to search for *UCPs* in fish and we took advantage of upcoming genome projects of the zebrafish (*Danio rerio*) and the pufferfish (*Fugu rubripes*). We identified three *UCP*-like sequences but except *UCP2*, their respective orthologues within the core UCP family could not be assigned using phylogenetic inference (Jastroch et al. 2005). Genomic mapping demonstrated identical synteny between genes neighbouring one of the novel fish *UCP*-genes and mammalian *UCP1*. The conserved synteny demonstrated the presence of a UCP1 orthologue in fish. Furthermore, the other novel *UCP* sequence displayed juxtapostion to fish *UCP2* in the genome, leading to the annotation of fish *UCP3*. Based on this finding we investigated regulation of fish UCP1 gene expression in the common carp, *Cyprinus carpio*. Carp UCP1 was expressed in liver, brain, kidneys, and intestine, but notably not in adipose tissue. UCP1 gene expression in liver was dramatically diminished in response to acute cold exposure (two days) and chronic cold acclimation (four weeks). These findings were in contrast to characteristics of rodent UCP1, which is exclusively expressed in BAT and recruited during cold exposure to increase heat production (9). We concluded that although the eutherian UCP1 was annotated as a thermogenic protein (also formerly called thermogenin), the physiological role in fish may be other than heat production.

Carp UCP1 broadly displays biochemical characteristics as found for eutherian UCP1

Previous findings impaired a thermogenic role of carp UCP1 but before drawing further speculations on the physiological role, we had to examine the protein function. We isolated liver mitochondria of cold-acclimated carp, expressing high levels of UCP1, and warm-acclimated carp, expressing low levels of UCP1, to measure mitochondrial proton conductance (Jastroch et al. 2007). Liver mitochondria from warm-acclimated but not from cold-acclimated carp showed a strong increase in proton conductance when palmitate (or 4-hydroxy-*trans*-2-nonenal, HNE)

was added, and this inducible proton conductance could be prevented by addition of GDP. This fatty acid sensitive proton leak was likely due to the expression of UCP1 in the liver of warm-acclimated carp. The observed biochemical properties of proton leak strongly suggested that carp UCP1 is a functional uncoupling protein with broadly the same activatory and inhibitory characteristics as mammalian UCP1. A thermogenic function of UCP1 in fish was still unlikely as no studies have shown heat production in the carp. Another physiological role may be related to mild uncoupling to prevent superoxide production, causing lipid peroxidation. We showed that carp UCP1 could be activated with HNE, a breakdown product of lipid peroxidation. All known UCPs (eutherian UCP1, UCP2, UCP3; avian UCP and plant UCP) increase proton leakage in response to superoxide or HNE (47,49,58,59) hinting a general role of UCPs to diminish superoxide production generated by the respiratory chain.

Complementing our previous studies on gene regulation, we observed in this study, that UCP1 gene expression is cold-induced in the carp brain. Increased UCP1 gene expression in the brain may be related to oxidative stress in the cold, but local thermogenesis could not be categorically excluded. Local endothermy occurs in the brain of some fish (60,61) but the molecular mechanism was attributed to futile calcium cycling. Considering that fish UCP1 was not known at that time, the role of UCP1 in the brain heater organ requires reinvestigation. In particular, if brain areas expressing *UCP1* show high oxidative capacity, thermogenesis will become more likely.

Our functional studies clearly demonstrated that uncoupling function of fish UCP1 was inducible by palmitate, a free fatty acid. During evolution, this biochemical characteristic probably facilitated the incorporation of the UCP1 protein into a complex signalling pathway, leading to adaptive heat production in eutherian BAT. The high thermogenic capacity of BAT is achieved by lipolysis, providing fatty acids as fuel for metabolism, but also as activator of UCP1, leading to the release of proton motive force as heat.

Characterisation of UCP1 and BAT in marsupials

Conserved synteny in the *UCP1* locus in fish and eutherians facilitated the identification of *UCP1* orthologues in other vertebrate classes. In the marsupial *M. domestica* we found *UCP*-like fragments in the trace archives of the *M. domestica* genome project. Screening of a *M. domestica* BAC genomic library, sequencing, mapping and gene analysis revealed the presence of *UCP1*, *UCP2* and *UCP3*. Although an ancestral UCP1 orthologue appears in fish, its physiological role is unknown so far and may be other than heat production. During evolution, UCP1 may have changed its physiological function towards heat production. The first unequivocal demonstration of UCP1 in marsupial was not only remarkable as previous studies failed to demonstrate presence of the *UCP1* gene but also as it showed a high tissue-specificity. UCP1 gene expression is targeted to adipose tissue of *M. domestica* and *S. crassicaudata*, in distinctive sites, where it also exerts thermogenic function in eutherians. Experiments in *M. domestica* implied that UCP1 was transiently expressed in the early ontogenetic phase and may be of major importance during nest vacation, when the juvenile experiences cold-stress for the first time. Similar transient expression of UCP1 was observed in neonates of large eutherians, like lambs, bovine and rabbits (62), and attributed to thermal stress during physiological birth.

In contrast to the South American marsupial *M. domestica*, we demonstrated cold-induced UCP1 expression in the interscapular fat deposit of the adult *S. crassicaudata*. In cold-acclimated *S. crassicaudata* of this study, we observed a transition from white to brown appearance of interscapular fat, increased oxidative capacity and UCP1 expression resembling the situation as found for cold-activated BAT in rodents. Induced oxidative capacity and UCP1 expression would provide the machinery, suggesting the presence of adaptive NST. Despite some evidence for NST in *S. crassicaudata* in previous studies (28), experiments demonstrating adaptive NST in response to cold are still required. The identification of BAT in *S. crassicaudata* now provides the basis to confirm the presence of adaptive NST in marsupials.

Phylogenetic distance of Southamerican and Australian marsupials, which diverged 80 MYA, did not explain differences in *UCP1* expression between *M. domestica* and *S. crassicaudata*. Our approach to compare two Australian dasyurids, *S. crassicaudata* and *A. flavipes*, under identical conditions revealed that different physiological significance is not dependent on phylogeny. *A. flavipes* and *S. crassicaudata* both belong to the Dasyuridae and diverged only about 25 million years ago. Based on this close phylogenetic relation, we expected to find UCP1 expression in both species but instead, *S. crassicaudata* expressed UCP1 whereas *A. flavipes* lacked UCP1 in the interscapular fat. The difference between these species may be explained by differences in body size and environmental temperature. Firstly, the dependence of BAT content and NST capacity is dependent on body size as shown for eutherians (5). Therefore, we have to consider that *S. crassicaudata* is significantly smaller (~18 g) than *A. flavipes* (~32 g). Secondly, *A. flavipes* was trapped in subtropical rainforest areas of Queensland with higher annual temperatures, ranging between 10°C to 30°C, whereas *S. crassicaudata* can be found in dry grassland throughout the southern half of Australia, diplaying lower annual mean temperatures and distinctive seasons. Different body size and environmental temperature fluctuations are both important affectors of NST capacity which may have selected for BAT in mature Dasyurids.

Although we detected BAT in marsupials, functional assays demonstrating uncoupling activity of UCP1 as well as the presence of adaptive NST are still required. Proton leak measurements were not possible as the amount of BAT in *S. crassicaudata* was insufficient to isolate mitochondria.

Demonstration of functional BAT in an ancient eutherian species, the rock elephant shrew, *Elephantulus myurus*

Functional interpendence of UCP1 and NST has only been convincingly demonstrated for modern eutherians like rodents. In Afrotheria, the phylogenetically oldest group of eutherians,

some evidence for NST was observed in the species *Elephantulus myurus* but could not be attributed to a molecular mechanism (63). We demonstrated the presence of UCP1 exclusively expressed in BAT of *E. myurus* (Mzilikazi, Jastroch, Meyer, and Klingenspor, submitted, Chapter VI) and show GDP-sensitive uncoupling activity of isolated BAT mitochondria. The uncoupling activity could be attributed to UCP1 as liver mitochondria lacked palmitate-induced GDP-sensitive proton conductance. Our results in isolated BAT mitochondria strongly suggested that NST in this species was mediated by UCP1 in BAT. Based on the phylogenetic position of *E. myurus* in the eutherian lineage, we concluded that BAT and UCP1 must have been thermogenic already 100 MYA.

Differently from small rodents, cold-acclimation did not increase NST capacity and UCP1 expression. We discussed that animals under the experimental laboratory conditions may display regulation of NST differently from the natural habitats. Further studies on captured free-ranging individuals around the annual cycle are required to confirm the absence of adaptive NST in *E. myurus*.

Proton conductance in myotubular mitochondria of the cold-acclimated marsupial *Antechinus flavipes* has a role in mild uncoupling but not in thermogenesis

We demonstrated that adult *M. domestica* and *A. flavipes* lack BAT. Alternative heating mechanisms must have evolved in marsupials, which are independent of BAT and complement heat production in small mammals. The identification of these mechanisms in *M. domestica* and *A. flavipes* may be of general significance in endotherms as birds also lack BAT but are capable of internal heat production. It has been suggested that skeletal muscle UCP3 might have a thermogenic role in mammals (Mills 2003). In particular, marsupials lacking BAT were thought to generate NST in skeletal muscle (36,64,65). Studies in the marsupial *Monodelphis domestica* demonstrated increased oxidative capacity and uncoupling protein 3 (UCP3) expression in

skeletal muscle leading to speculations on uncoupled respiration to sustain endothermy in the cold as found for BAT (65).

In *A. flavipes* we demonstrated UCP3-like immunological reactivity and increased protein levels in the cold (Jastroch et al. 2004b; Jastroch et al. in preparation, Chapter VII). Despite elevated UCP3 expression in the cold, we observed no change in basal proton conductance of isolated myotubular mitochondria (Jastroch et al. in preparation, Chapter VII). A thermogenic role for marsupial UCP3 by uncoupling is unlikely when compared to the situation of BAT mitochondria in eutherians: a high UCP1 concentration (reaching up to 5% of mitochondrial protein (66)) leads to elevated basal leak respiration, which can only be diminished by addition of inhibiting purine nucleotides like GDP. The high proportion of uncoupled respiration by UCP1 provides the basis for NST. In contrast to previous expectations, we exclude the contribution of UCP3-mediated thermogenic uncoupling activity as it is found for eutherian BAT. To substantiate the presence of NST in skeletal muscle, further studies have to demonstrate increased heat output independent of ST.

In the marsupial *A. flavipes*, proton conductance in myotubular mitochondria was induced by HNE selectively in the cold-acclimated group. In eutherians 4-hydroxynonenal (HNE) is an activator of mild uncoupling by UCP3 and ANT (adenine nucleotide translocase) conveying protection from lipid peroxidation and mitigating ROS production (49). In this study, induced uncoupling activity could be attributed to the ANT, as judged by inhibition with CAT (carboxyatractylate), while GDP, an inhibitor of UCPs, had no effect on HNE-induced uncoupling. Higher HNE-sensitivity of proton conductance indicated mechanisms mitigating reactive oxygen species by mild uncoupling during cold stress. Mild uncoupling activity in the cold was mediated by the ANT whereas the physiological role of UCP3 remained unclear.

Functional implications for UCP2 and UCP3 in vertebrates

The physiological function of UCP2 and UCP3 has not been resolved yet. This thesis focuses on the evolution of UCP1 but some results comparing regulation of gene expression cast light on the function of UCP2 and UCP3 in vertebrates. The fundamental base to study the evolution of UCPs was the comprehensive search and identification of UCPs in many organisms of the animal kingdom. Firstly, we found only one uncoupling protein in non-vertebrates like insects and the sea squirt while three different orthologues appeared in fish for the first time. In our phylogenetic studies on UCPs, UCP2 and UCP3 reflected the evolution of species and equal short branch lengths within the UCP2 and UCP3 subgroups represent continuous evolution rate, suggesting that UCP2 and UCP3 already had a derived function at the evolutionary stage of the teleost fish. In contrast, UCP1 displayed a high substitution rate between marsupials and eutherians and within the eutherian trait, suggesting changed function during evolution or selected mutation for high thermogenic capacity. Furthermore, UCP1 changed tissue-specificity during evolution. In accordance with a derived function, UCP2 and UCP3 show a specific gene expression pattern from fish to eutherians. UCP2 is ubiquitously expressed with highest expression levels found in spleen and blood cells (Jastroch et al. 2004a, Jastroch et al. 2005, (39)). Furthermore, the UCP2 orthologues from fish to mammals exhibited highest nucleotide and protein identity as compared to UCP1 and UCP3.

UCP3 is restricted to skeletal muscle in fish, birds, marsupials and eutherians. More importantly, UCP3 shows increased gene transcript and protein levels in response to fasting in all these vertebrates (Jastroch et al. 2005), (Jastroch et al. 2004a), (50,67)) illustrating that mechanisms regulating UCP3 expression have evolved early in the teleost fish – and were maintained during evolution. Most studies focus on rodents as models to study UCP2 and UCP3 function but our results highlighted, that further cross-species comparisons will assist in the functional annotation of UCP2 and UCP3 in vertebrates. A base for these comparative studies was our comprehensive

search for UCPs in the animal kingdom resulting in an improved phylogenetic tree at the end of this thesis (Fig. 8; compare to Fig. 7).

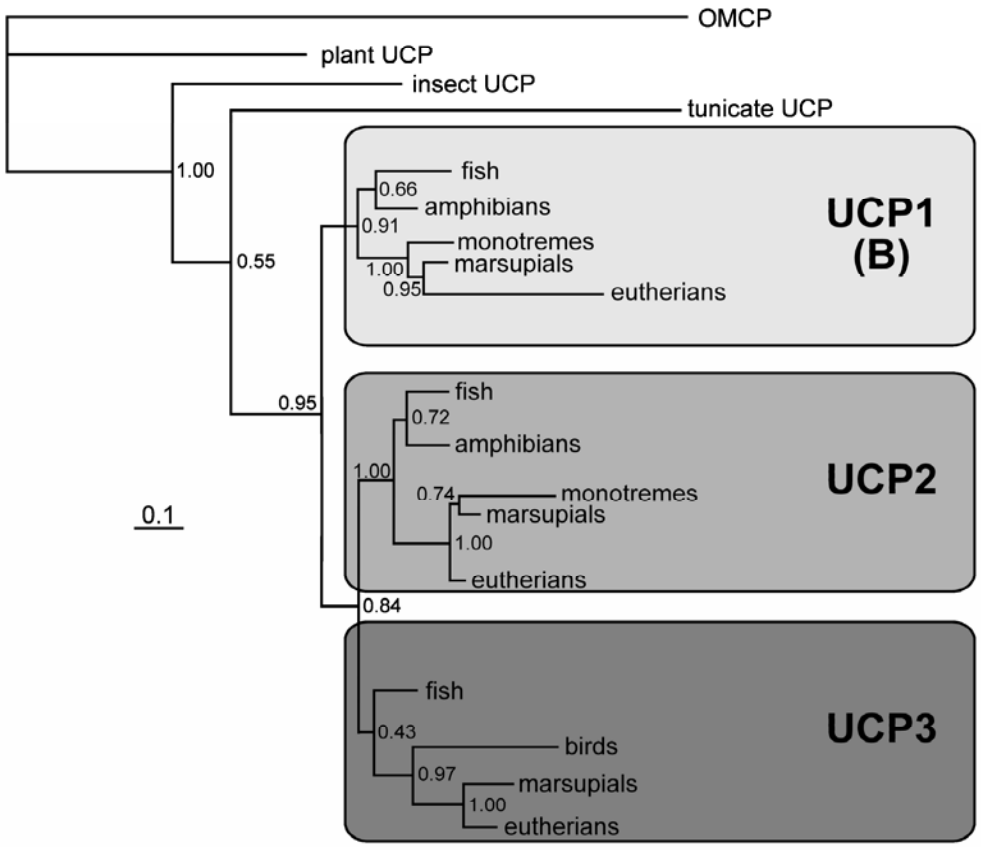

Fig. 8 Evolutionary tree of the core UCP family using the Bayesian statistics. The tree is taken from Chapter V and illustrates the extended knowledge about the distribution of the UCP family in the animal kingdom. The addition of further sequences including UCP1 of *M. domestica* and application of the Bayesian method for phylogenetic inference allowed for the first time a solid reconstruction of the UCP1, UCP2 and UCP3 subgroups.

Outlook: Introducing a cell system to study and to compare different UCPs

Comparisons of different UCP orthologues and paralogues in their native environment are hampered by different expression levels, different mitochondrial and genetical background. Ectopically expressed UCPs in yeast overcame these problems but the native function of UCPs in this model system has been repeatedly questioned in the past (68). Studies on UCP1 showed that mitochondria containing an inhibited UCP1 protein displayed state 4 (leak) respiration identical with empty controls (69). However, it was ignored that proton conductance was changed in yeast mitochondria expressing UCP1 as proton leak kinetics of mitochondria with inhibited UCP1 and mitochondria without UCP1 differed (70). We established a cell system stably expressing mouse UCP1 (71). Measuring mitochondrial respiration, we inhibited UCP1 with 1mM GDP and showed that oligomycin-sensitive respiration (state 4) was unchanged between UCP1-containing mitochondria and empty controls (Fig. 9A). In UCP1-containing mitochondria, ADP-induced state 3 respiration (as a measure for ATP-synthase activity) was increased (Fig. 9A) in comparison to empty controls, resulting in a higher RCR when UCP1 was inhibited (Fig. 9B). This result suggested that mitochondria may compensate proton conductance dissipated by UCP1. Indeed previous studies on yeast expressing UCP1 ectopically show increased expression of compounds belonging to the ATP-synthase (72). In contrast to the yeast system, we showed identical proton leak kinetics between mitochondria with inhibited UCP1 and empty controls (Fig. 9C). The expressed mouse UCP1 displayed native function in our system as it could be activated with palmitate (Fig. 9D) and inhibited with GDP (Fig. 9C and D).

In contrast to the yeast system, UCP1 in our cell system displays no artificial uncoupling activity and represents a solid basis to compare the function of different UCP orthologues and paralogues directly. Furthermore, amino acids can be exchanged and the function of the mutated proteins compared to the wild-type protein. Those experiments will elucidate the different functions of UCP paralogues, the evolution of function in different orthologues and structure-function relationships.

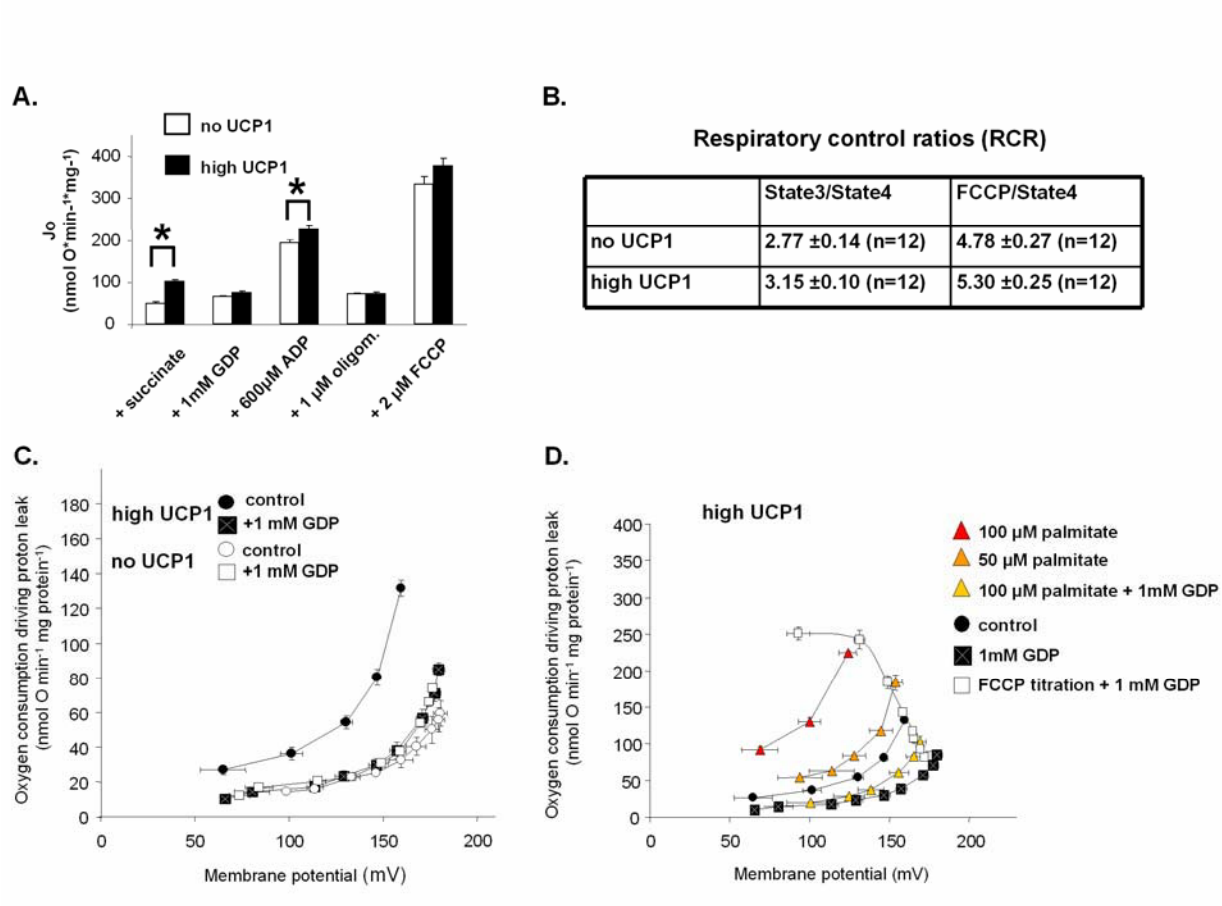

Fig. 9 Comparison of HEK293 cell mitochondria containing mouse UCP1 and no UCP1. A. Measurements of cell respiration. Mitochondria (0.175 mg ml^{-1}) were incubated with 8 µM rotenone to inhibit complex I, respiration was started by adding 6 mM succinate (state 2), 1 mM GDP was added to inhibit UCP1 and adjust respiration between high UCP1 and no UCP1 mitochondria. State 3 respiration was induced by addition of 600 µM ADP. After measuring stable state 3, mitochondria were transferred to state 4 with 1µM oligomycin. Finally, 2µM FCCP dissipated proton motive force and maximum respiration rate was measured. B. Respiratory control ratio (RCR) of GDP-inhibited mitochondria to assess coupling state. Dividing state 3 by state 4 determined the physiological RCR, dividing FCCP (artificial uncoupler) by state 4 determined the physical RCR. C. Proton conductance of UCP1-containing (black symbols) and mitochondria with no UCP1 (white symbols). Addition of 1 mM GDP (squares) adjusted differences in basal conductance (circles). D. Sensitive proton conductance in response to palmitate and GDP in UCP1-containing mitochondria. Proton leak kinetics responded to increasing amounts of palmitate and to 1 mM GDP thereby demonstrating native function as found for BAT mitochondria. 100 µM palmitate overcame 1 mM GDP inhibition suggesting competitive kinetics of UCP1. FCCP titration to dissipate proton motive force illustrated the kinetics of maximum respiration at different membrane potentials. All measurements were conducted in the presence of 0.3% defatted BSA**.**

References

(1) Ruben J. The evolution of endothermy in mammals and birds: from physiology to fossils. *Annu Rev Physiol.* 1995;57:69-95.

(2) Else PL, Hulbert AJ. Evolution of mammalian endothermic metabolism: "leaky" membranes as a source of heat. *Am J Physiol.* 1987;253(1 Pt 2):R1-R7.

(3) IUPS Thermal Commission. The Commission for Thermal Physiology of the International Union of Physiological Sciences. Glossary of terms physiology. *Pflügers Arch.* 1987;410:567-587.

(4) Böckler H, Heldmaier G. Interaction of shivering and non-shivering thermogenesis during cold exposure in seasonally-acclimatized Djungarian hamsters. *J therm Biol.* 1983;8:97-98.

(5) Heldmaier G. Zitterfreie Wärmebildung und Körpergröβe bei Säugetieren. *Z vergl Physiol.* 1971;73:222-248.

(6) Cannon B. Nonshivering thermogenesis in the newborn. *Molec Aspects Med.* 1980;3:119-223.

(7) Himms-Hagen J. Nonshivering thermogenesis. *Brain Res Bull.* 1984;12(2):151-160.

(8) Rafael J, Vsiansky P, Heldmaier G. Increased contribution of brown adipose tissue to nonshivering thermogenesis in the djungarian hamster during cold-adaptation. *J Comp Physiol [B].* 1985;155:717-722.

(9) Cannon B, Nedergaard J. Brown adipose tissue: function and physiological significance. *Physiol Rev.* 2004;84(1):277-359.

(10) Nicholls DG, Locke RM. Thermogenic mechanisms in brown fat. *Physiol Rev.* 1984;64:1-64.

(11) Golozoubova V, Hohtola E, Matthias A et al. Only UCP1 can mediate adaptive nonshivering thermogenesis in the cold. *FASEB J.* 2001;15(11):2048-2050.

(12) Berg F, Gustafson U, Andersson L. The uncoupling protein 1 gene (UCP1) is disrupted in the pig lineage: a genetic explanation for poor thermoregulation in piglets. *PLoS Genet.* 2006;2(8):e129.

(13) Klingenspor M. Cold-induced recruitment of brown adipose tissue thermogenesis. *Exp Physiol.* 2003;88(Pt 1):141-148.

(14) Klingenberg M, Winkler E. The reconstituted isolated uncoupling protein is a membrane potential driven H+ translocator. *EMBO J.* 1985;4(12):3087-3092.

(15) Garlid KD, Orosz DE, Modriansky M et al. On the mechanism of fatty acid-induced proton transport by mitochondrial uncoupling protein. *J Biol Chem.* 1996;271:2615-2620.

(16) Rial E, Aguirregoitia E, Jimenez-Jimenez J, Ledesma A. Alkylsulfonates activate the uncoupling protein UCP1: implications for the transport mechanism. *Biochim Biophys Acta.* 2004;1608(2-3):122-130.

(17) Shabalina IG, Jacobsson A, Cannon B, Nedergaard J. Native UCP1 displays simple competitive kinetics between the regulators purine nucleotides and fatty acids. *J Biol Chem.* 2004;279(37):38236-38248.

(18) Bininda-Emonds OR, Cardillo M, Jones KE et al. The delayed rise of present-day mammals. *Nature.* 2007;446(7135):507-512.

(19) Luo ZX, Ji Q, Wible JR, Yuan CX. An Early Cretaceous tribosphenic mammal and metatherian evolution. *Science.* 2003;302(5652):1934-1940.

(20) Dawson TJ, Dawson WR. Metabolic scope and conductance in response to cold of some dasyurid marsupials and australian rodents. *Comp Biochem Physiol.* 1982;71A:59-64.

(21) Geiser F, Drury RL, McAllan BM, Wang DH. Effects of temperature acclimation on maximum heat production, thermal tolerance, and torpor in a marsupial. *J Comp Physiol [B].* 2003;173(5):437-442.

(22) Hayward JS, Lisson PA. Evolution of brown fat: its absence in marsupials and monotremes. *Can J Zool.* 1992;70:171-179.

(23) Schaeffer PJ, Villarin JJ, Lindstedt SL. Chronic cold exposure increases skeletal muscle oxidative structure and function in Monodelphis domestica, a marsupial lacking brown adipose tissue. *Physiol Biochem Zool.* 2003;76(6):877-887.

(24) Loudon ASI, Rothwell NJ, Stock MJ. Brown fat, thermogenesis and physiological birth in a marsupial. *Comp Biochem Physiol.* 1985;81A:815-819.

(25) Nicol SC. Non-shivering thermogenesis in the potoroo, Potorous tridactylus (Kerr). *Comp Biochem Physiol.* 1978;59:33-37.

(26) Ye JM, Edwards SJ, Rose RW et al. alpha-adrenergic stimulation of thermogenesis in a rat kangaroo (Marsupialia, Bettongia gaimardi). *American Journal of Physiology.* 1996;40:R586-R592.

(27) Nicol SC, Pavlides D, Andersen NA. Nonshivering thermogenesis in marsupials: Absence of thermogenic response to beta 3-adrenergic agonists. *Comp Biochem Physiol A.* 1997;117:399-405.

(28) Clements F, Hope PJ, Daniels CB et al. Thermogenesis in the marsupial *Sminthopsis crassicaudata*: effect of catecholamines and diet. *Aust J Zool.* 1998;46:381-390.

(29) Opazo JC, Nespolo RF, Bozinovic F. Arousal from torpor in the chilean mouse-opposum (Thylamys elegans): does non-shivering thermogenesis play a role? *Comp Biochem Physiol A Mol Integr Physiol.* 1999;123:393-397.

(30) Reynolds W, Hulbert AJ. Cold acclimation in a small dasyurid marsupial: Antechinus stuartii. In: Archer M, editor. Mosman, N.S.W.: Royal Zoological Society of NSW, 1982: 278-83.

(31) May EL. Effects of cold acclimation on shivering intensity in the kowari (Dasyuroides byrnei), a dasyurid marsupial. *Journal of Thermal Biology.* 2003;28(6-7):477-487.

(32) Hope PJ, Pyle D, Daniels CB et al. Identification of brown fat and mechanisms for energy balance in the marsupial, Sminthopsis crassicaudata. *Am J Physiol.* 1997;42:R161-R167.

(33) Loncar D, Afzelius BA, Cannon B. Epididymal white adipose tissue after cold stress in rats. II. Mitochondrial changes. *J Ultrastruct Mol Struct Res.* 1988;101(2-3):199-209.

(34) Loncar D, Afzelius BA, Cannon B. Epididymal white adipose tissue after cold stress in rats. I. Nonmitochondrial changes. *J Ultrastruct Mol Struct Res.* 1988;101(2-3):109-122.

(35) Ricquier D, Raimbault S, Champigny O et al. Comment to Shinohara et al. (1991) FEBS Letters 293, 173-174. The uncoupling protein is not expressed in rat liver. *FEBS Lett.* 1992;303(1):103-106.

(36) Kabat AP, Rose RW, West AK. Non-shivering thermogenesis in a carnivorous marsupial Sarcophilus harrisii, in the absence of UCP1. *Journal of Thermal Biology.* 2003;28(5):413-420.

(37) Kabat AP, Rose RW, Harris J, West AK. Molecular identification of uncoupling proteins (UCP2 and UCP3) and absence of UCP1 in the marsupial Tasmanian bettong, Bettongia gaimardi. *Comp Biochem Physiol B Biochem Mol Biol.* 2003;134(1):71-77.

(38) Rose RW, West AK, Ye JM et al. Nonshivering thermogenesis in a marsupial (the tasmanian bettong Bettongia gaimardi) is not attributable to brown adipose tissue. *Physiol Biochem Zool.* 1999;72(6):699-704.

(39) Fleury C, Neverova M, Collins S et al. Uncoupling protein-2: a novel gene linked to obesity and hyperinsulinemia. *Nat Genet.* 1997;15(3):269-272.

(40) Boss O, Samec S, Kuhne F et al. Uncoupling protein-3 expression in rodent skeletal muscle is modulated by food intake but not by changes in environmental temperature. *J Biol Chem.* 1998;273(1):5-8.

(41) Mills EM, Banks ML, Sprague JE, Finkel T. Pharmacology: uncoupling the agony from ecstasy. *Nature.* 2003;426(6965):403-404.

(42) Giacobino JP. Effects of dietary deprivation, obesity and exercise on UCP3 mRNA levels. *Int J Obes Relat Metab Disord.* 1999;23 Suppl 6:S60-S63.

(43) von Praun C, Burkert M, Gessner M, Klingenspor M. Tissue-specific expression and cold-induced mRNA levels of uncoupling proteins in the Djungarian hamster. *Physiol Biochem Zool.* 2001;74(2):203-211.

(44) Nedergaard J, Cannon B. The 'novel' 'uncoupling' proteins UCP2 and UCP3: what do they really do? Pros and cons for suggested functions. *Exp Physiol.* 2003;88(1):65-84.

(45) Zhang CY, Baffy G, Perret P et al. Uncoupling protein-2 negatively regulates insulin secretion and is a major link between obesity, beta cell dysfunction, and type 2 diabetes. *Cell.* 2001;105(6):745-755.

(46) Gutteridge JM, Halliwell B. Free radicals and antioxidants in the year 2000. A historical look to the future. *Ann N Y Acad Sci.* 2000;899:136-147.

(47) Papa S, Skulachev VP. Reactive oxygen species, mitochondria, apoptosis and aging. *Mol Cell Biochem.* 1997;174(1-2):305-319.

(48) Echtay KS, Roussel D, St Pierre J et al. Superoxide activates mitochondrial uncoupling proteins. *Nature.* 2002;415(6867):96-99.

(49) Echtay KS, Esteves TC, Pakay JL et al. A signalling role for 4-hydroxy-2-nonenal in regulation of mitochondrial uncoupling. *EMBO J.* 2003;22(16):4103-4110.

(50) Raimbault S, Dridi S, Denjean F et al. An uncoupling protein homologue putatively involved in facultative muscle thermogenesis in birds. *Biochem J.* 2001;353(Pt 3):441-444.

(51) Laloi M, Klein M, Riesmeier JW et al. A plant cold-induced uncoupling protein. *Nature.* 1997;389:135-136.

(52) Stuart JA, Harper JA, Brindle KM, Brand MD. Uncoupling protein 2 from carp and zebrafish, ectothermic vertebrates. *Biochim Biophys Acta.* 1999;1413:50-54.

(53) Talbot DA, Duchamp C, Rey B et al. Uncoupling protein and ATP/ADP carrier increase mitochondrial proton conductance after cold adaptation of king penguins. *J Physiol.* 2004;558(Pt 1):123-135.

(54) Sweetlove LJ, Lytovchenko A, Morgan M et al. Mitochondrial uncoupling protein is required for efficient photosynthesis. *Proc Natl Acad Sci U S A.* 2006;103(51):19587-19592.

(55) Mzilikazi N, Lovegrove BG. Noradrenalin induces thermogenesis in a phylogenetically ancient eutherian mammal, the rock elephant shrew, Elephantulus myurus. *J Comp Physiol [B].* 2006;176(1):75-84.

(56) Reynarfarje B, Costa LE, Leninger AL. O2 solubility in aqueous media determined by kinetic methods. *Anal Biochem.* 1985;145:406-418.

(57) Rolfe DF, Hulbert AJ, Brand MD. Characteristics of mitochondrial proton leak and control of oxidative phosphorylation in the major oxygen-consuming tissues of the rat. *Biochim Biophys Acta.* 1994;1188(3):405-416.

(58) Smith AM, Ratcliffe RG, Sweetlove LJ. Activation and function of mitochondrial uncoupling protein in plants. *J Biol Chem.* 2004;279(50):51944-51952.

(59) Talbot DA, Hanuise N, Rey B et al. Superoxide activates a GDP-sensitive proton conductance in skeletal muscle mitochondria from king penguin (Aptenodytes patagonicus). *Biochem Biophys Res Commun.* 2003;312(4):983-988.

(60) Block BA. The billfish brain and eye heater: a new look at nonshivering thermogenesis. *News Physiol Sci.* 1987;2:208-213.

(61) Block BA, Finnerty JR, Stewart AF, Kidd J. Evolution of endothermy in fish: mapping physiological traits on a molecular phylogeny. *Science.* 1993;260(5105):210-214.

(62) Casteilla L, Champigny O, Bouillaud F et al. Sequential changes in the expression of mitochondrial protein mRNA during the development of brown adipose tissue in bovine and ovine species. Sudden occurrence of uncoupling protein mRNA during embryogenesis and its disappearance after birth. *Biochem J.* 1989;257(3):665-671.

(63) Mzilikazi N, Lovegrove BG. Noradrenalin induces thermogenesis in a phylogenetically ancient eutherian mammal, the rock elephant shrew, Elephantulus myurus. *J Comp Physiol [B].* 2006;176(1):75-84.

(64) Ye JM, Edwards SJ, Rose RW et al. Alpha-adrenergic stimulation of thermogenesis in a rat kangaroo (Marsupialia, Bettongia gaimardi). *Am J Physiol.* 1996;271(3 Pt 2):R586-R592.

(65) Schaeffer PJ, Villarin JJ, Pierotti DJ et al. Cost of transport is increased after cold exposure in Monodelphis domestica: training for inefficiency. *J Exp Biol.* 2005;208(Pt 16):3159-3167.

(66) Ricquier D, Mory G, Bouillaud F et al. Rapid increase of mitochondrial uncoupling protein and its mRNA in stimulated brown adipose tissue. *FEBS Lett.* 1984;178:240-244.

(67) Fromme T, Reichwald K, Platzer M et al. Chicken ovalbumin upstream promoter transcription factor II regulates uncoupling protein 3 gene transcription in Phodopus sungorus. *BMC Mol Biol.* 2007;8:1.

(68) Stuart JA, Harper JA, Brindle KM et al. A mitochondrial uncoupling artifact can be caused by expression of uncoupling protein 1 in yeast. *Biochem J.* 2001;356(Pt 3):779-789.

(69) Jimenez-Jimenez J, Zardoya R, Ledesma A et al. Evolutionarily distinct residues in the uncoupling protein UCP1 are essential for its characteristic basal proton conductance. *J Mol Biol.* 2006;359(4):1010-1022.

(70) Esteves TC, Parker N, Brand MD. Synergy of fatty acid and reactive alkenal activation of proton conductance through uncoupling protein 1 in mitochondria. *Biochem J.* 2006;395(3):619-628.

(71) Hirschberg V. Funktionelle Analyse von Entkopplerproteinen in humanen embyonalen Nierenzellen (HEK293). 2006.

(72) Douette P, Gerkens P, Navet R et al. Uncoupling protein 1 affects the yeast mitoproteome and oxygen free radical production. *Free Radic Biol Med.* 2006;40(2):303-315.

Physiol Genomics 17: 130–139, 2004.
First published February 17, 2004; 10.1152/physiolgenomics.00165.2003.

Uncoupling protein 2 and 3 in marsupials: identification, phylogeny, and gene expression in response to cold and fasting in *Antechinus flavipes*

Martin Jastroch,[1] Kerry Withers,[2] and Martin Klingenspor[1]

[1]*Animal Physiology, Department of Biology, Philipps-University Marburg, 35032 Marburg, Germany; and* [2]*Department of Biological and Physical Sciences, University of Southern Queensland, Toowoomba, Queensland 4350, Australia*

Submitted 26 September 2003; accepted in final form 13 February 2004

Jastroch, Martin, Kerry Withers, and Martin Klingenspor. Uncoupling protein 2 and 3 in marsupials: identification, phylogeny, and gene expression in response to cold and fasting in *Antechinus flavipes*. *Physiol Genomics* 17: 130–139, 2004. First published February 17, 2004; 10.1152/physiolgenomics.00165.2003.—We searched for the presence of uncoupling protein genes so far unknown in marsupials and monotremes and identified uncoupling protein 2 (UCP2) and UCP3 full-length cDNAs in libraries constructed from the marsupials *Antechinus flavipes* and *Sminthopsis macroura*. Marsupial UCP2 is 89–90% identical to rodent UCP2, whereas UCP3 exhibits 80% identity to mouse UCP3. A phylogenetic tree including all known UCPs positions the novel marsupial UCP2 and UCP3 at the base of the mammalian orthologs. In the 5′-untranslated region of UCP2 a second open reading frame encoding for a 36-amino acid peptide was identified which is highly conserved in all vertebrate UCP2 transcripts. Analysis of tissue specificity in *A. flavipes* with homologous cDNA probes revealed ubiquitous presence of UCP2 mRNA and striated muscle specificity of UCP3 mRNA resembling the known expression pattern in rodents. Neither UCP2 nor UCP3 gene expression was stimulated in adipose tissue and skeletal muscle of cold exposed *A. flavipes*. However, UCP3 mRNA expression was upregulated 6-fold in heart and 2.5-fold in skeletal muscle as reported for rodents in response to fasting. Furthermore, UCP3 mRNA seems to be coregulated with PDK4 mRNA, indicating a relation to enhanced lipid metabolism. In contrast, UCP2 gene expression was not regulated in response to fasting in adipose tissue and skeletal muscle but was diminished in the lung and increased in adipose tissue. Taken together, the sequence analysis, tissue specificity and physiological regulation suggest a conserved function of UCP2 and UCP3 during 130 million years of mammalian evolution.

Sminthopsis macroura; *Tachyglossus aculeatus*; pyruvate dehydrogenase 4; monotremes

IN EUTHERIAN MAMMALS, three uncoupling proteins (UCPs) related to the mitochondrial anion carrier family have been identified (3). The thermogenic UCP1 uncouples the respiratory chain from ATP synthesis in brown adipose tissue (BAT) mitochondria (41), but the function of more recently discovered UCPs has not been resolved (40). While UCP1 and UCP3 were so far only described in placental mammals, UCP2 was also found only in fish (58). Other members of the UCP family have been identified in plants (35).

Although some UCPs show rather distinct tissue-specific expression patterns, e.g., UCP1 in BAT only and UCP3 in BAT, heart, and skeletal muscle, UCP2 mRNA is present at variable levels in multiple tissues of eutherian mammals (5, 20, 37). The uncoupling activity of UCP1, UCP2, and UCP3 is increased by superoxides, suggesting a more general role of these mitochondrial anion carriers in detoxification of reactive oxygen species (ROS) (15). In contrast, other reports failed to demonstrate superoxide-induced uncoupling of UCP2 (11). The physiological function of UCPs other than UCP1 has not been finally resolved yet, and there exists considerable doubt as to whether UCP2 and UCP3 are indeed uncouplers of mitochondrial respiration (40). Alternative hypotheses on the putative function of UCP2 and UCP3 have been suggested and are currently under investigation. UCP3 is a potential modulator of fatty acid oxidation in mitochondria (24), whereas UCP2 may be involved in inflammatory responses and/or the regulation of insulin secretion from pancreatic β-cells (1, 18, 20, 29, 64). In rodents, the expression of UCP3 mRNA is induced in BAT but not in skeletal muscle after 48 h of cold exposure, whereas in response to fasting expression is only increased in skeletal muscle (7, 59). The highest UCP2 mRNA expression is found in tissues rich with macrophages and can be regulated in these cells by injection of lipopolysaccharides (LPS) as demonstrated in the rat (36). Pertaining to the thermogenic function, there is a long controversy as to whether UCPs, in particular UCP1, are present in marsupials and monotremes. In eutherian mammals nonshivering thermogenesis in BAT depends on UCP1-mediated uncoupling of respiration, but it is unclear whether this thermogenic mechanism is also utilized by marsupials and monotremes. Indeed, small body size and the seasonal fluctuations in environmental conditions of marsupial and monotreme habitats, e.g., low temperature and food shortage in the dry season, impose considerable requirements for physiological adaptation. Support for the presence of nonshivering thermogenesis in marsupials was obtained by several physiological studies which demonstrated adrenergic stimulation of resting oxygen consumption in several marsupial species (9, 12, 38, 42–44, 49, 50, 56, 63). Furthermore, GDP binding to interscapular adipose tissue mitochondria of Bennett's wallaby appeared to support the presence of UCP1 in marsupials (38). However, UCP2 and UCP3 also bind nucleotides, albeit with different affinity and specificity compared with UCP1 (14–16). Other molecular studies addressed the issue by immunologic detection of UCPs (25, 27) and PCR-based strategies (27). Prior to the discovery of the novel UCPs, Hope and coworkers (25) found in the interscapular adipose tissue depot of *Sminthopsis crassicaudata* a very weak signal corresponding to the molecular weight of UCP1 using an antibody raised against ground squirrel UCP1. At that time cross-reactivity with novel UCPs or other mitochondrial anion carriers could not be excluded. By Northern blot analysis using a rat UCP1 cDNA, no UCP-like transcript could be identified in adipose tissue of macropodids (50). Attempts to gather

Article published online before print. See web site for date of publication (http://physiolgenomics.physiology.org).

Address for reprint requests and other correspondence: M. Jastroch, Philipps-Univ. Marburg, Dept. of Biology, Animal Physiology, Karl-von-Frisch-Str. 8, 35043 Marburg, Germany (E-mail: jastroch@staff.uni-marburg.de).

molecular evidence for the presence of UCP2 and UCP3 orthologs in marsupials have been reported, but no study so far has published sequence data (9, 26, 27).

The objective of our study was to identify UCPs in different marsupial species (yellow-footed antechinus *Antechinus flavipes*, stripe-faced dunnart *S. macroura*, common brushtail possum *Trichosurus vulpecula*) and in the monotreme short-beaked echidna *Tachyglossus aculeatus*. The small nocturnal marsupial mammals span a body mass range from 15 g to 4.5 kg, whereas the monotreme *T. aculeatus* may weigh up to 7 kg (57). Two marsupial UCPs were identified and annotated as UCP2 and UCP3 by phylogenetic analysis. We chose the small carnivorous marsupial subspecies *A. flavipes flavipes*, whose weight ranges from 20 to 50 g in females and up to 80 g in males, to further investigate the regulation of UCP2 and UCP3 gene expression in response to cold exposure and food deprivation in selected tissues.

MATERIALS AND METHODS

Animal experiments. All experiments had been approved by the University of Southern Queensland Animal Ethics Committee (01REA121), National Parks Queensland and Environment Australia (PWS P2001585). Eighteen yellow-footed antechinus (*A. f. flavipes*) were captured with Elliott traps from several subtropical habitats in southeast Queensland (Australia) and housed individually for at least 7 days at 24°C (12:12 light/dark, lights on 0700 h) with free access to food and water (cat food pellets soaked in water, and mealworms). To investigate the effect of cold exposure, four individuals of *A. flavipes* were transferred to a climate chamber at 5°C for 2 days, whereas three controls remained at 24°C. Eight *A. flavipes* were food-deprived for 48 h, of which three animals were refed 24 h before tissue dissection. A stripe-faced dunnart (*S. macroura*) was housed in the animal facility of the University of Southern Queensland >6 mo prior to tissue dissection. In addition, road kills of a common brushtail possum (*T. vulpecula*) and an echidna (*T. aculeatus*) were collected from highways in the Darling Downs area.

Tissue dissection. After anesthesia, multiple tissues of *A. flavipes* (adipose tissue, heart, skeletal muscle, kidneys, liver, lung, stomach, and brain) were immediately sampled and snap frozen in liquid nitrogen. Blood was collected from individuals anesthetized with CO_2 by puncture of the vena cava posterior, then centrifuged at 16,000 *g* for 2 min, and sedimented blood cells were stored at −70°C. We also dissected spleen from *T. vulpecula*, spleen and interscapular adipose tissue from *S. macroura*, and adipose tissue, skeletal muscle, liver, kidneys, and spleen from *T. aculeatus*. All tissue samples were stored at −70°C and shipped in liquid nitrogen to Marburg, Germany. For DNA and RNA extractions all tissue samples were first powdered in liquid nitrogen.

Southern blot analysis. DNA was isolated from spleen and kidney tissue powder using a standard phenol-chloroform extraction protocol. Tissues were digested with 0.5 mg/ml proteinase K (Sigma) in NTES buffer (50 mM Tris·HCl, 100 mM EDTA pH 8.0, 100 mM NaCl, 1% SDS) at 55°C overnight and centrifuged for 5 min at 2,500 *g*. The clear supernatant was then incubated for 30 min with an equal volume of neutralized phenol-chloroform-isoamyl alcohol (25:24:1). After centrifugation (15 min, 14,000 *g*), the DNA (aqueous phase) was precipitated with 2 vol of ethanol and 1/10 vol of sodium acetate (3 M, pH 5.2) for 5 min at room temperature. The DNA was collected by centrifugation for 10 min at 14,000 *g*, washed in 70% ethanol, and dissolved in appropriate restriction buffers (Amersham). Twenty micrograms of photometrically quantified DNA was digested with *Ava*II, *Eco*RI, *Sma*I, *Xba*I, *Sac*I, and *Bam*HI (Amersham), subjected to electrophoresis in a 1% TAE-agarose gel, transferred in 20× SSC (1.5 M NaCl, 0.15 M sodium acetate, pH 7.0) to a nylon membrane (Hybond N+, Amersham), overnight and immobilized by UV cross-linking (UV-Stratalinker, Stratagene).

Northern blot analysis. Total RNA was isolated with TRIzol (GIBCO-BRL) according to the manufacturer's protocol (8). As an additional step, the RNA pellet was redissolved in a solution containing 6.3 M guanidinium thiocyanate, 40 mM sodium citrate pH 7, 0.8% sarcosyl, 8 mM 2-mercaptoethanol, precipitated with 1 vol isopropanol, washed in 75% ethanol, and finally dissolved in DEPC-treated water. Total RNA was photometrically quantified at 260 nm and stored at −70°C. Twenty micrograms of RNA was electrophoresed in a 1% denaturing agarose gel (5% formaldehyde, 0.02 M MOPS, 5 mM sodium acetate, 1 mM disodium EDTA, pH 8), transferred overnight in 10× SSC to a nylon membrane (Hybond N, Amersham), and UV cross-linked.

Reverse transcriptase-polymerase chain reaction. RNA was isolated from skeletal muscle of *A. flavipes* and used for first-strand cDNA synthesis (SuperScript II, GIBCO-BRL) according to the manufacturer's protocol. Consensus primers were obtained from MWG Biotech, Ebersberg, Germany (sense, 5′-CTG CAG CGC CAG ATG AGC TTC GCC; antisense, 5′-GTT CAT GTA CCG GGT CTT CAC CAC ATC C). 40 cycles of denaturation at 94°C (1 min), annealing at 56°C (1 min), and extension at 72°C (1 min) were performed. A final extension at 72°C was applied for 10 min and followed by rapid cooling to 4°C. The PCR product was gel-purified and ligated into a pGEMT-easy vector (Promega).

cDNA libraries. Poly(A)$^+$ mRNA was isolated by annealing biotin-labeled oligo(dT) primers coupled to beads (Oligotex mRNA kit Midi, Qiagen, Germany). Double-stranded cDNA was synthesized from 5 μg mRNA and unidirectionally inserted into a bacteriophage vector using the Zap Express XR Library Construction Kit (catalog no. 200451; Stratagene, La Jolla, CA). The libraries were screened for UCP homologs on nylon membranes using probes for UCP1, UCP2, and UCP3. Vectors containing positive cDNA inserts were processed into phagemids according to the manufacturer's protocol (55). Inserts were sequenced using vector-based primers. The full-length sequence was obtained by primer walking (MWG Biotech) and analyzed using BLAST software (GenBank).

Radioactive hybridization. cDNAs were random prime-labeled with [α-^{32}P]dCTP (Rediprime DNA labeling system, Amersham). Nylon membranes were prehybridized at 63°C with BSA solution (0.5M Na_2PO_4/NaH_2PO_4, pH 7.0, 1 mM EDTA, pH 8.0, 7% SDS, 1% BSA) for at least 1 h and hybridized overnight at 63°C with the ^{32}P-labeled probe. After hybridization, the blots were washed with 2× SSC/0.1% SDS for 20 min, 1× SSC/0.1% SDS for 10 min, and 0.5× SSC/0.1% SDS for 10 min at room temperature. Signal intensities were then monitored by exposure to a PhosphorScreen (Molecular Dynamics). The stringency of washing was subsequently increased to 0.1× SSC/0.1% SDS for 10 min at 60°C for the *A. flavipes* UCP2 probe. The hybridized probes were then detected by phosphor imaging (Storm 860, Molecular Dynamics), and signal intensities were quantified using ArrayVision 7.0 (Imaging Research). In the fasting-refeeding experiment UCP2 mRNA in skeletal muscle of *A. flavipes* was detected by autoradiography at −80°C for 2 days (X-OMAT AR-Film, Kodak) and quantified densitometrically (Scion Image Software 4.0.2).

All blots were hybridized with probes corresponding to the cDNA sequences of rat UCP1 (1,200 bp; GenBank accession number NM_012682.1), mouse UCP2 (1,000 bp; GenBank BC012967.1) and hamster UCP3 (826 bp; GenBank AF271265). The full-length UCP2 insert obtained from the spleen cDNA library of *A. flavipes* was ^{32}P-labeled and used for Northern blot analysis of gene expression in selected tissues. In addition, RNA extracted from the heart and skeletal muscle of *A. flavipes* was hybridized with hamster PDK4 cDNA (482 bp; GenBank AF321218).

Ethidium bromide staining of total RNA and hybridization with hamster 18S rRNA and mouse β-actin served to normalize gel loading. In between subsequent hybridizations, membranes were

stripped by shaking for 20 min at 64°C after addition of boiling 0.1× SSC. Data shown in columns represent mean values.

Phylogenetic inference. A comprehensive search for UCP sequences was performed in public databases using keywords and BLAST alignments (GenBank/EMBL and SwissProt). An alignment of the UCP amino acid sequences was generated using ClustalX 1.81 (**ftp://ftp-igbmc.u-strasbg.fr/pub/ClustalX**). Program modules of the PHYLIP software package were employed for cladistic analysis. For bootstrapping, the aligned data set was shuffled randomly 1,000 times (SEQBOOT) (19). Distances between pairs of protein sequences were calculated according to Dayhoff's empirical PAM matrix (13) using the PROTDIST and scaled in expected historical events per site with gaps considered as missing data. A phylogenetic tree was constructed by the neighbor joining method with PROTPARS (51). A majority-rule consensus tree was generated with CONSENSE. The oxaloacetate-malate carrier, considered as an "ancient" branch of the mitochondrial anion carrier family, was used as the outgroup. The choice of other mitochondrial anion carriers, namely "UCP4," "UCP5," ADP-ATP-translocase, or phosphate carrier protein, as the outgroup had no effect on the phylogenetic relationships within the core UCP family.

Statistical analysis. Statistical analysis was performed using SPSS 11.0 (SPSS Inc.). The effect of food deprivation and refeeding on the expression of UCP2 and UCP3 in different tissues was assessed by the nonparametric Kruskal-Wallis H-Test. The Mann-Whitney U-test was applied for two-sample comparisons. Results were considered statistically significant at $P < 0.05$.

RESULTS

The presence of UCP-related genes in marsupials and monotremes was first analyzed by Southern blot hybridization of genomic DNA with heterologous rodent cDNA probes for UCP1, UCP2, and UCP3. Mouse UCP2 cDNA clearly hybridized with several genomic restriction fragments of the marsupials *A. flavipes* and *T. vulpecula* (Fig. 1). A positive result for UCP2 was also obtained with DNA from *S. macroura* (data not shown) but not with DNA of the monotreme *T. aculeatus* (Fig. 1). Initial evidence for UCP2 gene expression in spleen of *A. flavipes* and *S. macroura* was obtained by Northern blot analysis using a heterologous mouse UCP2 probe. A single band was detected at a size corresponding to rodent UCP2 mRNA. Despite positive control hybridizations of mouse and hamster DNA with UCP1 or UCP3 probes, no signals were detected on marsupial or monotreme DNA. Similar results were obtained in this analysis when DNA was digested with other restriction enzymes (data not shown).

As Southern and Northern blot hybridizations with heterologous probes were not successful for UCP3, we tried an alternative approach. We hypothesized that eutherian UCP3 and avian UCPs are orthologs and therefore selected consensus primers from conserved regions for RT-PCR experiments. We amplified a 480-bp cDNA fragment by RT-PCR from skeletal muscle of *A. flavipes*, which showed high similarity to mouse UCP3. We then generated cDNA libraries from the marsupials *S. macroura* (spleen) and *A. flavipes* (spleen and skeletal muscle) to isolate full-length cDNAs of the marsupial UCP2 and UCP3.

Screening of the spleen cDNA libraries with a mouse UCP2 probe identified a 1,576-bp full-length clone from *A. flavipes* (GenBank AY233003) and a 1,076-bp fragment including a 5′ truncated partial coding sequence from *S. macroura* (GenBank AY232996). The deduced amino acid sequences of these marsupial UCP2 proteins are shown in Fig. 2. The open reading frame (ORF) of the cDNA from *A. flavipes* encodes a 310-amino acid protein. A GenBank query of both protein sequences revealed an average identity of 88–90% to rodent UCP2.

Screening the *A. flavipes* skeletal muscle cDNA library with the 480-bp UCP3 cDNA fragment identified a full-length UCP3 cDNA (GenBank AY519198). The deduced 312-amino acid protein exhibits 80% identity to mouse UCP3. Both marsupial UCPs showed an average identity to rodent UCP1 of 54–55%.

The sequence alignment with other UCPs demonstrates high conservation of the transmembrane domains, the nucleotide binding site (6), and associated pH sensors (E190 and H214) (31) (Fig. 2). The two histidine residues corresponding to H145 and H147 in hamster UCP1, which have been considered to be crucial for proton transport activity of UCP1 (2), are not present in marsupial UCP2 and UCP3.

For classification of marsupial UCP proteins and their relationship to other homologs, we performed phylogenetic analysis and generated a tree (Fig. 3). We retrieved 41 sequences from the core UCP family including plant UCPs from public databases, according to Borecky et al. (3). In our tree, the two marsupial UCP2 and the UCP3 cloned in the present study group together with their respective orthologs and are positioned at the base of the mammalian branch. The identity of marsupial and fish UCP2 is 80%. Our comprehensive search for UCPs further revealed so far unnamed protein products of the amphibians *Xenopus laevis* (GenBank AAH44682.1) and *Silurana tropicalis* (GenBank AAH63352), which we identified as UCP2. These amphibian sequences exhibit 81% identity to marsupial UCP2.

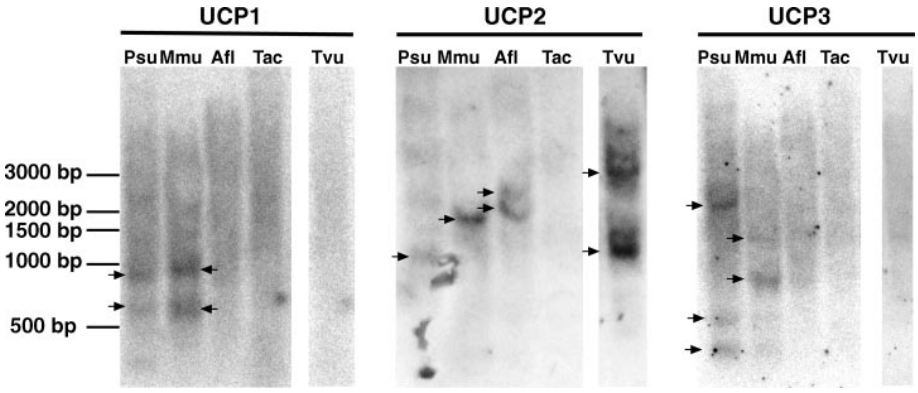

Fig. 1. Southern blot analysis of genomic DNA from several marsupial species and a monotreme. Twenty micrograms genomic DNA was digested with *Ava*II and hybridized with either rat uncoupling protein 1 (UCP1), mouse UCP2, or hamster UCP3 cDNA probes. Mouse and hamster DNA served as control. Arrows indicate specific signals. *Psu*, *Phodopus sungorus*; *Mmu*, *Mus musculus*; *Afl*, *Antechinus flavipes*; *Tac*, *Tachyglossus aculeatus*; *Tvu*, *Trichosurus vulpecula*.

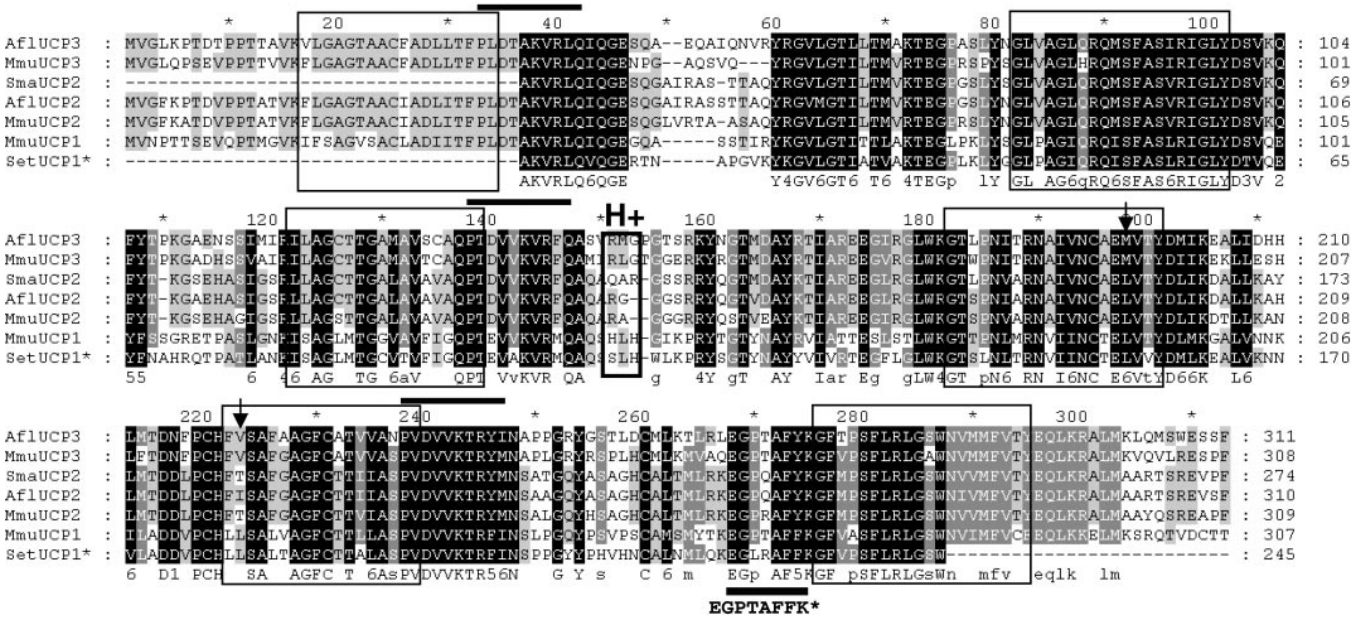

Fig. 2. Amino acid sequence alignment of UCP2 from *Sminthopsis macroura* (GenBank accession no. AY232996), *A. flavipes* (GenBank AY233003), and *M. musculus* (GenBank AAB17666), UCP3 from *A. flavipes* (GenBank AY519198) and *M. musculus* (GenBank PP56501), and UCP1 from *M. musculus* (GenBank P12242) and *Suncus etruscus* (30) using ClustalX 1.81 (**ftp://ftp-igbmc.u-strasbg.fr/pub/ClustalX**) and illustrated with GeneDoc 2.601 (**http://www.psc.edu/biomed/genedoc/**). Sequences are presented in single letter code. Gaps were introduced by ClustalX to optimize alignment score. Most conserved amino acids are highlighted in black; less conserved amino acids are in brighter background. Putative transmembrane regions are boxed, with arrows indicating amino acids involved in pH sensing of the nucleotide binding (31). H145 and H147, two amino acids involved in the proton transport of UCP1, are boxed and indicated with "H+" (2). Black bars above the alignment indicate the energy transfer protein signature; the black bar below indicates the position of a potential nucleotide binding domain (∗) found in UCP1 (6). Sma, *S. macroura*; Afl, *A. flavipes*; Mmu, *M. musculus*; Hsa, *Homo sapiens*; Set, *S. etruscus*.

Further analysis of the untranslated regions (UTR) of the *A. flavipes* marsupial UCP2 cDNA identified a second ORF in the 5′-UTR encoding for a putative peptide of 36 amino acids. This ORF contains three start codons (AUG) in frame. By alignment of all available 5′-UTRs from other UCP2 mRNAs, we observed a high degree of conservation of this ORF across vertebrates (Fig. 4). The marsupial UCP2 upstream ORF (uORF) exhibits 79–81% nucleotide identity and 66–69% amino acid identity to the ORF of eutherian mammals.

To investigate tissue-specific expression of UCP2 and UCP3, we analyzed total RNA from selected tissues by Northern blotting using the homologous *A. flavipes* cDNA probe. We detected high levels of UCP2 mRNA as a single band at ~1.7 kb in adipose tissue, lung, spleen, and blood cells. UCP2 mRNA was barely detectable in liver, skeletal muscle, heart, and stomach and not detectable in brain (Fig. 5). The highest abundance of UCP2 mRNA was observed in blood cells. Quantitative analysis demonstrated a 3.6-fold higher concentration of UCP2 mRNA in blood cells than in spleen and an even 4.5-fold higher concentration compared with lung and adipose tissue. UCP2 mRNA was also detected in spleen of *S. macroura*, *T. aculeatus* (Fig. 5), and *T. vulpecula* (data not shown), and in the monotreme, weak hybridization signals were observed in adipose tissue and liver. In contrast to this evidence for UCP2, no UCP3 mRNA was detectable with the *A. flavipes* UCP3 cDNA probe in any tissue of the monotreme (data not shown).

The expression of UCP3 mRNA in *A. flavipes* is restricted to heart and skeletal muscle (Fig. 5). As in rodents, the mRNA levels in heart were minor compared with skeletal muscle. In contrast to the mRNA isoforms known from rodents, only one splicing variant is visible on the blot, and the size corresponds to the size of UCP2 mRNA.

It has been proposed that novel UCPs could have a thermogenic function in marsupials, which most likely lack UCP1 (28, 50). Otherwise, UCP2 and UCP3 have been implicated in lipid mobilization and utilization in response to fasting. Therefore, we investigated the physiological regulation of UCP gene expression in selected tissues of *A. flavipes* exposed to cold and in response to fasting/refeeding. Cold exposure had no significant effect on UCP2 mRNA level in adipose tissue, and UCP2 as well as UCP3 mRNA were barely detectable in skeletal muscle of warm and cold exposed *A. flavipes* (data not shown).

In response to fasting, UCP3 mRNA level was 2.5-fold and 6-fold increased in skeletal muscle and heart, respectively, which was reversed upon refeeding for 24 h (Fig. 6, *A* and *B*). PDK4 mRNA levels in skeletal muscle and heart, taken as an index for the switch from carbohydrate to fatty acid metabolism in the fasted state, showed a threefold and sevenfold increase in skeletal muscle and heart, respectively (Fig. 6, *A* and *B*). UCP2 expression in response to fasting was decreased in lung and increased in adipose tissue but unaffected in spleen and skeletal muscle (Fig. 6*C*).

DISCUSSION

Previous studies provided suggestive evidence for the presence of uncoupling proteins in marsupial mammals, but unam-

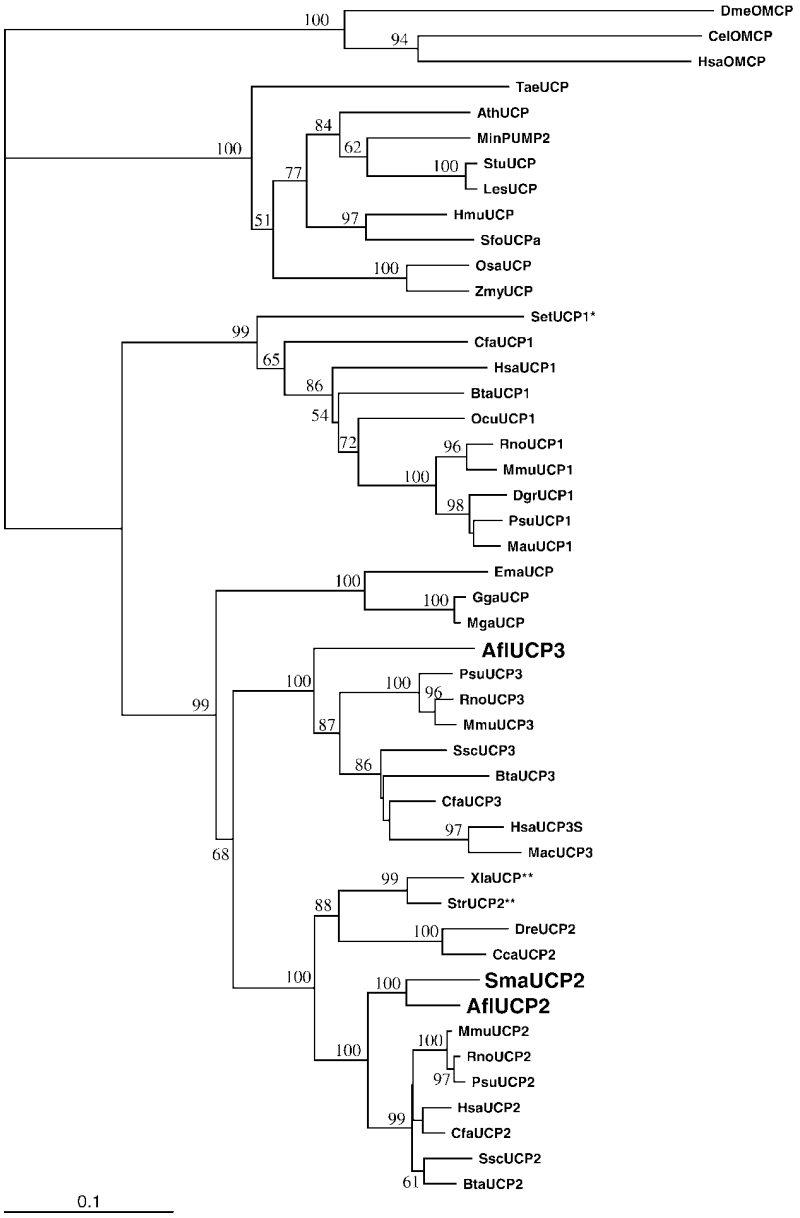

Fig. 3. Phylogenetic relationships of the UCP family including UCP2 and UCP3 of *A. flavipes* and UCP2 of *S. macroura*. A neighbor joining tree was derived from the amino acid alignment. Bootstrap values from 1,000 replications are given next to the internal branches. *Partial amino acid sequences. **Previously unnamed protein products, which we identified as members of the UCP superfamily. The oxaloacetate-malate carrier served as the outgroup. Afl, *A. flavipes*; Ath, *Arabidopsis thaliana*; Bta, *Bos Taurus*; Cca, *Cyprinus carpio*; Cfa, *Canis familiaris*; Dgr, *Dicrostonix groenlandicus*; Dre, *Danio rerio*; Ema, *Eupetomena macroura*; Gga, *Gallus gallus*; Hmu, *Helicodiceros muscivorus*; Hsa, *H. sapiens*; Les, *Lycopersicon esculentum*; Mac, *Macaca mulatto*; Mau, *Mesocricetus auratus*; Mga, *Meleagris gallopavo*; Min, *Mangifera indica*; Mmu, *M. musculus*; Ocu, *Oryctolagus cuniculus*; Osa, *Oryza sativa*; Psu, *P. sungorus*; Rno, *Rattus norvegicus*; Set, *Suncus etruscus*; Sfo, *Symplocarpus foetidus*; Sma, *S. macroura*; Ssc, *Sus scrofa*; Str, *Silurana tropicalis* Stu, *Solanum tuberosum*; Tae, *Triticum aestivum*; Xla, *Xenopus laevis*; Zmy, *Zea mays*. See the Supplementary Material (available online at the *Physiological Genomics* web site) for accession numbers of the sequences.

biguous molecular proof for their existence is lacking in metatheria as well as in prototheria. We here report on the sequence and tissue-specific expression pattern of marsupial UCP2 and UCP3.

First results suggesting the presence of UCP2 in metatheria and prototheria were obtained by comparative Southern and Northern blot analysis, whereas this approach was not successful for UCP1 and UCP3. We suggested a close relationship between avian UCPs and mammalian UCP3 based on the similar tissue-specific expression and physiological regulation (10, 17) and succeeded to amplify a 480-bp UCP3 cDNA fragment from skeletal muscle of *A. flavipes* using consensus primers.

Screening of cDNA libraries led to the identification of marsupial UCP2 (spleen, *A. flavipes* and *S. macroura*) and UCP3 (skeletal muscle, *A. flavipes*) (Fig. 2). In both proteins, transmembrane domains found in other members of the UCP family and several functional residues originally identified in UCP1 involved in pH sensing and nucleotide binding are conserved. This high degree of identity of marsupial and rodent UCP2 and UCP3 suggests a conserved function of the proteins in both mammalian subclasses.

We generated a phylogenetic tree with 44 sequences of UCP family members including the new marsupial UCP sequences and two previously nonannotated UCPs. UCP2 and UCP3 of *S. macroura* and *A. flavipes* are positioned at the base of their mammalian orthologs (Fig. 3).[1] Addition of the *A. flavipes* UCP3 sequence stabilized the node leading to the distinction between UCP2 and UCP3 sequences from 59% to 68% in our analysis. Beyond the comparison of marsupial UCPs with other mammalian orthologs, the phylogenetic analysis illustrates the

[1] The Supplementary Material for this article is available online at **http://physiolgenomics.physiology.org/cgi/content/full/00165.2003/DC1**.

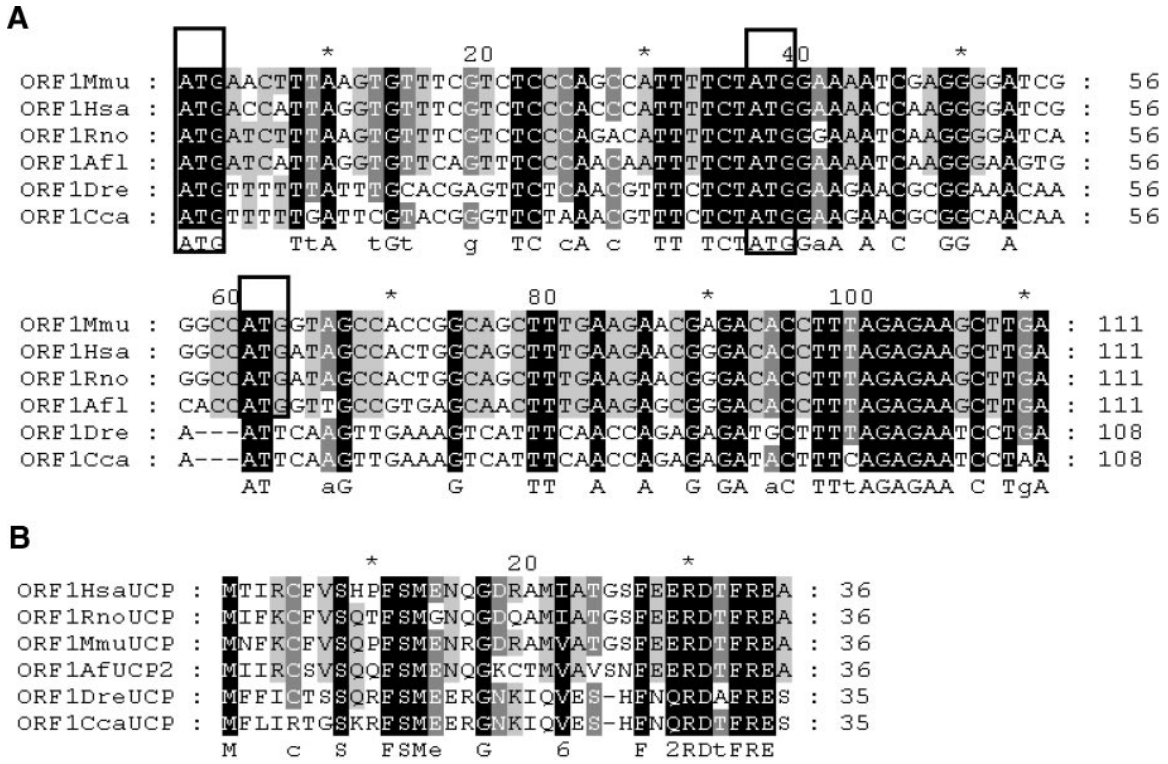

Fig. 4. Upstream open reading frame (ORF) found in the 5′-UTR of UCP2 mRNA from *A. flavipes*. The nucleotide sequence was aligned with all available UCP2 full-length mRNAs, and potential start cons (ATG) are boxed (*A*). The ORF was translated and aligned (*B*). Conserved nucleotides are highlighted with dark background. Mmu, *M. musculus*; Hsa, *H. sapiens*; Rno, *R. norvegicus*; Afl, *A. flavipes*; Dre, *D. rerio*; Cca, *C. carpio*.

broader relationships of UCP family members and enables the annotation of previously unnamed protein products. The present analysis provides the first demonstration of UCP2 in the animal class Amphibia.

The presence of UCP1 in marsupials remains unknown. Based on the phylogenetic tree, hypothesis can be generated on the presence of other UCPs in proto- and metatheria. Pertaining to UCP1, the presented tree questions the long-standing point of view that this protein is only found in placental mammals. Taking in account, the position of the node leading to the UCP1 cluster as well as the presence of UCP2 in fish and amphibians suggests that UCP1 (and UCP3) already exist(s) in lower vertebrates. Despite a high phylogenetic distance between amphibians, fish, and rodents, the UCP2 orthologs are very similar (~80%). In contrast, the comparison of UCP1 orthologs from phylogenetic distant species within eutherian mammals, as exemplified by shrew vs. mouse UCP1, reveals only 75% global identity based on 245 amino acids known from shrew. This indicates a rapid evolution of this protein within the eutherian infraclass. This may be one major complication in the attempt to determine the existence of an UCP1 ortholog in nonplacental mammals.

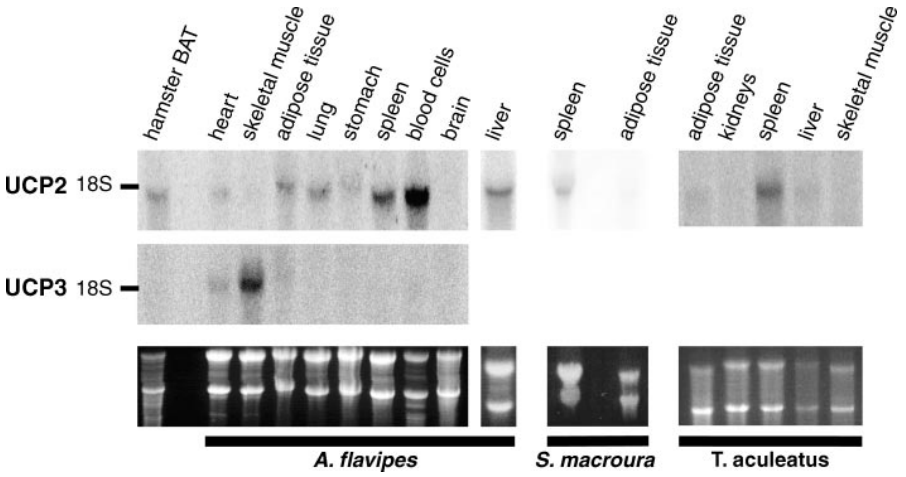

Fig. 5. Northern blot analysis of UCP expression in multiple tissues of the marsupials *A. flavipes* (UCP2 and UCP3) and *S. macroura* (UCP2) and the monotreme, the short-beaked echidna *T. aculeatus* (UCP2). Total RNA (20 μg) isolated from selected tissues was hybridized with the *A. flavipes* full-length UCP2 cDNA and *A. flavipes* UCP3 cDNA fragment. Total RNA from hamster brown adipose tissue served as a control.

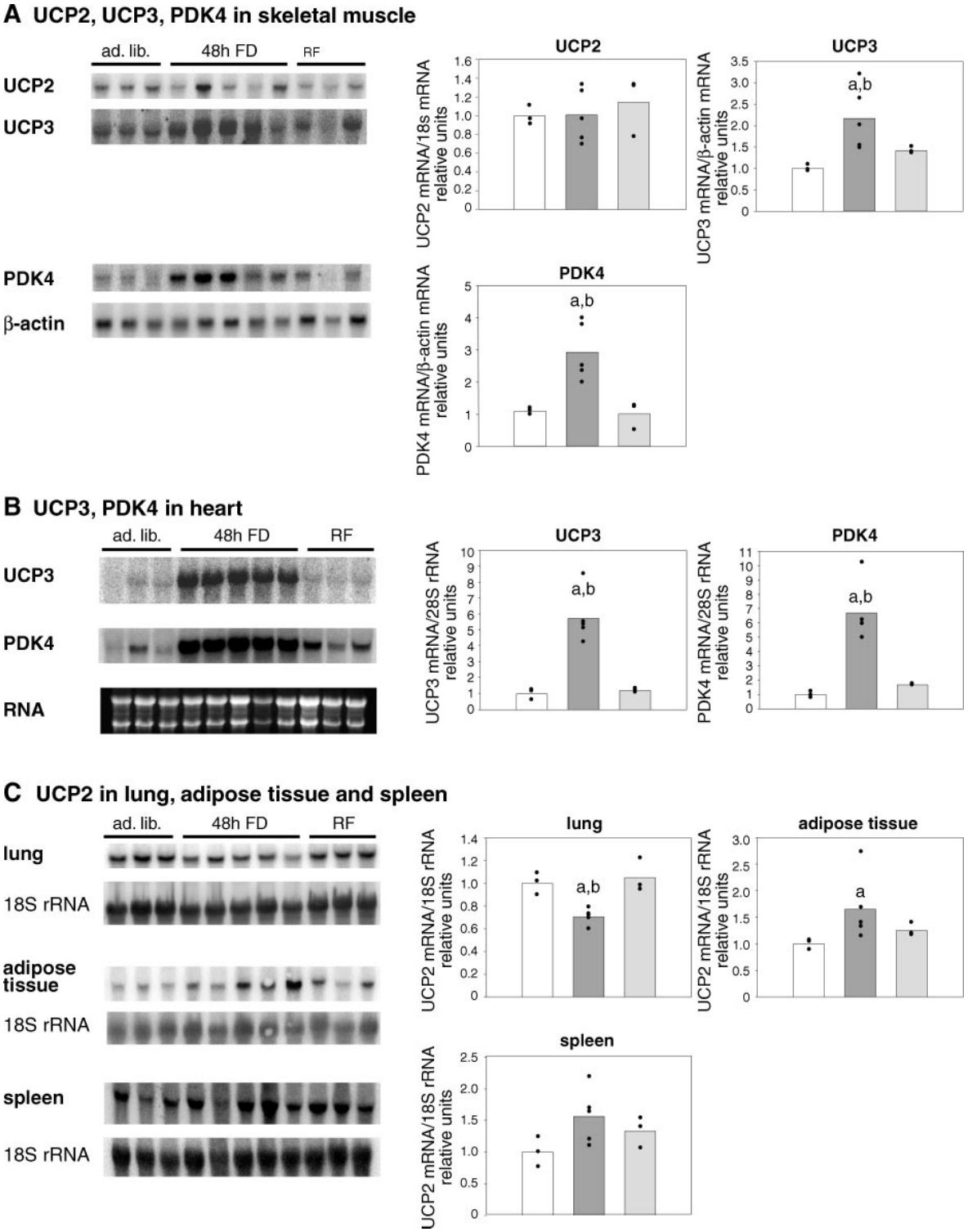

Fig. 6. Northern blot analysis in response to fasting in *A. flavipes* of UCP2, UCP3, and PDK4 mRNA in skeletal muscle (*A*), UCP3 and PDK4 mRNA in heart (*B*), and UCP2 in lung, adipose tissue, and spleen (*C*). Twenty micrograms total RNA from selected tissues of ad libitum-fed, food-deprived, and refed *A. flavipes* was hybridized with the *A. flavipes* full-length UCP2 cDNA and a 480-bp UCP3 cDNA fragment. *Right*: diagrams show individual UCP2 intensities (dots) and mean values of the ad libitum-fed group (open bar), 48-h fasted group (dark gray bar), and 24-h refed group (light gray bar). All intensities were normalized with either 18S rRNA or β-actin intensities. $^{a}P < 0.05$ for fasted vs. fed ad libitum; $^{b}P < 0.05$ for fasted vs. refed (Mann-Whitney U-Test).

We searched for conserved sequence motifs in the UTR of the *A. flavipes* UCP2 transcript, as others have demonstrated the presence of regulatory elements involved in translational regulation of the transcript (46). This led to the identification of a uORF in the 5′-UTR (Fig. 4). Surprisingly, the marsupial uORF is almost identical to an upstream ORF identified by Pecqueur and coworkers (47) in the transcripts of the mouse and human UCP2 genes. Functional analysis in cell systems revealed an inhibitory effect of the uORF on translation efficiency that depends on the utilized cell line (46, 47). The high level of conservation of this upstream ORF in metatheria emphasizes the functional significance for the regulation of UCP2 synthesis. Furthermore, we identified this uORF in the UCP2 full-length sequences of rat, zebrafish, and carp. So far there is no evidence for translation of this uORF. In all mammals, three AUG triplets are positioned in identical position in the uORF, whereas in fish, only two of them can be found (Fig. 4). The translation of eukaryotic mRNA is dependent on structures of the leader and the Kozak sequence (33, 45). Elements of the 5′-UTR control protein synthesis and especially upstream AUGs correlate negatively with translation efficiency (22, 32, 39, 48). Binding of ribosomes to uAUGs instead of the actual translational start codon would result in a lower translation rate. This control element for translational efficiency seems to be conserved during the evolution of vertebrates.

Following the unequivocal demonstration of UCP2 and UCP3 in marsupials, we subsequently investigated in *A. flavipes* the tissue-specific expression pattern and physiological regulation of gene expression in response to cold exposure and fasting by selecting tissues in which these physiological stimuli have been reported to alter the expression of UCP2 and UCP3 in mice and rats. Tissue specificity of UCP2 and UCP3 gene expression in marsupials is very similar to placental mammals (40). *A. flavipes* UCP3 mRNA is restricted to heart and skeletal muscle with higher levels in the latter tissue. In contrast, a ubiquitous tissue distribution of UCP2 mRNA was found in *A. flavipes* as described previously in rodents (Fig. 5), with strongest expression levels observed in tissue sites rich with macrophages, like lung and spleen (20, 59). We detected the highest abundance of UCP2 mRNA in blood cells. This is consistent with findings in rodents and humans where high levels of UCP2 expression have been observed in monocytes and macrophages (34). However, we analyzed RNA from the total blood cell population in which white blood cells make up only 0.1% of the total cell number, and it is unlikely that erythrocytes and blood platelets, which lack mitochondria, express significant amounts of UCP2. Thus, if UCP2 expression is restricted to white blood cells, then the cell-specific mRNA abundance must be extremely high (Fig. 5). In blood and macrophage-rich tissues the level of UCP2 expression appears to regulate the generation of ROS, indicating a function in the modulation of the mammalian immune system. UCP2 knockout mice gain resistance against *Toxoplasma gondii* infection (1), and downregulation of UCP2 in macrophages promotes the generation of bactericidal substances (29).

UCP2 and UCP3 have been proposed to be either related to thermogenesis, lipid oxidation, or ROS defense (15, 21). However, in accordance with rodent studies, cold exposure for 2 days affected neither UCP2 (adipose tissue, skeletal muscle) nor UCP3 (skeletal muscle) mRNA levels in *A. flavipes*. In only one study of rat soleus muscle was an increase of UCP2 mRNA level in response to cold reported (4), but the functional significance has not been resolved.

We, as well as others, have failed to demonstrate the presence of UCP1 in marsupials, but it has been speculated that marsupial UCP2 and UCP3 could be involved in nonshivering thermogenesis (28). However, based on the lack of cold-induced expression in adipose tissue and skeletal muscle, such a thermogenic function of UCP2 and UCP3 appears unlikely. In the mouse only UCP1 ablation results in a defect of adaptive thermogenesis in the cold (23). Furthermore, the two-histidine motif conserved in UCP1 (H145/H147 in hamster) and involved in the unique proton transport capacity is not present in rodent UCP2 and UCP3 (2). Therefore, it was suggested that only UCP1 is able to uncouple the respiratory chain. However, the functional significance of the two-histidine motif must be questioned, as H145 is not conserved in shrew UCP1 (Fig. 2). Moreover, Echtay and coworkers (14–16) found that superoxides and coenzyme Q not only stimulate the uncoupling activity of UCP1, but also activate UCP2 and UCP3. Even if marsupial UCP2 exhibits uncoupling activity, it is not induced in response to cold.

In eutherian mammals UCP2 and UCP3 expression is increased in response to fasting in skeletal muscle (4, 7, 52, 53, 60). In fasted *A. flavipes* UCP3 mRNA level is increased in skeletal muscle and in heart and diminished by refeeding (Fig. 6). Interestingly, physiological regulation of UCP2 expression in skeletal muscle of *A. flavipes* in fasting/refeeding was absent. In this fasting/refeeding experiment PDK4 expression, taken as a marker for a metabolic switch toward lipid oxidation (61, 62), closely resembled the changes in UCP3 mRNA levels. This suggests that UCP3 is recruited when muscle metabolism preferentially oxidizes lipids. Recent reports substantiate the hypothesis that UCP3 may function as a fatty acid anion exporter, thereby preventing the accumulation of nonesterified fatty acids in the mitochondrial matrix (24, 54). In conclusion, the regulation of skeletal muscle UCPs (avian UCP, marsupial UCP3, and placental UCP3) in response to fasting and refeeding across a broad range of endotherms suggests an identical physiological function.

UCP2 mRNA level was significantly decreased in lung and increased in adipose tissue but not altered in spleen and skeletal muscle (Fig. 6). Regulation of UCP2 expression in lung and adipose tissue has not been reported for rodents (46), and the functional significance of this interspecific difference is unclear. However, UCP2 mRNA expression does not reflect UCP2 protein levels, which have been shown to increase in the absence of mRNA regulation (49). Furthermore, the high UCP2 mRNA levels found in blood cells may have to be considered in this respect. Results obtained in UCP2 gene expression studies using total tissue RNA may be affected by tissue blood volume. Alteration of tissue blood volume in response to physiological challenges like fasting or cold exposure may result in apparent changes in UCP2 gene expression. In situ hybridization studies, as already published for UCP2 in the brain, could rule out this possible source of error in future experiments.

In summary, we unequivocally identified UCP2 and UCP3 in marsupials and provided first evidence for the expression of UCP2 in a monotreme. Sequence elements of the marsupial UCPs are strongly conserved during evolution of the 130

million year old marsupial lineage, suggesting an identical protein function that is further corroborated by the similar tissue expression pattern and physiological regulation of gene expression in marsupials and placental mammals. We found no indication for the involvement of marsupial UCPs in adaptive nonshivering thermogenesis. Further comparative analysis of UCP2 and UCP3 from evolutionary distinct species will assist in testing different hypotheses pertaining to the functional annotation of these mitochondrial anion carrier proteins.

ACKNOWLEDGMENTS

We are grateful to the University of Queensland, Dr. Geoff Lundie-Jenkins from Queensland Parks, Environment Australia, and the staff of the Department of Natural Resources, Inglewood, for use of their facilities. We also want to thank Queensland Museum for providing us with tissues from a variety of Australian marsupials and several Queensland farmers for permission to trap on their properties.

GRANTS

This research was supported by Deutsche Forschungsgemeinschaft DFG KL973/7 (to M. Klingenspor) and by a grant to Kerry Withers from the Department of Biological and Physical Sciences, University of Southern Queensland.

REFERENCES

1. **Arsenijevic D, Onuma H, Pecqueur C, Raimbault S, Manning BS, Miroux B, Couplan E, Alves-Guerra MC, Goubern M, Surwit R, Bouillaud F, Richard D, Collins S, and Ricquier D.** Disruption of the uncoupling protein-2 gene in mice reveals a role in immunity and reactive oxygen species production. *Nat Genet* 26: 435–439, 2000.
2. **Bienengraeber M, Echtay KS, and Klingenberg M.** H+ transport by uncoupling protein (UCP-1) is dependent on a histidine pair, absent in UCP-2 and UCP-3. *Biochemistry* 37: 3–8, 1998.
3. **Borecky J, Maia IG, and Arruda P.** Mitochondrial uncoupling proteins in mammals and plants. *Biosci Rep* 21: 201–212, 2001.
4. **Boss O, Samec S, Dulloo AG, Seydoux J, Muzzin P, and Giacobino JP.** Tissue-dependent upregulation of rat uncoupling protein-2 expression in response to fasting or cold. *FEBS Lett* 412: 111–114, 1997.
5. **Boss O, Samec S, Paolonigiacobino A, Rossier C, Dulloo AG, Seydoux J, Muzzin P, and Giacobino JP.** Uncoupling protein-3: A new member of the mitochondrial carrier family with tissue-specific expression. *FEBS Lett* 408: 39–42, 1997.
6. **Bouillaud F, Arechaga I, Petit PX, Raimbault S, Levimeyrueis C, Casteilla L, Laurent M, Rial E, and Ricquier D.** A sequence related to a DNA recognition element is essential for the inhibition by nucleotides of proton transport through the mitochondrial uncoupling protein. *EMBO J* 13: 1990–1997, 1994.
7. **Cadenas S, Buckingham JA, Samec S, Seydoux J, Din N, Dulloo AG, and Brand MD.** UCP2 and UCP3 rise in starved rat skeletal muscle but mitochondrial proton conductance is unchanged. *FEBS Lett* 462: 257–260, 1999.
8. **Chomczynski P and Sacchi N.** Single-step method of RNA isolation by acid guanidinium thiocyanate-phenol-chloroform extraction. *Anal Biochem* 162: 156–159, 1987.
9. **Clements F, Hope PJ, Daniels CB, Chapman I, and Wittert G.** Thermogenesis in the marsupial *Sminthopsis crassicaudata*: effect of catecholamines and diet. *Aust J Zool* 46: 381–390, 1998.
10. **Collin A, Malheiros RD, Moraes VM, Van As P, Darras VM, Taouis M, Decuypere E, and Buyse J.** Effects of dietary macronutrient content on energy metabolism and uncoupling protein mRNA expression in broiler chickens. *Br J Nutr* 90: 261–269, 2003.
11. **Couplan E, Mar Gonzalez-Barroso M, Alves-Guerra MC, Ricquier D, Goubern M, and Bouillaud F.** No evidence for a basal, retinoic, or superoxide-induced uncoupling activity of the uncoupling protein 2 present in spleen or lung mitochondria. *J Biol Chem* 277: 26268–26275, 2002.
12. **Dawson TJ and Olson JM.** Thermogenic capabilities of the opossum *Monodelphis domestica* when warm and cold acclimated: similarities between American and Australian marsupials. *Comp Biochem Physiol A* 89: 85–91, 1988.
13. **Dayhoff MO.** *Atlas of Protein Sequence and Structure*. Washington, DC: National Biomedical Research Foundation, 1979.
14. **Echtay KS, Murphy MP, Smith RA, Talbot DA, and Brand MD.** Superoxide activates mitochondrial uncoupling protein 2 from the matrix side. Studies using targeted antioxidants. *J Biol Chem* 277: 47129–47135, 2002.
15. **Echtay KS, Roussel D, St Pierre J, Jekabsons MB, Cadenas S, Stuart JA, Harper JA, Roebuck SJ, Morrison A, Pickering S, Clapham JC, and Brand MD.** Superoxide activates mitochondrial uncoupling proteins. *Nature* 415: 96–99, 2002.
16. **Echtay KS, Winkler E, Frischmuth K, and Klingenberg M.** Uncoupling proteins 2 and 3 are highly active H(+) transporters and highly nucleotide sensitive when activated by coenzyme Q (ubiquinone). *Proc Natl Acad Sci USA* 98: 1416–1421, 2001.
17. **Evock-Clover CM, Poch SM, Richards MP, Ashwell CM, and McMurtry JP.** Expression of an uncoupling protein gene homolog in chickens. *Comp Biochem Physiol A Mol Integr Physiol* 133: 345–358, 2002.
18. **Faggioni R, Shigenaga J, Moser A, Feingold KR, and Grunfeld C.** Induction of UCP2 gene expression by LPS: a potential mechanism for increased thermogenesis during infection. *Biochem Biophys Res Commun* 244: 75–78, 1998.
19. **Felsenstein J.** Confidence limits on phylogenies: an approach using the bootstrap. *Evolution* 39: 783–791, 1985.
20. **Fleury C, Neverova M, Collins S, Raimbault S, Champigny O, Levi-Meyrueis C, Bouillaud F, Seldin MF, Surwit RS, Ricquier D, and Warden CH.** Uncoupling protein-2: a novel gene linked to obesity and hyperinsulinemia. *Nat Genet* 15: 269–272, 1997.
21. **Fleury C and Sanchis D.** The mitochondrial uncoupling protein-2: current status. *Int J Biochem Cell Biol* 31: 1261–1278, 1999.
22. **Geballe AP and Morris DR.** Initiation codons within 5′-leaders of mRNAs as regulators of translation. *Trends Biochem Sci* 19: 159–164, 1994.
23. **Golozoubova V, Hohtola E, Matthias A, Jacobsson A, Cannon B, and Nedergaard J.** Only UCP1 can mediate adaptive nonshivering thermogenesis in the cold. *FASEB J* 15: 2048–2050, 2001.
24. **Himms-Hagen J and Harper ME.** Physiological role of UCP3 may be export of fatty acids from mitochondria when fatty acid oxidation predominates: an hypothesis. *Exp Biol Med (Maywood)* 226: 78–84, 2001.
25. **Hope PJ, Pyle D, Daniels CB, Chapman I, Horowitz M, Morley JE, Trayhurn P, Kumaratilake J, and Wittert G.** Identification of brown fat and mechanisms for energy balance in the marsupial, *Sminthopsis crassicaudata*. *Am J Physiol Regul Integr Comp Physiol* 273: R161–R167, 1997.
26. **Hope PJ, Turnbull H, Breed W, Morley JE, Horowitz M, and Wittert GA.** The effect of ovarian steroids and photoperiod on body fat stores and uncoupling protein 2 in the marsupial *Sminthopsis crassicaudata*. *Physiol Behav* 69: 463–470, 2000.
27. **Kabat AP, Rose RW, Harris J, and West AK.** Molecular identification of uncoupling proteins (UCP2 and UCP3) and absence of UCP1 in the marsupial Tasmanian bettong, *Bettongia gaimardi*. *Comp Biochem Physiol B Biochem Mol Biol* 134: 71–77, 2003.
28. **Kabat AP, Rose RW, and West AK.** The devil's crucible: non-shivering thermogenesis in the Tasmanian devil, *Sarcophilus harrisii* (Abstract) [Online]. Conference Proceeding, oral presentation at the Australia and New Zealand Society for Comparative Physiology and Biochemistry conference, Adelaide, December 2001. http://www.zoology.uwa.edu.au/ANZSCPB/images/ANZSCPB2001abstracts.pdf. (See p.13)
29. **Kizaki T, Suzuki K, Hitomi Y, Taniguchi N, Saitoh D, Watanabe K, Onoe K, Day NK, Good RA, and Ohno H.** Uncoupling protein 2 plays an important role in nitric oxide production of lipopolysaccharide-stimulated macrophages. *Proc Natl Acad Sci USA* 99: 9392–9397, 2002.
30. **Klaus S, Raimbault S, Bouillaud F, Ricquier D, Gessner M, and Jürgens KD.** Sequence of the brown adipose tissue specific uncoupling protein UCP from the Etruscan shrew (*Suncus etruscus*). In: *Adaptations to the Cold: Tenth International Hibernation Symposium*, edited by Geiser F, Hulbert AJ, and Nicol SC. Armidale, NSW: University of New England Press, 1996, p. 293–298.
31. **Klingenberg M, Echtay KS, Bienengraeber M, Winkler E, and Huang SG.** Structure-function relationship in UCP1. *Int J Obes* 23: S24–S29, 1999.
32. **Kochetov AV, Ischenko IV, Vorobiev DG, Kel AE, Babenko VN, Kisselev LL, and Kolchanov NA.** Eukaryotic mRNAs encoding abundant and scarce proteins are statistically dissimilar in many structural features. *FEBS Lett* 440: 351–355, 1998.

33. **Kozak M.** An analysis of 5′-noncoding sequences from 699 vertebrate messenger RNAs. *Nucleic Acids Res* 15: 8125–8148, 1987.
34. **Krauss S, Zhang CY, and Lowell BB.** A significant portion of mitochondrial proton leak in intact thymocytes depends on expression of UCP2. *Proc Natl Acad Sci USA* 99: 118–122, 2002.
35. **Laloi M, Klein M, Riesmeier JW, Mullerrober B, Fleury C, Bouillaud F, and Ricquier D.** A plant cold-induced uncoupling protein. *Nature* 389: 135–136, 1997.
36. **Larrouy D, Laharrague P, Carrera G, Viguerie-Bascands N, Levi-Meyrueis C, Fleury C, Pecqueur C, Nibbelink M, Andre M, Casteilla L, and Ricquier D.** Kupffer cells are a dominant site of uncoupling protein 2 expression in rat liver. *Biochem Biophys Res Commun* 235: 760–764, 1997.
37. **Ledesma A, de Lacoba MG, and Rial E.** The mitochondrial uncoupling proteins. *Genome Biol* 3: REVIEWS3015, 2002.
38. **Loudon ASI, Rothwell NJ, and Stock MJ.** Brown fat, thermogenesis and physiological birth in a marsupial. *Comp Biochem Physiol* 81A: 815–819, 1985.
39. **Morris DR and Geballe AP.** Upstream open reading frames as regulators of mRNA translation. *Mol Cell Biol* 20: 8635–8642, 2000.
40. **Nedergaard J and Cannon B.** Pros and cons for suggested functions. *Exp Physiol* 88: 65–84, 2003.
41. **Nicholls DG and Locke RM.** Thermogenic mechanisms in brown fat. *Physiol Rev* 64: 1–64, 1984.
42. **Nicol SC.** Non-shivering thermogenesis in the potoroo, *Potorous tridactylus* (Kerr). *Comp Biochem Physiol C* 59: 33–37, 1978.
43. **Nicol SC, Pavlides D, and Andersen NA.** Nonshivering thermogenesis in marsupials: absence of thermogenic response to beta 3-adrenergic agonists. *Comp Biochem Physiol A Physiol* 117: 399–405, 1997.
44. **Opazo JC, Nespolo RF, and Bozinovic F.** Arousal from torpor in the chilean mouse-opposum (*Thylamys elegans*): does non-shivering thermogenesis play a role? *Comp Biochem Physiol A Mol Integr Physiol* 123: 393–397, 1999.
45. **Pain VM.** Initiation of protein synthesis in eukaryotic cells. *Eur J Biochem* 236: 747–771, 1996.
46. **Pecqueur C, Alves-Guerra MC, Gelly C, Levi-Meyrueis C, Couplan E, Collins S, Ricquier D, Bouillaud F, and Miroux B.** Uncoupling protein 2, in vivo distribution, induction upon oxidative stress, and evidence for translational regulation. *J Biol Chem* 276: 8705–8712, 2001.
47. **Pecqueur C, Cassard-Doulcier AM, Raimbault S, Miroux B, Fleury C, Gelly C, Bouillaud F, and Ricquier D.** Functional organization of the human uncoupling protein-2 gene, and juxtaposition to the uncoupling protein-3 gene. *Biochem Biophys Res Commun* 255: 40–46, 1999.
48. **Rogozin IB, Kochetov AV, Kondrashov FA, Koonin EV, and Milanesi L.** Presence of ATG triplets in 5′ untranslated regions of eukaryotic cDNAs correlates with a "weak" context of the start codon. *Bioinformatics* 17: 890–900, 2001.
49. **Rose RW, Kuswanti N, and Colquhoun EQ.** Development of endothermy in a Tasmanian marsupial, *Bettongia gaimardi* and its response to cold and noradrenaline. *J Comp Physiol [B]* 168: 359–363, 1998.
50. **Rose RW, West AK, Ye JM, McCormick GH, and Colquhoun EQ.** Nonshivering thermogenesis in a marsupial (the tasmanian bettong *Bettongia gaimardi*) is not attributable to brown adipose tissue. *Physiol Biochem Zool* 72: 699–704, 1999.
51. **Saitou N and Nei M.** The neighbor-joining method: a new method for reconstructing phylogenetic trees. *Mol Biol Evol* 4: 406–425, 1987.
52. **Samec S, Seydoux J, and Dulloo AG.** Interorgan signaling between adipose tissue metabolism and skeletal muscle uncoupling protein homologs: is there a role for circulating free fatty acids? *Diabetes* 47: 1693–1698, 1998.
53. **Samec S, Seydoux J, and Dulloo AG.** Role of UCP homologues in skeletal muscles and brown adipose tissue: mediators of thermogenesis or regulators of lipids as fuel substrate? *FASEB J* 12: 715–724, 1998.
54. **Schrauwen P, Hoeks J, Schaart G, Kornips E, Binas B, Van De Vusse GJ, Van Bilsen M, Luiken JJ, Coort SL, Glatz JF, Saris WH, and Hesselink MK.** Uncoupling protein 3 as a mitochondrial fatty acid anion exporter. *FASEB J* 17: 2272–2274, 2003.
55. **Short JM and Sorge JA.** In vivo excision properties of bacteriophage lambda ZAP expression vectors. *Methods Enzymol* 216: 495–508, 1992.
56. **Smith BK and Dawson TJ.** Effect of cold and warm acclimation on the thermal balance of a marsupial (*Dasyuroides byrnei*). *Thermal Physiol* 9: 3199–3204, 1984.
57. **Strahan R.** *The Mammals of Australia*. Sydney, Australia: Reed Books, 1995.
58. **Stuart JA, Harper JA, Brindle KM, and Brand MD.** Uncoupling protein 2 from carp and zebrafish, ectothermic vertebrates. *Biochim Biophys Acta* 1413: 50–54, 1999.
59. **von Praun C, Burkert M, Gessner M, and Klingenspor M.** Tissue-specific expression and cold-induced mRNA levels of uncoupling proteins in the Djungarian hamster. *Physiol Biochem Zool* 74: 203–211, 2001.
60. **Weigle DS, Selfridge LE, Schwartz MW, Seeley RJ, Cummings DE, Havel PJ, Kuijper JL, and Beltrandelrio H.** Elevated free fatty acids induce uncoupling protein 3 expression in muscle: a potential explanation for the effect of fasting. *Diabetes* 47: 298–302, 1998.
61. **Wu P, Inskeep K, Bowker-Kinley MM, Popov KM, and Harris RA.** Mechanism responsible for inactivation of skeletal muscle pyruvate dehydrogenase complex in starvation and diabetes. *Diabetes* 48: 1593–1599, 1999.
62. **Wu P, Sato J, Zhao Y, Jaskiewicz J, Popov KM, and Harris RA.** Starvation and diabetes increase the amount of pyruvate dehydrogenase kinase isoenzyme 4 in rat heart. *Biochem J* 329: 197–201, 1998.
63. **Ye JM, Edwards SJ, Rose RW, Steen JT, Clark MG, and Colquhoun EQ.** alpha-adrenergic stimulation of thermogenesis in a rat kangaroo (Marsupialia, *Bettongia gaimardi*). *Am J Physiol Regul Integr Comp Physiol* 271: R586–R592, 1996.
64. **Zhang CY, Baffy G, Perret P, Krauss S, Peroni O, Grujic D, Hagen T, Vidal-Puig AJ, Boss O, Kim YB, Zheng XX, Wheeler MB, Shulman GI, Chan CB, and Lowell BB.** Uncoupling protein-2 negatively regulates insulin secretion and is a major link between obesity, beta cell dysfunction, and type 2 diabetes. *Cell* 105: 745–755, 2001.

Supplementary Table

Abbreviation	Species name	Protein	Acc No.	Common name
Afl	*Antechinus flavipes*	UCP2 UCP3	AY233003 AY519198	Yellow-footed Antechinus
Ath	*Arabidopsis thaliana*	UCP	CAA11757.1	Mouse-ear cress
Bta	*Bos Taurus*	UCP1 UCP2 UCP3	P10861_partial AAD29672_partial AAD33339	Cow
Cca	*Cyprinus carpio*	UCP2	Q9W725	Carp
Cel	*Caenorhabditis elegans*	OMCP	NP_493694.1	
Cfa	*Canis familiaris*	UCP1 UCP2 UCP3	BAB11684 Q9N2J1 BAA90458	Dog
Dgr	*Dicrostonix groenlandicus*	UCP1	AAM49148	Lemming
Dme	*Drosophila melanogaster*	OMCP	AAF56907	Vinegar fly
Dre	*Danio rerio*	UCP2	Q9W720	Zebrafish
Ema	*Eupetomena macroura*	UCP	AAK16829	Swallow-tailed hummingbird
Gga	*Gallus gallus*	UCP	AF287144	Chicken
Hmu	*Helicodiceros muscivorus*	UCP	BAC06495.1	Hairy arum
Hsa	*Homo sapiens*	UCP1 UCP2 UCP3S OMCP	G01858 XP_035029 NP_073714 A56650	Human
Les	*Lycopersicon esculentum*	UCP	AAL82482	Tomato
Mac	*Macaca mulatto*	UCP3	7008155	Rhesus monkey
Mau	*Mesocricetus auratus*	UCP1	P04575	Golden hamster
Mga	*Meleagris gallopavo*	UCP	AAL28138	Turkey
Min	*Mangifera indica*	PUMP2	AAK70939_partial	Mango

Mmu	*Mus musculus*	UCP1 UCP2 UCP3	P12242 AAB17666 P56501	Mouse
Ocu	*Oryctolagus cuniculus*	UCP1	CAA32826	Rabbit
Osa	*Oryza sativa*	UCP	BAB40658.1	Japanese rice
Psu	*Phodopus sungorus*	UCP1 UCP2 UCP3	AAG33983 AAG33984_partial AAG33985_partial	Dsungarian hamster
Rno	*Rattus norvegicus*	UCP1 UCP2 UCP3	P04633 AAC98733 P56499	Rat
Set	*Suncus etruscus*	UCP1	Literature (32)	White-toothed pygmy shrew
Sfo	*Symplocarpus foetidus*	UCPa	BAA92172.1	Shunk cabbage
Sma	*Sminthopsis macroura*	UCP2	AY232996	Stripe-faced Dunnert
Ssc	*Sus scrofa*	UCP2 UCP3	AAD05201 AAD08811	Pig
Str	*Silurana tropicalis*	UCP2	AAH63352	Western clawed frog
Stu	*Solanum tuberosum*	UCP	T07793	Potato
Tae	*Triticum aestivum*	UCP	AB042429	Bread wheat
Xla	*Xenopus laevis*	UCP2	AAH44682	African clawed frog
ZmyUCP	*Zea mays*	UCP	AF461732_1	Maize

A Quest for the Origin of Mammalian Uncoupling Proteins

MARTIN JASTROCH,[1] SIGRID STÖHR,[1] KERRY WITHERS,[2] AND MARTIN KLINGENSPOR[1]
[1] Philipps University of Marburg, Department of Biology, Animal Physiology, Germany
[2] Department of Biological and Physical Sciences, University of Southern Queensland, Toowoomba, Queensland, Australia

Abstract. Nonshivering thermogenesis is dependent on the presence of UCP1 in brown adipose tissue. The function of UCP2 and UCP3 is most likely related to mitochondrial superoxide metabolism and/or fatty acid oxidation. These three members of the core UCP family are known in eutherians but had not been found in marsupials and monotremes so far. The objective of our search is to determine the origin of UCP1 and classical nonshivering thermogenesis. Furthermore, our approach to characterize UCP2/UCP3 in distantly related animal species will assist in the functional annotation of these proteins.

We recently reported on the molecular identification, tissue-distribution, and physiological regulation of UCP2 and UCP3 mRNA in the marsupial *Antechinus flavipes* (yellow-footed Antechinus). Despite separate evolution of the marsupial lineage since 130 million years, our data suggest a conserved physiological role of these UCPs. Here, we present the immunological detection of marsupial UCP3 in skeletal muscle using antibodies raised against mouse/rat UCP3. A comprehensive phylogenetic analysis led us to hypothesize that all uncoupling proteins were already present at the evolutionary stage of modern teleost fishes and questions the unique presence of UCP1 in placental mammals. However, the search for UCP1 in nonplacental mammals has been unsuccessful so far and is most likely hampered by the more rapid evolution of UCP1 as compared to other UCPs.

Life in the Cold: Evolution, Mechanisms, Adaptation, and Application. Twelfth International Hibernation Symposium. Biological Papers of the University of Alaska, number 27. Institute of Arctic Biology, University of Alaska Fairbanks, Alaska, USA.

The Quest for UCP1 in Nonplacental Mammals

In placental mammals, uncoupling protein 1 (UCP1) is responsible for nonshivering thermogenesis in brown adipose tissue mitochondria. The protein is inserted with six α helical transmembrane domains into the inner mitochondrial membrane and catalyzes proton flux into the matrix. Protonmotive force normally driving ATP synthesis is thereby dissipated as heat. In mice acutely exposed to the cold this unique mechanism of heat production is essential for survival (Enerbäck et al., 1997), and in small placental hibernators, brown adipose tissue mass is increased in relation to body mass as compared to nonhibernating mammals (Heldmaier, 1971). In the past, physiologists, morphologists, and biochemists have repeatedly questioned the common view that brown adipose tissue and UCP1 are monophyletic traits of placental mammals. In some marsupial species, treatment with sympathomimetics increased resting metabolic rate, resembling the adrenergic stimulation of nonshivering thermogenesis in brown adipose tissue of placental mammals (Loudon et al., 1985), but this finding was not confirmed in other studies. The interscapular fat deposit of Bennett's wallaby consists of multilocular adipocytes (Loudon et al., 1985), but so do white adipocytes in cold-stressed placental mammals (Loncar et al., 1988). The brownish appearance of the interscapular fat depot in the small marsupial carnivores *Sminthopsis macroura* and *Antechinus flavipes* (unpublished observation) indicates a high tissue content of mitochondria, but only the identification of UCP1 in marsupial adipose tissue and the demonstration of uncoupled mitochondrial respiration would provide hard evidence for the existence of brown adipose tissue in marsupials.

It is well established that purine nucleotides bind to UCP1 and inhibit proton transport activity in the absence of free fatty acids (Klingenspor, 2003). Indeed, increased GDP-binding to interscapular brown adipose tissue mitochondria of the Benett's wallaby suggested the presence of UCP1 (Loudon et al., 1985). Furthermore, UCP1-like immunoreactivity was reported in the interscapular fat deposit of *Sminthopsis crassicaudata* using an antibody raised against squirrel UCP1 (Hope et al., 1997). However, by using rodent probes or primers deduced from rodent UCP1 sequences, UCP1 mRNA could not be detected in the Tasmanian bettong (Rose et al., 1999) and the Tasmanian devil (Kabat et al., 2003). In our laboratory the attempts to identify UCP1 mRNA in marsupial adipose tissue with heterologous probes were futile as well. Previously, the use of a labelled oligomer from a conserved region of UCP1 had been successful to detect the mRNA in a variety of placentals (Brander et al., 1993). However, in our

hands several attempts to amplify marsupial UCP1 by RT-PCR using different primers deduced from conserved regions of the UCP1 coding sequence failed. Taken together, the monophyletic nature of the UCP1 gene in placental mammals has not been seriously challenged, as sequence data providing unambiguous proof for the presence of UCP1 in nonplacental mammals have not been reported.

Identification of Uncoupling Proteins in Marsupials

Even in tissues other than brown adipose tissue, a significant portion of mitochondrial respiration is due to proton leakage across the inner mitochondrial membrane but the biochemical cause for this leak has not been resolved (Rolfe and Brown, 1997). In 1997, paralogous proteins similar to UCP1 were found (Boss et al., 1997; Fleury et al., 1997). Because of their sequence and structural similarity, and their uncoupling activity in certain experimental conditions, they were named UCP2 and UCP3. In placental mammals UCP2 is ubiquitously expressed in multiple tissues, whereas UCP3 is restricted to skeletal and heart muscle. Pertaining to their phylogenetic distribution, UCP2 and UCP3 are described in placental mammals. Moreover, UCP2 is also found in fish (Stuart et al., 1999) and a UCP-like protein is present in birds (Raimbault et al., 2001). None of the core UCP family members have been identified so far in invertebrates.

A thermogenic function of UCP2 and UCP3 in brown adipose tissue is unlikely since they do not compensate for defective thermogenesis in UCP1 ablated mice, and ablation of the UCP2 or UCP3 gene does not impair energy balance, cold resistance, or nonshivering thermogenesis in rodents (Cannon and Nedergaard, 2004). However, a recent study suggests a possible thermogenic activity of UCP3 in skeletal muscle of mice in response to extasy treatment (Mills et al., 2003). Accumulating evidence suggests that UCP3 may play a role in mitochondrial lipid metabolism operating as a fatty acid anion exporter (Himms-Hagen and Harper, 2001; Schrauwen et al., 2003). Other nonthermogenic-uncoupling functions have been assigned to UCP2, including the reduction of superoxide generation in mitochondria by mild uncoupling, diminished pancreatic insulin secretion by lowering the cytosolic ATP/ADP ratio, neuroprotection and modulation of the immune system (Nedergaard and Cannon, 2003).

We cloned full-length marsupial UCP2 and UCP3 cDNAs in *Antechinus flavipes* and a UCP2 cDNA in *Sminthopsis macroura* (stripe-faced dunnart) (Jastroch et al., 2004). Initial hybridization analyses using heterologous probes from mouse and hamster revealed the presence of the UCP2 gene and transcript

but not UCP1 and UCP3. Since the marsupial UCP3 sequence was not detectable using heterologous rodent cDNA probes, we applied an alternative cloning strategy based on conserved blocks within the UCP3 coding sequence. We deduced consensus oligomers from placental UCP3, also including bird UCP. We suggest that the latter is most likely the avian orthologue of UCP3, which is supported by the physiological regulation of gene expression (Evock-Clover CM et al., 2002) and phylogenetic relation to mammalian UCP3 (Fig. 3). We amplified a 480 bp cDNA fragment from skeletal muscle cDNA of *A. flavipes,* which we used to isolate a full-length UCP3 clone (Genbank Acc. #AY519198) from a cDNA library.

In *A. flavipes* exposed to 5° C for two days, the mRNA levels of UCP2 and UCP3 in interscapular adipose tissue and in skeletal muscle were not increased (Jastroch et al., 2004), which appears to exclude a potential role in adaptive thermogenesis in marsupials. However, we recently achieved the immunological detection of UCP3 in protein extracts from skeletal muscle (Fig. 1). UCP3 protein levels in cold-exposed *A. flavipes* were elevated nearly 2-fold. In contrast to the mRNA data, this finding suggests a role of UCP3 for muscle thermogenesis.

We also studied the regulation of UCP2 and UCP3 mRNA in response to two days of food deprivation. Whereas UCP2 mRNA remained unchanged in most tissues investigated, UCP3 mRNA was upregulated 6-fold in heart and 2.5-fold in skeletal muscle. This mode of physiological regulation is consistent with the upregulation of UCP3 expression in skeletal muscle of rodents induced by fasting but not compatible with a thermogenic function of UCP3. Since muscle energy expenditure in fasted animals is lowered, the efficiency of mitochondrial ATP synthesis is unlikely to be reduced in this negative state of energy balance.

When Did the UCP1 Gene Emerge in Vertebrate Evolution?

One hundred thirty million years of evolution separated marsupials and eutherian mammals, leading to sequence variations in the UCP genes that may impose some difficulties in their identification in marsupials. In this respect, the search for UCP2 orthologues is less difficult due to the high sequence conservation in distantly related taxa, such as amphibians, fish, and rodents. In retrospect, the high identity of rodent and marsupial cDNA sequences (90%) facilitated detection of the marsupial gene and the corresponding mRNA by heterologous hybridization assays. However, for UCP3 this approach completely failed due to only 80% global identity between marsupial and rodent UCP3. The search for regions in the coding sequence conserved across phylogenetically distinct species

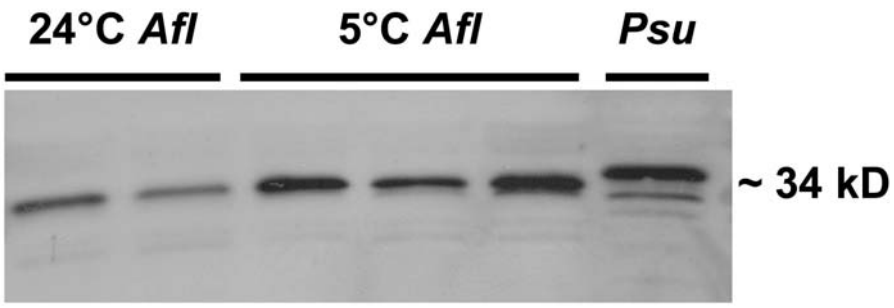

*Fig. 1: Immunological detection of UCP3 in cold and warm acclimated yellow-footed antechinus (*Antechinus flavipes, *Afl). Forty micrograms of protein from skeletal muscle per lane were subjected to Western blot analysis using an antibody against mouse/rat UCP3. An equal amount of skeletal muscle protein from the Djungarian hamster (*Phodopus sungorus, *Psu) served as a control.*

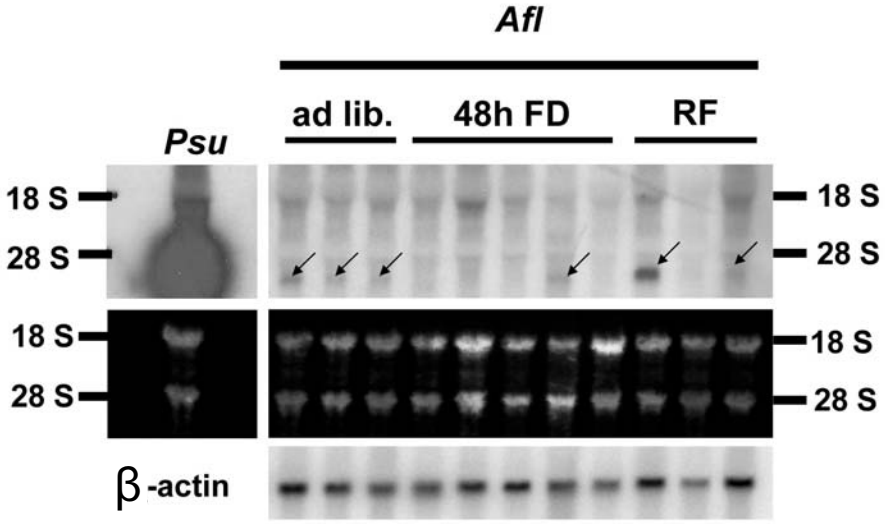

Fig. 2: Northern blot of skeletal muscle from fed, fasted, and refed A. flavipes. *Twenty micrograms of total RNA were analysed by Northern blotting with a rat UCP1 cDNA probe, as well as a mouse UCP2 and* β*-actin probe. Arrows indicate the apparent detection of marsupial UCP1. Afl:* Antechinus flavipes, *Psu:* Phodopus sungorus, *ad lib.:* ad libitum, *FD: food-deprived for 48 hours, RF: refed for 24 hours.*

led to successful PCR amplification of a marsupial UCP3 cDNA fragment. Notably, the full-length marsupial UCP3 cDNA probe did not hybridize with hamster UCP3 mRNA on Northern blots of total skeletal muscle RNA, whereas a clear albeit weaker hybridization signal was observed probing hamster spleen RNA with the marsupial UCP2 cDNA (Jastroch et al., 2004). This illustrates the limitations of heterologous hybridization assays in the search for orthologues in distantly related species.

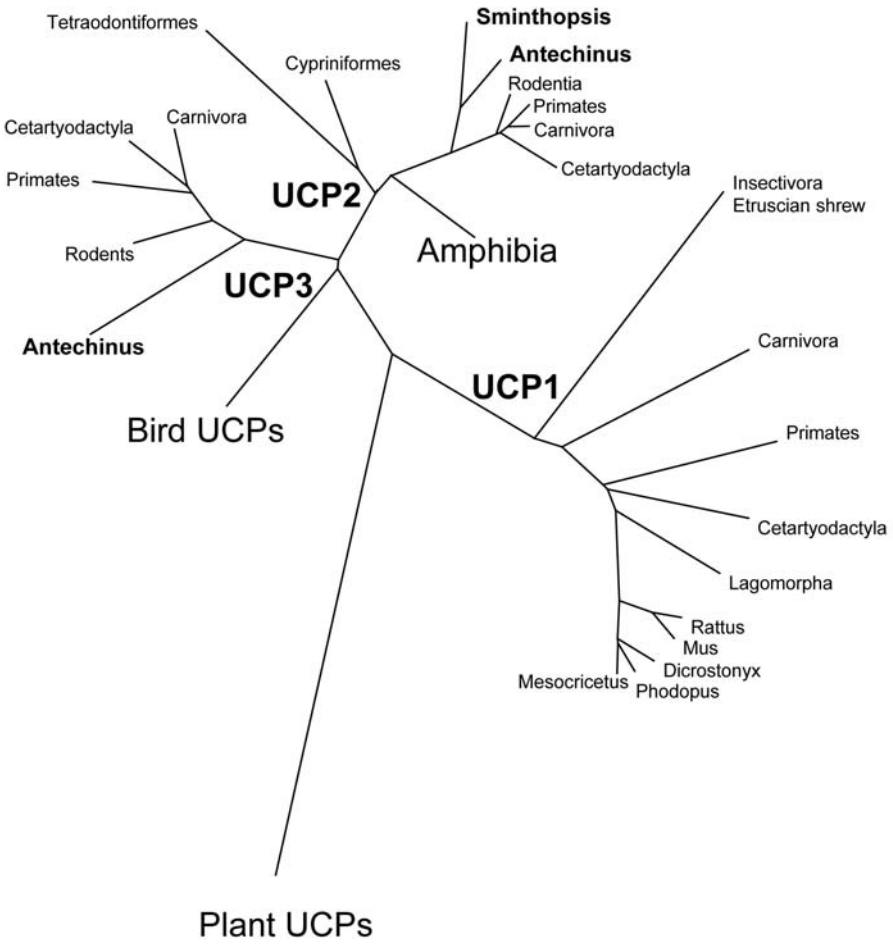

Fig. 3: Unrooted phylogenetic tree of the core UCP family using the neighbor-joining method.

Knowing this, we definitely cannot conclude that nonplacental mammals lack the UCP1 gene. We speculate that the search for marsupial UCP1 was not successful yet, since the sequence similarity to eutherian UCP1 can be expected to be rather low. Even within eutherian mammals, the comparison of UCP1 orthologues from phylogenetic distant taxa, as exemplified by comparison of Etruscan shrew UCP1 and mouse UCP1, reveals only 75% global identity (based on 245 amino acids known from shrew). Klaus and colleagues reported that the signal intensity for Etruscan shrew UCP1 mRNA is strongly diminished when using a heterologous rodent probe for hybridization analysis (Klaus et al., 1996). This indicates a rapid evolution of this protein within the eutherian infraclass and certainly complicates straightforward attempts to identify the eutherian orthologue of UCP1 in nonplacental mammals.

Despite these theoretical considerations, we screened multiple tissues sampled from fed, fasted, and refed *A. flavipes* by Northern blot analysis for the presence of UCP1 mRNA with a full-length radio-labelled rat UCP1 cDNA probe. Surprisingly, in skeletal muscle of several individuals we observed a barely detectable hybridization signal when Northern blots were washed at low stringency (indicated by arrows in Fig. 3). This apparent detection of marsupial UCP1 mRNA in skeletal muscle did not depend on feeding state and may rather be related to life history of the animals or variation in tissue sampling. Rehybridization of the same blot with UCP2 and UCP3 definitely excluded possible cross-hybridization, as judged from transcript size. Screening of skeletal muscle cDNA libraries will reveal whether the detected transcript indeed represents marsupial UCP1.

Regarding the phylogenetic tree of all known UCPs, it is well possible that UCP1 not only occurs in placental mammals. Using different outgroups, e.g., plant UCPs (Fig. 3), brain mitochondrial carrier protein (BMCP1), or the oxalacetate-malate carrier, the branching of UCP1 occurs at least at the evolutionary stage of modern teleost fish. Thus, UCP1 and UCP3 may also be found in ectothermic vertebrates unless these genes went extinct in the living species.

Orthologues are defined as proteins sharing common ancestry and function. However, if an uncoupling protein gene sharing a common ancestor with mammalian UCP1 does exist in ectothermic vertebrates, a global thermogenic function appears unlikely. The thermogenic function may rather represent a new property of UCP1 that evolved in the mammalian lineage. Despite the fact that UCP1 is regarded as a marker protein for brown adipose tissue in eutherian mammals, the expression of this protein if present might not be restricted to

adipose tissue in nonplacental mammals and ectothermic vertebrates. Notably, an involvement of UCP1 in intestinal relaxation was suggested by a study in UCP1-ablated mice (Shabalina et al., 2002), adding to the ongoing discussion as to whether the UCP1 gene is also expressed in smooth longitudinal muscle of rodents (Nibbelink et al., 2001; Rousset et al., 2003).

We therefore conclude that the search for UCP1 in nonplacental mammals has to be intensified on the molecular level.

Acknowledgements

This study was funded by the Deutsche Forschungsgemeinschaft (KL 973/7). We are grateful to Lawrence Slieker (Eli Lilly) for providing the UCP3 antibody and to Dr. Geoff Lundie Jenkins from Queensland Parks and Environment Australia. M. Jastroch is supported by the International Max Planck Research School in Marburg.

Reference List

Boss O, Samec S, Paolonigiacobino A, Rossier C, Dulloo AG, Seydoux J, Muzzin P, Giacobino JP (1997) Uncoupling protein-3: A new member of the mitochondrial carrier family with tissue-specific expression. *FEBS Lett* 408: 39–42.

Brander F, Keith JS, Trayhurn P (1993) A 27-mer oligonucleotide probe for the detection and measurement of the mRNA for uncoupling protein in brown adipose tissue of different species. *Comp Biochem Physiol B* 104(1):125–31.

Cannon B, Nedergaard J (2004) Brown adipose tissue: Function and physiological significance. *Physiol Rev* 84:277–359.

Enerbäck S, Jacobsson A, Simpson EM, Guerra C, Yamashita H, Harper ME, Kozak LP (1997) Mice lacking mitochondrial uncoupling protein are cold-sensitive but not obese. *Nature* 387:90–94.

Evock-Clover CM, Poch SM, Richards MP, Ashwell CM, McMurtry JP (2002) Expression of an uncoupling protein gene homolog in chickens. *Comp Biochem Physiol A Mol Integr Physiol* 133(2):345–58.

Fleury C, Neverova M, Collins S, Raimbault S, Champigny O, Levi-Meyrueis C, Bouillaud F, Seldin MF, Surwit RS, Ricquier D, Warden CH (1997) Uncoupling protein-2: A novel gene linked to obesity and hyperinsulinemia. *Nat Genet* 15:269–272.

Heldmaier G (1971) Zitterfreie Wärmebildung und Körpergröβe bei Säugetieren. *Z vergl Physiol* 73:222–248.

Himms-Hagen J, Harper ME (2001) Physiological role of UCP3 may be export of fatty acids from mitochondria when fatty acid oxidation predominates: An hypothesis. *Exp Biol Med (Maywood)* 226:78–84.

Hope PJ, Pyle D, Daniels CB, Chapman I, Horowitz M, Morley JE, Trayhurn P, Kumaratilake J, Wittert G (1997) Identification of brown fat and mechanisms for energy balance in the marsupial, *Sminthopsis crassicaudata. Amer J Physiol-Regul Integr C* 42:R161–R167.

Jastroch M, Withers K, Klingenspor M (2004) Uncoupling protein 2 and 3 in marsupials: Identification, phylogeny and gene expression in response to cold and fasting in *Antechinus flavipes. Physiol Genomic* 17:130–139.

Kabat AP, Rose RW, West AK (2003) Nonshivering thermogenesis in a carnivorous marsupial *Sarcophilus harrisii,* in the absence of UCP1. *J Thermal Biol* 28:413–420.

Klaus S, Raimbault S, Bouillaud F, Ricquier D, Gessner M, Jürgens KD (1996) Sequence of the brown adipose tissue specific uncoupling protein UCP from the Etruscan shrew (*Suncus etruscus*). In Geiser F, Hulbert AJ, Nicol SC (eds), *Adaptations to the Cold: Tenth International Hibernation Symposium*, Armidale: University of New England Press. Pp. 293–298.

Klingenspor M (2003) Cold-induced recruitment of brown adipose tissue thermogenesis. *Exp Physiol* 88:141–148.

Loncar D, Afzelius, BA, Cannon B (1988) Epididymal white adipose tissue after cold stress in rats. *J Ultrastr Molecul Struct Res* 101:199–209.

Loudon ASI, Rothwell NJ, Stock MJ (1985) Brown fat, thermogenesis and physiological birth in a marsupial. *Comp Biochem Physiol* 81A:815–819.

Mills EM, Banks ML, Sprague JE, Finkel T (2003) Pharmacology: uncoupling the agony from ecstasy. *Nature* 426:403–404.

Nedergaard J, Cannon B (2003) The "novel" "uncoupling" proteins UCP2 and UCP3: What do they really do? Pros and cons for suggested functions. *Exp Physiol* 88:65–84.

Nibbelink M, Moulin K, Arnaud E, Duval C, Penicaud L, Casteilla L (2001) Brown fat UCP1 is specifically expressed in uterine longitudinal smooth muscle cells. *J Biol Chem* 276:47291–47295.

Raimbault S, Dridi S, Denjean F, Lachuer J, Couplan E, Bouillaud F, Bordas A, Duchamp C, Taouis M, Ricquier D (2001) An uncoupling protein homologue putatively involved in facultative muscle thermogenesis in birds. *Biochem J* 353:441–444.

Rolfe DFS, Brown GC (1997) Cellular energy utilization and molecular origin of standard metabolic rate in mammals. *Physiol Rev* 77:731–758.

Rose RW, West AK, Ye JM, McCormick GH, Colquhoun EQ (1999) Nonshivering thermogenesis in a marsupial (the Tasmanian bettong *Bettongia gaimardi*) is not attributable to brown adipose tissue. *Physiol Biochem Zool* 72: 699–704.

Rousset S, Alves-Guerra MC, Ouadghiri-Bencherif S, Kozak LP, Miroux B, Richard D, Bouillaud F, Ricquier D, Cassard-Doulcier AM (2003) Uncoupling protein 2, but not uncoupling protein 1, is expressed in the female mouse reproductive tract. *J Biol Chem* 278:45843–45847.

Schrauwen P, Hoeks J, Schaart G, Kornips E, Binas B, Van De Vusse GJ, Van Bilsen M, Luiken JJ, Coort SL, Glatz JF, Saris WH, Hesselink MK (2003) Uncoupling protein 3 as a mitochondrial fatty acid anion exporter. *FASEB J* 17:2272–2274.

Shabalina I, Wiklund C, Bengtsson T, Jacobsson A, Cannon B, Nedergaard J (2002) Uncoupling protein-1: Involvement in a novel pathway for beta-adrenergic, cAMP-mediated intestinal relaxation. *Am J Physiol Gastrointest Liver Physiol* 283:G1107–G1116.

Stuart JA, Harper JA, Brindle KM, Brand MD (1999) Uncoupling protein 2 from carp and zebrafish, ectothermic vertebrates. *Biochim Biophys Acta* 1413: 50–54.

Physiol Genomics 22: 150–156, 2005.
First published May 10, 2005; 10.1152/physiolgenomics.00070.2005.

CALL FOR PAPERS | *Comparative Genomics*

Uncoupling protein 1 in fish uncovers an ancient evolutionary history of mammalian nonshivering thermogenesis

Martin Jastroch,[1] Sven Wuertz,[2] Werner Kloas,[2] and Martin Klingenspor[1]

[1]*Department of Animal Physiology, Biology Faculty, Philipps-University Marburg, Marburg; and* [2]*Department of Inland Fisheries, Leibniz-Institute of Freshwater Ecology and Inland Fisheries, Berlin, Germany*

Submitted 23 March 2005; accepted in final form 5 May 2005

Jastroch, Martin, Sven Wuertz, Werner Kloas, and Martin Klingenspor. Uncoupling protein 1 in fish uncovers an ancient evolutionary history of mammalian nonshivering thermogenesis. *Physiol Genomics* 22: 150–156, 2005. First published May 10, 2005; 10.1152/physiolgenomics.00070.2005.—Uncoupling proteins (UCPs) increase proton leakage across the inner mitochondrial membrane. Thereby, UCP1 in brown adipose tissue dissipates proton motive force as heat. This mechanism of nonshivering thermogenesis is considered as a monophyletic trait of endothermic placental mammals that emerged about 140 million years ago and provided a crucial advantage for life in the cold. The paralogues UCP2 and UCP3 are probably not thermogenic proteins but convey mild uncoupling, which may serve to reduce the rate of mitochondrial reactive oxygen species production. Both are present in endotherms (mammals and birds), but so far only UCP2 has been identified in ectothermic vertebrates (fish and amphibia). The evolution of UCPs is of general interest in the search for the origin of mammalian UCP1-mediated nonshivering thermogenesis. We here show the presence of UCP1 and UCP3 in ectothermic teleost fish species using comparative genomics, phylogenetic inference, and gene expression analysis. In the common carp (*Cyprinus carpio*), UCP1 is predominantly expressed in the liver and strongly diminished in response to cold exposure, thus contrasting the cold-induced expression of mammalian UCP1 in brown adipose tissue. UCP3 mRNA is only found in carp skeletal muscle with expression levels increased fivefold in response to fasting. Our findings disprove the monophyletic nature of UCP1 in placental mammals and demonstrate that all three members of the core UCP family were already present before the divergence of ray-finned and lobe-finned vertebrate lineages about 420 million years ago.

proton leak; brown adipose tissue; common carp; uncoupling protein 2; uncoupling protein 3

IN BROWN ADIPOCYTES, thermogenic uncoupling protein (UCP)1 increases proton leakage of the mitochondrial inner membrane and thereby dissipates proton motive force as heat (23). UCP1-mediated proton leakage is activated by fatty acids and inhibited by purine nucleotides. This molecular mechanism catalyzes nonshivering thermogenesis in newborns, small mammals, and hibernators. The biological role of UCP2 and UCP3 is controversial. There is speculation on the involvement of UCP3 in skeletal muscle thermogenesis of mammals and birds (21, 36), whereas others address the function of UCP3 to the export of redundant fatty acids from the mitochondrial matrix (15, 33). Several physiological functions have been proposed for UCP2 including the regulation of ATP-to-ADP ratios in pancreatic β-cells (42) or the modulation of reactive oxygen species production in the defence system of macrophages (19, 22). In fact, all members of the core UCP family are activated by superoxides and/or carbon-centerd radicals conveying mild uncoupling, which through prevention of reverse electron transfer may function to diminish endogenous superoxide production in the mitochondrial matrix (11, 12, 36). It has been suggested recently that this mild uncoupling could be the original ancient function of UCPs serving to protect cells against oxidative damage (7). Verification of this hypothesis requires the identification and comparative functional analysis of UCPs in phylogenetically ancient vertebrates.

The evolution of UCPs and their contribution to proton leak-dependant adaptive nonshivering thermogenesis are of general interest as this invention may have facilitated the development of endothermy. Evidence for nonshivering thermogenesis in vertebrates other than placental mammals, e.g., birds (10) and marsupials (30), as well as in brain heater cells of the billfish and butterfly mackerel (3), has been reported. In the billfish and butterfly mackerel, nonshivering thermogenesis in brain heater cells is responsible for cranial endothermy, but the involvement of UCPs could not be proven by immunodetection with heterologous antibodies (2). In nonplacental mammals, physiological evidence for and against nonshivering thermogenesis was found (24), but neither morphological nor molecular proof for the existence of brown adipose tissue and UCP1 could be found (14, 17, 18). Therefore, it was concluded that brown adipose tissue and UCP1 evolved about 140 million years ago in placental mammals, providing them with the crucial advantage to maintain high body temperature in the cold (4, 8). Pertaining to UCP3, of which the physiological function remains to be resolved, orthologues have so far been identified in endotherms, including marsupials (17), placentals (5), and birds (28, 39), but not in ectothermic vertebrates.

Here, we demonstrate that all three UCPs are already present at the evolutionary stage of ectothermic teleost fish. As exemplified in the common carp (*Cyprinus carpio*), gene expression of UCP1 and UCP3 is regulated in response to cold and fasting in a tissue-specific manner.

MATERIALS AND METHODS

Phylogenetic inference and comparative genomics. We conducted a comprehensive search for *Ucp* genes by blasting zebrafish (*Danio rerio*) and pufferfish (*Fugo rubripes*) genomes with full-length coding se-

Article published online before print. See web site for date of publication (http://physiolgenomics.physiology.org).

Address for reprint requests and other correspondence: M. Klingenspor, Philipps-Univ. Marburg, Biology Faculty, Dept. of Animal Physiology, Karl-von-Frisch-Strasse 8, 35043 Marburg, Germany (E-mail: klingens@staff.uni-marburg.de).

quences of mammalian UCPs (Ensembl Genome Browser, http://www.ensembl.org). To verify the membership of identified candidates to the core UCP family, the predicted protein sequences of putative fish UCPs were aligned [ClustalX, ftp://ftp-igbmc.u-strasbg.fr/pub/ClustalX/ (37)] together with all known UCP protein sequences available in public databases and subjected to phylogenetic inference using the Neighbour joining method (Felsenstein J. *PHYLIP Phylogeny Inference Package version 3.6.* Distributed by the author. Seattle, WA: Univ. of Washington, 2004. http://evolution.genetics.washington.edu/phylip.html). Bootstrapping involved 1,000 replicates, and the consensus tree was illustrated using TreeView (http://taxonomy.zoology.gla.ac.uk/rod/treeview.html). Physical gene maps of verified *Ucp* loci were scaled based on assemblies of the Ensembl Genome Browser (http://www.ensembl.org). Genes located up- and downstream of *Ucp* genes in these loci were blasted against mammalian genomes for the highest score.

Cold acclimation and fasting of the common carp. Six-month-old common carps (*C. carpio*) provided by the Department of Inland Fisheries (Berlin, Germany) were kept under a natural photoperiod (September to October) in 0.13-m^3 tanks (water exchange rate: 1.5 vol/h). They were fed ~0.5% of their body weight per day and acclimated to water temperatures of 8 and 20°C for 4 wk. A fourth group was kept at 20°C, and food was deprived for 4 wk. Animals were killed, and tissues were dissected and immediately snap frozen in liquid nitrogen. Animal care and performance of experiments were approved by the Institutional Animal Care and Use Committees of IGB (Leibniz-Institut für Gewässerökologie und Binnenfisherei, Berlin, Germany) and the LaGetSi (Landesamt für Gesundheit und technische Sicherheit, Berlin, Germany).

RT-PCR amplification and cDNA library screening. To study gene expression, all three UCP cDNAs of the common carp (*C. carpio*) were cloned. RNA was isolated from the liver (UCP1), spleen (UCP2), and skeletal muscle (UCP3) and used for first-strand synthesis (SuperScript II, GIBCO-BRL) according to the manufacturer's protocol. Consensus PCR primers for UCP1 (forward 5′-ATCGGCCTCTACGACAACGTCAA-3′ and reverse 5′-ACCAGTTCTGTGCAGTTGACCAG-3′) and UCP3 (forward 5′-GGCACCATCACCACTATGGTTCG-3′ and reverse 5′-CAATCGTGGTGCAGAAACCAGCG-3′) were generated on the basis of zebrafish and pufferfish genes, whereas PCR primers for UCP2 (forward 5′-GTTTCTCTATGGAAGAACGCGG-3′ and reverse 5′-TGCTTAAAGAGGAGTGGCCCAG-3′) were deduced from the published carp sequence (35).

The PCR cycler was programmed to 40 cycles of denaturation at 94°C (1 min), annealing at 58°C (1 min), and extension at 72°C (2 min), followed by a final extension for 10 min at 72°C and rapid cooling to 4°C. A cDNA library (Zap Express XR Library Construction Kit, catalog no. 200451, Stratagene; La Jolla, CA) was generated from the carp liver and screened with the RT-PCR product obtained with the UCP1 primers (300 bp). RNA was extracted from tissues of the common carp (*C. carpio*), quantified photometrically, and blotted and hybridized as described before (17). A 1,512-bp UCP1 cDNA (Genbank Accession No. AY461434) as well as a 1,141-bp UCP2 and 490-bp UCP3 (Genbank Accession No. AY505343) PCR fragment served as templates for Northern blot analysis. Signals were quantified by phosphor imaging and normalized to 18S rRNA expression as a loading control.

RESULTS

Genomic identification of UCP1, UCP2, and UCP3 in teleost fish. In the search for UCP orthologues in the animal kingdom, heterologous hybridizations are not applicable due to limited gene conservation (16). Therefore, the nearly completed genome projects of the zebrafish (*D. rerio*) and pufferfish (*F. rubripes*) were searched for the presence of UCP genes. In addition to *Ucp2*, which has been previously identified in fish expressed sequence tag (EST) libraries (35), we discovered two novel *Ucp*-like genes in the databases of both teleost genomes. On the amino acid level, their intraspecific identities with zebrafish UCP2 were 68% and 74%, respectively.

To elucidate the relationship of these novel *Ucp*-like genes to the known mammalian orthologues, we compared their genomic location in mammals and fish. Pertaining to mammalian *Ucp1*, an identical order of neighboring genes is seen, thereby demonstrating a region of conserved synteny within the mammalian lineage (Fig. 1). Surprisingly, this region of conserved synteny is also found in the genomes of the zebrafish and pufferfish and encloses one of the novel fish *Ucp* genes. On zebrafish chromosome 1, a region spanning ~50 kb contains this novel *Ucp* gene flanked by *gene A* (ENSDART00000026397) and *gene B* (ENSDART00000034884), of which orthologous counterparts also neighbor *Ucp1* in mammals (Fig. 1). Therefore, this *Ucp* gene is unequivocally identified as the *Ucp1* orthologue in fish.

The second novel *Ucp*-like gene is located in direct vicinity of the zebrafish *Ucp2* gene resembling the juxtaposition of *Ucp2* and *Ucp3* in the human and mouse (26), rat (www.ensembl.org), and bovine (34). Furthermore, homologous genes neighboring the *Ucp2–Ucp3* cluster were also conserved in both mammalian and fish genomes, forming a region of conserved synteny (Fig. 1). Therefore, the second novel *Ucp* is annotated as the *Ucp3* orthologue in fish.

Phylogenetic inference. UCP1 and UCP3 protein sequences were deduced from the respective genes identified in the zebrafish and pufferfish (www.ensembl.org). The intraspecific identity of UCP1 to UCP2 and UCP3 is 68% and 71%, respectively, whereas the identity of UCP2 to UCP3 amounts to 74%. In cross-species alignments of UCPs, we highlighted regions of particular interest previously identified by the study of structure-function relationships (Fig. 2). Phylogenetic inference definitely grouped all three proteins into the core UCP family and positioned UCP2 within the respective vertebrate orthologues (Fig. 3). However, despite the unambigious annotation of fish UCP1 and UCP3 based on conserved synteny, the phylogenetic relationship to their respective orthologues within the UCP core family could not be resolved (Fig. 3).

Regulation of gene expression. To investigate tissue-specific expression as well as the regulation in response to cold exposure and fasting, we cloned cDNAs of all three UCPs in the common carp (*C. carpio*). RT-PCR amplified a 300-bp UCP1 fragment from liver cDNA, a 490-bp UCP3 fragment from skeletal muscle cDNA, and a 1,141-bp UCP2 fragment from spleen cDNA. These PCR products were cloned into pGEM-T-easy (Promega) and sequenced. The UCP1 cDNA fragement served to screen the carp liver cDNA library. UCP2 and UCP3 cDNAs were directly used to generate probes for Northern blot analysis.

We demonstrated differential tissue-specific mRNA expression patterns of the three UCPs in the carp (Fig. 4*A*). Multiple-tissue Northern blot analysis revealed preferential expression of carp UCP1 mRNA in metabolically active tissues, with highest levels in the liver, moderate levels in the brain and functional kidneys (meso- and metanephros), and lowest levels in the intestine. Carp UCP3 mRNA is exclusively expressed in skeletal muscle, with higher levels observed in red (oxidative) compared with white (glycolytic) muscle. UCP2 mRNA was found in all tissues included in the analysis, with the highest expression levels found in blood cells, the intestine, and gills.

For further physiological characterization of carp UCP1 and UCP3, we investigated the regulation of gene expression. In mammals, UCP1 gene expression in brown adipose tissue (BAT)

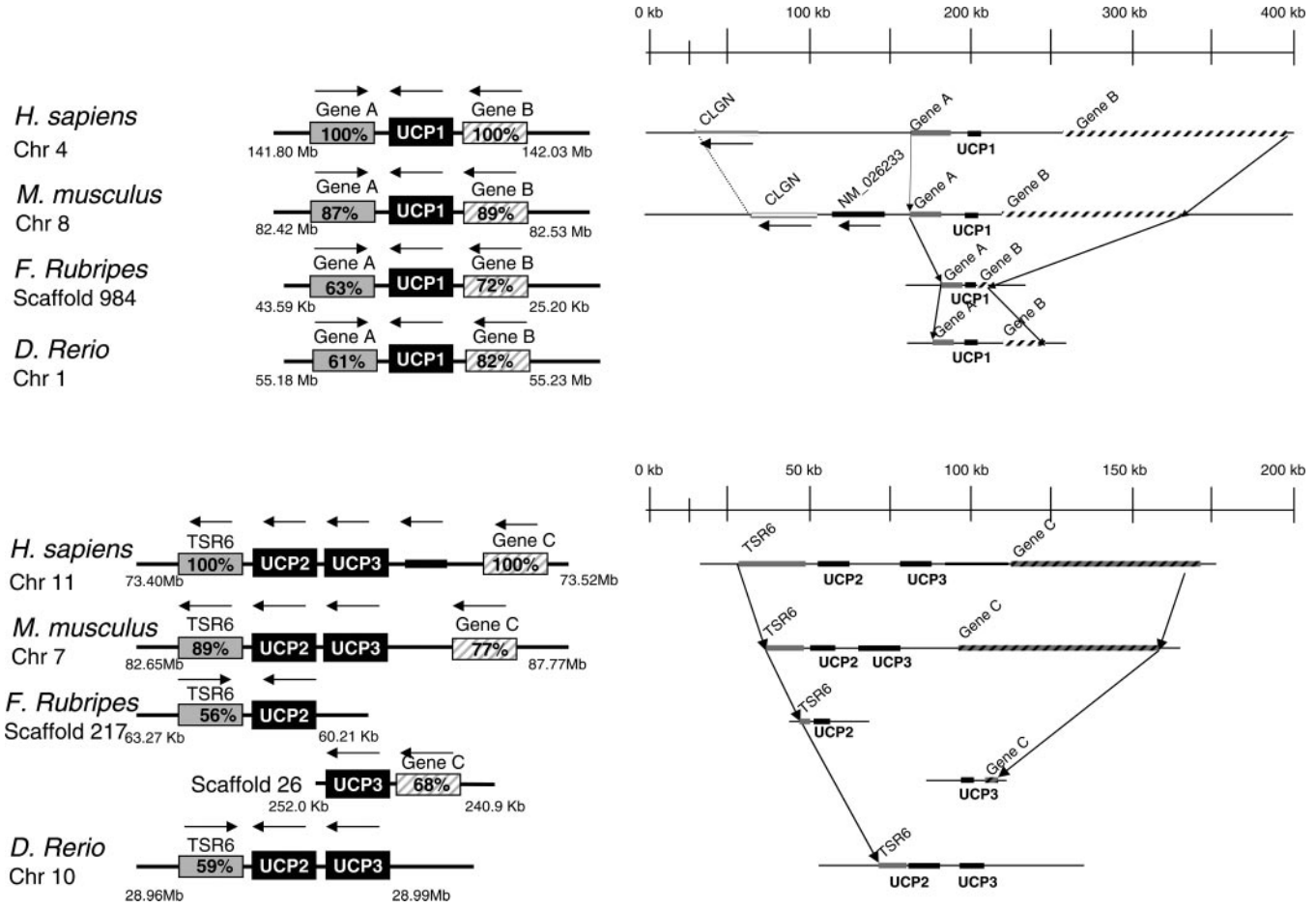

Fig. 1. Schematic (*right*) and physical gene maps (*left*) of the conserved syntenic regions of the uncoupling protein (UCP) 1, 2, and 3 genes (*Ucp1*, *Ucp2*, and *Ucp3*, respectively) in the genomes of the human (*Homo sapiens*), mouse (*Mus musculus*), pufferfish (*Fugu rubripes*), and zebrafish (*Danio rerio*). *Ucp* genes are shown as solid boxes, and gene orientations are indicated by arrows. The protein identity of *Ucp* neighbours is calculated as a percentage of the human orthologues. *Top*: conserved synteny at the *Ucp1* locus. Orthologues of *gene A* in *H. sapiens* (NM_153702), *M. musculus* (NM_178736), *F. rubripes* (SINFRUT00000155541), and *D. rerio* (ENSDART00000026397) are shown as shaded boxes; orthologues of *gene B* in *H. sapiens* (094958), *M. musculus* (NM_027758), *F. rubripes* (SINFRUT00000173715), and *D. rerio* (ENSDART00000034884) are shown as hatched boxes. *Bottom*: conserved synteny at the *Ucp2-Ucp3* locus. *TSR6* orthologues are shown as shaded boxes; orthologues of *gene C* in *H. sapiens* (Q8NDH7), *M. musculus* (Q8BXE5), and *F. rubripes* (SINFRUT00000136711) are shown as hatched boxes. *Right*: physical gene distances referring to the Ensembl genome browser (www.ensembl.org). Chr, chromosome; TSR6, testis spermatocyte apoptosis-related gene 6 protein; CLGN, calmegin.

is induced in the cold, whereas UCP3 mRNA levels in skeletal muscle and the heart are elevated in the fasted state. Therefore, cold exposure and fasting were chosen as the physiological stimuli most likely to affect UCP1 and UCP3 gene expression in the carp. In the liver, UCP1 mRNA levels were almost diminished in carp transferred from 20 to 8°C for either 2 days or 4 wk (Fig. 4*B*). In contrast, UCP1 mRNA levels in the kidneys were not affected by cold exposure (ANOVA on ranks, $P > 0.3$; data not shown).

UCP3 gene expression in skeletal muscle was not affected by cold. However, in response to 4 wk of fasting, UCP3 mRNA levels in glycolytic white skeletal muscle increased fivefold (Fig. 4*B*). No systematic effect of fasting on UCP1 gene expression in the liver and kidneys was observed (data not shown).

DISCUSSION

In the present study, we localized all three members of the core *Ucp* gene family in zebrafish and pufferfish genomes by comparative genomics and demonstrate tissue-specific regulation of their gene expression in the common carp (*C. carpio*). Our comprehensive search for *Ucp* genes initially corroborated the presence of the *Ucp2* gene in fish, as expected from the previous identification of UCP2 cDNA in EST libraries from carp (*C. carpio)* and zebrafish (*D. rerio)* (35). However, our search also revealed two novel *Ucp* genes, which were identified as new members of the core UCP family by phylogenetic inference. On the basis of conserved synteny, these novel *Ucp* genes were unequivocally annotated as *Ucp1* and *Ucp3* (Fig. 1). This comparative analysis of *Ucp* loci in different species illustrates the utility of syntenic relationships (1, 27, 41).

UCP1 plays a key role in nonshivering thermogenesis and was previously regarded as a monophyletic trait of placental mammals only expressed in brown adipose tissue (8). Moreover, UCP3, of which the physiological function remains to be resolved, has so far only been identified in marsupials (17) and placental mammals (5) as well as in birds (28, 39). The presence of all three *Ucp* genes in ectothermic fish, including *Ucp1*, is therefore unexpected and indicates an ancient evolutionary divergence of the core UCP family.

To further characterize the fish *Ucp* genes, we cloned the respective cDNAs from the common carp (*C. carpio*) and investigated tissue-specific expression as well as regulation in response to cold and fasting. We demonstrated that tissue distribution of UCP1 mRNA in fish is broader than in placental mammals occurring in metabolically active tissues like the liver, kidney, brain, and intestine but notably not in adipose tissue (Fig. 4*A*). In cold-exposed carp, UCP1 mRNA was

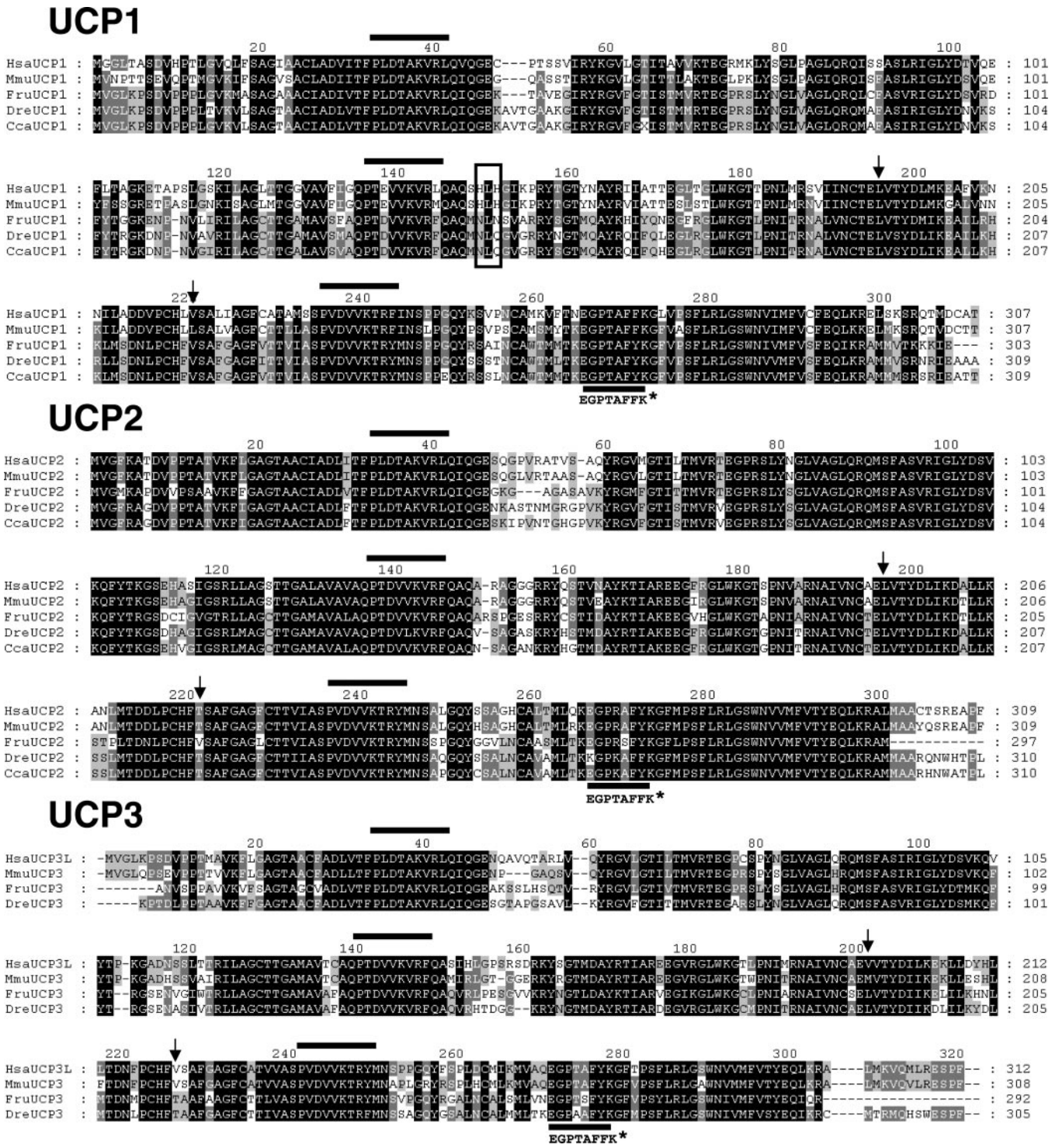

Fig. 2. Amino acid sequence alignments of UCP1, UCP2, and UCP3. Sequences from *H. sapiens* (Hsa), *M. musculus* (Mmu), *F. rubripes* (Frau), *D. rerio* (Dre), and *Cyprinus carpio* (Cca) were aligned using ClustalX 1.81 (ftp://ftp-igbmx.u-strasbg.fr/pub/ClustalX) and illustrated with Genedoc 2.601 (http://www.psc.edu/biomed/genedoc/). Most conserved amino acids are highlighted in black, with less conserved amino acids shown with a brighter background. Arrows indicate amino acids involved in pH sensing of the nucleotide binding (20). Positions of two histidins, putatively involved in the proton transport of mammalian UCP1, are boxed. Solid bars above the alignment indicate the energy transfer protein signature; the solid bar below the alignment indicates the position of a potential nucleotide binding domain (*) found in UCP1 (6).

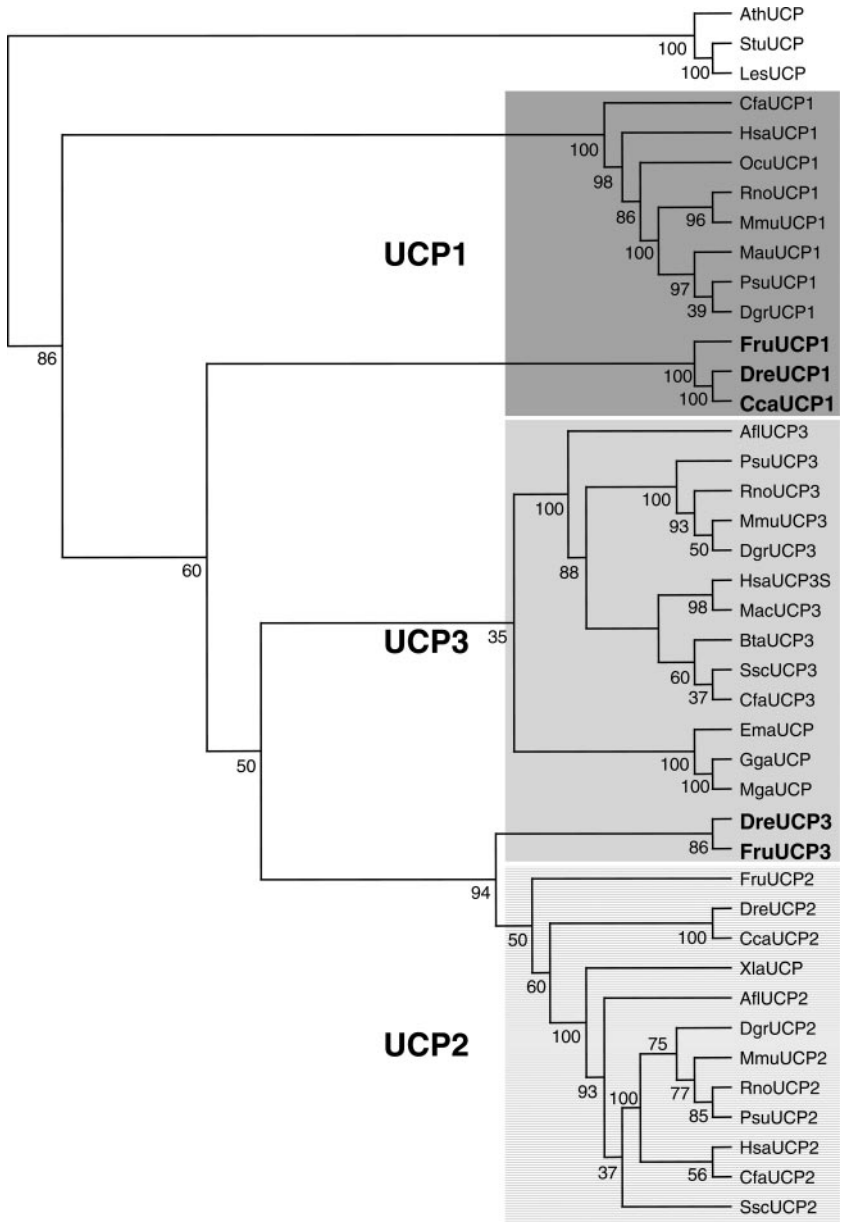

Fig. 3. Phylogenetic neighbor joining tree of the UCP core family. Bootstrap values from 1,000 replicates are given next to the internal branches. The plant UCPs served as distantly related outgroup. Complete protein sequences were used. Afl, *Antechinus flavipes*; Ath, *Arabidopsis thaliana*; Bta, *Bos taurus*; Cca: *C. carpio*; Cfa, *Canis familiaris*; Dgr, *Dicrostonix groenlandicus*; Dre, *D. rerio*; Ema, *Eupetomena macroura*; Fru, *F. rubripes*; Gga, *Gallus gallus*; Has, *H. sapiens*; Les, *Lycopersicon esculentum*; Mac, *Macaca mulatto*; Mau, *Mesocricetus auratus*; Mga, *Meleagris gallopavo*; Mmu, *M. musculus*; Ocu, *Oryctolagus cuniculus*; Psu, *Phodopus sungorus*; Rno, *Rattus norvegicus*; Ssc, *Sus scrofa*; Stu, *Solanum tuberosum*; Xla, *Xenopus laevis*.

almost diminished in the liver, whereas expression levels remained unaffected in the kidney. The cold-induced downregulation in the liver was a rapid event as minimal expression levels were attained after 2 days and maintained in carp cold acclimated for 4 wk. This may serve to increase coupled respiration and efficiency of ATP synthesis and could be one mechanism by which the carp reduces metabolic rate and saves chemical energy at low water temperatures.

The evolution of UCPs is of major interest in the attempt to trace the origin of UCP1-mediated nonshivering thermogenesis in placental mammals. Physiological evidence for nonshivering thermogenesis in birds (10), marsupials (30), and billfish (3) has been reported, but either the involvement of UCPs could not be proven or experimental data suggest alternative thermogenic mechanisms. Given the presence of a UCP1 orthologue at the evolutionary level of fish, we must now conclude that the common ancestors of ray-finned and lobe-finned vertebrates already disposed of this gene about 420 million years ago. Consequently, the presence of UCP1-mediated nonshivering thermogenesis in all endothermic vertebrates has to be reconsidered. In this respect, the observed conserved synteny in the *Ucp1* locus and the high sequence identity of one neighboring gene (*gene B* in Fig. 1, *top*) in fish and mammals should facilitate the identification of UCP1 orthologues in other vertebrate classes. Alternatively, the ancient *Ucp1* gene may have provided the raw material to develop thermogenic UCP1 in mammals but went extinct in other vertebrate classes.

All known UCP1 orthologues catalyze a net proton translocation, and there is evidence that UCP2, UCP3, and plant UCP increase proton leakage (9, 12), but for fish UCP1 experimental data demonstrating this function are lacking at the present state. Most teleosts, like the carp, are ectotherms not able to raise and maintain their body temperature significantly above water temperature by endogenous heat production. It is therefore evident that in most fishes UCP1 does not serve as a

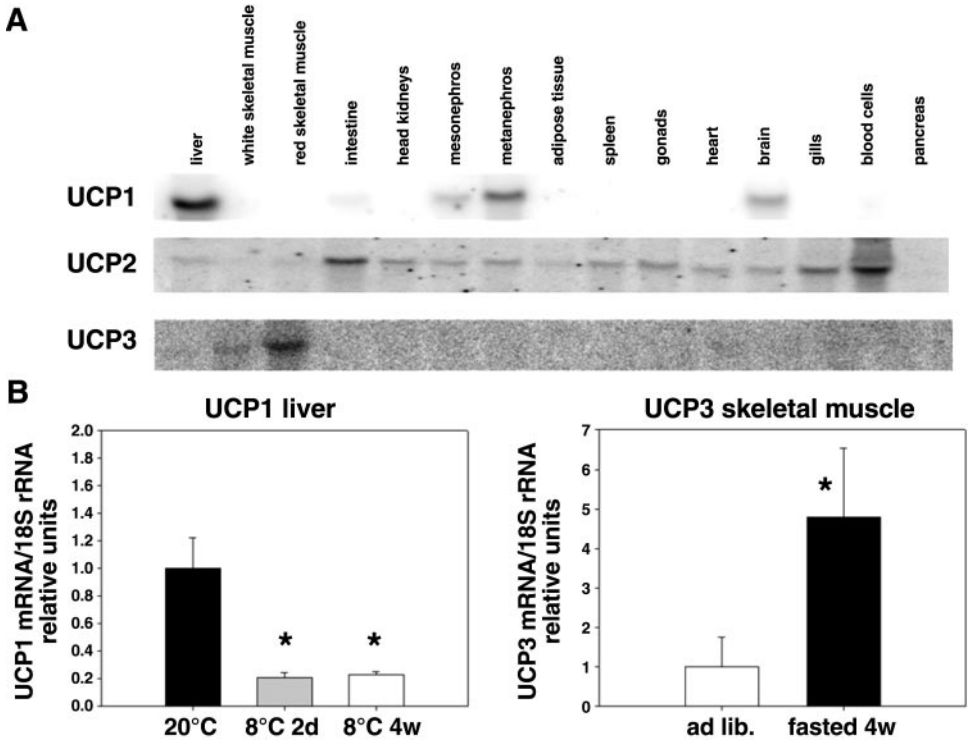

Fig. 4. Regulation of carp UCP gene expression. *A*: Northern blot showing tissue-specific expression of UCP1, UCP2, and UCP3. Twenty micrograms of total RNA were hybridized with homologous UCP probes. *B*: UCP1 mRNA expression levels in response to cold (liver; *left*) and UCP3 mRNA expression levels in response to fasting (skeletal muscle; *right*). Radioactive intensities of specific signals are shown as relative units. Each group consisted of five carps. Ad libitum (ad lib.)-fed carps were either acclimated to 20°C or exposed to 8°C for 2 days (2d) and 4 wk (4w) or fasted at 20°C for 4 wk (fasted 4w). The effect of cold acclimation on liver UCP1 mRNA was evaluated by ANOVA on ranks ($P < 0.01$) followed by the Tukey test for multiple comparisons. *Significant difference compared with 20°C ad libitum-fed group ($P < 0.05$). The effect of fasting on skeletal muscle UCP3 mRNA was confirmed by Student's *t*-test. *$P <$ 0.01.

thermogenic protein defending elevated core body temperature. However, cranial endothermy has been reported in several species including the billfish (swordfish, sailfish, and blue marlin, *Xiphiidae* and *Istiophoridae*) as well as the butterfly mackerel (*Scombridae)* (3).These endothermic fish possess a brain heater organ, which is derived from extraocular muscles and warms the brain and the eye up to 20°C above water temperature. Previous biochemical studies indicated that the underlying thermogenic mechanism in the modified muscle cells of the brain heater may utilize the free energy of ATP for futile calcium cycling across the sarcoplasmic reticulum membrane, thereby enabling high rates of mitochondrial respiration and energy dissipation as heat. Immunological studies have questioned the presence of UCP in heater cells, but, obviously, this issue now has to be reinvestigated (2). Notably, we detected UCP1 mRNA in the brain of the carp. The presence and thermogenic function of UCP1 in neuronal tissue or directly in brain heater cells of the billfish and butterfly mackerel would cast a new light on the evolution of nonshivering thermogenesis in vertebrates.

UCP2 gene expression in the carp is ubiquitous, reflecting the situation in marsupials (17) and placentals (5, 13, 40). Interestingly, carp UCP3 gene expression was restricted to skeletal muscle, resembling the tissue specificity of mammalian UCP3. The observed preferential expression of UCP3 in red oxidative muscle in the carp may be related to the higher mitochondrial content of this fiber type. Conversely, in ad libitum-fed rats, no significant difference in UCP3 mRNA was reported when soleus (oxidative) and gastrocnemius (glycolytic) muscle were compared (32). In the carp, we investigated the fasting response of UCP3 gene expression in white glycolytic muscle as it is known in the rat that the fasting response of UCP3 expression is most pronounced in this muscle fiber type (31). Indeed, fasting caused a fivefold upregulation of UCP3 mRNA levels. In situations of high lipid oxidation, like fasting, it has been suggested that mammalian UCP3 protects mitochondria and cells from oxidative damage either by mild uncoupling activity preventing excess mitochondrial superoxide production (7) or by fatty acid anion export impeding their accumulation and peroxidation in the mitochondrial matrix (15, 33). There is also speculation on the involvement of UCP3 in skeletal muscle thermogenesis of mammals and birds (21, 36), but the observed upregulation of UCP3 gene expression in a physiological state associated with decreased energy expenditure appears to weaken this hypothesis. Regardless of the physiological function, the high similarity in tissue distribution and fasting response of UCP3 gene expression in the rat and carp indicates that its function and the mechanisms of gene regulation are most likely conserved during evolution.

It has been suggested that teleost fish have more genes than mammals, although it is still a matter of debate whether this is due to frequent independent duplications or the result of one ancient fish-specific genome duplication at the time of modern teleostei radiation ~320 million years ago (1, 25, 29, 38). However, our search for *Ucp* genes in zebrafish and pufferfish genomes only revealed the three orthologues known in mammals but no further sister genes. Either *Ucp* genes were exempt from genome duplication in ancient times or excess paralogues went extinct during the evolution of modern teleostei. Notably, the maintenance of gene redundancy in mammals supports the idea that each orthologue exhibits a distinct physiological function.

Taken together, our data disprove the monophyletic nature of UCP1 in placental mammals. All three members of the core UCP family were already present before the divergence of ray-finned (*Actinopterygii*) and lobe-finned (*Sarcopterygii*) vertebrate lineages about 420 million years ago, which suggests an ancient evolutionary history of UCPs and nonshivering thermogenesis in vertebrates.

GRANTS

This study was supported by Deutsche Forschungsgemeinschaft Grant KL 973/7 (to M. Klingenspor). M. Jastroch held a scholarship at the International Max Planck Graduate School.

REFERENCES

1. **Amores A, Force A, Yan YL, Joly L, Amemiya C, Fritz A, Ho RK, Langeland J, Prince V, Wang YL, Westerfield M, Ekker M, and Postlethwait JH.** Zebrafish hox clusters and vertebrate genome evolution. *Science* 282: 1711–1714, 1998.
2. **Block BA.** The billfish brain and eye heater: a new look at nonshivering thermogenesis. *News Physiol Sci* 2: 208–213, 1987.
3. **Block BA.** Thermogenesis in muscle. *Annu Rev Physiol* 56: 535–577, 1994.
4. **Borecky J, Maia IG, and Arruda P.** Mitochondrial uncoupling proteins in mammals and plants. *Biosci Rep* 21: 201–212, 2001.
5. **Boss O, Samec S, Paolonigiacobino A, Rossier C, Dulloo AG, Seydoux J, Muzzin P, and Giacobino JP.** Uncoupling protein-3: A new member of the mitochondrial carrier family with tissue-specific expression. *FEBS Lett* 408: 39–42, 1997.
6. **Bouillaud F, Arechaga I, Petit PX, Raimbault S, Levimeyrueis C, Casteilla L, Laurent M, Rial E, and Ricquier D.** A sequence related to a DNA recognition element is essential for the inhibition by nucleotides of proton transport through the mitochondrial uncoupling protein. *EMBO J* 13: 1990–1997, 1994.
7. **Brand MD, Affourtit C, Esteves TC, Green K, Lambert AJ, Miwa S, Pakay JL, and Parker N.** Mitochondrial superoxide: production, biological effects, and activation of uncoupling proteins. *Free Radic Biol Med* 37: 755–767, 2004.
8. **Cannon B and Nedergaard J.** Brown adipose tissue: function and physiological significance. *Physiol Rev* 84: 277–359, 2004.
9. **Considine MJ, Goodman M, Echtay KS, Laloi M, Whelan J, Brand MD, and Sweetlove LJ.** Superoxide stimulates a proton leak in potato mitochondria that is related to the activity of uncoupling protein. *J Biol Chem* 278: 22298–22302, 2003.
10. **Duchamp C, Barre H, Delage D, Rouanet JL, Cohen-Ahad F, and Minaire Y.** Nonshivering thermogenesis and adaptation to fasting in king penguin chicks. *Am J Physiol Regul Integr Comp Physiol* 257: R744–R751, 1989.
11. **Echtay KS, Esteves TC, Pakay JL, Jekabsons MB, Lambert AJ, Portero-Otin M, Pamplona R, Vidal-Puig AJ, Wang S, Roebuck SJ, and Brand MD.** A signalling role for 4-hydroxy-2-nonenal in regulation of mitochondrial uncoupling. *EMBO J* 22: 4103–4110, 2003.
12. **Echtay KS, Roussel D, St Pierre J, Jekabsons MB, Cadenas S, Stuart JA, Harper JA, Roebuck SJ, Morrison A, Pickering S, Clapham JC, and Brand MD.** Superoxide activates mitochondrial uncoupling proteins. *Nature* 415: 96–99, 2002.
13. **Fleury C, Neverova M, Collins S, Raimbault S, Champigny O, Levi-Meyrueis C, Bouillaud F, Seldin MF, Surwit RS, Ricquier D, and Warden CH.** Uncoupling protein-2: a novel gene linked to obesity and hyperinsulinemia. *Nat Genet* 15: 269–272, 1997.
14. **Hayward JS and Lisson PA.** Evolution of brown fat: its absence in marsupials and monotremes. *Can J Zool* 70: 171–179, 1992.
15. **Himms-Hagen J and Harper ME.** Physiological role of UCP3 may be export of fatty acids from mitochondria when fatty acid oxidation predominates: an hypothesis. *Exp Biol Med (Maywood)* 226: 78–84, 2001.
16. **Jastroch M, Stöhr S, Withers K, and Klingenspor M.** A quest for the origin of mammalian uncoupling proteins. In: *Life in the Cold: Evolution, Mechanisms, Adaptation, and Application*, edited by Barnes B M and Carey HV. Fairbanks, AL: Univ. of Alaska, 2004, p. 417–426.
17. **Jastroch M, Withers K, and Klingenspor M.** Uncoupling protein 2 and 3 in marsupials: identification, phylogeny, and gene expression in response to cold and fasting in *Antechinus flavipes*. *Physiol Genomics* 17: 130–139, 2004.
18. **Kabat AP, Rose RW, Harris J, and West AK.** Molecular identification of uncoupling proteins (UCP2 and UCP3) and absence of UCP1 in the marsupial Tasmanian bettong, *Bettongia gaimardi*. *Comp Biochem Physiol B Biochem Mol Biol* 134: 71–77, 2003.
19. **Kizaki T, Suzuki K, Hitomi Y, Taniguchi N, Saitoh D, Watanabe K, Onoe K, Day NK, Good RA, and Ohno H.** Uncoupling protein 2 plays an important role in nitric oxide production of lipopolysaccharide-stimulated macrophages. *Proc Natl Acad Sci USA* 99: 9392–9397, 2002.
20. **Klingenberg M, Echtay KS, Bienengraeber M, Winkler E, and Huang SG.** Structure-function relationship in UCP1. *Int J Obes* 23: S24–S29, 1999.
21. **Mills EM, Banks ML, Sprague JE, and Finkel T.** Pharmacology: uncoupling the agony from ecstasy. *Nature* 426: 403–404, 2003.
22. **Negre-Salvayre A, Hirtz C, Carrera G, Cazenave R, Troly M, Salvayre R, Penicaud L, and Casteilla L.** A role for uncoupling protein-2 as a regulator of mitochondrial hydrogen peroxide generation. *FASEB J* 11: 809–815, 1997.
23. **Nicholls DG and Locke RM.** Thermogenic mechanisms in brown fat. *Physiol Rev* 64: 1–64, 1984.
24. **Nicol SC, Pavlides D, and Andersen NA.** Nonshivering thermogenesis in marsupials: absence of thermogenic response to beta 3-adrenergic agonists. *Comp Biochem Physiol A* 117: 399–405, 1997.
25. **Ohno S.** Gene duplication and the uniqueness of vertebrate genomes circa 1970–1999. *Semin Cell Dev Biol* 10: 517–522, 1999.
26. **Pecqueur C, Cassard-Doulcier AM, Raimbault S, Miroux B, Fleury C, Gelly C, Bouillaud F, and Ricquier D.** Functional organization of the human uncoupling protein-2 gene, and juxtaposition to the uncoupling protein-3 gene. *Biochem Biophys Res Commun* 255: 40–46, 1999.
27. **Postlethwait JH, Woods IG, Ngo-Hazelett P, Yan YL, Kelly PD, Chu F, Huang H, Hill-Force A, and Talbot WS.** Zebrafish comparative genomics and the origins of vertebrate chromosomes. *Genome Res* 10: 1890–1902, 2000.
28. **Raimbault S, Dridi S, Denjean F, Lachuer J, Couplan E, Bouillaud F, Bordas A, Duchamp C, Taouis M, and Ricquier D.** An uncoupling protein homologue putatively involved in facultative muscle thermogenesis in birds. *Biochem J* 353: 441–444, 2001.
29. **Robinson-Rechavi M, Marchand O, Escriva H, Bardet PL, Zelus D, Hughes S, and Laudet V.** Euteleost fish genomes are characterized by expansion of gene families. *Genome Res* 11: 781–788, 2001.
30. **Rose RW, West AK, Ye JM, McCormick GH, and Colquhoun EQ.** Nonshivering thermogenesis in a marsupial (the tasmanian bettong *Bettongia gaimardi*) is not attributable to brown adipose tissue. *Physiol Biochem Zool* 72: 699–704, 1999.
31. **Samec S, Seydoux J, and Dulloo AG.** Role of UCP homologues in skeletal muscles and brown adipose tissue: mediators of thermogenesis or regulators of lipids as fuel substrate? *FASEB J* 12: 715–724, 1998.
32. **Samec S, Seydoux J, Russell AP, Montani JP, and Dulloo AG.** Skeletal muscle heterogeneity in fasting-induced upregulation of genes encoding UCP2, UCP3, PPARgamma and key enzymes of lipid oxidation. *Pflügers Arch* 445: 80–86, 2002.
33. **Schrauwen P, Hoeks J, Schaart G, Kornips E, Binas B, Van De Vusse GJ, Van Bilsen M, Luiken JJ, Coort SL, Glatz JF, Saris WH, and Hesselink MK.** Uncoupling protein 3 as a mitochondrial fatty acid anion exporter. *FASEB J* 17: 2272–2274, 2003.
34. **Stone RT, Rexroad CE, III, and Smith TP.** Bovine UCP2 and UCP3 map to BTA15. *Anim Genet* 30: 378–381, 1999.
35. **Stuart JA, Harper JA, Brindle KM, and Brand MD.** Uncoupling protein 2 from carp and zebrafish, ectothermic vertebrates. *Biochim Biophys Acta* 1413: 50–54, 1999.
36. **Talbot DA, Duchamp C, Rey B, Hanuise N, Rouanet JL, Sibille B, and Brand MD.** Uncoupling protein and ATP/ADP carrier increase mitochondrial proton conductance after cold adaptation of king penguins. *J Physiol* 558: 123–135, 2004.
37. **Thompson JD, Gibson TJ, Plewniak F, Jeanmougin F, and Higgins DG.** The CLUSTAL_X windows interface: flexible strategies for multiple sequence alignment aided by quality analysis tools. *Nucleic Acids Res* 25: 4876–4882, 1997.
38. **Vandepoele K, De Vos W, Taylor JS, Meyer A, and Van de PY.** Major events in the genome evolution of vertebrates: paranome age and size differ considerably between ray-finned fishes and land vertebrates. *Proc Natl Acad Sci USA* 101: 1638–1643, 2004.
39. **Vianna CR, Hagen T, Zhang CY, Bachman E, Boss O, Gereben B, Moriscot AS, Lowell BB, Bicudo JE, and Bianco AC.** Cloning and functional characterization of an uncoupling protein homolog in hummingbirds. *Physiol Genomics* 5: 137–145, 2001.
40. **Von Praun C, Burkert M, Gessner M, and Klingenspor M.** Tissue-specific expression and cold-induced mRNA levels of uncoupling proteins in the Djungarian hamster. *Physiol Biochem Zool* 74: 203–211, 2001.
41. **Woods IG, Kelly PD, Chu F, Ngo-Hazelett P, Yan YL, Huang H, Postlethwait JH, and Talbot WS.** A comparative map of the zebrafish genome. *Genome Res* 10: 1903–1914, 2000.
42. **Zhang CY, Baffy G, Perret P, Krauss S, Peroni O, Grujic D, Hagen T, Vidal-Puig AJ, Boss O, Kim YB, Zheng XX, Wheeler MB, Shulman GI, Chan CB, and Lowell BB.** Uncoupling protein-2 negatively regulates insulin secretion and is a major link between obesity, beta cell dysfunction, and type 2 diabetes. *Cell* 105: 745–755, 2001.

J Comp Physiol B
DOI 10.1007/s00360-007-0171-6

ORIGINAL PAPER

Functional characterisation of UCP1 in the common carp: uncoupling activity in liver mitochondria and cold-induced expression in the brain

Martin Jastroch · Julie A. Buckingham · Michael Helwig · Martin Klingenspor · Martin D. Brand

Received: 16 March 2007 / Revised: 18 May 2007 / Accepted: 21 May 2007

Abstract Mammalian uncoupling protein 1 (UCP1) mediates nonshivering thermogenesis in brown adipose tissue. We previously reported on the presence of a UCP1 orthologue in ectothermic fish and observed downregulation of UCP1 gene expression in the liver of the common carp. Neither the function of UCP1, nor the mode of UCP1 activation is known in carp liver mitochondria. Here, we compared the proton conductance at 25°C of liver mitochondria isolated from carp either maintained at 20°C (warm-acclimated, WA) or exposed to 8°C (cold-acclimated, CA) water temperature for 7–10 days. Liver mitochondria from WA carp had higher state four rates of oxygen consumption and greater proton conductance at high membrane potential. Liver mitochondria from WA, but not from CA, carp showed a strong increase in proton conductance when palmitate (or 4-hydroxy-*trans*-2-nonenal, HNE) was added, and this inducible proton conductance was prevented by addition of GDP. This fatty acid sensitive proton leak is likely due to the expression of UCP1 in the liver of WA carp. The observed biochemical properties of proton leak strongly suggest that carp UCP1 is a functional uncoupling protein with broadly the same activatory and inhibitory characteristics as mammalian UCP1. Significant UCP1 expression was also detected in our previous study in whole brain of the carp. We here observed a twofold increase of UCP1 mRNA in carp brain following cold exposure, suggesting a role of UCP1 in the thermal adaptation of brain metabolism. In situ hybridization located the UCP1 gene expression to the optic tectum responsible for visual system control, the descending trigeminal tract and the solitary tract. Taken together, this study characterises uncoupling protein activity in an ectotherm for the first time.

Keywords Uncoupling protein 1 · Proton leak · *Cyprinus carpio* · 4-hydroxynonenal · Liver

Abbreviations

ADP	Adenosine 5′-(trihydrogen diphosphate)
BSA	Bovine serum albumin
CA	Cold-acclimated
DEPC	Diethylpyrocarbonate
DTT	Dithiothreitol
EDTA	Ethylenediaminetetraacetic acid
EGTA	Ethylene glycol bis (2-aminoethyl ether)-N,N,N′N′-tetraacetic acid
FCCP	Carbonyl cyanide p-trifluoro-methoxyphenylhydrazone
GDP	Guanosine 5′-diphosphate
HEPES	4-(2-Hydroxyethyl)-1-piperazineethanesulfonic acid
PBS	Phosphate buffered saline
SSC	Sodium chloride sodium citrate buffer
^{35}S-UTP	Uridine 5′-[α-^{35}S]thiotriphosphate
TEA	Triethanolamine
TPMP	Triphenylmethylphosphonium

Communicated by G. Heldmaier.

Electronic supplementary material The online version of this article (doi:10.1007/s00360-007-0171-6) contains supplementary material, which is available to authorized users.

M. Jastroch (✉) · M. Helwig · M. Klingenspor
Animal Physiology, Department of Biology,
Philipps University Marburg, Karl-von-Frisch-Str. 8,
Marburg 35032, Germany
e-mail: Jastroch@staff.uni-marburg.de

J. A. Buckingham · M. D. Brand
Medical Research Council Dunn Human Nutrition Unit,
Hills Road, Cambridge, CB2 2XY, UK

Tris–HCl	(Hydroxymethyl) aminomethane-hydrochloride
WA	Warm-acclimated

Introduction

Uncoupling protein 1 (UCP1) executes nonshivering thermogenesis in brown adipose tissue of newborn humans, small mammals and hibernating mammals. The protein catalyses proton leakage through the inner membrane of mitochondria in brown adipocytes, decreasing the proton motive force and resulting in increased oxygen consumption and heat generation without concomitant ATP generation (Nicholls and Locke 1984). Paralogous proteins have been identified in vertebrates (UCP2, UCP3 and avian UCP) and in plants (plant UCP) but their physiological role remains controversial (Brand and Esteves 2005). Further proteins were named UCP4 and UCP5 but typical UCP1-like biochemical properties of these other proteins have not yet been demonstrated and phylogenetic inference excludes them from the core UCP protein family (Cannon and Nedergaard 2004).

The thermogenic role of mammalian UCP1 has been clearly identified and until recently the phylogenetic distribution of UCP1 was broadly accepted as restricted to placental mammals (Jastroch et al. 2005). In placental mammals, signal transduction at the brown adipocyte leads to an immediate breakdown of triglycerides, releasing free fatty acids into the cytosol. These fatty acids not only activate uncoupling by UCP1 (Lowell 1998) but are also fed into the respiratory chain of brown adipocyte mitochondria and serve as fuel. Direct activation of uncoupling activity by fatty acids has only been unambiguously demonstrated for UCP1 (Cunningham et al. 1986). Proton transport of all uncoupling proteins can be potently inhibited with purine nucleoside di- and triphosphates, including ADP, GDP, ATP and GTP. The activatory role of fatty acids remains unclear. There are three competing models: (a) fatty acids are required cofactors facilitating transport of protons (Klingenberg and Winkler 1985); (b) cycling of fatty acids is required for proton transport (UCP1 transports fatty acid anion from the matrix to the intermembrane space, and this is followed by protonation and flip-flop of the acid back to the matrix) (Garlid et al. 1996) or (c) there is no mechanistic requirement for fatty acids but they overcome nucleotide inhibition by simple competitive kinetics (Rial et al. 2004; Shabalina et al. 2004).

As one feature common to all known UCPs proton transport resulting in mild uncoupling can be activated by exposure of mitochondria to superoxide, which is prevented in the presence of purine nucleotides. 4-hydroxy-trans-2-nonenal (HNE), a reactive alkenal that also activates UCPs, may be one mediator of this mild uncoupling in response to the superoxide pathway (Echtay et al. 2003; Considine et al. 2003). Based on this activation of UCPs by reactive oxygen species produced by the respiratory chain a general role of UCPs in protection from oxidative cell damage has been proposed.

A recent study demonstrates the expression of UCP1, UCP2 and UCP3 in the common carp (*Cyprinus carpio*), an ectothermic vertebrate, providing a departure point for further investigation on the evolution of UCP1-mediated thermogenesis in placental mammals and the general function of UCPs in vertebrates (Jastroch et al. 2005). Interestingly, UCP1 mRNA in carp liver is diminished in response to cold, in contrast to expression of mammalian UCP1 in brown adipose tissue, which is cold induced. In the present paper we measured proton conductance in liver mitochondria from carp to resolve the function of UCP1. No previous studies have demonstrated uncoupling activity of UCP1 in an ectothermic vertebrate like the common carp, and the functional characterisation will assist in understanding the general roles of UCPs in the animal kingdom.

Materials and methods

Animal experiments

Common carp (400–600 g body weight) were kept in a temperature-controlled recirculating water system (Living stream, Frigid units) maintained at 20°C for at least 2 weeks. Three individuals were transferred to a second system and water temperature was gradually lowered (2°C per day) to 8°C. It has been demonstrated that 48 h of exposure to 8°C diminishes UCP1 mRNA levels dramatically (Jastroch et al. 2005). In the present study, carp were cold-exposed at 8°C for 7–10 days before use to induce metabolic acclimatisation processes. Animals were killed within UK Home Office rules by stunning, puncture of the heart and cerebral dislocation.

Isolation of liver mitochondria

Mitochondria for proton conductance measurements were always isolated in parallel from two carp, one taken from the warm and the other from the cold water tank in order to control for possible day-by-day variability in the quality of mitochondrial preparations. The liver was removed and immediately placed in ice-cold isolation medium (250 mmol l^{-1} sucrose, 5 mmol l^{-1} Tris–HCl, 2 mmol l^{-1} EGTA pH 7.4) containing 1% (w/v) defatted BSA (Sigma). The tissue was minced with scissors and disrupted using a Dounce homogeniser with a medium-fitting pestle. The homogenate was centrifuged at 8,500*g* for 10 min at 4°C and the pellet was resuspended in isolation medium and spun at 1,047*g* for 10 min; the resulting supernatant was subjected to a high-speed spin cycle (11,630*g*, 10 min, and

4°C). The pellet was resuspended in medium without BSA. The high-speed spin cycle was repeated twice and the final pellet resuspended in a minimal volume of isolation medium. Protein concentration was determined using the biuret method with fatty acid-free bovine serum albumin as standard (Gornall et al. 1949).

Measurement of oxygen consumption and membrane potential

Oxygen consumption was measured using a Clark-type oxygen electrode (Rank Brothers Ltd, United Kingdom) maintained at 25°C and calibrated with air-saturated medium (120 mmol l^{-1} KCl, 5 mmol l^{-1} KH_2PO_4, 3 mmol l^{-1} HEPES, 1 mmol l^{-1} EGTA, and 0.3% (w/v) defatted BSA, pH 7.2), which was assumed to contain 479 nmol O ml^{-1} (Reynafarje et al. 1985). Prior to the first measurements, the RCR =*respiratory control ratio*, dividing state three respiration (ADP-induced) by state 4 (leak respiration) of liver mitochondria was measured to ascertain the integrity of the carp liver mitochondria during the mitochondrial isolation procedure. Simultaneously with oxygen consumption, membrane potential was measured using a $TPMP^+$ sensitive electrode (Brand 1995). Mitochondria were suspended at 1.5 mg ml^{-1} in 2.5 ml medium and incubated with 8 µM rotenone to inhibit complex I, with 4 µg ml^{-1} oligomycin to inhibit phosphorylation of ADP, and with 110 ng ml^{-1} nigericin to abolish ΔpH. The $TPMP^+$ electrode was calibrated with sequential additions up to 2.5 µmol l^{-1} $TPMP^+$. Succinate (6 mmol l^{-1}) was added to start the reaction. Oxygen consumption and membrane potential were titrated through sequential steady states by successive additions of malonate up to 1 mmol l^{-1} for skeletal muscle mitochondria and up to 4 mmol l^{-1} for liver mitochondria. Where indicated, 1 mmol l^{-1} GDP, 35 µmol l^{-1} HNE or 100 µmol l^{-1} sodium palmitate dissolved in ethanol were added at the beginning of each run. The equation to calculate the binding of palmitate to bovine serum albumin (BSA) at 37°C by Richieri and coworkers (Richieri et al. 1993) was used to estimate free palmitate levels in our measurements containing 0.3% BSA (50.1 µmol l^{-1}): Free palmitate (nmol l^{-1}) = 4.4n − 0.03 + 0.23 exp (1.16n), where n is the molar ratio of palmitate to albumin.

Northern blot analysis and in situ hybridisation of the carp brain

The carp skull was opened; the brain carefully removed and immediately snap frozen in liquid nitrogen. All brain samples were stored at −70°C. Prior to RNA extraction the whole brain was first powdered in liquid nitrogen. Isolation of total RNA and Northern blotting was performed as described previously (Jastroch et al. 2004). The blot was hybridised with a probe corresponding to the full-length cDNA sequence of carp UCP1 (Jastroch et al. 2005). The hybridised probe was then detected by phospor imaging (Storm 860, Molecular Dynamics), and relative expression levels quantified using ArrayVision 7.0 (Imaging Research).

Coronal and sagittal brain sections (20 µm) were processed using a cryosectioning microtome (Leica CM 3050) and transferred to precooled object slides. A riboprobe complementary to carp UCP1 was generated from a linearised cloned cDNA. 50 µl of the ^{35}S-UTP-labelled probe was mixed in a volume of 256 µl with 3.9 mg ml^{-1} tRNA, 20 µl 1M DTT, 74 µl DEPC-treated water and added to 1 ml dextran sulphate and 1.5 ml hybridisation buffer (1M NaCl, 3.4× Denhardts, 34 mmol l^{-1} Tris (pH 8), 3.4 mmol l^{-1} EDTA (pH 8)). Prior to hybridisation, the slides were fixed in 4% paraformaldehyde in PBS (137 mmol l^{-1} NaCl, 10 mmol l^{-1} phosphate, 2.7 mmol l^{-1} KCl, pH 7.4) for 20 min on ice followed by 2 × 5 min washes in 0.1 mol l^{-1} PBS, immersed in 250 ml, 0.1 mol l^{-1} TEA (2 min) and transferred to 0.1 mol l^{-1} TEA containing 625 µl of acetic anhydride for 10 min. Slides were dehydrated through a gradient of increasing concentration of ethanol (50, 70, 95 and 100%) for 3 min each step. For hybridisation, 50 µl of hybridisation cocktail was loaded on each slide and incubated for 16 h at 60°C. Post hybridisation, object slides were transferred to 4× SSC (150 mmol l^{-1} NaCl, 15 mmol l^{-1} Na_3-citrate), cover slides were removed, and washed four times for 5 min in 4× SSC. After incubation in RNase solution (0.5 mol l^{-1} NaCl, 10 mmol l^{-1} Tris (pH 8), 1 mmol l^{-1} EDTA, 2 µg ml^{-1} RNase) at 37°C for 30 min, washing was repeated in descending concentrations of SSC (2× SSC twice for 5 min each, 1× SSC for 10 min and 0.5× SSC for 10 min at room temperature plus 0.1× SSC incubation for 30 min at 60°C). Dried slides were exposed to BioMax MR Film (Kodak) for two weeks. A control was performed by hybridising sections with equal length sense riboprobes of UCP1 resulting in no signal.

Statistical analysis

Values are means ± SEM. For comparisons of warm-acclimated (WA) and cold-acclimated (CA) carp, unpaired Student's *t* tests were performed. Activation and inhibition of proton conductance was tested using one-way ANOVA and Tukey's post hoc test with the level of significance set to $P < 0.05$.

Results

Morphology of liver from WA and CA carp

Prior to tissue removal, we observed an altered morphological appearance of the carp liver at different acclimation

temperatures (Supplemental photograph). In CA carp, the liver appeared enlarged and enshrouded other organs (e.g. spleen, intestine) indicating that significant physiological adaptations occurred due to cold acclimation. In accordance with our observations, the positive effect of cold exposure on liver mass seems to be a common adaptational process in fish as it was also described in the eel (*Anguilla anguilla* L.) (Wodtke 1974) or in the canal catfish (Kent et al. 1988).

State 4 respiration and basal proton conductance of liver mitochondria from WA and CA carp

We first compared the values of resting (state 4) oxygen consumption and membrane potential in liver mitochondria from WA and CA carp (Fig. 1). The mitochondrial assays were done under standardised 25°C conditions so that effects of the acclimation procedures (which happen to be at different temperatures) could be directly compared.

When respiring on succinate, state 4 respiration of mitochondria from WA fish tended to be higher than from CA fish (9.77 ± 0.73 compared to 7.72 ± 0.36 nmol O min^{-1} mg^{-1} of protein, *t* test, $P = 0.065$, $n = 3$, Fig. 1). In contrast, the CA group trends towards higher state 4 potential (168.5 ± 2.6 vs. 162.2 ± 0.7 mV, *t* test, $P = 0.097$, $n = 3$, Fig. 1). Lower respiration rate and higher membrane potential shows that state 4 proton leakage in carp liver mitochondria is decreased in response to cold acclimation.

We next compared the full kinetic response at 25°C of proton leak (monitored as oxygen consumption rate) to stepwise changes in its driving force, membrane potential,

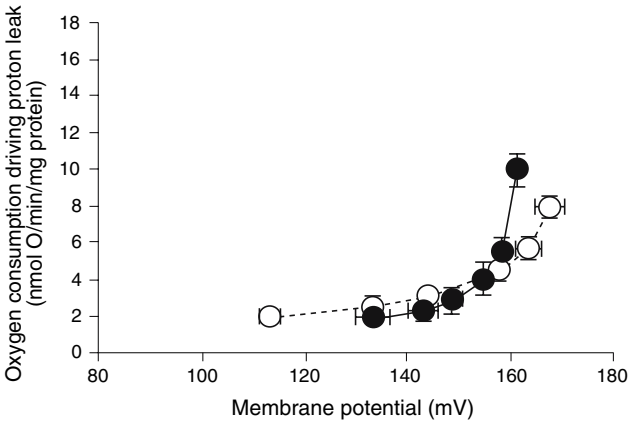

Fig. 1 Kinetics of basal proton conductance in liver mitochondria from CA and WA carp. Oxygen consumption driving proton leak in the absence of ATP synthesis is plotted against different membrane potentials imposed by malonate titration of succinate oxidation in isolated carp liver mitochondria to display the kinetic dependence of proton leak on its driving force, membrane potential, at 25°C. For details see "Materials and methods". *Filled circle* warm-acclimated (WA) carp; *open circle* cold-acclimated (CA) carp. Data are mean ± SEM of three (carp) independent experiments each performed in duplicate

in liver mitochondria from WA and CA carp (Fig. 1). As proton leak is a nonlinear function of membrane potential, to make comparisons between the two acclimation temperatures we compared the oxygen consumption driving proton leak at a common membrane potential. At the highest common potential of about 162 mV (the state 4 potential of mitochondria from WA carp), oxygen consumption was significantly ($P < 0.05$) decreased from 9.77 ± 0.73 in WA to 5.21 ± 0.56 nmol O min^{-1} mg^{-1} of protein in mitochondria from CA carp, indicating a twofold drop in the proton conductance of liver mitochondria from CA carp. However, this effect was only apparent at the highest membrane potentials.

Palmitate activation and GDP inhibition of proton conductance in carp liver mitochondria

Carp acclimated to 20°C express relatively high amounts of UCP1 mRNA in liver, whereas UCP1 mRNA levels are diminished after exposure to 8°C (Jastroch et al. 2005). The proton leak kinetics of UCPs have two major characteristics: activation by fatty acids (Locke et al. 1982), superoxide and alkenals (Echtay et al. 2003); (Considine et al. 2003) and inhibition by purine nucleoside di- or triphosphates (Nicholls and Locke 1984). We investigated if the kinetics of proton leak in carp liver mitochondria are affected by well characterized UCP1 activators and inhibitors, and whether the effects of these compounds are altered when UCP1 mRNA levels are diminished in response to cold acclimation.

Figure 2a shows that addition of palmitate (100 µmol l^{-1} total, which would result in about 11 nmol l^{-1} free palmitate according to (Richieri et al. 1993) in the presence of 0.3% BSA) increased the proton leakiness of liver mitochondria from WA carp. At the highest common potential of 154 mV, oxygen consumption was increased significantly from 3.63 ± 0.69 to 11.95 ± 1.44 nmol O min^{-1} mg^{-1} of protein, indicating a 3–4-fold stimulation of proton conductance (Fig. 2c). The increase in proton conductance was fully prevented by 1 mmol l^{-1} GDP (Fig. 2a, c), as expected if it was caused by palmitate activation of proton conductance through UCP1. In liver mitochondria from CA carp, palmitate had a negligible effect on proton conductance (Fig. 2b, d). Additionally, we observed that GDP without the addition of palmitate had no further effect on lowering proton conductance neither in the warm acclimated nor in the CA carp (data not shown). This experiment shows that GDP-sensitive fatty acid activation of proton conductance occurs in liver mitochondria from the common carp just as it does in UCP1-containing mitochondria from brown adipose tissue and implies that carp UCP1 is a functional fatty acid activated proton transporter. This conclusion is greatly strengthened by the lack of fatty acid and GDP effects in

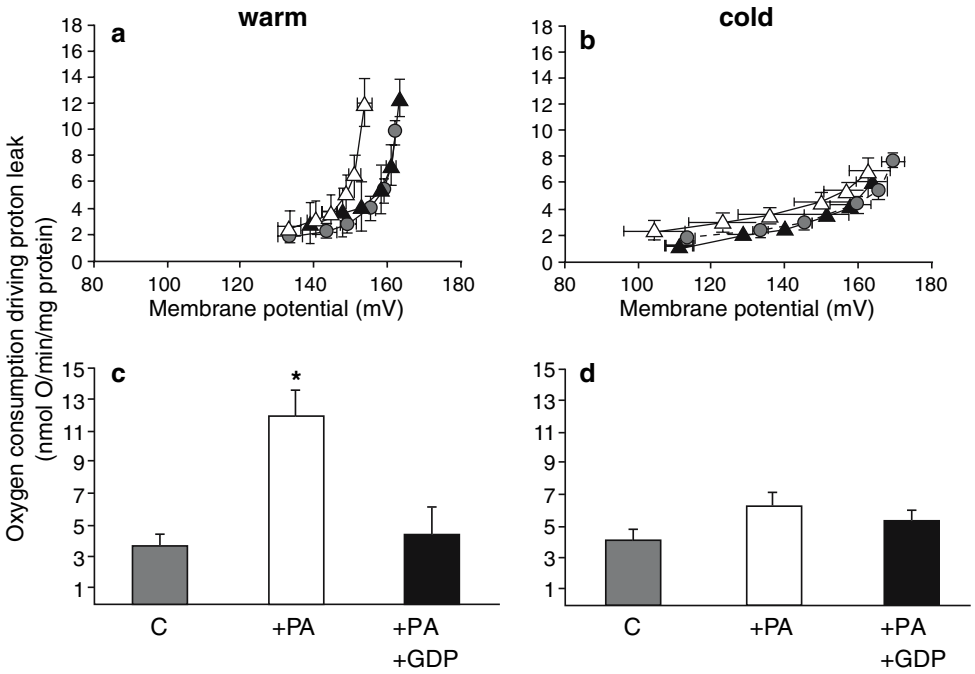

Fig. 2 Palmitate induced GDP-sensitive proton conductance in carp liver mitochondria. The kinetics of proton leak at 25°C were measured as described in Fig. 1. **a** and **b** show the kinetic curves; **c** and **d** show the derived rates of proton leak at the highest common potential (154 mV). Liver mitochondria were from (**a**, **c**) 20°C WA or (**b**, **d**) 8°C CA common carp. *Circle*, control; Δ, 100 µmol l^{-1} M palmitate; *filled triangle*, 100 µmol l^{-1} palmitate + 1 mmol l^{-1} GDP. All data are mean ± SEM of three independent experiments each performed in duplicate. *Asterisk* significant compared to control and GDP-inhibition ($P < 0.05$, one way ANOVA followed by Tukey's post hoc test); *C* control; *PA* palmitate

liver mitochondria from CA carp, in which UCP1 mRNA expression is lower (Jastroch et al. 2005).

HNE activation and GDP inhibition of proton conductance in carp liver mitochondria

HNE activates the proton conductance of mammalian UCP1, UCP2 and UCP3 (Echtay et al. 2003) and plant UCP (Smith et al. 2004). Figure 3a shows that addition of 35 µmol l^{-1} HNE to liver mitochondria from WA carp increased the proton conductance. At the highest common potential of about 151 mV, oxygen consumption driving proton leak was elevated 3–4-fold, from 3.06 ± 0.63 to 10.87 ± 1.13 nmol O min^{-1} mg^{-1} of protein (Fig. 3c). Although the proton conductance of mammalian adenine nucleotide translocase is also activated by HNE, activation of UCPs can be distinguished from this effect by its sensitivity to addition of GDP to inhibit specifically UCPs (Echtay et al. 2003). Figure 3a and c show that HNE-activated proton conductance could be partially inhibited with 1 mmol l^{-1} GDP. Once again, these effects were absent in liver mitochondria from CA carp (Fig. 3b, d), suggesting that they were caused by UCP1 and not by the adenine nucleotide translocase. Addition of both palmitate and HNE gave similar results to palmitate or HNE alone (Fig. 3e–h), suggesting no additivity or synergy of activation of carp UCP1 by fatty acids and alkenals under our assay conditions.

UCP1 in the brain of the common carp

In the studies reported above, we used mitochondria from carp liver to elucidate a possible function of UCP1. These experiments were based on the rationale that in liver we previously found the highest UCP1 gene expression of all carp tissues investigated (Jastroch et al. 2005) and the isolation of large amounts of coupled mitochondria was convenient. However, UCP1 mRNA is also expressed in carp brain (Jastroch et al. 2005). We therefore investigated in the carp brain the effect of cold acclimation on UCP1 expression and the neuroanatomical localisation of UCP1 mRNA.

Whereas UCP1 in carp liver is downregulated in the cold (Jastroch et al. 2005), UCP1 mRNA levels in the carp brain were upregulated about 2.4-fold in response to 7–10 days of cold acclimation (Fig. 4a). We furthermore scrutinised the neuroanatomical expression sites by in situ hybridisation. Figure 4b shows a representative autoradiograph of a sagittal brain section of a CA carp and the corresponding scheme adapted from the brain atlas of the goldfish (Canosa et al. 2004). A coronal section in the anterior part of the brain shows clear hybridisation of the UCP1 probe in the periventricular grey zone of the optic tectum (Fig. 4c). In the posterior region consisting of neuronal hindbrain structures, the descending trigeminal tract and the solitary tract show specific binding of the UCP1 probe (Fig. 4d).

Discussion

Our results demonstrate that the proton conductance of carp liver mitochondria can be stimulated by palmitate or HNE and inhibited by GDP. This regulated proton conductance was, however, only found in mitochondria isolated from carp acclimated to 20°C, but absent in carp acclimated to 8°C. We previously reported that UCP1 mRNA is most

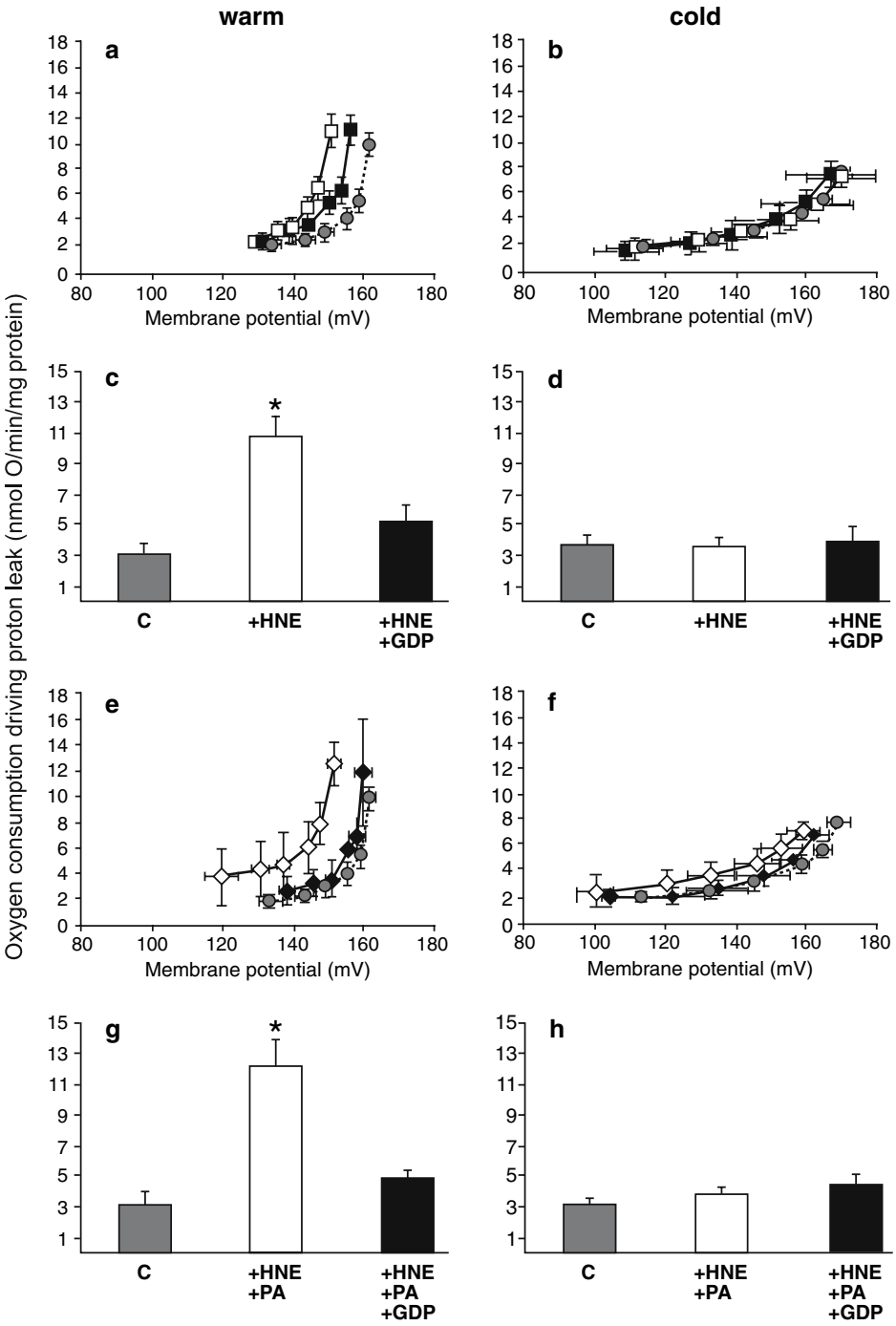

Fig. 3 HNE and palmitate induced GDP-sensitive proton conductance in carp liver mitochondria. The kinetics of proton leak at 25°C were measured as described in Fig. 1. **a**, **b**, **e**, **f** show the kinetic curves; **c**, **d**, **g**, **h** show the derived rates of proton leak at the highest common potential (151 mV). Liver mitochondria were from (**a**, **c**, **e**, **g**) 20°C WA or (**b**, **d**, **f**, **h**) 8°C CA common carp. *Circle*, control; *open square*, 35 µmol l^{-1} HNE; *filled square*, 35 µmol l^{-1} HNE + 1 mmol l^{-1} GDP; *open diamond*, 35 µmol l^{-1} HNE + 100 µmol l^{-1} palmitate; *filled diamond* 35 µmol l^{-1} HNE + 100 µmol l^{-1} palmitate + 1 mmol l^{-1} GDP. All data are mean ± SEM of three independent experiments except the treatment with "HNE and palmitate" which was performed twice in duplicate. *Asterisk* significant compared to control and GDP-inhibition ($P < 0.05$, one way ANOVA followed by Tukeys post hoc test); *C* control; *PA* palmitate

abundant in carp liver and strongly down regulated in response to cold (Jastroch et al. 2005). This coincidence strongly suggests that the observed GDP-sensitive induction of proton conductance by fatty acids and HNE is due the presence of UCP1 in liver mitochondria of WA carp. Unfortunately, available antibodies raised against mammalian UCP1 do not cross-react with the carp UCP1 orthologue. In future studies, the generation of a fish-specific UCP1 antibody and the use of UCP1 gene knockout or iRNA methodology is definitely required to further corroborate the function of carp UCP1. We have to consider that the rather weak expression of UCP2 in carp liver may also explain the presence of inducible proton conductance. However, a study investigating UCP2 expression in the liver of a temperate marine fish, the common eelpout *Zoarces viviparous*, shows an upregulation of UCP2 in response to cold (Mark et al. 2006). Based on the assumption that UCP2 expression is similarly regulated in the temperate carp, inducible proton conductance would therefore, be more pronounced in the CA carp which was not the case. Further

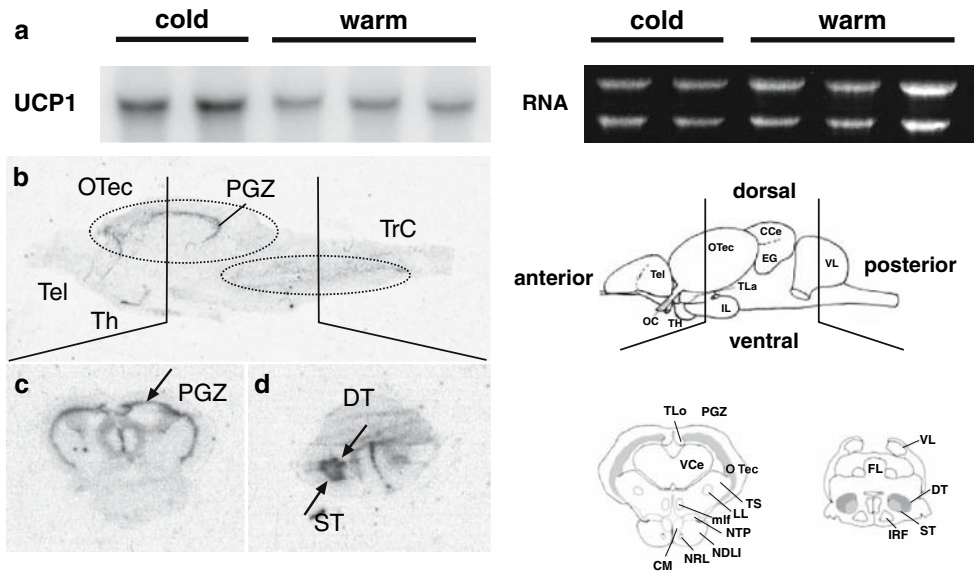

Fig. 4 Northern blot analysis of UCP1 in carp brain and autoradiographs of carp brain sections. **a** Twenty micrograms total RNA from the brain of WA or CA carp were hybridised with the carp UCP1 full-length cDNA (*left*). Loading of RNA was checked by ethidium–bromide staining of the agarose gel (*right*). **b** Sagittal section of carp brain, labelled according to the schematic representation (*right*) of whole goldfish brain anatomy modified from (Canosa et al. 2004). **c** Coronal and **d** sagittal sections located as indicated in **b**, labelled according to the schematic representation (*right*) of coronal and sagittal sections of the goldfish brain (10). *CCe* cerebellar body; *CM* mammilar body; *DT* descending trigeminal tract; *EG* eminentia granularis; *FL* facial lobe; *IL* inferior lobe; *IRF* inferior reticular formation; *LL* lateral lemniscus; *mlf* medial longitudinal fascicules; *NDLI* diffuse nucleus of the inferior lobe; *NRL* nucleus of the lateral recess; *NTP* posterior thalamic nucleus; *OC* optic chiasma; *OTec* optic tectum; *PGZ* periventricular grey zone of OTec; *ST* solitary tract; *Tel* telencephalon; *TH* thalamus; *TLA* lateral thalamus; *TLo* torus longitudinalis; *TrC* truncus cerebri; *TS* torus semicircularis; *VCe* cerebellar valve; *VL* vagal lobe. Terminology according to (10)

indication that we do not measure UCP2 activity is provided by studies of their mammalian species orthologues: the conserved central matrix loop of mammalian UCP1 is required for fatty acid activation which is absent for UCP2 and UCP3 (Jimenez-Jimenez et al. 2006).

The fatty acid induced uncoupling of mitochondrial proton conductance resembles the action of UCP1 in mammalian brown adipose tissue mitochondria. Even though the alkenal HNE activated carp UCP1 per se, palmitate activation of carp UCP1 required no further addition of metabolites of the superoxide activatory pathway, closely reflecting the situation reported for UCP1 in mammalian mitochondria (Klingenberg and Echtay 2001). Fatty acid induced uncoupling can also be mediated by other proton translocases like the adenine nucleotide transporter or the phosphate carrier protein but high GDP sensitivity is so far a common feature for UCPs. A recent study suggested a dual-site model of UCP1 regulation including fatty acids and reactive alkenals interacting at separate sites. It cannot be excluded, however, that endogenous alkenals are required for UCP1 activity as they are released continuously by oxidising natural membranes (Esteves et al. 2006). In contrast, all other members of the core UCP family so far investigated (UCP2, UCP3, potato UCP, penguin UCP) (Considine et al. 2003; Talbot et al. 2004; Echtay et al. 2002) experimentally required the addition of alkenals before they catalysed proton conductance in mitochondria (Brand et al. 2004).

Our study on UCP1 in carp emphasises the strength of parallel measurements of oxygen consumption and membrane potential for the quantification of proton leakage. In numerous studies, state 4 oxygen consumption alone has been taken as a surrogate for the proton leakiness of the mitochondrial inner membrane. Higher leak should result in an increased pump activity of the respiratory chain to maintain the membrane potential. The activation of UCP1 in brown adipose tissue decreases the membrane potential dramatically but the high oxidative capacity strongly defends this potential resulting in increased oxygen consumption. Thus, respiration of brown adipose tissue mitochondria can be induced several fold with palmitate and is a good index of UCP1 function. With carp liver mitochondria, activation of proton leak leads to little elevation of oxygen consumption (Figs. 1, 2), but simultaneous measurement of both oxygen consumption and membrane potential clearly resolves the increase of proton conductance. In these mitochondria of low oxidative capacity, oxygen consumption is not dramatically increased to defend the membrane potential but the membrane potential is rather decreased.

Among the teleost fish, the common carp is a "cold-inactive" species: winter-acclimatised carp have reduced activity and metabolism. Several studies demonstrate a recruitment of mitochondrial density and respiratory capacity during cold acclimation in skeletal muscle (Guderley 1990). In liver, however, no evidence has been reported that the respiratory capacity, using cytochrome c oxidase as a marker, is increased (Wodtke 1981). On the other hand the metabolic capacity of the Krebs cycle, as judged from liver citrate synthase activity, appears to be augmented during cold acclimation (Lucassen et al. 2006). In the "cold-inactive" species the requirement for ATP in vivo is strongly reduced which likely results in a depressed state 3 respiration of hepatocytes. In this situation the contribution of proton leak (state 4 respiration) to the cellular oxygen consumption would dominate. Accordingly, the observed reduction in proton leakage in CA carp mitochondria (Fig. 1) serves to save energy and increases the efficiency of mitochondrial ATP production. Our findings on the reduction of mitochondrial proton leak are consistent with physiological findings in other ectothermic vertebrates during metabolic depression. Basal proton leak rate is reduced in skeletal muscle mitochondria of hypometabolic frogs because of decreased activity of the electron transport chain (St Pierre et al. 2000), and it is reduced in hepatopancreas cells from aestivating snails compared to controls because of changes in mitochondrial proton conductance (Bishop and Brand 2000).

Alterations in proton conductance might be caused by alterations in membrane properties. In carp, the proportion of unsaturated fatty acids rapidly increases within less than a week in response to cold (Wodtke 1978; Trueman et al. 2000; Tiku et al. 1996). The influence of phospholipid fatty acid composition on proton conductance has been intensively discussed in the past. Whereas, a correlation between proton conductance and fatty acid composition is observed in mitochondria, the proton permeability of liposomes made from mitochondrial inner membranes does not depend on phospholipid composition (Porter et al. 1996; Brookes et al. 1997). Given an assay temperature of 25°C, we would expect higher membrane fluidity in accordance with homeoviscous adaptation in mitochondria of CA carp and perhaps a higher proton conductance due to a higher degree of unsaturation (Guderley 2004). In contrast, we observed a lower basal proton conductance in mitochondria from the CA group (Fig. 1). Liver mitochondria from CA carp were measured at an assay temperature of 25°C to allow comparisons of UCP1 function between WA and CA carp. Therefore, the biological relevance of lower proton conductance might be impaired, as the cold-exposed mitochondria might not work properly at a higher temperature. Anyway, the high temperature does not disrupt the mitochondrial inner membrane, as damaged mitochondria would lose proton motive force. Instead, the membrane potential was even higher as in the warm-acclimated liver mitochondria. Other studies investigating basal proton leak kinetics in fish found similar proton conductance in carp and goldfish liver mitochondria at 25°C (J Baca, K Dickson, JA Buckingham, J St Pierre and MD Brand, unpublished observations) whereas proton conductance of trout liver mitochondria at 20°C was about twice as high (Brookes et al. 1998).

What is the physiological function of carp UCP1? One might speculate that it either mediates thermogenesis, protects against oxidative stress by causing mild uncoupling, or has some role in fatty acid metabolism. To date, adaptive heat production has not been detected in the liver of ectotherms. Furthermore, the thermogenic function of UCP1 in mammalian brown adipose tissue is supported by high mitochondrial density, high respiratory capacity and high protein density of UCP1, features either lacking or not yet investigated in carp liver. Most fish are obligate ectotherms and recorded body temperatures always range within 1 or 2°C of ambient water temperature (Block 1994; Crawshaw 1976), but the possibility of local thermogenesis cannot be categorically excluded. One precedent is the brain heater organ of Scombroid fish (billfish, swordfish and butterfly mackerel) (Carey 1982). However, in Scombroid fish, counter-current heat exchangers and calcium cycling activity underlie local heat production and speculations on a thermogenic or thermocompensatory role of UCP1 in fish brain are not substantial.

In carp brain, we detected the highest abundance of UCP1 in the periventricular grey zone of the optic tectum containing nuclei of descending neurons into the optic tectum. The physiological role of the optic tectum is related to the control of sensory functions (e.g., the visual system). Descending nerve fibres control motor functions and metabolic homeostasis of the carp. Temperature compensation mechanisms in the neuronal system are suggested (Montgomery and Macdonald 1990) and in carp, rapid temperature drops even led to an increase of neuronal activity in the preoptic area (van den Burg et al. 2005). Under these conditions, peroxidation products are most likely increased and UCP1 might be required as a protective protein to prevent lipid peroxidation. Intriguingly, brain UCP1 mRNA levels were twofold increased after 7–10 days of cold acclimation in our study. For further studies, it would be of interest to cover the dynamic changes of UCP1 mRNA levels during cold acclimation in a time-course experiment as responses often occur in the earliest phase of cold stress.

If we focus on the activation of proton conductance in carp liver mitochondria by HNE, an involvement in the defense system against reactive oxygen species seems to be the most likely. The degree of activation correlates well with the previously reported UCP1 expression levels and

can be inhibited with GDP, leading to the conclusion that UCP1 is mediating HNE-activated proton conductance. Nevertheless, GDP inhibition could not be observed in rodent liver mitochondria (Echtay et al. 2003).

Considering the depressed metabolic state of CA carp during winter, reduced metabolism in the liver may result in decreased lipid peroxidation and less need for mild uncoupling. It has been hypothesised that the ability of superoxide and reactive alkenals to activate the proton conductance of all the major branches of the UCP core family suggests that the "ancestral" function of the UCPs was related to the response to radicals rather than to thermogenesis. In contrast, increased incorporation of polyunsaturated fatty acids in the phospholipids of mitochondrial membranes of CA carp should rather increase the risk for lipid peroxidation, a situation in which increased capacity for mild uncoupling would be of benefit. On this background it is currently difficult to judge whether the presence of fatty acid induced proton leak in WA carp, but not in CA fish, hints towards a role in the mitigation of superoxide production.

Fatty acid activation of proton conductance in carp UCP1 demonstrates that the biochemical properties of the common ancestor of the fish and mammalian protein already possessed the potential to be functional in the thermogenic machinery of brown adipose tissue later in mammalian evolution. We postulate that all orthologues of UCP1 upstream from the fish/mammal common ancestor will exhibit fatty acid activated proton conductance. Future studies on these proteins will help to define the onset point of UCP1-mediated adaptive thermogenesis. On the molecular level, the identification of orthologues earlier in the evolutionary tree will help to trace back the evolutionary origin of fatty acid sensitivity and will further extend our understanding of its biological significance.

Acknowledgments We thank Helen Boysen, Ian Goldstone and Sigrid Stöhr for excellent technical assistance, and the Department of Zoology, Cambridge University for providing us with their animal facilities. This study was funded by the Medical Research Council, the DAAD and the DFG (Grant KL 973/7).

References

Bishop T, Brand MD (2000) Processes contributing to metabolic depression in hepatopancreas cells from the snail *Helix aspersa*. J Exp Biol 203:3603–3612

Block BA (1994) Thermogenesis in muscle. Ann Rev Physiol 56:535–577

Brand MD (1995) Measurement of mitochondrial protonmotive force. In: Brown GC (ed) Bioenergetics: a practical approach. IRL Press, Oxford, pp 39–62

Brand MD, Affourtit C, Esteves TC, Green K, Lambert AJ, Miwa S, Pakay JL, Parker N (2004) Mitochondrial superoxide: production, biological effects, and activation of uncoupling proteins. Free Radic Biol Med 37:755–767

Brand MD, Esteves TC (2005) Physiological functions of the mitochondrial uncoupling proteins UCP2 and UCP3. Cell Metab 2:85–93

Brookes PS, Buckingham JA, Tenreiro AM, Hulbert AJ, Brand MD (1998) The proton permeability of the inner membrane of liver mitochondria from ectothermic and endothermic vertebrates and from obese rats: correlations with standard metabolic rate and phospholipid fatty acid composition. Comp Biochem Physiol B Biochem Mol Biol 119:325–334

Brookes PS, Hulbert AJ, Brand MD (1997) The proton permeability of liposomes made from mitochondrial inner membrane phospholipids: no effect of fatty acid composition. Biochim Biophys Acta 1330:157–164

Cannon B, Nedergaard J (2004) Brown adipose tissue: function and physiological significance. Physiol Rev 84:277–359

Canosa LF, Cerda-Reverter JM, Peter RE (2004) Brain mapping of three somatostatin encoding genes in the goldfish. J Comp Neurol 474:43–57

Carey FG (1982) A brain heater in the swordfish. Science 216:1327–1329

Considine MJ, Goodman M, Echtay KS, Laloi M, Whelan J, Brand MD, Sweetlove LJ (2003) Superoxide stimulates a proton leak in potato mitochondria that is related to the activity of uncoupling protein. J Biol Chem 278:22298–22302

Crawshaw LI (1976) Effect of rapid temperature change on mean body temperature and gill ventilation in carp. Am J Physiol 231:837–841

Cunningham SA, Wiesinger H, Nicholls DG (1986) Quantification of fatty acid activation of the uncoupling protein in brown adipocytes and mitochondria from the guinea-pig. Eur J Biochem 157:415–420

Echtay KS, Esteves TC, Pakay JL, Jekabsons MB, Lambert AJ, Portero-Otin M, Pamplona R, Vidal-Puig AJ, Wang S, Roebuck SJ, Brand MD (2003) A signalling role for 4-hydroxy-2-nonenal in regulation of mitochondrial uncoupling. EMBO J 22:4103–4110

Echtay KS, Roussel D, St Pierre J, Jekabsons MB, Cadenas S, Stuart JA, Harper JA, Roebuck SJ, Morrison A, Pickering S, Clapham JC, Brand MD (2002) Superoxide activates mitochondrial uncoupling proteins. Nature 415:96–99

Esteves TC, Parker N, Brand MD (2006) Synergy of fatty acid and reactive alkenal activation of proton conductance through uncoupling protein 1 in mitochondria. Biochem J 395:619–628

Garlid KD, Orosz DE, Modriansky M, Vassanelli S, Jezek P (1996) On the mechanism of fatty acid-induced proton transport by mitochondrial uncoupling protein. J Biol Chem 271:2615–2620

Gornall AG, Bardawill CJ, David MM (1949) Determination of serum proteins by means of the biuret reaction. J Biol Chem 177:751–766

Guderley H (1990) Functional significance of metabolic responses to thermal acclimation in fish muscle. Am J Physiol 259:R245–R252

Guderley H (2004) Metabolic responses to low temperature in fish muscle. Biol Rev Camb Philos Soc 79:409–427

Jastroch M, Withers K, Klingenspor M (2004) Uncoupling protein 2 and 3 in marsupials: identification, phylogeny, and gene expression in response to cold and fasting in *Antechinus flavipes*. Physiol Genomics 17:130–139

Jastroch M, Wuertz S, Kloas W, Klingenspor M (2005) Uncoupling protein 1 in fish uncovers an ancient evolutionary history of mammalian nonshivering thermogenesis. Physiol Genomics 22:150–156

Jimenez-Jimenez J, Ledesma A, Zaragoza P, Gonzalez-Barroso MM, Rial E (2006) Fatty acid activation of the uncoupling proteins requires the presence of the central matrix loop from UCP1. Biochim Biophys Acta 1757:1292–1296

Kent J, Koban M, Prosser CL (1988) Cold-acclimation-induced protein hypertrophy in channel catfish and green sunfish. J Comp Physiol [B] 158:185–198

Klingenberg M, Echtay KS (2001) Uncoupling proteins: the issues from a biochemist point of view. Biochim Biophys Acta 1504:128–143

Klingenberg M, Winkler E (1985) The reconstituted isolated uncoupling protein is a membrane potential driven H^+ translocator. EMBO J 4:3087–3092

Locke RM, Rial E, Nicholls DG (1982) The acute regulation of mitochondrial proton conductance in cells and mitochondria from the brown fat of cold-adapted and warm-adapted guinea pigs. Eur J Biochem 129:381–387

Lowell BB (1998) Adaptive thermogenesis: turning on the heat. Curr Biol 8:R517–520

Lucassen M, Koschnick N, Eckerle LG, Portner HO (2006) Mitochondrial mechanisms of cold adaptation in cod (*Gadus morhua* L.) populations from different climatic zones. J Exp Biol 209:2462–2471

Mark FC, Lucassen M, Portner HO (2006) Thermal sensitivity of uncoupling protein expression in polar and temperate fish. Comp Biochem Physiol D—Genomics Proteomics 1:365–374

Montgomery JC, Macdonald JA (1990) Effects of temperature on nervous system: implications for behavioral performance. Am J Physiol 259:R191–R196

Nicholls DG, Locke RM (1984) Thermogenic mechanisms in brown fat. Physiol Rev 64:1–64

Porter RK, Hulbert AJ, Brand MD (1996) Allometry of mitochondrial proton leak: Influence of membrane surface area and fatty acid composition. Am J Physiol 40:R1550–R1560

Reynafarje B, Costa LE, Lehninger AL (1985) O_2 solubility in aqueous media determined by a kinetic method. Anal Biochem 145:406–418

Rial E, Aguirregoitia E, Jimenez-Jimenez J, Ledesma A (2004) Alkylsulfonates activate the uncoupling protein UCP1: implications for the transport mechanism. Biochim Biophys Acta 1608:122–130

Richieri GV, Anel A, Kleinfeld AM (1993) Interactions of long-chain fatty acids and albumin: determination of free fatty acid levels using the fluorescent probe ADIFAB. Biochemistry 32:7574–7580

Shabalina IG, Jacobsson A, Cannon B, Nedergaard J (2004) Native UCP1 displays simple competitive kinetics between the regulators purine nucleotides and fatty acids. J Biol Chem 279:38236–38248

Smith AM, Ratcliffe RG, Sweetlove LJ (2004) Activation and function of mitochondrial uncoupling protein in plants. J Biol Chem 279:51944–51952

St Pierre J, Brand MD, Boutilier RG (2000) Mitochondria as ATP consumers: cellular treason in anoxia. Proc Nat Acad Sci USA 97:8670–8674

Talbot DA, Duchamp C, Rey B, Hanuise N, Rouanet JL, Sibille B, Brand MD (2004) Uncoupling protein and ATP/ADP carrier increase mitochondrial proton conductance after cold adaptation of king penguins. J Physiol 558:123–135

Tiku PE, Gracey AY, Macartney AI, Beynon RJ, Cossins AR (1996) Cold-induced expression of delta 9-desaturase in carp by transcriptional and posttranslational mechanisms. Science 271:815–818

Trueman RJ, Tiku PE, Caddick MX, Cossins AR (2000) Thermal thresholds of lipid restructuring and delta(9)-desaturase expression in the liver of carp (Cyprinus carpio L). J Exp Biol 203:641–650

van den Burg EH, Peeters RR, Verhoye M, Meek J, Flik G, Van der LA (2005) Brain responses to ambient temperature fluctuations in fish: reduction of blood volume and initiation of a whole-body stress response. J Neurophysiol 93:2849–2855

Wodtke E (1974) Effects of acclimation temperature on the oxidative metabolism of the eel (*Anguilla anguilla* L.). J Comp Physiol [B] 91:309–332

Wodtke E (1978) Lipid adaptation in liver mitochondrial membranes of carp acclimated to different environmental temperatures: phospholipid composition, fatty acid pattern and cholesterol content. Biochim Biophys Acta 529:280–291

Wodtke E (1981) Temperature adaptation of biological membranes Compensation of the molar activity of cytochrome c oxidase in the mitochondrial energy-transducing membrane during thermal acclimation of the carp (*Cyprinus carpio* L). Biochim Biophys Acta 640:710–720

The molecular identification of uncoupling protein 1 in marsupials sheds light on the evolution of brown adipose tissue in mammals

Jastroch M. [1#], Withers K. W. [2], Taudien S. [3], Frappell P. B. [4], Helwig M. [1], Fromme T. [1], Hirschberg V. [1], Heldmaier G. [1], McAllan B. M. [5], Firth B.T. [6], Burmester T. [7], Platzer M. [3], and Klingenspor M. [1]

[1] Department of Animal Physiology, Faculty of Biology, Philipps-Universität Marburg, Karl-von-Frisch-Str. 8, 35043 Marburg, Germany,
[2] Department of Biological and Physical Sciences, University of Southern Queensland, Toowoomba, Qld, Australia,
[3] Genome Analysis, Leibniz-Institute for Age Research – Fritz Lipmann Institute, D-07745 Jena, Germany
[4] Adaptational and Evolutionary Respiratory Physiology Laboratory, Department of Zoology, La Trobe University, Melbourne 3086, Vic., Australia
[5] Environmental Control of Physiology, Bosch Institute, The University of Sydney, Sydney 2006, NSW Australia
[6] Department of Anatomical Sciences, University of Adelaide, Adelaide, Australia
[7] Institute of Zoology, Biozentrum Grindel, University of Hamburg, Martin-Luther-King-Platz 3, D-20146 Hamburg, Germany

To whom correspondence should be addressed: Martin Jastroch, Department of Animal Physiology, Faculty of Biology, Philipps-Universität Marburg, Karl-von-Frisch-Str. 8, 35043 Marburg, Germany, Email: Jastroch@staff.uni-marburg.de,Phone: +49-6421-2823389, Fax: +49-6421-282893

Abstract

Brown adipose tissue (BAT) expressing uncoupling protein 1 (UCP1) is responsible for adaptive nonshivering thermogenesis giving mammals crucial advantage to survive the cold. Although BAT has been well characterized in eutherian mammals, its emergence during evolution remained unknown as the identification of UCP1 failed in marsupials, which diverged from eutherians 150 MYA. We here unequivocally identified the *UCP1* gene in a genomic library of the South American marsupial *Monodelphis domestica* by conserved synteny and phylogenetic inference. The subsequent identification of UCP1 in the Australian dasyurid marsupial *Sminthopsis crassicaudata* demonstrated the presence of UCP1 in the two major marsupial groups which separated 80 MYA by continental drift. Whereas UCP1 expression was only detectable in a *M. domestica* juvenile, we observed cold-induced UCP1 gene expression in interscapular fat deposits of *S. crassicaudata*, just as found for eutherians. These differences between the South American *M. domestica* and the Australian dasyurid *S. crassicaudata* are not based on phylogenetic distance as the dasyurid *A. flavipes* also lacks BAT in the adult state.

Taken together, our data suggest that an archetypal BAT expressing UCP1 was present at least 150 MYA allowing mammals to adapt nonshivering thermogenesis to the cold and produce endogenous heat without dependence on shivering and activity.

Introduction

The evolution of brown adipose tissue (BAT) and its thermogenic uncoupling protein 1 (UCP1) is of major interest in the understanding of successful mammalian radiation. Adaptive nonshivering thermogenesis (NST) generated in BAT enables small eutherian mammals to maintain high body temperature independent of daily and seasonal temperature fluctuations (Cannon and Nedergaard 2004). Although BAT was first described in 1551 (Gesner 1551), its thermogenic role was not recognized until the 1960s (Dawkins and Hull 1964); (Smith 1962) and it is now established that BAT contributes significantly to adaptive NST of rodents, hibernators and newborns (Cannon and Nedergaard 2004). During cold exposure, sympathetic postganglions release noradrenaline (NA) and activate BAT by stimulation of lipolysis and futile UCP1-dependent mitochondrial respiration. UCP1, a mitochondrial carrier protein, is located in the inner membrane of BAT mitochondria and provides the molecular basis for NST (Nicholls and Locke 1984). The protein increases proton conductance and uncouples oxidative phosphorylation from ATP synthesis by dissipating proton motive force as heat. All eutherian species investigated so far possess UCP1, with the exception of pigs where a naturally disrupted *UCP1* gene results in poor thermoregulation and sensitivity to cold exposure (Berg et al. 2006). The observation that UCP1-knockout mice are unable to defend their body temperature when exposed to the cold (Golozoubova et al. 2001) confirms that UCP1 is crucial for adaptive NST. In contrast to previous expectations, an ancient UCP1 orthologue could be identified in the ectothermic teleost fish but the physiological function might be other than heat production (Jastroch et al. 2005).

Evidence for NST in marsupial mammals which separated from eutherians about 150 MYA (Bininda-Emonds et al. 2007) remains controversial. In macropods the injection of noradrenaline led to an increase of metabolic rate (Loudon et al. 1985); (Nicol 1978) a response attributed to skeletal muscle by others (Ye et al. 1996); (Nicol et al. 1997). It was suggested that adaptive

nonshivering thermogenesis may be of major importance in Australian dasyurids as they belong to the smallest marsupials. Indeed, a small thermogenic response to NA could be observed in *Sminthopsis crassicauda* kept at 24°C (Clements et al. 1998). However, no response to noradrenaline was observed in *Antechinus stuartii* (5°C or 30°C acclimated) (Reynolds and Hulbert 1982). Similarly, there was a lack of response in Southamerican marsupials (Dawson and Olson 1988); (Opazo et al. 1999). Notably, albeit evidence for NST in some marsupials, no study demonstrated that NST was adaptive in the cold. Nevertheless, marsupials are well capable of thermoregulation and defend stable body temperature during cold exposure (Schaeffer et al. 2003); (Dawson and Dawson 1982); (Geiser et al. 2003). Studies on the kowari (*Dasyuroides byrney*) for example provided indirect indication of adaptive NST replacing shivering thermogenesis (May 2003). Cold-acclimated (CA) compared to warm-acclimated (WA) individuals showed a decrease in shivering tremor during cold exposure.

Morphological studies revealed BAT characteristics like multilocular fat droplets and vascularisation in the interscapular region of Benett's wallaby pouch youngs (*Macropus rufogriseus rufogriseus*)(Loudon et al. 1985). However, another study investigating 38 different marsupial and one monotreme species precluded the presence of BAT in marsupials by pointing out that morphological features for BAT also occured in white adipose tissue during cold stress (Hayward and Lisson 1992); (Loncar et al. 1988b); (Loncar et al. 1988a). Morphological features are therefore inappropriated for the identification of BAT. Furthermore, they led to the erroneous conclusion that birds possess BAT (Oliphant 1983).

The discovery of UCP1 (Heaton et al. 1978); (Ricquier and Kader 1976) and the cloning of the cDNA sequence (Bouillaud et al. 1985); (Aquila et al. 1985) in rodents 25 years ago stimulated studies to identify UCP1 and its genomic presence in marsupials. One early study showed weak UCP1-like immunoreactivity in the interscapular fat deposit of *Sminthopsis crassicaudata* (Hope et al. 1997). However, it is generally accepted that UCP1 antibodies cross-react with other mitochondrial carriers (Ricquier et al. 1992) or UCP2/3 which have been recently identified in

marsupials (Jastroch et al. 2004). Unequivocal detection of UCP1 requires genomic or gene transcript sequence data. However, several attempts to identify the UCP1 sequence have failed so far (Kabat et al. 2003a); (Kabat et al. 2003b); (Rose et al. 1999); (Jastroch et al. 2004).

In this study we searched for the presence of BAT and UCP1 in one South American (*M. domestica*) and two Australian marsupial species (*S. crassicaudata* and *A. flavipes*). Our approach was to search the genomic trace archives of the National Center for Biotechnology Information for UCP-like sequence fragments of *M .domestica*, to screen a genomic library and to annotate the sequence by genomic mapping and gene analysis. Subsequent studies on gene expression strongly suggested that an archetypal BAT existed before the divergence of eutherian and marsupial mammals 150 MYA.

Materials and Methods

Isolation of genomic DNA of *M. domestica* and polymerase chain reactions

DNA was isolated from a tail tip of a female adult *M. domestica* using a standard phenol-chloroform extraction protocol as described previously (Jastroch et al. 2004). 50ng of photometrically quantified DNA was subjected to polymerase chain reaction. A “eutherian” UCP1 consensus sequence was blasted against *M. domestica* whole genome shotgun data (http://www.ncbi.nlm.nih.gov/Traces/trace.fcgi) and led to the identification of several fragments with high identity to “eutherian” UCP1. The fragments were assembled according to the intron-exon structure of mouse *Ucp1*. Primers were generated (MWG Biotech, Ebersberg, Germany) to amplify a *UCP1*-like fragment.

“forEx3”: 5'-AGTGGCACAGCCTACAGATGT-3'

“revEx4”: 5'-CTTGGAACGTCATC ATGTTTG-3'

A second primer pair served to amplify a *M. domestica UCP2*-like fragment

"forUCP2": 5'-GCCTACAAGACTATTGCCCGAGAGGAG-3';

"revUCP2": 5'-AAGCGGAGAAAGGAAGGCATGAACCC-3'

40 cycles of denaturation at 94°C for 1 min, annealing at 54°C (or 58°C for UCP2) for 1 min, and extension at 72°C for 1 min (2 min for UCP2) were performed. A final extension at 72°C was applied for 10 min and followed by rapid cooling to 4°C. The PCR product was gel-purified and ligated into a pGEMT-easy vector (Promega) for sequencing. Intron-sequence was excised by gene SOEing (see suppl. 1) and used as a probe for Northern blotting. Nested oligonucleotides were used for the screening of a genomic *M. domestica* BAC library.

Mapping, sequencing and gene analysis of opossum clones

High density arrayed grids of the genomic opossum (*Monodelphis domestica*) BAC library VMRC-6 (Virginia Mason Research Center, distributed by BACPAC Resources, Oakland, CA; http://bacpac.chori.org) were screened by hybridization with radioactively end-labeled (T4-Polynucleotidekinase, Roche) oligonucleotides (Galgoczy et al. 2001):

The primers were:	md1.F	5'-GGGACTTTCCATGCCTACAA-3'	
	md2.R	5'-CAATAGCATTTCTTGCCACG-3'	
	md3.F	5'-AATAGCATCCGCAGAAGGAA-3'	
	md4.R	5'-CGTCCCTGGAAAGAGGAAAT-3'	(mdUCP1 specific)
and	md5.F	5'-CTCTTGCAGGTGGCATCC-3'	
	md6.R	5'-GACATTGGGCGAAGTTCCT-3'	(mdUCP2 specific).

The identified BACs were verified by PCR using the probe oligos as primers. BACs VMRC6-66F14 (GenBank Acc.no. AC171738, containing md*UCP*1) and VMRC6-60O3 (GenBank Acc.no. AC171737, containing md1*UCP2* and md*UCP3*) were sequenced by a combination of shotgun and directed approaches (Wen et al. 2005). Base calling and assembly were performed by Phred/Phrap. Finishing was performed in accordance to the Human Genome Project standards

(http://genomeold.wustl.edu/Overview/g16stand.php) with the support of external *Monodelphis domestica* whole genome shotgun data (http://www.ncbi.nlm.nih.gov/Traces/trace.fcgi).

Phylogenetic inference

We deduced the coding sequence and subsequently the amino acid sequence from the *M. domestica UCP1*, *UCP2* and *UCP3* genes. A comprehensive search for UCP sequences was performed in public databases (Ensembl genome browser, www.ensemb.org/ NCBI, www.ncbi.nlm.nih.gov) by employing the Blast algorithm (Altschul et al. 1990). An alignment of the UCP amino acid sequences was generated using ClustalX 1.81 (ftp://ftp-igbmc.u-strasbg.fr/pub/ClustalX) and converted into a *.nex* file. For Bayesian phylogenetic analyses, MRBAYES 3.1.2 (http://mrbayes.csit.fsu.edu/**)** was employed assuming the Whelan and Goldmann model combined with the Coversio-model (Ronquist and Huelsenbeck 2003). The analyses were run for 1,000,000 generations and trees sampled every 100th generation. Posterior probabilities were estimated on the last 3000 trees (burnin = 7000). The tree was illustrated using Treeview (http://taxonomy.zoology.gla.ac.uk/rod/treeview) and probabilities are shown as internal edge labels.

Animal Experiments

The gray short-tailed opossums (*Monodelphis domestica*) were kindly donated by P. Giere and U. Zeller (Museum für Naturkunde, Humboldt-Universität zu Berlin, Germany). The opossums were individually kept in the animal facility at the Philipps-Universität Marburg on a 12-hour/12-hour light/dark cycle at an ambient temperature (T_a) of 24 °C ± 2 °C (relative humidity: 40% to 50%) and fed cat food, curd mixed with fruit, and insects. For cold acclimation experiments, two individuals were transferred into a separate chamber maintained at 12°C for 14 days.

Seven yellow-footed Antechinus (*Antechius flavipes*) were captured with Elliott traps in several subtropical habitats in Southeast Queensland (Australia) between January and March 2005. Fourteen fat-tailed dunnarts (*Sminthopsis crassicaudata*) were obtained from a breeding colony at La Trobe University, Melbourne. All animals were housed individually in the animal facility of the University of Southern Queensland (12:12 light/dark, lights on at 0700h) with free access to water and food (mealworms and cat food mix including calcium carbonate). All animals were kept at 24°C. To investigate the effect of cold, seven *S. crassicaudata* and four *A. flavipes* were transferred to a climate chamber adjusted to 10°C for 17 – 22 days whereas the other individuals remained at 24°C. Ten *S. crassicaudata* used for COX activity assays were acclimated to 13.5 and 27.5°C in the animal facility of the University of Adelaide in November 1990.

Experimental protocols for the use of Australian marsupials were approved by the Animal Ethics Committee of the University of Southern Queensland, Queensland Environmental Protection Agency (permit number WISP02633304) and Environment Australia (export number WT2005-12380). Animal experiments involving *M. domestica* were performed in accordance with the German Animal Welfare Laws.

Tissue dissection

Two 22 and 25 days old *M. domestica* embryos were immediately frozen on dry ice and stored at –70°C prior to cryosectioning. All other individuals of *M. domestica, S. crassicaudata* and *A. flavipes* were euthanased (carbon dioxide) and tissues dissected. The samples were immediately snap frozen in liquid nitrogen. Frozen tissue samples were stored at –70°C. Liver, skeletal muscle and adipose tissue of *S. crassicaudata* and *A. flavipes* were shipped from Australia in liquid nitrogen to Marburg, Germany.

***In situ* hybridisation of *M. domestica* embryos**

Sagittal body sections (20 μm) were processed using a cryosectioning microtome (Leica CM 3050) and were transferred to precooled object slides. A riboprobe complementary to *M. domestica* UCP1 (225 bp; primers forEx3, revEx4) and UCP2 (350 bp; forUCP2, revUCP2) was generated from a linearised cloned cDNA. Radioactive riboprobes using [^{35}S]-UTP (1-2 x 10^7 cpm ml^{-1}), pre- and posthybridisation procedures were performed as described previously (Jastroch et al. 2007). Controls were performed by hybridising sections with equal length sense riboprobes of UCP1 and UCP2.

RNA isolation and reverse transcriptase - polymerase chain reaction

Total RNA was isolated with TRIzol (GIBCO-BRL) according to the manufacturer's protocol. As an additional step, the RNA pellet was redissolved in a solution containing 6.3 mol L^{-1} guanidinium thiocyanate, 40 mmol L^{-1} sodium citrate pH 7, 0.8% sarcosyl, 8 mmol L^{-1} 2-mercaptoethanol, precipitated with 1 volume isopropanol, washed in 75% ethanol, and finally dissolved in DEPC-treated water. Total RNA was photometrically quantified at 260 nm and stored at –70°C. The isolated RNA was used for first strand cDNA synthesis (SUPERSCRIPT II, GIBCO/BRL) according to the manufacturer's protocol.

M. domestica UCP1 primers 5'-AGGTGAAGCCCAGACCATGGAT-3'

5'-GGCTGACACAAAGTGGCAAGGT-3'

comprising 6.7 kb of the *UCP1* gene and resulting in 550 bp cDNA sequence, were subjected to polymerase chain reaction with cDNAs of selected tissues. 40 cycles of 94°C (1 min), 59°C (1 min) and 72°C (1 min) were performed and terminated by a 10 min extension at 72°C. The PCR products were gel-purified and ligated into a pJET vector (Fermentas).

The full coding sequence of *S. crassicaudatastica* UCP1 including 5'- and 3'-UTR was amplified using the smart RACE cDNA amplification kit (Clontech) combined with gene specific primers deduced from *M. domestica*

UCP1 3'-UTR: 5'-CTACAGATGTGGTGAAAGTCAGAC-3'

5'-UTR: 5'-GGCTGACACAAAGTGGCAAGGT-3'.

Northern blot analysis

RNA was electrophoresed, blotted on a nylon membrane and hybridised as described previously (Jastroch et al. 2004). After hybridization, the blots were washed with 2x SSC/0.1% SDS for 20 min, 1x SSC/0.1% SDS for 10 min, 0.5x SSC/0.1% SDS for 10 min at room temperature, blots where then transferred to 0.1x SSC/0.1% SDS and washed for 10 min at 60°C. Signal intensities were then monitored by exposure to a PhosphorScreen (Molecular Dynamics). The hybridized probes were then detected by phosphor imaging (Storm 860, Molecular Dynamics), and signal intensities were quantified using ArrayVision 7.0 (Imaging Research). Ethidium bromide staining of total RNA served to normalize gel loading.

Cytochrome c oxidase (COX) activity

COX activity of interscapular fat deposits was measured polarographically at 25°C with a Hansa Tech oxygen electrode chamber as described in (Heldmaier and Buchberger 1985) and (Klaus et al 1988).

Statistical Analysis

Values are means ± S.E.M. The Mann-Whitney U test was applied for two-sample comparisons. Results were considered statistically significant at $P < 0.05$.

Results

Identification of UCP1 in M. domestica

We initially searched the *M. domestica* trace archives provided by the National Center for Biotechnology Information for *UCP*-like sequence fragments using a consensus UCP1 coding sequence deduced from available eutherian sequences. A 346 bp fragment was amplified from genomic DNA of *M. domestica* containing an 121 bp intron. The 225 bp partial coding sequence displayed highest identity to eutherian UCP1 (76%) but lower similarity to eutherian UCP2 and UCP3 (69%). A second fragment was amplified using UCP2 primers exhibiting high identity to UCP2 of *A. flavipes* (92%) (summarized in suppl. 1). A genomic *M. domestica* BAC library was screened using homologous primers deduced from the cloned *UCP* fragments. The isolated BAC clones were sequenced, genes analysed and physically mapped (Fig. 1). VMRC6-66F14 (GenBank AC171738) contained a *UCP1*-like gene and VMRC6-60O3 (GenBank *AC171737*) contained *UCP2* and *UCP3*. Compared to the corresponding human UCP orthologues, the deduced amino acid sequence of *M. domestica* UCP2 exhibited highest identity (91%; 95% similarity), followed by *M. domestica* UCP3 (82%; 90% similarity) and *M. domestica* "UCP1-like" (65%; 77% similarity). The protein blast algorithm (http://www.ncbi.nlm.nih.gov/blast) could resolve the position of the *UCP1*-like gene product relating it closer to *H. sapiens* UCP2 than to *H. sapiens* UCP1.

For genomic annotation, we characterized the *M. domestica UCP* genes by physical mapping. The *UCP1*-like gene of BAC clone VMRC6-66F14 was flanked by highly conserved orthologues of human ELMOD2 and human KIAA0882 thereby displaying syntenic regions identical to human *UCP1*. Conserved synteny of the *UCP1* locus in vertebrates unequivocally identified *M. domestica UCP1* as an orthologue of human *UCP1*. *M. domestica UCP2* and *UCP3* were not only found in a juxtaposition as human *UCP2* and *UCP3* but were also enclosed by the orthologues of human DNAJB13 and DKFZP586P0123.

We searched in 10 kb genomic sequence upstream of the transcriptional start *M. domestica* for the presence of the enhancer box containing response elements which are crucial for tissue-specific and cold-induced UCP1 expression in eutherians (Silva and Rabelo 1997). We identified the enhancer box in all eutherians under investigation by plotting the *UCP1* upstream region of the mouse against the other species (suppl. 2). Using this method, the enhancer box could not be identified in the upstream region of *M. domestica*.

Phylogenetic inference

For the classification of the UCP sequences from *M. domestica*, we generated a phylogenetic tree using Bayesian statistics. Our comprehensive search for UCPs in public databases resulted in 81 UCP sequences in the animal kingdom. Phylogenetic inference including *M. domestica* UCP1 resolved phylogenetic relations within in the UCP family (Fig. 2A, simplified to major vertebrate groups). In contrast to previously published phylogenetic trees, the addition of further UCP1 sequences including the *M. domestica* sequence and the use of Bayesian statistics clearly clustered fish UCP1 to the UCP1 orthologues. The UCP1 branch is featured in Fig. 2B, the full tree can be viewed in suppl. 3. The position of *M. domestica* UCP1 between monotremes (represented by the platypus) and eutherian mammals reflects the phylogeny of species. In contrast, UCP1 of the Afrotherian species, *Echinops telfairi*, is expected at the base of placental mammals but clustered with the rodent UCP1. The branch lengths are mean branch lengths of the consensus tree representing substitution rates. Notably, the branch length between *M. domestica* UCP1 and eutherian UCP1 is exceptionally long reflecting a high substitution rate. While the distance to ectotherm amphibian UCP1 is 0.125 relative units, the distance to eutherian UCP1 is 0.25 relative units. In contrast, the branch length of marsupial UCP2 and UCP3 is shorter to eutherians than to the orthologues in ectotherms.

Tissue-specific expression in the South American marsupial M. domestica

Based on the identification of the *UCP1* gene in *M. domestica*, we investigated UCP1 gene expression. We first performed whole-body *in situ* hybridisation of a 22- and a 25-day old embryo and show the lack of UCP1 expression (Fig. 3A). UCP2 mRNA was ubiquitously expressed with highest levels in spleen, heart and liver. Non-specific signals, as judged by comparing to the sense-control, occured in calcified bone tissue.

We then acclimated two 12-weeks old *M. domestica* to 12°C for fourteen days while two individuals remained at 24°C. Using a *M. domestica* UCP1 cDNA fragment as a probe, we detected no UCP1 mRNA in any tissue of CA and WA individuals (Fig. 3B). Post-hybridization procedures under less stringent conditions visualized cross-reactivity to mouse UCP1 in BAT whereas *M. domestica* UCP1 remained undetectable. Notably, UCP1 mRNA expression in the interscapular fat, a typical BAT site in eutherians, was undetectable in CA individuals. When hybridised with a *M. domestica* UCP2 probe, we detected mRNA in all fat tissues, spleen and intestine. UCP2 mRNA levels in interscapular fat were not upregulated during exposure. We finally sampled 14 different tissues from a juvenile (70 days, post nest vacation). Dispersed adipose tissue deposits (brownish appearance) were found on the ribcage of a juvenile embedded in between pectoral muscle fibres (pectoral fat). We isolated RNA and subjected the corresponding cDNAs to polymerase chain reaction. *M. domestica* UCP1 primers comprising 6.7 kb of genomic sequence were used to amplify a 550 bp cDNA fragment in adipose tissue embedded in the breast region (Fig. 3A). Subsequent sequencing clearly identified UCP1 cDNA. Expression levels were low as Northern blotting analysis with a UCP1 probe was insensitive (data not shown).

Tissue-specific expression in the Australian marsupials S. crassicaudata and A. flavipes

In *S. crassicaudata*, we detected UCP1 mRNA using the *M. domestica* UCP1 probe (Fig. 3 A). On the representative blot, we subjected total RNA from liver, skeletal muscle and interscapular fat of a WA (24°C) and a CA (10°C) *S. crassicaudata* and *A. flavipes*. The UCP1 probe detected expression exclusively in the interscapular fat deposit of *S. crassicaudata*. Notably, UCP1 was not detectable in interscapular fat of *A. flavipes*. To confirm the absence of UCP1 mRNA expression in *A. flavipes*, we repeated Northern blot analysis on selected tissues including interscapular fat deposits of all *A. flavipes* kept at 10°C. However, when probed with a UCP2 fragment cloned from *Sminthopsis macroura* (Jastroch et al. 2004), we detected highest UCP2 mRNA levels in the interscapular fat region of *S. crassicaudata* and *A. flavipes* whereas mRNA levels in liver and skeletal muscle were rather low. Cross-reactivity of the UCP1 probe to UCP2 could be excluded as the UCP1 probe exhibited only 61 to 69% identity to *Sminthopsis* and *Antechinus* UCP2, respectively. Using a *A. flavipes* UCP3 probe, we detected UCP3 mRNA in skeletal muscle of both species confirming a previous study (Jastroch et al. 2004).

Primers leading to the amplification of *M. domestica* cDNA were used to amplify a 250 bp UCP1 cDNA fragment of *S. crassicaudata*. Using 5'- and 3'-RACE-PCR, we identified 1386 bp of UCP1 transcript including the full coding sequence (Genbank Acc. No. EF622232). The deduced protein sequence was included in the phylogenetic inference and an alignment of the *S. crassicaudata* UCP1 coding sequence showed highest identity with *M. domestica* UCP1 (92%), lower identity to eutherian and marsupial UCP2 and UCP3 (70 –75%) (suppl. 3).

Effect of cold exposure on BAT of S. crassicaudata

Adaptive NST in rodents requires the recruitment of mitochondria and UCP1 to increase heat production. In a pilot study on *S. crassicaudata* in 1990, we found a tendency towards increased COX activity in the interscapular fat deposit of CA individuals (Fig. 4B) but we were not able to

detect UCP1 mRNA by Northern blotting using a rat UCP1 cDNA probe, even under low stringency (data not shown). In the present study, we isolated total RNA from the interscapular fat deposit of *S. crassicaudata* and by using a marsupial UCP1 probe, we demonstrated an up-regulation of UCP1 gene expression in response to cold. UCP1 mRNA levels of CA *S. crassicaudata* increased 2-fold ($n = 7$, $p = 0.018$) (Fig. 4C). Furthermore, appearance of the interscapular fat deposit changed from white to brown in of *S. crassicaudata* (Fig. 4D), a transition that was absent in *M. domestica* and *A. flavipes* (unpublished observation).

Discussion

The successful radiation of eutherian mammals to cold environments may have been facilitated by classical adaptive NST depending on BAT and its crucial protein UCP1 (Cannon and Nedergaard 2004). However the origin and evolution of the thermogenic organ is unknown. Whereas UCP1 and BAT were regarded as absent in marsupials (Dawson and Olson 1988); (Hayward and Lisson 1992); (Jastroch et al. 2004); (Kabat et al. 2003a); (Kabat et al. 2003b); (Nicol et al. 1997); (Schaeffer et al. 2003), this study represents the first unequivocal demonstration of UCP1 gene expression in adipose tissue of both South American and Australian marsupials.

Conserved genomic synteny unambiguously identifies the three *M. domestica UCP* genes as orthologues of eutherian *UCP1, UCP2* and *UCP3*. Although an ancestral UCP1 orthologue appears in the vertebrate lineage as early as the divergence of ray-finned and lobe-finned fish 460 million years ago (Jastroch et al. 2005), UCP1 went extinct during evolution in the bird lineage (e.g. the chicken genome, unpublished observation) and rendered function in eutherian pigs (Berg et al. 2006). In previous studies, phylogenetic approaches could not resolve the position of fish UCP1 within the evolutionary tree, indicating a weak node between fish UCP1 and the UCP2/3 subgroup which was likely to collapse (Jastroch et al. 2004); (Jimenez-Jimenez et al. 2006). The addition of further sequences including UCP1 of *M. domestica* and application of the Bayesian method for phylogenetic inference allows for the first time a solid reconstruction of the UCP1, UCP2 and UCP3 subgroups with fish UCP1 clearly clustering to the UCP1 orthologues. In contrast to UCP2 and UCP3, the phylogenetic distance of UCP1 orthologues between marsupials and eutherians is longer, reflecting higher mutation rate as an indicator for rapidly driven evolution.

The physiological role of the ancient fish UCP1 is unknown so far and may be other than heat production. Functional studies suggested that carp UCP1 is a functional uncoupling protein with broadly the same activatory and inhibitory characteristics as mammalian UCP1 (Jastroch et al. 2007). During evolution, UCP1 may have changed the physiological function towards heat production. For this reason, the finding of marsupial UCP1 is not only remarkable as previous studies failed to demonstrate UCP1 in marsupials but also represents a protein sequence intermediate to ectothermic fish UCP1 and the highly thermogenic placental UCP1. Natural mutation and selection of UCP1 favouring increased thermogenic function offers new insights into protein function by projecting mutations inserted by natural selection onto structure-function relationships.

In *M. domestica*, we only found UCP1 mRNA in dispersed adipose tissue deposits around the ribcage of a juvenile embedded in between pectoral muscle fibres suggesting that physiological significance of UCP1 is restricted to a short time frame during ontogeny. We did not detect UCP1 expression in ectothermic embryos and surprisingly, we also found no cold-induced UCP1 mRNA expression in the interscapular fat deposit, which is a typical region for BAT in eutherians. Although the observed expression pattern in *M. domestica* is different from rodents, we have to consider that numerous eutherians do not possess significant amounts of BAT during their whole lifespan. Rabbits lose the ability to express UCP1 one month after birth (Cambon 1998), in bovine and lambs UCP1 expression is of significance only two days after physiological birth (Casteilla 1989). BAT in marsupials may therefore only be of importance to overcome cold-stress around pouch or nest vacation. Noradrenaline responses coincide with pouch vacation as shown in the wallaby (Loudon et al. 1985) or in the Eastern barred bandicoot (*Perameles gunnii*) (Ikomnomoupoulou 2006). With the identification of marsupial UCP1 in this study, these observations can be revisited and the contribution of BAT investigated. Marsupials provide an excellent model to study the significance of BAT in NST during early ontogeny as the living exteriorised fetus can be easily investigated.

In rodents and humans, an enhancer box in the upstream promotor region contains condensed elements targeting UCP1 expression to BAT and allows responsiveness to the cold (for review see (Silva and Rabelo 1997)). The fish *UCP1* gene lacks the enhancer box and not surprisingly, carp UCP1 is only expressed in liver and brain but not in adipose tissue (Jastroch et al. 2005). We searched the promotor upstream region of the *M. domestica UCP1* gene *in silico* for causative response elements. Our search for the enhancer box controlling BAT-specific UCP1 expression revealed a clear conservation among eutherians (even in the ancient Afrotherian species *Echinops telfairi*). *M. domestica* lacks this distinct region suggesting that the enhancer box is an invention of eutherian mammals. However, the respective response elements may be dispersed across the promotor upstream region and the presence cannot be categorically excluded.

Despite the lack of the enhancer box, marsupial UCP1 shows a remarkably high tissue-specificity targeting gene expression to distinct adipose tissue sites of *M. domestica* and *S. crassicaudata*. Furthermore, *S. crassicaudata* UCP1 gene expression responds to cold exposure.

In contrast to the South American marsupial, we clearly demonstrate cold-induced UCP1 expression in the interscapular fat deposit of the adult *S. crassicaudata*. One might speculate, that phylogenetic distance of Southamerican and Australian marsupials which diverged 80 MYA may explain differences in UCP1 expression between *M. domestica* and *S. crassicaudata*. Our approach to compare two Australian dasyurids, *S. crassicaudata* and *A. flavipes*, under identical conditions demonstrate that different physiological significance is not dependent on phylogeny. *A. flavipes* and *S. crassicaudata* both belong to the Dasyuridae and diverged only about 25 million years ago. Based on the close relation, we expected to find UCP1 expression in both species but we show that *S. crassicaudata* expresses UCP1 whereas *A. flavipes* lacks UCP1 in the interscapular fat.

Previous studies in *Sminthopsis* and *Antechinus* species support the interdependence of NST and marsupial UCP1. In accordance with the presence of BAT, *Sminthopsis spec.* elevate metabolic rate by 30% in response to 0.25 mg kg^{-1} noradrenaline at 24°C (*S. crassicaudata*) (Clements 1998), or in response to cold exposure (*S. macroura*) (Geiser 2001). In contrast, *Antechinus stuartii*, a close relative of *A. flavipes* does not show a thermogenic response to NA (Reynolds and Hulbert 1982).

Why is UCP1 and BAT required in one species whereas the closely related species seemingly relies on alternative thermogenic mechanisms? Firstly, the dependence of BAT content and NST capacity is dependent on body size as shown for eutherians (Heldmaier 1971). Therefore, we have to consider that *S. crassicaudata* is significantly smaller (~18 g) than *A. flavipes* (~32 g). Secondly, *A. flavipes* was trapped in subtropical rainforest areas of Queensland with higher annual temperatures ranging between 10°C to 30°C whereas *S. crassicaudata* can be found in dry grassland throughout the southern half of Australia diplaying lower annual mean temperatures and distinctive seasons. Body size and environmental temperature are both important affectors of NST capacity which may have selected species-specific for BAT in mature mammals.

Despite some evidence for NST in *S. crassicaudata*, studies demonstrating adaptive NST in response to cold are definitely lacking. In CA *S. crassicaudata* of this study, we observed a transition from white to brown appearance of interscapular fat, increased oxidative capacity and UCP1 expression resembling the situation as found for cold-activated BAT in rodents. Induced oxidative capacity and UCP1 expression provide the thermogenic machinery that strongly suggests the presence of adaptive thermogenesis. The identification of BAT in *S. crassicaudata* now provides the basis to confirm the presence of adaptive NST in marsupials.

A distinct difference to eutherians is the lack of UCP1 in adult *A. flavipes* and *M. domestica*. As mentioned, differences in the development of BAT also occur within the eutherian trait but based

on our knowledge from eutherians, we would have expected BAT in these small marsupials in the size range of mice and rats. Alternative heating mechanisms must have evolved in marsupials which are independent of BAT and complement heat production. The identification of these mechanisms in *M. domestica* and *A. flavipes* may be of general significance in endotherms as birds also lack BAT.

Taken together, we unequivocally identified UCP1 in marsupials. In some marsupials UCP1 may be recruited transiently during early stages of development and is lost during adulthood. *S. crassicaudata* recruits BAT in the cold and represents a model to investigate adaptive nonshivering thermogenesis in marsupials. In this study, the characterization of BAT in different marsupials provides the basis for further studies on the physiological significance and evolution of UCP1-mediated NST.

Our results demonstrate the evolution of an archetypal BAT before the divergence of marsupials and eutherians more than 150 million years ago that may have given early mammals the advantage to persist in the cold.

Acknowledgements

This research was supported by Deutsche Forschungsgemeinschaft DFG KL973/7 (to M. K.) and by the *Centre for rural and environmental biology*, Department of Biological and Physical Sciences, University of Southern Queensland (to K.W. and M.J.). We thank Sigrid Stöhr for excellent technical assistance.

References

1. **Altschul, S. F., Gish, W., Miller, W., Myers, E. W., and Lipman, D. J.** (1990). Basic local alignment search tool. *J Mol.Biol*, **215**, 403-410.
2. **Aquila, H., Link, T. A., and Klingenberg, M.** (1985). The uncoupling protein from brown fat mitochondria is related to the mitochondrial ADP/ATP carrier. Analysis of sequence homologies and of folding of the protein in the membrane. *EMBO J*, **4**, 2369-2376.
3. **Berg, F., Gustafson, U., and Andersson, L.** (2006). The uncoupling protein 1 gene (UCP1) is disrupted in the pig lineage: a genetic explanation for poor thermoregulation in piglets. *PLoS Genet.*, **2**, e129-
4. **Bininda-Emonds, O. R., Cardillo, M., Jones, K. E., MacPhee, R. D., Beck, R. M., Grenyer, R., Price, S. A., Vos, R. A., Gittleman, J. L., and Purvis, A.** (2007). The delayed rise of present-day mammals. *Nature*, **446**, 507-512.
5. **Bouillaud, F., Ricquier, D., Thibault, J., and Weissenbach, J.** (1985). Molecular approach to thermogenesis in brown adipose tissue: cDNA cloning of the mitochondrial uncoupling protein. *Proc.Natl.Acad.Sci.U S A*, **82**, 445-448.
6. **Cannon, B. and Nedergaard, J.** (2004). Brown adipose tissue: function and physiological significance. *Physiol Rev.*, **84**, 277-359.
7. **Clements, F., Hope, P. J., Daniels, C. B., Chapman, I., and Wittert, G.** (1998). Thermogenesis in the marsupial *Sminthopsis crassicaudata*: effect of catecholamines and diet. *Aust J Zool*, **46**, 381-390-
8. **Dawkins, M. J. R. and Hull, D.** (1964). Brown adipose tissue and the response of new-born rabbits to cold. *J Physiol*, **172**, 216-238.
9. **Dawson, T. J. and Dawson, W. R.** (1982). Metabolic scope and conductance in response to cold of some dasyurid marsupials and australian rodents. *Comp Biochem Physiol*, **71A**, 59-64.
10. **Dawson, T. J. and Olson, J. M.** (1988). Thermogenic capabilities of the opossum Monodelphis domestica when warm and cold acclimated: similarities between American and Australian marsupials. *Comp Biochem Physiol A*, **89**, 85-91.
11. **Galgoczy, P., Rosenthal, A., and Platzer, M.** (2001). Human-mouse comparative sequence analysis of the NEMO gene reveals an alternative promoter within the neighboring G6PD gene. *Gene.*, **271**, 93-98.
12. **Geiser, F., Drury, R. L., McAllan, B. M., and Wang, D. H.** (2003). Effects of temperature acclimation on maximum heat production, thermal tolerance, and torpor in a marsupial. *Journal of comparative physiology.B, Biochemical, systemic, and environmental physiology.*, **173**, 437-442.
13. **Gesner, C.** (1551). *Medici Tigurini Historiae Animalium Liber I de Quadrupedibusuiuiparis*, 840-844.
14. **Golozoubova, V., Hohtola, E., Matthias, A., Jacobsson, A., Cannon, B., and Nedergaard, J.** (2001). Only UCP1 can mediate adaptive nonshivering thermogenesis in the cold. *FASEB J*, **15**, 2048-2050.

15. **Hayward, J. S. and Lisson, P. A.** (1992). Evolution of brown fat: its absence in marsupials and monotremes. *Can J Zool*, **70**, 171-179.

16. **Heaton, G. M., Wagenvoord, R. J., Kemp, A., and Nicholls, D. G.** (1978). Brown-adipose-tissue mitochondria: photoaffinity labelling of the regulatory site of energy dissipation. *Eur J Biochem*, **82**, 515-521.

17. **Heldmaier, G.** (1971). Zitterfreie Wärmebildung und Körpergröbe bei Säugetieren. *Z vergl Physiol*, **73**, 222-248.

18. **Hope, P. J., Pyle, D., Daniels, C. B., Chapman, I., Horowitz, M., Morley, J. E., Trayhurn, P., Kumaratilake, J., and Wittert, G.** (1997). Identification of brown fat and mechanisms for energy balance in the marsupial, Sminthopsis crassicaudata. *American Journal of Physiology*, **42**, R161-R167.

19. **Jastroch, M., Buckingham, J. A., Helwig, M., Klingenspor, M., and Brand, M. D.** (2007). Functional characterisation of UCP1 in the common carp: uncoupling activity in liver mitochondria and cold-induced expression in the brain. *Journal of comparative physiology.B, Biochemical, systemic, and environmental physiology.*, **DOI 10.1007/s00360-007-0171-6**,

20. **Jastroch, M., Withers, K., and Klingenspor, M.** (2004). Uncoupling protein 2 and 3 in marsupials: identification, phylogeny, and gene expression in response to cold and fasting in *Antechinus flavipes*. *Physiol Genomics*, **17**, 130-139.

21. **Jastroch, M., Wuertz, S., Kloas, W., and Klingenspor, M.** (2005). Uncoupling protein 1 in fish uncovers an ancient evolutionary history of mammalian nonshivering thermogenesis. *Physiol Genomics*, **22**, 150-156.

22. **Jimenez-Jimenez, J., Zardoya, R., Ledesma, A., Garcia, de Lacoba, Zaragoza, P., Mar Gonzalez-Barroso, M., and Rial, E.** (2006). Evolutionarily distinct residues in the uncoupling protein UCP1 are essential for its characteristic basal proton conductance. *J Mol.Biol*, **359**, 1010-1022.

23. **Kabat, A. P., Rose, R. W., Harris, J., and West, A. K.** (2003a). Molecular identification of uncoupling proteins (UCP2 and UCP3) and absence of UCP1 in the marsupial Tasmanian bettong, Bettongia gaimardi. *Comp Biochem Physiol B Biochem Mol Biol*, **134**, 71-77.

24. **Kabat, A. P., Rose, R. W., and West, A. K.** (2003b). Non-shivering thermogenesis in a carnivorous marsupial Sarcophilus harrisii, in the absence of UCP1. *Journal of Thermal Biology*, **28**, 413-420.

25. **Loncar, D., Afzelius, B. A., and Cannon, B.** (1988a). Epididymal white adipose tissue after cold stress in rats. I. Nonmitochondrial changes. *J Ultrastruct.Mol.Struct.Res.*, **101**, 109-122.

26. **Loncar, D., Afzelius, B. A., and Cannon, B.** (1988b). Epididymal white adipose tissue after cold stress in rats. II. Mitochondrial changes. *J Ultrastruct.Mol.Struct.Res.*, **101**, 199-209.

27. **Loudon, A. S. I., Rothwell, N. J., and Stock, M. J.** (1985). Brown fat, thermogenesis and physiological birth in a marsupial. *Comp Biochem Physiol*, **81A**, 815-819.

28. **May, E. L.** (2003). Effects of cold acclimation on shivering intensity in the kowari (Dasyuroides byrnei), a dasyurid marsupial. *Journal of Thermal Biology*, **28**, 477-487.

29. **Nicholls, D. G. and Locke, R. M.** (1984). Thermogenic mechanisms in brown fat. *Physiol Rev*, **64**, 1-64.

30. **Nicol, S. C.** (1978). Non-shivering thermogenesis in the potoroo, Potorous tridactylus (Kerr). *Comp Biochem Physiol*, **59**, 33-37.

31. **Nicol, S. C., Pavlides, D., and Andersen, N. A.** (1997). Nonshivering thermogenesis in marsupials: Absence of thermogenic response to beta 3-adrenergic agonists. *Comp Biochem Physiol A*, **117**, 399-405.

32. **Oliphant, L. W.** (1983). First observations of brown fat in birds. *Condor*, **85**, 350-354.

33. **Opazo, J. C., Nespolo, R. F., and Bozinovic, F.** (1999). Arousal from torpor in the chilean mouse-opposum (Thylamys elegans): does non-shivering thermogenesis play a role? *Comp Biochem Physiol A Mol Integr Physiol*, **123**, 393-397.

34. **Reynolds, W. and Hulbert, A. J.** (1982). Cold acclimation in a small dasyurid marsupial: Antechinus stuartii. (ed. Archer, M.), pp. 278-283. Mosman, N.S.W.: Royal Zoological Society of NSW.

35. **Ricquier, D. and Kader, J. C.** (1976). Mitochondrial protein alteration in active brown fat: a soidum dodecyl sulfate-polyacrylamide gel electrophoretic study. *Biochem Biophys.Res.Commun.*, **73**, 577-583.

36. **Ricquier, D., Raimbault, S., Champigny, O., Miroux, B., and Bouillaud, F.** (1992). Comment to Shinohara et al. (1991) FEBS Letters 293, 173-174. The uncoupling protein is not expressed in rat liver. *FEBS Lett.*, **303**, 103-106.

37. **Ronquist, F. and Huelsenbeck, J. P.** (2003). MrBayes 3: Bayesian phylogenetic inference under mixed models. *Bioinformatics*, **19**, 1572-1574.

38. **Rose, R. W., West, A. K., Ye, J. M., McCormick, G. H., and Colquhoun, E. Q.** (1999). Nonshivering thermogenesis in a marsupial (the tasmanian bettong Bettongia gaimardi) is not attributable to brown adipose tissue. *Physiological and biochemical zoology : PBZ.*, **72**, 699-704.

39. **Schaeffer, P. J., Villarin, J. J., and Lindstedt, S. L.** (2003). Chronic cold exposure increases skeletal muscle oxidative structure and function in Monodelphis domestica, a marsupial lacking brown adipose tissue. *Physiol.Biochem Zool*, **76**, 877-887.

40. **Silva, J. E. and Rabelo, R.** (1997). Regulation of the uncoupling protein gene expression. *Eur.J Endocrinol.*, **136**, 251-264.

41. **Smith, R. E.** (1962). Thermoregulation by brown adipose tissue in cold. *Fed Proc*, **21**, 221-221.

42. **Wen, G., Ramser, J., Taudien, S., Gausmann, U., Blechschmidt, K., Frankish, A., Ashurst, J., Meindl, A., and Platzer, M.** (2005). Validation of mRNA/EST-based gene predictions in human Xp11.4 revealed differences to the organization of the orthologous mouse locus. *Mamm.Genome*, **16**, 934-941.

43. **Ye, J. M., Edwards, S. J., Rose, R. W., Steen, J. T., Clark, M. G., and Colquhoun, E. Q.** (1996). alpha-adrenergic stimulation of thermogenesis in a rat kangaroo (Marsupialia, Bettongia gaimardi). *American Journal of Physiology*, **40**, R586-R592.

Figure legends

Fig.1: Conservation of *UCP1*, *UCP2*, *UCP3* and their flanking genes between human and opossum (*M. domestica*).

Fig. 2: Phylogenetic relations of the core UCP family in vertebrates including marsupial UCP1 (*M. domestica* and *S. crassicaudata*). An alignment of all available UCP sequences was analysed by MrBayes 3.1.2, assuming a Whelan and Goldmann model of evolution. Bayesian posterior probabilities are given at the branch nodes. A. Simplified tree resolving the phylogenetic relations of the core UCP family. The oxalacetate-malate carrier (OMCP) represents the outgroup. B. Detailed illustration of the UCP1 subgroup. Bayesian probabilities are given at the nodes and a scale for branch lengths is given next to the tree.

Fig. 3: Regulation of UCP1 and UCP2 gene expression in multiple tissues of the developing marsupial *M. domestica.* Homologous radioactively-labelled cDNA, riboprobes and primers were used.

A. Representative sagittal section showing whole-body in situ hybridisation of 22 – 25 old embryos. The UCP2 antisense riboprobe clearly hybridised with UCP2 mRNA in spleen, heart and liver while no UCP1 signals could be detected using a *M. domestica* UCP1 antisense riboprobe (left panel). All riboprobes hybridised artificially with calcified bone as judged by comparison to sense controls (right panel). A photograph of a sagittal transection served to assign radioactive signals to organs. B. Multiple tissue Northern blot analysis of three months old *M. domestica* incl. interscapular fat of WA and CA individuals (n = 4); and mouse BAT controls. Total RNA (10 μg) isolated from selected tissues was hybridised with a 225 bp UCP1 and a 350 bp *M. domestica* UCP2 cDNA fragment. Total RNA from mouse brown adipose tissue served as a control. Post-hybridisation for UCP1 was performed under less stringent conditions,

detecting mouse UCP1. The *M. domestica* UCP2 probe detected mRNA in spleen, inguinal and interscapular fat of *M. domestica*. C. Low levels of UCP1 cDNA detected by PCR in multiple tissues of a 70 days old juvenile. The 550 bp UCP1 fragment was amplified from adipose tissue embedded in the ribcage (pectoral fat). β-actin mRNA served as a cDNA quality control. Skm, skeletal muscle; int.fat, interscapular fat deposit; ing. fat, inguinal fat; ax. fat, axilliar fat.

Fig. 4: A. UCP expression in selected tissues of the marsupials *S. crassicaudata* and *A. flavipes*. Ten micrograms of total RNA were hybridised with a *M. domestica* UCP1, *S. macroura* (S.cr.) UCP2 and a *A. flavipes* (A. fl.) UCP3 probe. Skm, skeletal muscle; int.fat, interscapular fat deposit. B. COX activity in interscapular adipose tissue homogenates of WA and CA *S. crassicaudata*. C. The effect of cold exposure (10°C) on UCP1 gene expression in *S. crassicaudata*. Radioactive intensities of specific signals are shown as relative units corrected by ethidium bromide staining of the 18S rRNA. The effects of cold acclimation was evaluated by Mann Whitney U test; *$p < 0.05$. D. Appearance of interscapular fat due to cold exposure. The photograph shows a dorsal view on the interscapular fat deposits of a WA and a CA *S. crassicaudata*.

Figure 1

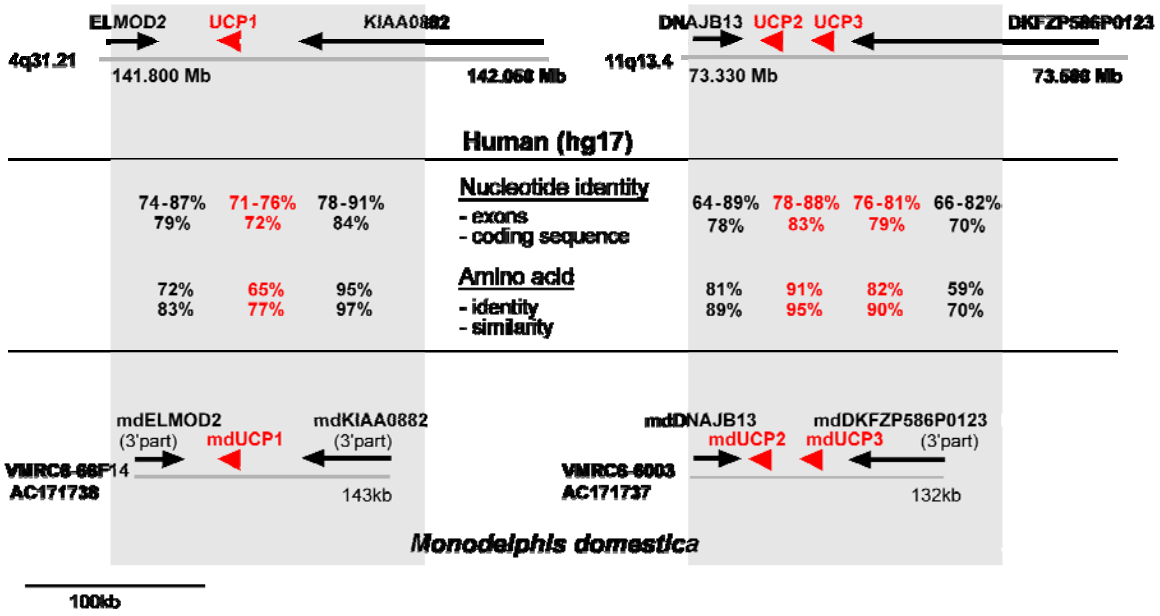
ELMOD2
UCP1
KIAA0882
4q31.21
141.800 Mb
142.068 Mb
DNAJB13
UCP2
UCP3
DKFZP586P0123
11q13.4
73.330 Mb
73.688 Mb
Human (hg17)
Nucleotide identity
- exons
- coding sequence
74-87%
79%
71-76%
72%
78-91%
84%
64-89%
78%
78-88%
83%
76-81%
79%
66-82%
70%
Amino acid
- identity
- similarity
72%
83%
65%
77%
95%
97%
81%
89%
91%
95%
82%
90%
59%
70%
mdELMOD2
(3'part)
mdUCP1
mdKIAA0882
(3'part)
VMRC6-68F14
AC171738
143kb
mdDNAJB13
mdUCP2
mdUCP3
mdDKFZP586P0123
(3'part)
VMRC6-6003
AC171737
132kb
Monodelphis domestica
100kb

Figure 2

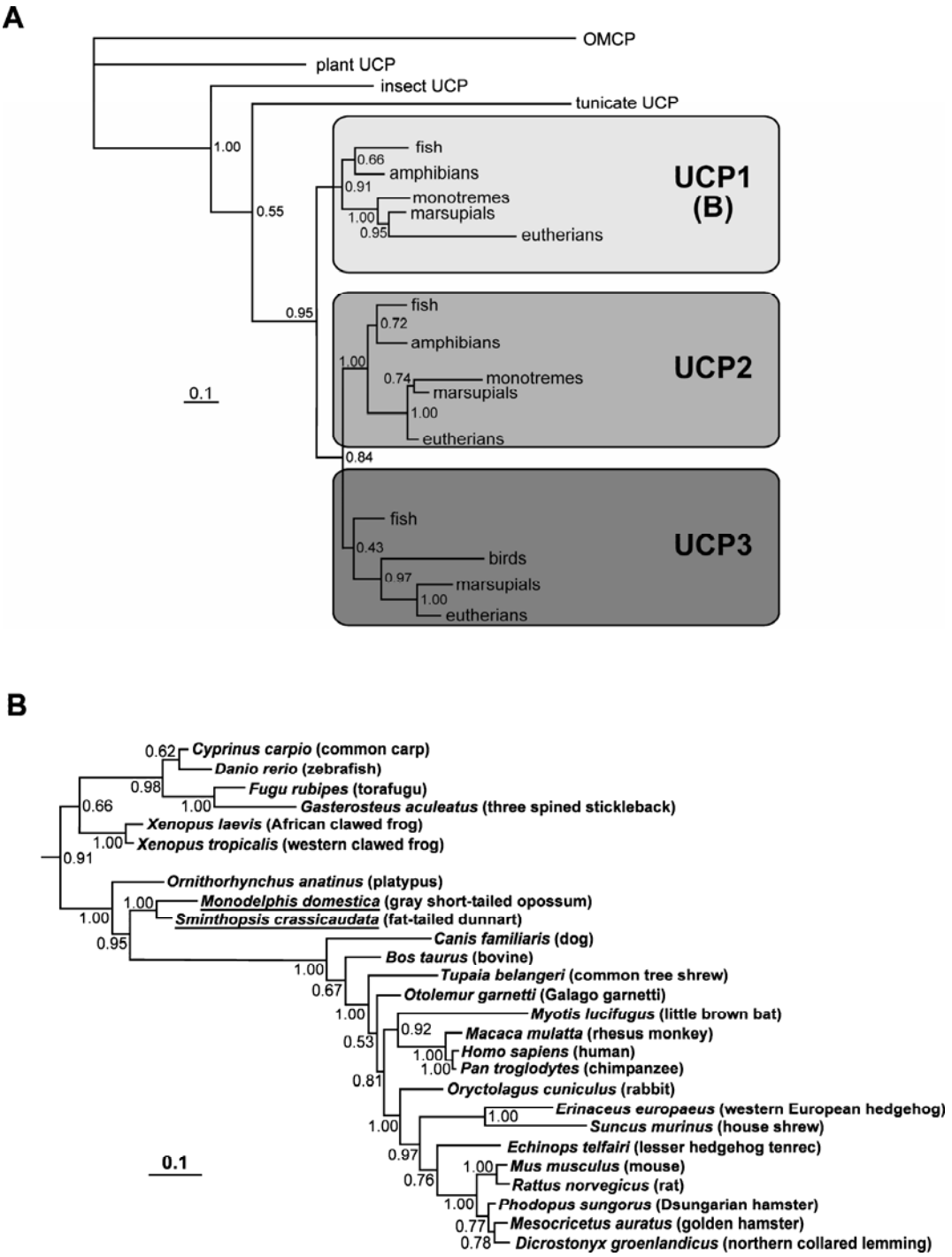
A
OMCP
plant UCP
insect UCP
tunicate UCP
1.00
0.55
0.95
0.84
fish
0.66
amphibians
0.91
monotremes
1.00
marsupials
0.95
eutherians
UCP1
(B)
fish
0.72
amphibians
1.00
0.74
monotremes
marsupials
1.00
eutherians
UCP2
0.1
fish
0.43
birds
0.97
marsupials
1.00
eutherians
UCP3
B
0.62
Cyprinus carpio (common carp)
Danio rerio (zebrafish)
0.98
Fugu rubipes (torafugu)
0.66
1.00
Gasterosteus aculeatus (three spined stickleback)
Xenopus laevis (African clawed frog)
1.00
Xenopus tropicalis (western clawed frog)
0.91
Ornithorhynchus anatinus (platypus)
1.00
Monodelphis domestica (gray short-tailed opossum)
1.00
Sminthopsis crassicaudata (fat-tailed dunnart)
0.95
Canis familiaris (dog)
1.00
Bos taurus (bovine)
Tupaia belangeri (common tree shrew)
0.67
Otolemur garnetti (Galago garnetti)
1.00
Myotis lucifugus (little brown bat)
0.92
0.53
Macaca mulatta (rhesus monkey)
1.00
Homo sapiens (human)
1.00
Pan troglodytes (chimpanzee)
0.81
Oryctolagus cuniculus (rabbit)
1.00
Erinaceus europaeus (western European hedgehog)
1.00
Suncus murinus (house shrew)
0.97
Echinops telfairi (lesser hedgehog tenrec)
1.00
Mus musculus (mouse)
0.76
Rattus norvegicus (rat)
1.00
Phodopus sungorus (Dsungarian hamster)
0.77
Mesocricetus auratus (golden hamster)
0.78
Dicrostonyx groenlandicus (northern collared lemming)
0.1

Figure 3

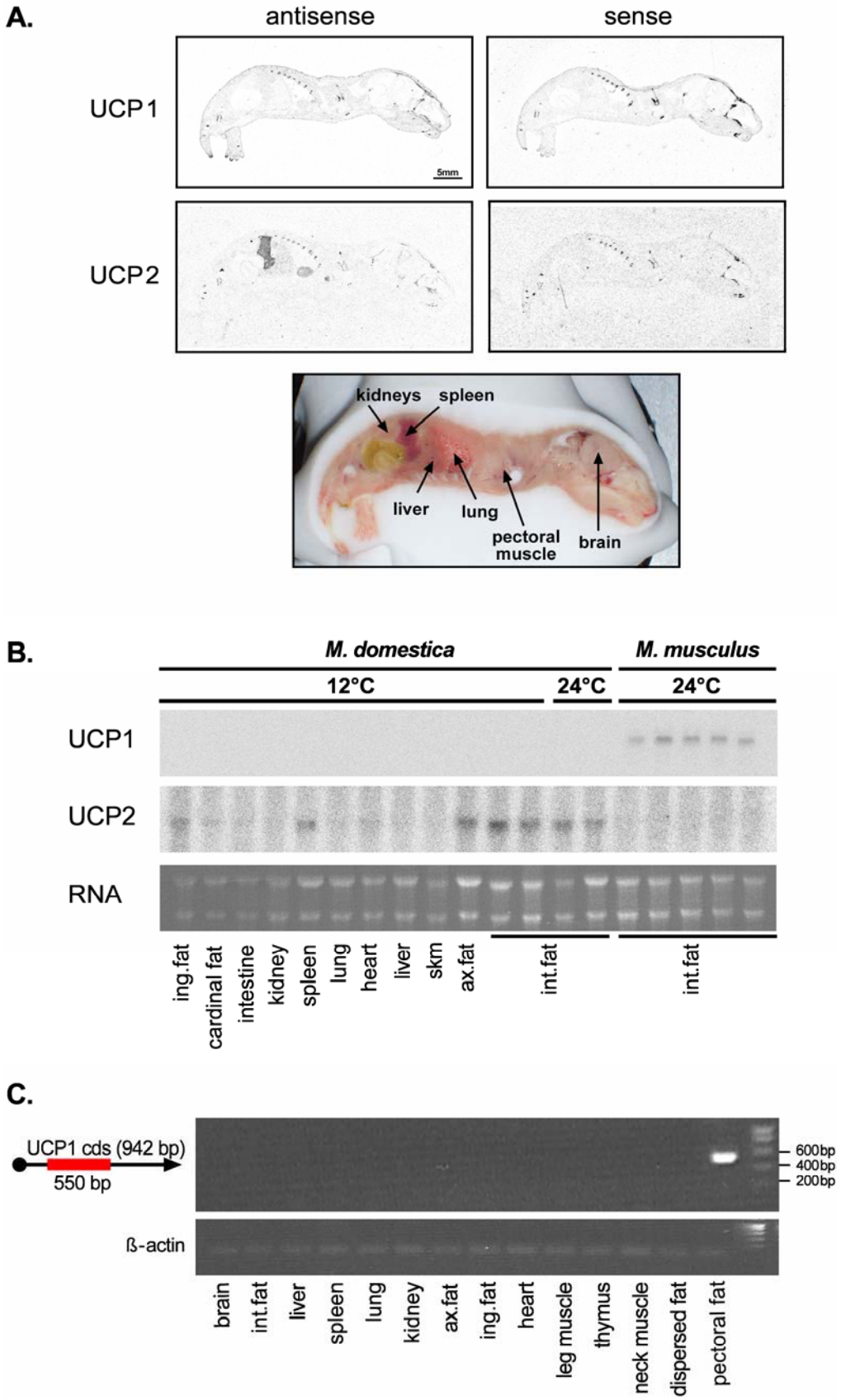
A.
antisense
sense
UCP1
UCP2
5mm
kidneys
spleen
liver
lung
pectoral muscle
brain
B.
M. domestica
M. musculus
12°C
24°C
24°C
UCP1
UCP2
RNA
ing.fat
cardinal fat
intestine
kidney
spleen
lung
heart
liver
skm
ax.fat
int.fat
int.fat
C.
UCP1 cds (942 bp)
550 bp
600bp
400bp
200bp
ß-actin
brain
int.fat
liver
spleen
lung
kidney
ax.fat
ing.fat
heart
leg muscle
thymus
neck muscle
dispersed fat
pectoral fat

Figure 4

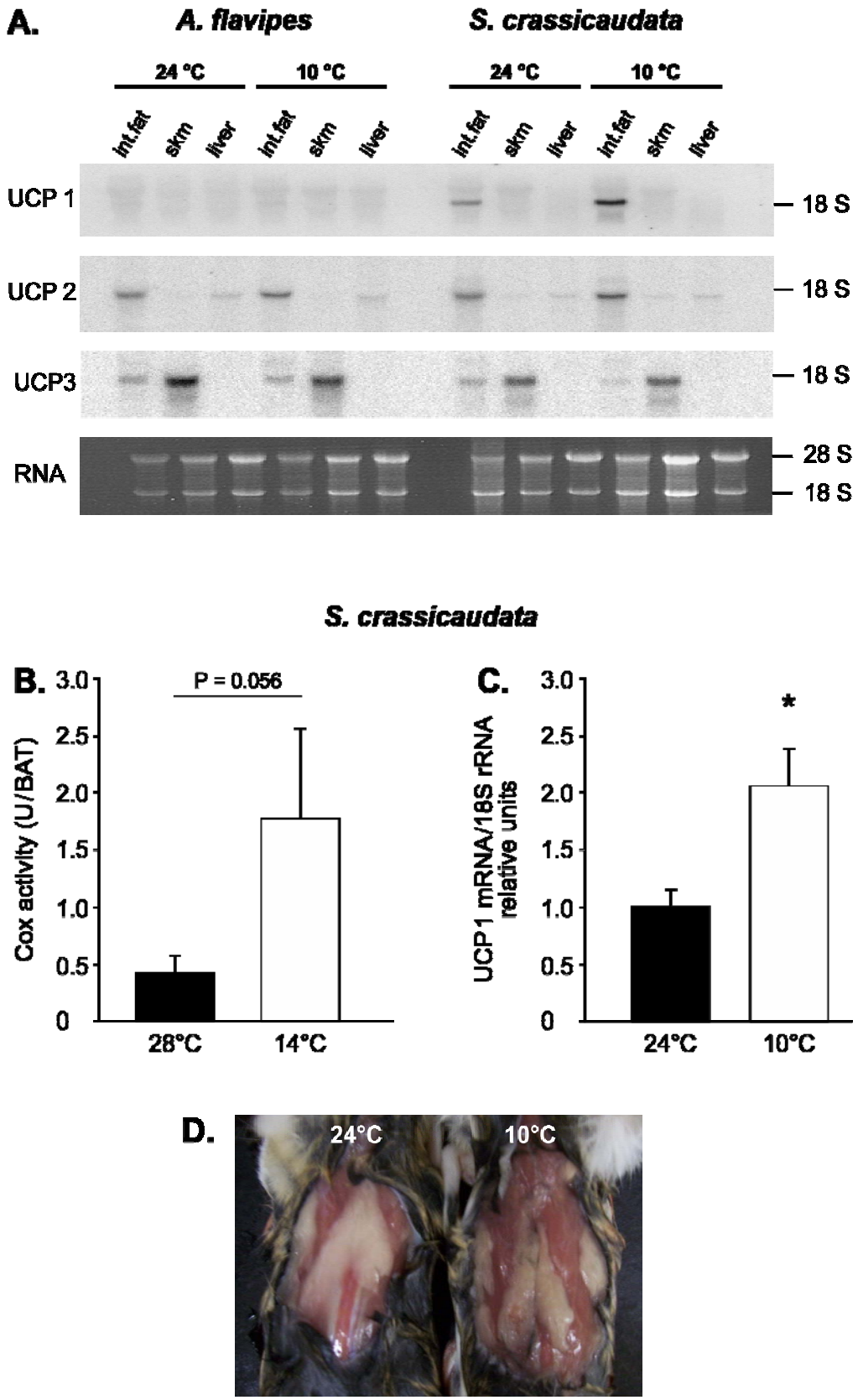
A.
A. flavipes
S. crassicaudata
24 °C
10 °C
24 °C
10 °C
int.fat
skm
liver
int.fat
skm
liver
int.fat
skm
liver
int.fat
skm
liver
UCP 1
UCP 2
UCP3
RNA
18 S
18 S
18 S
28 S
18 S
S. crassicaudata
B.
Cox activity (U/BAT)
P = 0.056
3.0
2.5
2.0
1.5
1.0
0.5
0
28°C
14°C
C.
UCP1 mRNA/18S rRNA relative units
*
3.0
2.5
2.0
1.5
1.0
0.5
0
24°C
10°C
D.
24°C
10°C

Supplemental material

Material and Methods

S1 Gene soeing

Northern blot analysis required the excision of intron sequence from the genomic UCP1 fragment of *M. domestica*. Therefore, we excised intron 3/4 using PCR based gene SOEing (Horton RM, Ho SN, Pullen JK, Hunt HD, Cai Z, Pease LR (1993) Gene splicing by overlap extension. Methods Enzymol. 217:270-279). The *M. domestica* exon 3 fragment (amplified by using primers "forEx3" and 5'-CATCGTCCCTTTCCAAAGCC -3') and exon 4 fragment (using primers forward 2: CTTTGGAAAGGGACGATGCC and "revEx4") were amplified separately (30 cycles of 94° C (20s), 54°C (30s), and 72°C (1 min) with a final extension at 72°C (10 min)). Both fragments were subjected to a single PCR with an annealing temperature of 52°C using primers "forEx3" and "revEx4". The resulting fragment was cloned and used as a template for radioactively labelled probing.

Figure legend:

S1 Amplification of genomic UCP fragment from M. domestica

Upper panel: Gel electrophoresis of a 324 bp *UCP1*-like genomic fragment (lane 2) of *M. domestica*. Excision of the intron using geneSOEing resulted in a 225 bp fragment (lane 1). Lower panel: Gel electrophoresis of a 1200 bp *UCP2* fragment from genomic DNA of *M. domestica* (lane 1/2).

S2 Syntenic promotor region

The lack of the UCP1-specific enhancer box controlling UCP1 expression in *M. domestica*. – 10000 bp to 0 bp upstream region of *UCP1* transcriptional start was retrieved from the ensembl genome browser (www.ensembl.org) and searched for the presence of the UCP1-enhancer box in selected placental mammals and *M. domestica*. 2A. The *M. musculus* upstream region (x-axis) was plotted against the upstream region of the other species (y-axis) using the dotplot function of

the spin module (Staden Package; http://staden.sourceforge.net/). Red dots indicate a score 9 out of 10. A 45° virtuell line indicates conserved regions. The predicted enhancer box is marked with a circle and magnified. 2B. The predict regions for the enhancer box were aligned using clustalX.

Figure legend:

S2.1 Lack of the UCP1-enhancer box in M. domestica

The *M. musculus* upstream region (x-axis) was plotted against the upstream region of the other species (y-axis). Red dots indicate a score 9 out of 10. A 45° virtuell line indicates conserved regions. The predicted enhancer box is marked with a circle and magnified

S2.2 Conservation of the UCP1-enhancer box in eutherians

Alignment of the UCP1-enhancer box from selected placental species. Dark shading indicates conservation, responsive elements are underscored, published in blue and novel predicted in red.

S3 Bayesian phylogenetic tree

For methods see material and methods section.

Figure legend

S3 Bayesian phylogenetic tree

Phylogenetic relations of the UCP family in vertebrates including UCP1 of marsupials using Bayesian statistics. The oxaloacetate-malate carrier served as the outgroup. P-values are given as internal node labels. UCP sequences other than marsupials were either found predicted in public databases or found by search genomic sequence. The table contains species names, abbreviations of the species and sequence accession numbers.

S4 Alignment of *Sminthopsis crassicaudata* UCP1

The *S. crassicaudata* UCP1 protein sequence was alignment with *M. domestica* UCP1 and the mouse UCPs using clustalX. The alignment is illustrated in the conservation mode of genedoc.

S1 Amplification of a genomic UCP1 and UCP2 cDNA fragment from *M. domestica*

UCP1:

lane 1 225 bp product of gene SOEing

lane 2 346 bp fragment

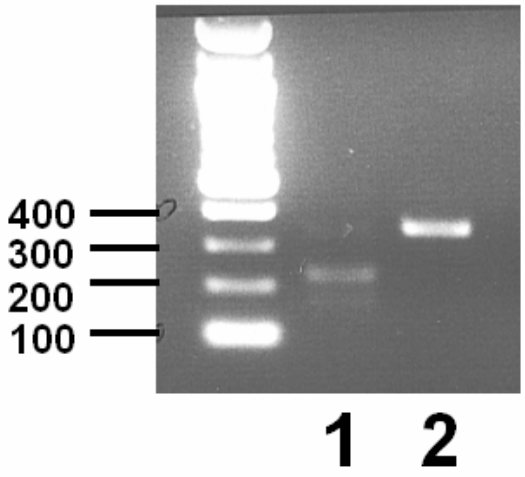

UCP2:

lane 1/2 1200 bp fragment

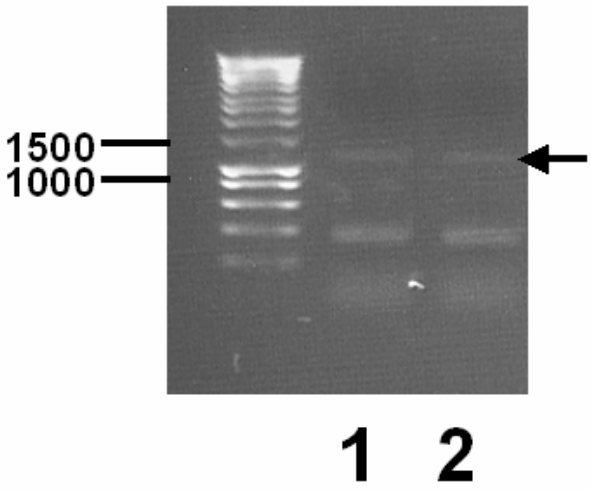

S2.1 Conservation of the UCP1-enhancer box – dot blots

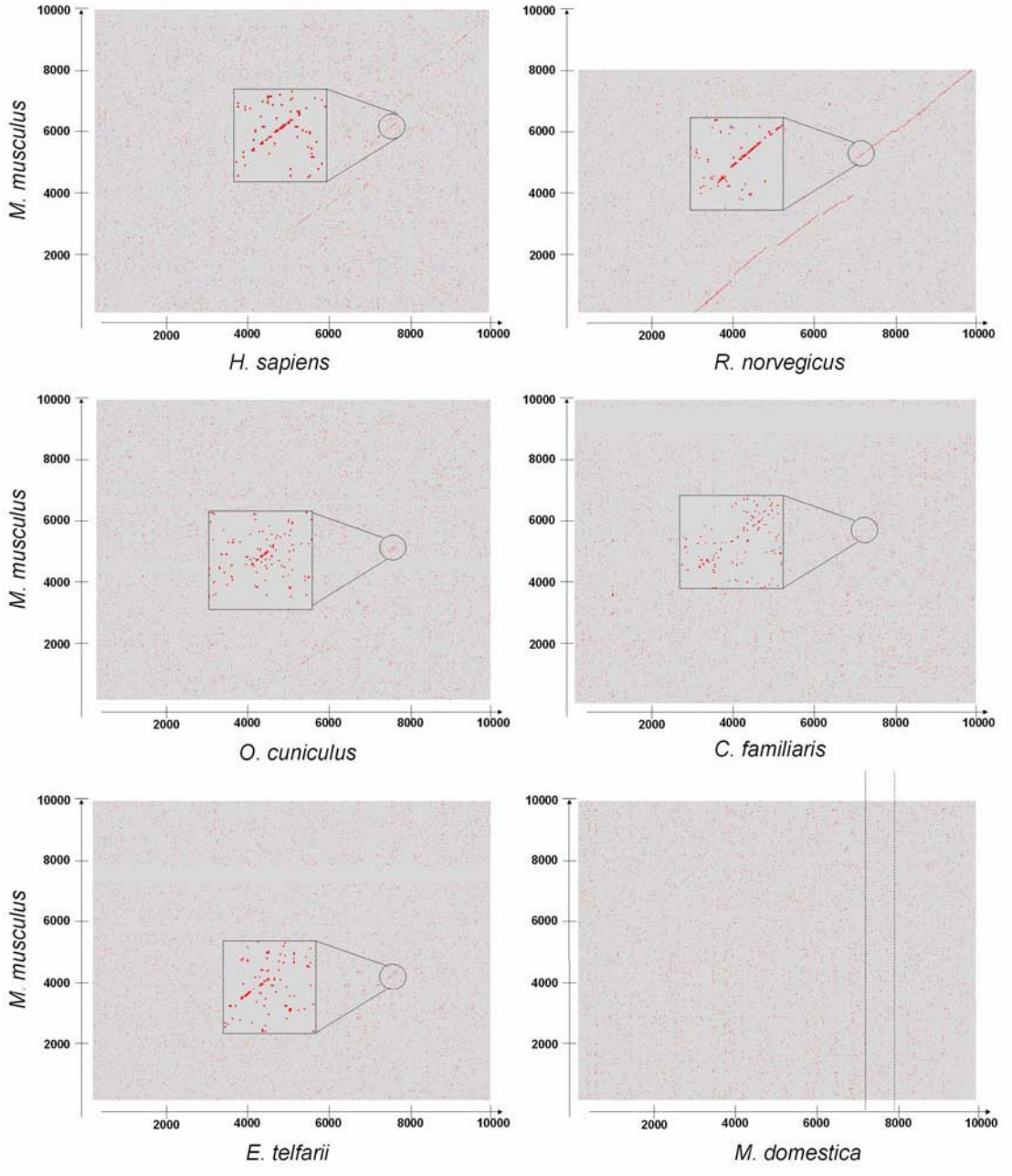

S2.2 Conservation of the UCP1-enhancer box - alignment

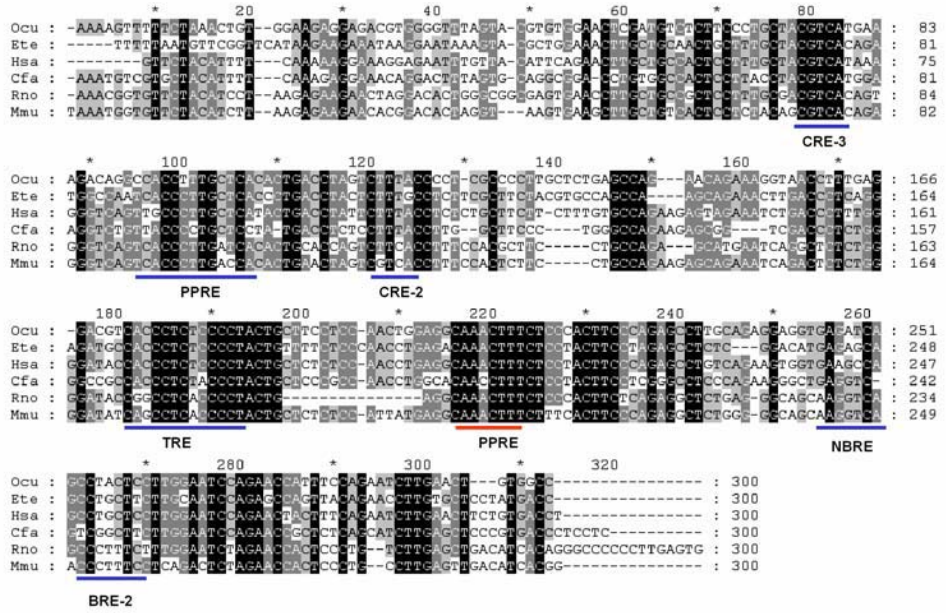

S3 Bayesian tree of the UCP family

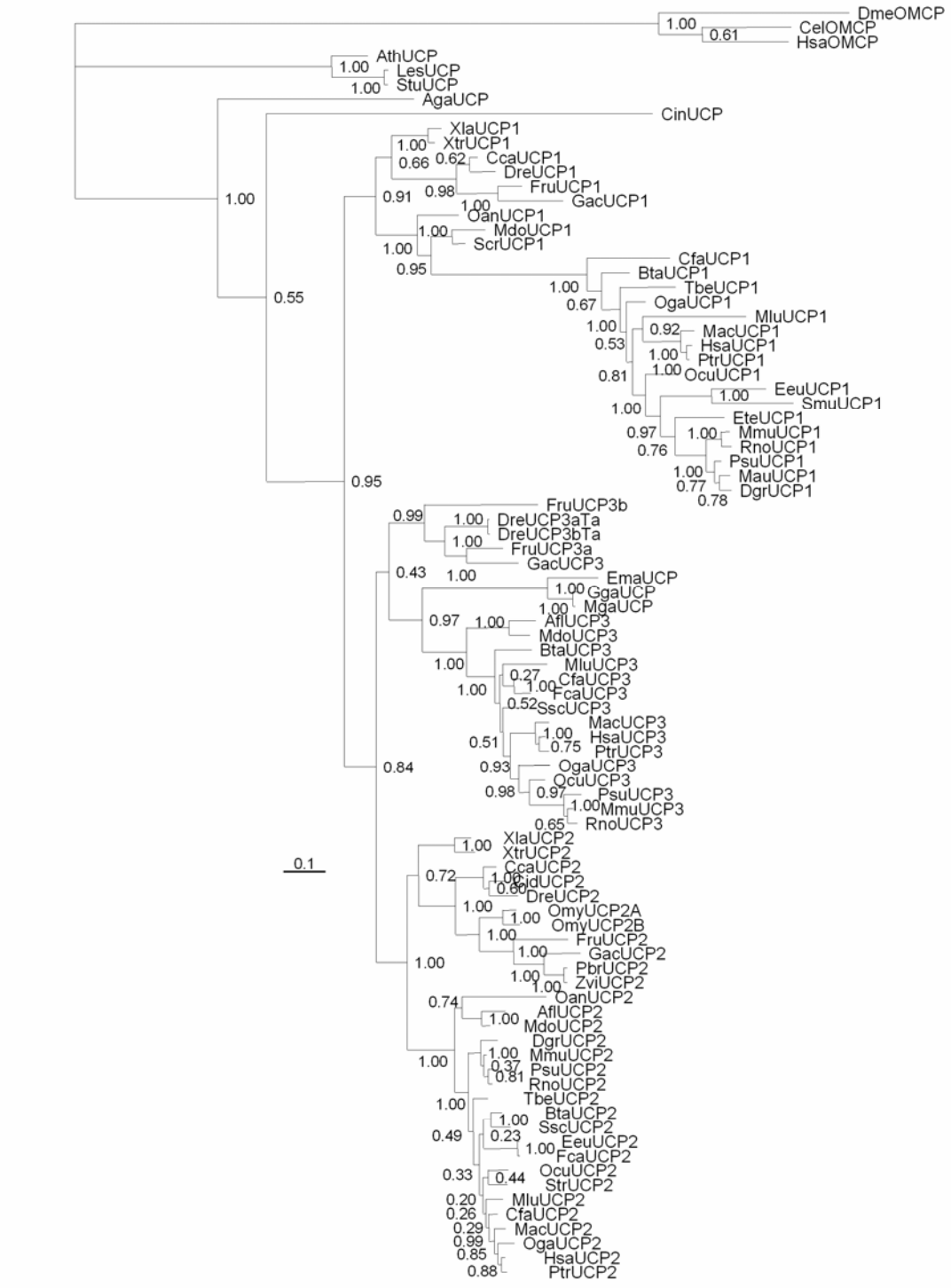

Uncoupling Protein Sequences used for phylogenetic inference

Species	Abbreviation	Common name	UCP1	UCP2	UCP3	UCPX
Anopheles gambiae	Aga	African malaria mosquito				XM_552584
Antechnius flavipes	Afl	yellow-footed Antechinus		AY233003	AY519198.1	
Arabidopsis thaliana	Ath	thale-cress		CAA11757.1		
Bos Taurus	Bta	bovine, domestic Cattle	XP_616977.2	AAI02840.1	AAD33339	
Canis familiaris	Cfa	dog	BAB11684	Q9N2J1	BAA90458	
Ciona intestinalis	Cin	sea squirt				GENSCAN00000088333
Ctenopharyngodon idella	Cid	grass carp		AAX49553.1		
Cyprinus carpio	Cca	common carp	AAS10175.2	Q9W725		
Danio rerio	Dre	zebrafish	ENSDARG00000023151	Q9W720	UCP3a/b identified by Taudien	
Dicrostonyx groenlandicus	Dgr	lemming	AF515781	AY484518		
Echinops telfairi	Ete	lesser hedgehog Tenrec	ENSETEG00000010924			
Erinaceus europaeus	Eeu	hedgehog	ENSEEUG00000005182	ENSEEUT00000007970		
Eupetomena macroura	Ema	swallow-tailed hummingbird			AAK16829	
Felix catus	Fca	cat		Q1LZN3_FELCA	ENSFCAT00000005034	
Fugu rubripes	Fru	pufferfish	Identified by Taudien	SINFRUT00000167188	UCP3a/b identified by Taudien	
Gallus gallus	Gga	chicken			AF287144	
Gasterosteus aculeatus	Gac	stickleback	ENSGACT00000022876	ENSGACT00000026955	ENSGACT00000026952	
Homo sapiens	Has	human	G01858	XP_035029	NP_073714	
Lycopersicon esculentum	Les	tomato				AAL82482
Macaca mulatta	Mac	Rhesus monkey	XP_001090457.1	Q9N1D9_MACMU	Q9N1D8_MACMU	
Meleagris gallopavo	Mga	turkey			AAL28138	
Mesocricetus auratus	Mau	golden hamster	P04575			
Monodelphis domestica	Mdo	oppossum	MS	MS	MS	

Mus musculus	Mmu	Mouse	P12242	AAB17666	P56501	
Myotis lucifugus	Mlu	microbat	ENSMLUT00000009572	ENSMLUT00000012109	ENSMLUT00000012116	
Oncorhynchus mykiss	Omy	rainbow trout		A: ABC00183.1/ B: ABC00185.1		
Ornithorhynchus anatinus	Oan	platypus	ENSOANT00000024079	ENSOANT00000011476		
Oryctolagus cuniculus	Ocu	rabbit	CAA32826	ENSOCUT00000012590	ENSOCUT00000014607	
Otolemur garnettii	Oga	bushbaby	ENSOGAT00000006809	ENSOGAT00000001699	ENSOGAT00000002909	
Pachycara brachycephalum	Pbr	Antarctic eelpout		AAT99593.1		
Pan troglodytes	Ptr	chimpanzee	ENSPTRT00000030601	ENSPTRT00000007559	ENSPTRT00000007561	
Phodopus sungorus	Psu	Djungarian hamster	AAG33983	AAG33984	AAG33985	
Rattus norvegicus	Rno	rat	P04633	AAC98733	P56499	
Solanum tuberosum	Stu	potato				T07793
Spermophilus tridecemlineatus	Str	thirteen-lined ground squirrel		ENSSTOT00000010715		
Suncus murinus	Smu	Asian house shrew	BAE96411.1			
Sus scrofa	Ssc	pig	Extinct	AAD05201	AAD08811	
Tetraodon nigroviridis	Tni	pufferfish	CR640550	Taudien	UCP3a/b identified by Taudien	
Tupaia_belangeri	Tbe	treeshrew	ENSTBET00000000042	ENSTBET00000001469		
Xenopus laevis	Xla	African clawed frog	AAH86297.1	AAH44682.1		
Xenopus tropicalis	Xtr	Western clawed frog	ENSXETT00000032640	ENSXETT00000055772	Identified by Taudien	
Zoarces viviparus	Zvi	Viviparous blenny		AAT99594.1		

S4 Alignment of *Sminthopsis crassicaudata* and *Monodelphis domestica* UCP1 with mouse UCPs

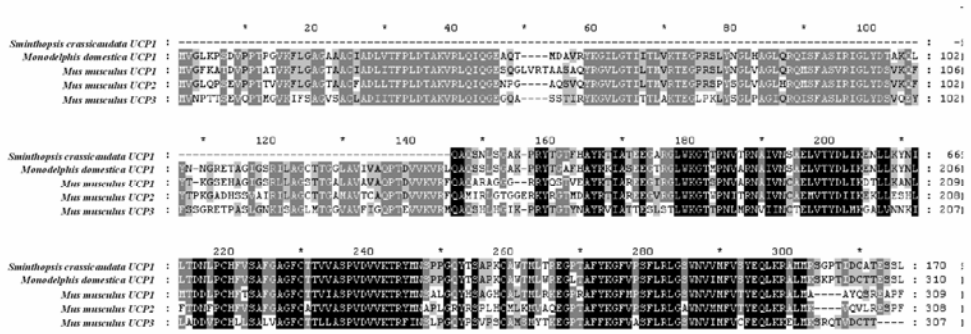

The molecular and biochemical basis of non-shivering thermogenesis in a phylogenetically ancient eutherian mammal, the rock elephant shrew, *Elephantulus myurus*

[1]Nomakwezi Mzilikazi*, [2]Martin Jastroch, [2]Carola Meyer and [2]Martin Klingenspor

*To whom correspondence should be addressed

[1]Department of Zoology, Nelson Mandela Metropolitan University, P.O. Box 77000, Port Elizabeth, 6031, SOUTH AFRICA

Email: nomakwezi.mzilikazi@nmmu.ac.za

Tel: +27 41 504 2421

Fax: +27 41 504 2317

[2]Department of Animal Physiology, Faculty of Biology, Philipps Universität Marburg, Karl von Frisch Str.8, Marburg, 35043, GERMANY

klingens@staff.uni-marburg.de

Abstract

Uncoupling protein 1 (UCP1) mediated non-shivering thermogenesis (NST) in brown adipose tissue (BAT) is an important avenue of thermoregulatory heat production in many mammalian species. Until recently, UCP1 was thought to occur exclusively in eutherians. In the light of the recent finding that UCP1 is already present in fish, it is of interest to investigate when UCP1 gained a thermogenic function in the vertebrate lineage. We elucidated the basis of NST in a phylogenetically ancient mammal, the rock elephant shrew, *Elephantulus myurus* (Afrotheria: Macroscelidea). We sequenced *Ucp1* and detected *Ucp1* mRNA and protein restricted to brown fat deposits. We found that cytochrome c oxidase activity was highest in these deposits when compared with liver and skeletal muscle. Consistent with a thermogenic function of UCP1 isolated BAT mitochondria showed increased state 4 respiration in the cold as well as palmitate induced, GDP sensitive proton conductance, which was absent in liver mitochondria. On the whole animal level, evidence of thermogenic function was further corroborated by an increased metabolic response to noradrenaline (NA) injection. Cold acclimation (18°C) led to an increased basal metabolic rate relative to warm acclimation (28°C) in *E. myurus* but there was no evidence of additional recruitment of NA induced NST capacity in response to cold acclimation. In summary, we showed that BAT and functional UCP1 are already present in these phylogenetically ancient mammals, but the seasonal regulation and adaptive value of NST in Afrotherians remains to be elucidated.

Keywords: basal metabolic rate; uncoupling protein 1; proton leak kinetics; brown adipose tissue

Running head: Basis of nonshivering thermogenesis in *E. myurus*

Introduction

The success of early mammals is often attributed to the ability to produce heat endogenously through non-shivering thermogenesis (NST) (8, 27). In eutherian mammals NST is known to occur in brown adipose tissue (BAT) where uncoupling protein 1 (UCP1) works to generate heat instead of ATP (8, 15, 17, 39). However, the often repeated statement that all eutherians exhibit BAT is based on only a few representatives of the subclass. Until recently UCP1 was thought to be associated exclusively with NST in eutherian mammals. However, it has been demonstrated by conserved synteny that UCP1 appears in the vertebrate line as early as before the divergence of ray finned and lobe-finned fishes (19) although a thermogenic function of fish UCP1 is unlikely. This finding begs the question of where in the vertebrate lineage UCP1 gained a thermogenic function as well as the adaptive significance of UCP1 presence.

Within the Marsupialia and the Monotremata the presence and function of UCP1 remains controversial. The elephant shrews belong to the Afrotheria, a group of mammals thought to be at the base of the eutherian radiation (38). Their phylogenetic placement thus makes them an excellent model in the quest for the presence of UCP1 and BAT mediated thermogenesis. In addition, the rock elephant shrew, *Elephantulus myurus* shows a pronounced thermogenic response to noradrenalin (NA) injection (31) which is often taken as an indicator of BAT-mediated NST (7, 8). However, at present it is unclear whether this NA-induced thermogenesis observed in *E. myurus* is indicative of classical NST and whether it is of any adaptive value, i.e. can be recruited in the cold.

Classical, adaptive, cold mediated NST is accompanied by a pronounced recruitment of BAT and enhanced thermogenic capacity (8, 14, 17, 23). This adaptive thermogenic capacity is evident as changes in physiological and biochemical parameters such as high mitochondrial density and respiratory capacity in BAT, a high UCP1 concentration in BAT mitochondria of cold acclimated mammals (21, 23) as well as a higher metabolic response to NA injection when

compared to warm acclimated animals. Furthermore, in rodents, UCP1 increases proton leak in the presence of free-fatty acids, in a GDP-sensitive manner (35). In addition, basal metabolic rate (BMR) is also increased in the cold, a response thought to be associated with increased blood flow to intestinal organs and increased peripheral vascularization (12).

Drastic seasonal changes in thermogenic capacity are often associated with high latitude species. However, it is becoming increasingly clear that phenotypic plasticity is selected for, even in those species from tropical and subtropical environments because plasticity allows organisms to match environmental variability at an ecological scale (28, 29, 34). We might therefore expect the African-endemic elephant shrews to exhibit adaptive changes in their thermogenic properties during warm and cold acclimation.

The aim of the study was therefore two-fold. Firstly, we aimed to elucidate the molecular and biochemical basis of nonshivering thermogenesis in rock elephant shrew, *E. myurus*. Our approach was to investigate the occurrence of BAT and the patterns of tissue expression of UCP1 in *E. myurus* as well as to characterize UCP1 function by measuring the proton leak kinetics of isolated BAT mitochondria. Secondly, we investigated whether parameters associated with thermoregulation and cold adaptation such as BMR, NST capacity, amount of UCP1, cytochrome c oxidase activity were regulated in response to cold and warm acclimation.

Materials and methods

Study animals

Adult *E. myurus* (n = 12) were captured on the MacKay farm, 17 km east of Estcourt (28°56.749'S 30°00.848'E), KwaZulu-Natal, South Africa, in June 2006. They were then flown to Germany and housed in the Department of Animal Physiology, Philipps Universität Marburg. Within 3 weeks of arrival, 3 of the animals died, presumably due to stress associated with capture and handling.

The animals were individually housed in large Makrolon Type IV cages and provided with sawdust bedding and nesting boxes. They were maintained at 24°C under a 12L: 12D photoperiod. Food and water was available ad libitum throughout the study. The animals were fed ProNutro, a commercial high protein cereal (22% protein, 59% carbohydrate and 6% fat) mixed with water. This diet was alternated with canned dog food and was supplemented with fresh lettuce and cockroaches. The food was replenished once every 24 hrs.

Experimental sequence

All experiments complied with the German Animal Welfare Laws and are fully compliant with the American Physiological Society's "Guiding Principles for Research Involving Animals and Human Beings."

The metabolic measurements were made in October – December 2006. Our approach was to first measure BMR and NST capacity of animals acclimated to 24°C, after which the animals were divided into two groups, the warm acclimated (WA) group (n = 4) at 28°C and the cold acclimated (CA) group (n = 5) at 18°C. We expected that both BMR and NST capacity would increase and decrease under cold and warm acclimation, respectively. The BMR of the animals was measured at 31°C. This temperature is within the known thermoneutral zone for

this species (26). After measurement of BMR, the NST capacity of the animals was tested by measurement of the metabolic response to NA injection. The animals were then maintained at their respective acclimation temperatures for at least 3 weeks before repeat BMR and NST capacity measurements were made. After four weeks the animals were sacrificed so as to ascertain the biochemical and molecular basis of non-shivering thermogenesis in this species.

Measurement of BMR and NST capacity

Animals were placed in 1.8ℓ metabolic chambers inside a constant environment cabinet. Oxygen consumption (VO_2) was measured using an open-flow through system using an electrochemical analyzer (S-3A/II, Ametek). Air was pumped through the metabolic chambers at flow rates *ca*. 50ℓ hr^{-1}. The use of solenoid relay valves for each chamber allowed us to measure three animals and a control channel sequentially in 1min intervals. Measurements were therefore obtained for each animal every four minutes. During the determination of NST capacity, we measured single animals and therefore increased the resolution of measurement to two minutes. Further details of the respirometry have been described previously in (13).

All metabolic measurements were made during the daytime, the known rest phase for this species (33). On each measurement day, animals were removed from their cages around 09h00 and measurements commenced shortly thereafter. The animals were kept in the metabolic chambers for at least 6 hours and the BMR was taken as the mean of the three lowest consecutive measurements, equivalent to 12 min, obtained during the last two hours of data measurements. The length of time spent in the metabolic chambers coupled with the fact that the animals were not fed prior to measurement ensured that the animals were post absorptive at the time of BMR determination. Animals were allowed at least 3 days of recovery from BMR measurements, after which their capacity for NST was determined through the injection of noradrenaline (NA).

The measurements of response to NA were made at 25°C, so as to avoid hyperthermia (34). We used 85% of the dose recommended by Wunder and Gettinger (1996; 0.458 mg/kg) because Mzilikazi and Lovegrove demonstrated that the maximal NA induced thermogenesis in this species can already be elicited at this dose (31). Animals were injected with NA at least 2 hours after they were initially placed in the respirometers. For each animal the NST capacity was determined as the difference between the highest NA-induced VO_2 and the BMR.

Cloning of Ucp1 cDNA and phylogenetic inference

Total RNA was isolated from selected tissues and cDNA synthesized as described previously (18). Primers were deduced from the lower hedgehog tenrec (*Echinops telfairi*) genome found at www.ensembl.org. Primers (forward 5′-GACTATGGGGGTGAAGATCTTC-3′; reverse 5′-AAAGGCCGGCAGCCCTTCCTTG-3′) were used for polymerase chain reaction on cDNAs of the interscapular fat deposit of *E. myurus*. 40 cycles of denaturation at 94°C (1min), annealing at 59°C (1 min) and elongation at 72°C (1 min) were performed. A final extension at 72°C was applied for 10 minutes and followed by rapid cooling to 4°C. The PCR product was gel-purified and ligated into a pJET1/blunt cloning vector (Fermentas). Inserts were sequenced using vector based primers.

Three plant UCPs, three bird UCPs, 22 UCP2, 16 UCP3, and 22 UCP1 sequences including the novel *E. myurus* sequence were aligned and subjected to phylogenetic analysis using Neighbour-joining method as described previously (18). For bootstrap analysis the alignment dataset was shuffled 1000 times. The oxalacetate-malate carrier (OMCP) served as the distantly related outgroup.

Northern blot analysis

Five micrograms of RNA were electrophoresed in a 1% denaturing agarose gel (5% formaldehyde, 0.02 MOPS, 5mM sodium acetate, 1mM disodium EDTA, pH 8), transferred overnight in 10X SSC to a nylon membrane (Hybond N, Amersham), and UV cross-linked. All

blots were hybridized with probes corresponding to the cDNA sequences of *Elephantulus myurus* UCP1. The cDNA probes were labeled by random priming with [α^{32}P] dATP. Nylon membranes were prehybridized at 63°C with BSA solution (0.5M Na_2HPO_4/NaH_2PO_4, pH 7.0, 1mM EDTA, pH 8.0, 0.7% SDS, 1% BSA) for at least one hour and hybridized overnight at 63°C with the ^{32}P-labelled probe. After hybridization , the blots were washed with 2X SSC/0.1% SDS for 30 min, 1X SSC/0.1% SDS for 10min, 0.5X SSC/0.1% SDS for 10 min and 0.1X SSC/0.1% for 10 min at room temperature. Signal intensities were then monitored by exposure to a PhosphoScreen (Molecular Dynamics). The hybridized probes were then detected by phosphor imaging (Storm 860, Molecuar Dynamics) and the signal intensities were quantified using ArrayVision 7.0 (Imaging Research). Signal intensities were normalized to ethidium-bromide stained 28S rRNA.

Immunological detection of UCP1

Samples of frozen tissues were homogenized in sample buffer (100 mM KH_2PO_4/K_2HPO_4, 2mM EDTA pH 7.5) after which the protein concentration was determined by the Bradford method. Protein samples were then run on a SDS-polyacrylamide gel (3% stacking gel and 12.5% running gel). The protein was then transferred to a nitrocellulose membrane (Hybond-C, Amersham Biosciences). After blocking against non-specific binding with 5% Slimfast for at least 1 h at room temperature, the membrane was incubated with a rabbit polyclonal antibody to hamster UCP1 (1: 10 000) for 1 h and then treated with a second antibody, goat-anti-rabbit-IgG, HRPO-conjugate 1: 10 000) for another 1 h at room temperature. The membrane was then washed before being incubated for 2 min with ECL reagents for peroxidase detection. The signals were detected by exposing the membrane to autoradiography film for 30 sec.

Isolation of interscapular fat mitochondria

Clearly identifiable fat deposits from the interscapular region were excised from the animal and quickly transferred to an excess of ice-cold isolation medium A (250mM Sucrose, 10mM TES, 1mM EDTA, 0.4% (w/v) BSA, pH 7.2). The tissue was then minced in the buffer, on ice, with fine scissors. The tissue was then transferred to a glass-teflon homogenizer. The tissue was homogenized with 6 strokes of a loose-teflon pestle, filtered through a layer of gauze and centrifuged for 10 min at 8740 g. The lipid layer was removed through aspiration, the supernatant was discarded, and the lipid remaining on the inside walls of the tube was removed using tissue paper. The mitochondria pellet was suspended in isolation medium B (250 mM Sucrose, 10mM TES, 1mM EGTA, 0.4% w/v BSA, pH 7.2) and centrifuged at 950 g for 10 min and the resulting supernatant was transferred to a new tube and centrifuged at 8740 g for 10 minutes. The final mitochondrial pellet was suspended in a buffer containing 100mM KCl, 20mM TES, 1mM EGTA, pH 7.2). Protein concentration was determined using the Biuret method.

Isolation of liver mitochondria

The liver was removed and immediately placed in ice cold isolation medium (250 mM Sucrose, 5mM Tris-HCl, 2mM EGTA, pH 7.4). The tissue was minced with scissors and disrupted using a Dounce homogenizer with a medium-fitting pestle. The homogenate was centrifuged at 8500 g for 10 min at 4°C and the pellet was re-suspended in isolation medium and spun at 1047 g for 10 min. The resulting supernatant was subjected to a high speed cycle (11630 g, 10 min, 4°C). The pellet was re-suspended in medium without BSA. The high speed cycle was repeated twice and the final pellet re-suspended in a minimal volume of isolation medium. Protein concentration was determined using the Biuret method.

Proton leak kinetics: measurement of oxygen consumption and membrane potential

Oxygen consumption of BAT mitochondria was measured using a Clark-type electrode (Rank Brothers Ltd., UK) maintained at 37°C and calibrated with air-saturated medium (50mM KCl, 5mM TES, 2mM $MgCl_2$ x $6H_2O$, 4mM KH_2PO_4, 1mM EGTA, 0.4% (w/v) BSA, pH 7.2). For the liver mitochondria, the measuring medium contained 120 mM KCl, 5mM KH_2PO_4, 3mM HEPES, 1mM EGTA and 0.3% (w/v) BSA, pH 7.2. The measuring medium was assumed to contain 406 nmol O/ml (36). Oxygen consumption and membrane potential were measured simultaneously using an electrode sensitive to the potential-sensitive probe, $TPMP^+$ (triphenylmethylphosphonium), a method previously described (2; 4). Briefly, the kinetics of the mitochondrial proton leak were measured by determining the dependence of the respiration rate required to drive the proton leak on membrane potential. BAT and liver mitochondria were incubated at protein levels of 0.3 mg/ml and 0.7 mg/ml, respectively in 2.5 ml of medium containing 8μM rotenone to inhibit complex I, (4μg ml^{-1}) oligomycin to inhibit phosphorylation of ADP and (110ng ml^{-1}) nigericin to abolish ΔpH. The $TPMP^+$ electrode was calibrated with sequential additions up to 2.5μM $TPMP^+$. Succinate (6 mmol l^{-1}) was provided as the substrate for respiration. Oxygen consumption and membrane potential were titrated through sequential steady states by successive additions of malonate up to 2mM for BAT mitochondria and up to 4mM for liver mitochondria. Finally, 0.3μM FCCP was added to dissipate the membrane potential and release all the $TPMP^+$ from the mitochondria, allowing for correction of baseline drift. Respiration at each steady state was then plotted against the appropriate membrane potential so as to display the dependence of proton leak rate on potential.

Cytochrome c oxidase activity measurements

Cytochrome c oxidase (COX) activity was measured polarographically (37) in BAT mitochondria, BAT, liver and skeletal muscle tissue homogenates. All tissues were weighed and were then homogenized in tissue buffer containing 100mM KH_2PO_4 /K_2HPO_4, 2mM EDTA, pH 7.5. The homogenate was incubated at 25°C with 1ml air-saturated medium (79 mM K_2HPO_4 x $3H_2O$, KH_2PO_4, 5 mM EDTA-Na_2, pH 7.4) assumed to contain 479 nmol O/ml with 43µL 3mM cytochrome c, and 71µL of 0.25M ascorbic acid added. The tissue homogenate was diluted 1:2 up to 1:6 for BAT, liver and skeletal muscle, and 1:15 for BAT mitochondria, with polyoxyethylenether W1, 1.5% (w/v) no longer than ten minutes before the assay.

All mean values are reported ± SEM. Differences between groups were analyzed using t-tests, paired t- tests and ANOVAs as appropriate.

Results

Body mass

The mean ± SEM body mass of all the animals acclimated to 24°C was 63.5 ± 2.1g. After three weeks of respective temperature acclimation the body mass of both WA and CA had decreased to 59.2 ± 3.1 and 59.4 ± 1.8g, respectively and did not differ significantly between the groups ($t = 0.07$; $p > 0.05$).

Basal metabolic rate and non-shivering thermogenesis

The mean BMR of all animals acclimated to 24°C was 1.23 ± 0.03 ml $O_2.g^{-1}.hr^{-1}$. There was no significant difference in the BMR of the two groups before they were transferred to their respective acclimation temperatures. However, there was a pronounced cold acclimation effect on the BMR of the rock elephant shrews (Fig. 1). Except for one individual, the WA animals either maintained the same BMR as at 24°C or decreased BMR. Overall, the BMR of the WA group (1.31 ± 0.07ml $O_2.g^{-1}.h^{r-1}$) was not significantly different to that measured at 24°C. In contrast, all the CA animals exhibited a significant increase in BMR (1.64 ± 0.04 ml $O_2.g^{-1}.hr^{-1}$). This BMR increase was on average 37.9 ± 1.6% and ranged from 35 – 42%. Overall, there was a significant difference in the BMR of cold and warm acclimated animals ($t = 4.65$; $p = 0.002$).

The injection of NA caused an increase in VO_2 which was observed within 45 min of administration. These high metabolic rates following NA injection were not associated with activity as the animals typically spread out their bellies on the metabolic chambers, presumably to dissipate heat. The increase in VO_2 caused by NA injection was in most cases up to 4x BMR values. The NST capacity for all animals at 24°C was 2.75 ± 0.69 ml.$O_2.g^{-1}.hr^{-1}$ and there were no differences in the NST capacity of the animals that were placed in the respective acclimation groups (data not shown). Surprisingly, cold acclimation did not lead to an increase in the NST capacity of rock elephant shrews (Fig. 1; 2.65 ± 0.65 ml $O_2.g^{-1}.hr^{-1}$). Similarly, warm acclimation did not lead to a decrease in the NST capacity (2.53 ± 0.18 ml $O_2.g^{-1}.hr^{-1}$). Overall there were no significant differences in NST capacity of cold and warm acclimated animals ($t = -0.09$;

$p = 0.93$).

Cloning of the Ucp1 cDNA and phylogenetic inference

We amplified a 726bp cDNA fragment by RT-PCR from the interscapular fat deposit (Genbank Acc. No EF 121740) which had the characteristics of eutherian brown fat, extensive blood supply as well as abundant mitochondria, giving it a brownish colour. For classification of the deduced *E. myurus* UCP1 protein sequence and its relationship to other homologues, we performed phylogenetic analyses and generated a tree. Phylogenetic inference revealed that *E. myurus* UCP1 groups amongst other known eutherian UCP1 orthologues (Fig. 2). It is most closely related to the tenrec UCP1 sequence with 81% amino acid identity, has 76 % identity to mouse UCP1, 55% identity to mouse UCP2 and 53% to mouse UCP3.

UCP1 expression patterns and regulation

We analyzed the tissue distribution of UCP1 both at the mRNA as well as the protein level in the elephant shrews. Northern blot hybridization of total RNA with a *E. myurus* UCP1 cDNA probe selectively detected a transcript in interscapular adipose tissue but not in WAT or any of the other tissues dissected from *E. myurus* (Fig. 3A). Accordingly, on Western blots our polyclonal hamster UCP1 antibody only detected a 32kD protein in the interscapular fat pad (Fig. 3B). Weak signals detected in the other tissues represent cross reactivity of the antibody with unknown proteins of different molecular mass. Cold acclimation did not increase UCP1 mRNA expression in the interscapular fat (Fig. 3C; CA = 0.7±0.1, WA = 1.0 ±0.2; $t = -1.24$, $p = 0.25$). We then analyzed the UCP1 concentration in protein extracts prepared from tissue homogenates (Fig. 3D) and in isolated mitochondria (Fig. 3E). The UCP1 protein levels in the interscapular fat of warm and cold acclimated elephant shrews was not significantly different (CA = 1.0 ± 0.1 WA = 1.1 ± 0.1; $t = -0.51$, $p = 0.62$).

Cytochrome c oxidase (COX) activity

The enzyme COX is a reliable indicator of respiratory capacity in a tissue. We therefore investigated whether there were differences in COX activity in the BAT, liver and skeletal muscle of CA and WA animals. COX activity was highest in BAT, followed by skeletal muscle and the lowest enzyme activity was observed in the liver (Fig. 4A). However, none of the tissues showed increased COX activity during cold acclimation. In addition to investigating COX activity at tissue level, we also measured COX activity in BAT mitochondria. There was a tendency towards increased activity in the mitochondria of CA animals, although this did not amount to a statistically significant difference (Fig. 4B; $t = -1.29$, $p = 0.24$). We also compared state 4 respiration (in the presence of 5mM GDP) of BAT mitochondria from CA and WA animals. The state 4 respiration of CA mitochondria (151.9 ± 4.4 nmol O min^{-1}. mg^{-1} protein) was significantly higher than that of WA animals (130.3 ± 7.1 nmol O min^{-1}.mg^{-1} protein) ($t = 2.72$, $p = 0.03$), suggesting a higher respiratory capacity in CA animals (Fig. 4C). There were no differences in the state 4 respiration of liver mitochondria from CA (54.4 ± 6.1 nmol O min^{-1}. mg^{-1} protein) and WA (55.9 ± 6.7 nmol O min^{-1}. mg^{-1} protein) animals ($t = -0.16$, $p = 0.87$).

Proton leak kinetics and functional characterization of UCP1

We were interested in whether the presence of UCP1 in the BAT of *E. myurus* was associated with uncoupled respiration (proton leakage) representing the molecular mechanism of NST. Proton leakage catalyzed by UCP1 has two distinct characteristics: inhibition by purine nucleotide di- or triphosphates as well as activation by fatty acids (35). We therefore investigated if the proton leak kinetics in elephant shrew BAT mitochondria were affected by GDP and palmitate in CA and WA elephant shrews.

Firstly, we titrated the effect of GDP on mitochondria isolated from BAT and liver of rock elephant shrews. Because proton leak is a non-linear function of membrane potential, we compared the oxygen consumption driving the proton leak at a common membrane potential of

135mV in the presence of 0, 1, 3, and 5 mM GDP. There was a clear sensitivity of proton conductance to GDP presence in BAT mitochondria whereas this sensitivity could not be discerned on liver mitochondria (Figure 5A). In the absence of GDP the oxygen consumption required to balance the proton leak in BAT mitochondria was quite substantial and decreased with increasing GDP concentration (Fig. 5B).

The addition of 100μM palmitate increased proton conductance (Fig. 6). In the absence of GDP, palmitate almost completely dissipated the membrane potential whilst stimulating respiration. We therefore used 3mM GDP in our assay. Under this condition, palmitate caused a strong increase in proton leakage as evidenced by the increased oxygen consumption and decreased membrane potential. At 3mM GDP the proton leak induced by palmitate was even higher than that observed in the absence of GDP (0mM) and palmitate. However, palmitate had no discernible effect on oxygen consumption of liver mitochondria (Fig. 6). The increased proton leakage due to palmitate combined with the observed GDP inhibition was consistent with an uncoupling function of UCP1.

There always remains the possibility that the GDP sensitive proton conductance in the BAT mitochondria was due to the adenine nucleotide translocase (ANT), a mitochondrial anion carrier that exchanges ADP for ATP across the mitochondrial inner membrane (5, 11). ANT can be potently inhibited by carboxyatractylate (CAT). As the uncoupling effect of ANT is so strong in rat liver and kidney mitochondria, Skulachev and co-workers have suggested that the recoupling effect of GDP on mitochondria cannot be considered as a specific probe for the involvement of a UCP in fatty acid-mediated uncoupling and that GDP suppresses ANT function (20). However, addition of 100μM CAT in the absence of GDP did not result in any observable change in proton conductance in BAT mitochondria of cold acclimated *E. myurus*. In fact, in the presence of CAT (no GDP), the BAT mitochondria were more uncoupled than when 1mM GDP was present in our assay (data not shown). This suggests that the proton leakage induced by fatty acids in this study was mediated by UCP1 and not by ANT. In addition, 5mM ADP had an

effect even more potent than that of 5mM GDP, demonstrating strong purine nucleotide sensitivity.

We then compared kinetics of proton conductance in BAT mitochondria from CA and WA animals. The oxygen consumption driving the proton leak in the absence of ATP synthesis was plotted against different membrane potentials imposed by malonate titration of succinate oxidation to display the kinetic dependence of proton leak on its driving force, the membrane potential at 37°C. We then assessed similarities and differences in proton leak rate curves by the overlap or non-overlap of standard error bars as has been done in other studies (1, 3, 6, 16). In agreement with our other results, the proton leak curves of BAT mitochondria overlapped for cold and warm acclimated animals, indicating similar proton leak kinetics under the two acclimation treatments

(Fig. 7), suggesting that BAT mitochondria from CA animals were no more uncoupled than those from WA animals. Similarly, there were no significant differences in the proton leak kinetics of liver mitochondria between groups (data not shown).

Discussion

The overall aim of this study was to elucidate the basis of nonshivering thermogenesis in the rock elephant shrew, *Elephantulus myurus* by integrating measurements at the molecular, subcellular, tissue and whole animal levels. We have demonstrated the presence of the *Ucp1* gene as well as its protein UCP1 whose expression was BAT specific in a member of the Afrotheria. The orthologue of UCP1 has already been demonstrated in fish although a thermogenic role in ectotherms is unlikely (19). It is therefore imperative that in addition to showing occurrence of UCP1, uncoupling thermogenic function should also be demonstrated if it

is to be implicated in nonshivering thermogenesis. We therefore characterized the function of UCP1 and investigated proton leak kinetics and demonstrated that addition of fatty acids to isolated BAT mitochondria increases proton conductance in a GDP-sensitive manner. To fully display thermogenesis, an organ requires high oxidative capacity to oxidize metabolic substrates and a leak (such as UCP1 to release heat) to uncouple oxidative phosphorylation (22). We demonstrated that BAT of the elephant shrew displays highest oxidative capacity in comparison to skeletal muscle and liver. Taken together, our data show that in this ancient eutherian, UCP1 has a thermogenic function and that NST in the elephant shrew occurs in BAT and is UCP1 mediated.

We expected adaptive recruitment of thermogenic capacity during cold acclimation, the hallmarks of which are increases in the expression of the *Ucp1* gene and its associated UCP1, and mitochondrial biogenesis (21). We found no evidence of recruitment of cold-induced thermogenic capacity in BAT when investigating NA-induced response, *Ucp1* mRNA, mitochondrial UCP1 levels and amounts of tissue UCP1 in rock elephant shrews. We also could not find any differences in the rate of proton leakage from mitochondria of cold and warm acclimated animals. Instead, of all the parameters considered, the principal adjustment in response to cold acclimation was only evident in BMR and state 4 respiration rate of BAT mitochondria.

Although in highly seasonal species such as the Djungarian hamster, uncoupled respiration has a dominating role during cold acclimation, with the total amount of UCP1 in BAT estimated to increase by a nearly 20-fold magnitude (12), it has been widely documented that small mammals increase their BMR in response to cold acclimation (9, 25, 34). This elevated BMR is thought to improve total thermogenic capacity, as well as extend the thermoneutral zone to lower T_as and is partly associated with blood distribution to the intestinal organs, whose metabolic activities are presumably increased (12).

The higher state 4 respiration suggests a higher respiratory capacity in the BAT mitochondria of cold acclimated animals. Cytochrome c oxidase is a marker enzyme for the inner mitochondrial membrane and can be used to estimate the amount of mitochondrial protein in BAT and respiratory capacity of mitochondria (21). Increased COX activity also points towards increased respiratory capacity and is often accompanied by a pronounced stimulation of UCP1 gene expression, thus elevating the capacity of BAT for NST (24). The high COX activity in BAT compared to skeletal muscle and liver does support a thermogenic function of this tissue. In addition, although there were no significant differences in COX activity between groups, both at tissue and mitochondrial level, we did find a tendency towards higher respiratory capacity in the BAT mitochondria of cold acclimated animals.

It is tempting to ask whether pronounced differences might have been observed between the two groups had the animals in the cold acclimation group been placed at a much lower ambient temperature or cold/warm acclimated for longer. It is true that in most studies animals are often acclimated to ambient temperatures below 10°C and that acclimating our animals to lower ambient temperatures for longer might have yielded significant differences between the two groups. Nevertheless, comparable temperature gradients such as used in this study have been shown to induce changes in thermogenic capacity of mice. For example, mice acclimated to 21°C and then transferred to 33°C decreased BAT mass, mitochondrial protein as well as UCP1 content within 48 hrs (10).

We are interested in the extent to which ambient temperature fluctuations influence physiological responses of animals in their natural habitats. We therefore considered that placing the animals at lower ambient temperatures may not necessarily have been ecologically relevant because even in winter in their natural habitat, the rock elephant shrews would not experience consistently low ambient temperatures. Instead, in its natural range, this species is exposed to fluctuating diel ambient temperature cycles, with cool nights (ca. 5°C) and warm days (> 20°C). We suggest that the animals may not have increased their thermogenic capacity

during our cold acclimation conditions simply because NST is not an exclusive source of heat gain for this species. In fact, it has been shown previously that during winter when *E. myurus* use daily torpor they accrue significant energy saving by exogenous passive heating during arousal from torpor (30, 32). The apparent lack of NST recruitment may therefore be explained simply by considering the ambient temperature cycles that occur in this species' natural habitat. In addition, Lovegrove et al. (2001) predicted that metabolic rate of *E. myurus* acclimated to 18°C was 3.01 ± 0.15 ml $O_2.g^{-1}.hr^{-1}$ at 0°C (Figure 5C, Lovegrove et al. 2001). Since there were no differences in NST capacity of cold and warm acclimated animals in this study, we pooled our results and found that the mean maximum NA-induced oxygen consumption was 4.03 ± 0.22 ml $O_2.g^{-1}.hr^{-1}$. This implies that at 28°C *E. myurus* have already acquired BAT providing them with enough NST capacity to deal with T_as below freezing. Since T_as seldom decrease below 0°C in *E. myurus*' natural habitat the BAT recruited at 28°C is sufficient for survival and meets their ecological requirements. On the other hand the maintenance of functional BAT at high T_as (28°C) might allow them to deal with unpredictable and aseasonal cold spells known to occur in this species' range.

In nature, ambient temperature and photoperiod often act in concert to bring about seasonal physiological adjustments. In retrospect, it remains possible that had we coupled cold and warm acclimation with short and long photoperiod, respectively, we might have observed some differences between the two groups. Nevertheless, in a study investigating phenotypic plasticity of physiological variables between species, (25) found that after controlling for latitude and phylogenetic effects, the seasonal changes in NST cannot (as yet) be reliably associated with any independent predictor variable.

In conclusion, we show that BAT and functional UCP1 are already present in the rock elephant shrew, a member of the Afrotheria and a basal eutherian mammal although they did not show any evidence of additional recruitment of NST capacity when cold acclimated. This does

not necessarily mean that NST is not adaptive in this species. We suggest that what is likely to be most informative regarding the seasonal regulation and the adaptive nature of thermoregenic parameters in any species will be to capture free-ranging individuals, during the different seasons and immediately measuring the parameters of interest without prior acclimation. An understanding of interseasonal and interannual plasticity in physiological responses is likely to be important during seasonal climate perturbations resulting from large scale climate anomalies.

Acknowledgements

This study was financed by the Alexander von Humboldt Foundation (postdoctoral research fellowship to NM), the National Research Foundation of South Africa, the Nelson Mandela Metropolitan University and a DFG grant (KL973/7) to MK. Any opinions, findings and conclusions or recommendations expressed in this material are those of the authors and the NRF does not accept any liability in regard thereto. We are grateful to the Ezemvelo KwaZulu Natal Wildlife for capture and export permits and Mr and Mrs Bruce McKay for granting permission to work and capture animals on their farm in Estcourt, South Africa. We thank Sigrid Stöhr for excellent technical assistance.

Reference

1. **Brand MD, Couture P, Else PL, Withers K and Hulbert AJ**. Evolution of energy and metabolism. *Biochem J* 275: 81-86, 1991.
2. **Brand MD**. Measurement of the mitochondrial proton motive force. In: Bioenergetics - a practical approach, edited by Brown GC. Oxford: IRL Press, 1995, p. 39-62.
3. **Brand M, Couture P, Else PL, Withers K and Hulbert AJ**. Evolution of energy and metabolism. *Biochem J* 275: 81-86, 1991.
4. **Brand M, Pakay J, Ocloo A, Kokoszka J, Wallace D and Brookes P**. The basal proton conductance of mitochondria depends on adenine nucleotide translocase content. *Biochem J* 392: 353-362, 2005.
5. **Brand M, Pakay J, Ocloo A, Kokoszka J, Wallace D, Brookes P and Cornwall E**. The basal proton conductance of mitochondria depends on adenine nucleotide translocase content. *Biochem J* 392: 353-362, 2005.
6. **Brookes P, Buckingham J, Tenreiro A, Hulbert AJ and Brand M**. The proton permeability of the inner membrane of liver mitochondria from ectothermic and endothermic vertebrates and from obese rats: correlations with standard metabolic rate and phospholipid fatty acid composition. *Comp Biochem Physiol* 119B: 325-334, 1998.
7. **Cannon B and Nedergaard J**. The biochemistry of an inefficient tissue: brown adipose tissue. *Essays Biochem* 20: 110-164, 1985.
8. **Cannon B and Nedergaard J**. Brown adipose tissue: Function and physiological significance. *Physiol Rev* 84: 277-359, 2004.
9. **Chaffee R and Roberts J**. Temperature acclimation in birds and mammals. *Annu Rev Physiol* 33: 155-202, 1971.
10. **Desautels M**. Mitochondrial thermogenin content is unchanged during atrophy of BAT of fasting mice. *Am J Physiol* 249: E99-E106, 1985.
11. **Echtay K, Esteves T, Pakay J, Jekabsons M, Lambert A, Portero-Otín M, Pamplona R, Vidal-Puig A, Wang S, Roebuck S and Brand M**. A signalling role for 4-hydroxy-2nonenal in regulation of mitochondrial uncoupling. *EMBO J* 22: 4103-4110, 2003.
12. **Heldmaier G, Klaus S, Wiesinger H, Friedrichs U and Wenzel M**. Cold acclimation and thermogenesis. In: Life in the Cold II, edited by Malan A and Canguilhem B. Montrouge, France: John Libbey Eurotext, 1989, p. 347-358.
13. **Heldmaier G and Ruf T**. Body temperature and metabolic rate during natural hypothermia in endotherms. *J Comp Physiol B* 162: 696-706, 1992.
14. **Heldmaier G, Klaus S and Wiesinger H**. Seasonal adaptation of thermoregulatory heat production in small mammals. In: Thermoreception and temperature regulation, edited by Bligh J and Voigt K. Berlin: Springer-Verlag, 1990, p. 235-243.
15. **Heldmaier G, Steinlechner S, Rafael J and Vsiansky P**. Photoperiodic control and effects of melatonin on nonshivering thermogenesis and brown adipose tissue. *Science* 212: 917-919, 1981.

16. **Hulbert AJ, Else PL, Manolis S and Brand M**. Proton leak in hepatocytes and liver mitochondria from archosaurs (crocodiles) and allometric relationships for ectotherms. *J Comp Physiol B* 172: 387-397, 2002.

17. **Jansky L**. Non-shivering thermogenesis and its thermoregulatory significance. *Biol Rev* 48: 85-132, 1973.

18. **Jastroch M, Withers K and Klingenspor M**. Uncoupling protein 2 and 3 in marsupials: identification, phylogeny and gene expression in response to cold and fasting in *Antechinus flavipes*. *Physiol Genomics* 17: 130-139, 2004.

19. **Jastroch M, Wuertz S, Kloas W and Klingenspor M**. Uncoupling protein 1 in fish uncovers an ancient evolutionary history of mammalian non-shivering thermogenesis. *Physiol Genomics* 22: 150-156, 2005.

20. **Khailova L, Prikhodko E, Dedukhova V, Mokhova E, Popov V and Skulachev V**. Participation of ATP/ADP antiporter in oleate and oleate-hydroperoxide-induced uncoupling suppresed by GDP and carboxyatractylate. *Biochim et Biophys Acta* 1757: 1324-1329, 2006.

21. **Klaus S, Heldmaier G and Ricquier D**. Seasonal acclimation of bank voles and wood mice: nonshivering thermogenesis and thermogenic properties of brown adipose tissue mitochondria. *J Comp Physiol B* 158: 157-164, 1988.

22. **Klingenspor M**. Cold-induced recruitment of brown adipose tissue thermogenesis. *Exp Physiol* 88: 141-148, 2003.

23. **Klingenspor M**. Cold-induced recruitment of brown adipose tissue thermogenesis. *Exp Physiol* 88: 141-148, 2003.

24. **Klingenspor M, Ivemeyer M, Wiesinger HK, Heldmaier G and Wiesner R**. Biogenesis of thermogenic mitochondria in brown adipose tissue of Djungarian hamsters during cold acclimation. *Biochem J* 316: 607-613, 1996.

25. **Lovegrove BG**. Seasonal thermoregulatory responses in mammals. *J Comp Physiol B* 175: 231-247, 2005.

26. **Lovegrove BG, Raman J and Perrin MR**. Heterothermy in elephant shrews (*Elephantulus* spp.): hibernation or daily torpor? *J Comp Physiol B* 171: 1-10, 2001.

27. **Malan A**. The origins of hibernation: a reappraisal. In: Adaptations to the cold: Tenth International Hibernation Symposium, edited by Geiser F, Hulbert AJ and Nicol SC. Armidale: University of New England Press, 1996, p. 1-6.

28. **McKechnie AE, Chetty K and Lovegrove BG**. Phenotypic flexibility in the basal metabolic rate of laughing doves: responses to short-term thermal acclimation. *J Exp Biol* 210: 97-106, 2007.

29. **McKechnie AE and Wolf BO**. Partitioning of evaporative water loss in white-winged doves: plasticity in response to short-term thermal acclimation. *J Exp Biol* 207: 203-210, 2004.

30. **Mzilikazi N and Lovegrove BG**. Daily torpor in free-ranging rock elephant shrews, Elephantulus myurus: A year-long study. *Physiol Biochem Zool* 77: 285-296, 2004.

31. **Mzilikazi N and Lovegrove BG**. Noradrenalin induces thermogenesis in a phylogenetically ancient eutherian mammal, the rock elephant shrew, *Elephantulus myurus*. *J Comp Physiol B* 176: 75-84, 2006.

32. **Mzilikazi N, Lovegrove BG and Ribble D**. Exogenous passive heating during torpor arousal in free-ranging rock elephant shrews, Elephantulus myurus. *Oecologia* 133: 307-314, 2002.

33. **Mzilikazi N and Lovegrove B**. Daily torpor during the active phase in free-ranging rock elephant shrews, *Elephantulus myurus*. *J Zool ,Lond* 267: 103-111, 2005.

34. **Nespolo R, Bacigalupe L, Rezende E and Bozinovic F**. When nonshivering thermogenesis equals maximum metabolic rate: thermal acclimation and phenotypic plasticity of fossorial *Spalacopus cyanus* (Rodentia). *Physiol Biochem Zool* 74: 325-332, 2001.

35. **Nicholls D and Locke R**. Thermogenic mechanisms in brown fat. *Physiol Rev* 64: 1-64, 1984.

36. **Reynafarje B, Costa L and Lehninger A**. O2 solubility in aqueous media determined by a kinetic method. *Anal Biochem* 145: 406-418, 1985.

37. **Smith L and Camerino P**. Comparison of polarographic and spectrophotometric assays for cytochrome c oxidase activity. *Biochem* 2: 1428-1432, 1963.

38. **Springer MS, Cleven GC, Madsen O, de Jong WW, Waddell VG, Amrine HM and Stanhope MJ**. Endemic African mammals shake the phylogenetic tree. *Nature* 388: 61-64, 1997.

39. **Wunder BA and Gettinger RD**. Effects of body mass and temperature acclimation on the nonshivering thermogenic response of small mammals. In: Adaptations to the Cold: Tenth International Hibernation Symposium, edited by Geiser F, Hulbert AJ and Nicol SC. Armidale: University of New England Press, 1996, p. 131-139.

Figure legends

Figure 1: Basal metabolic rate (BMR) and maximum oxygen consumption (VO_2 max) induced by noradrenalin (NA) injection in (A) cold acclimated and (B) warm acclimated *Elephantulus myurus*. The NST capacity was calculated as the difference between VO_2 max and BMR.

Figure 2: Phylogenetic relationships of known eutherian UCP1. A neighbour joining tree was derived from the amino acid alignment. Bootstrap values from 1000 replications are given next to the internal branches. The oxaloacetate-malate carrier served as the outgroup.

Figure 3: (A) Northern blot analysis of UCP1 expression in multiple tissues of *Elephantulus myurus*. Total RNA (5µg) isolated from multiple tissues was hybridized with ^{32}P-radiolabelled cDNA corresponding to a *E. myurus* UCP1 fragment.
(B) Western blot analysis of UCP 1 expression in multiple tissues of *E. myurus*. (C). Northern blot analysis of BAT UCP1 mRNA showing no significant differences in the levels of expression in response to cold and warm acclimation. Ten µg RNA were used in this analysis. (D) Western blot analysis of UCP1 levels in BAT homogenate and (E) BAT mitochondria of cold and warm acclimated *E. myurus*.

Figure 4: (A) Cytochrome c oxidase (COX) activity in brown adipose tissue, liver and skeletal muscle homogenate of cold and warm acclimated *E. myurus*. There were no significant differences between groups in any of the tissues measured. (B) Cytochrome c oxidase activity measured in isolated BAT mitochondria of cold and warm acclimated *E.myurus*. (C) State 4 respiration of isolated *E. myurus* BAT mitochondria respiring on succinate in the presence of 5mM GDP. Respiration was significantly higher in the mitochondria from cold acclimated animals.

Figure 5: (A) Dependence of proton leak rate (measured as the respiration rate driving proton leak) in the presence of oligomycin on membrane potential of isolated BAT (open circles) and liver (closed circles) mitochondria of cold acclimated *E.myurus* in the presence of 0, 1, 3 and 5mM GDP. Replicate measurements were performed on each mitochondrial preparation and averaged. Values are ± SEM from five independent preparations. The broken line indicates the highest common potential (135.3 mV).

(B) The relationship between proton leak rate at the highest common potential (measured as the respiration rate driving proton leak) at 135.3 mV in (A) and GDP concentration.

Figure 6: Dependence of proton leak rate (measured as the respiration rate driving proton leak) in the presence of oligomycin on membrane potential of isolated BAT (open circles) and liver (closed circles) mitochondria of cold acclimated *E.myurus* in the presence of 0, and 3 mM GDP as well as 100 μM palmitate (in the presence of 3mM GDP). Replicate measurements were performed on each mitochondrial preparation and averaged. Values are ± SEM from five independent preparations.

Figure 7: Dependence of proton leak rate (measured as the respiration rate driving proton leak) in the presence of oligomycin on membrane potential of isolated BAT mitochondria from cold (open circles) and warm (closed circles) acclimated *E.myurus* in the presence of 1, 3 and 5mM GDP. There were no observable differences in the mitochondrial proton leak kinetics of the animals from the two groups. Replicate measurements were performed on each mitochondrial preparation and averaged. Values are ± SEM from five and four independent preparations of cold and warm acclimated animals, respectively.

Figure 1

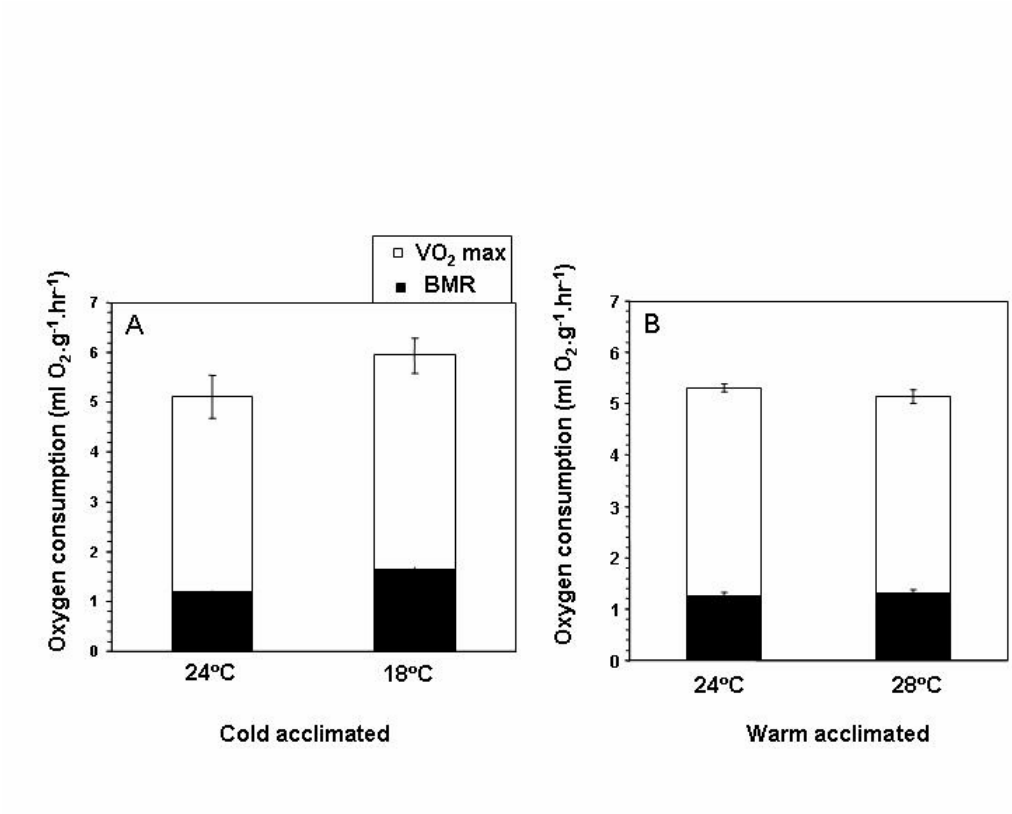
VO2 max
BMR
A
B
Oxygen consumption (ml O2.g-1.hr-1)
0
1
2
3
4
5
6
7
24ºC
18ºC
28ºC
Cold acclimated
Warm acclimated

Figure 2

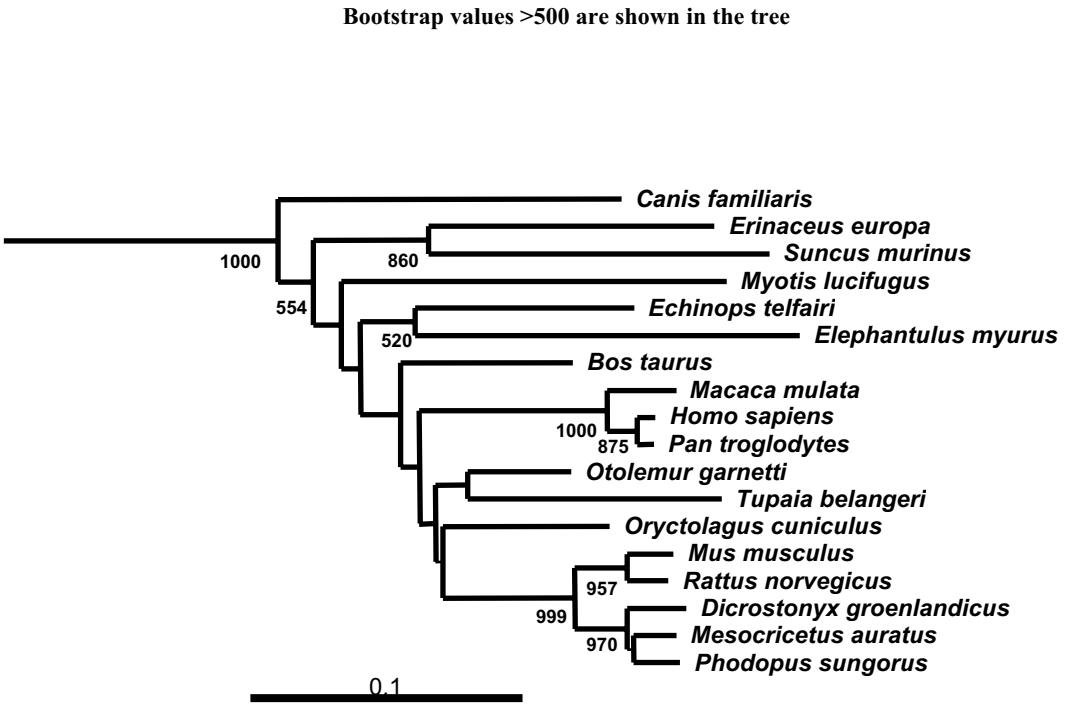
Bootstrap values >500 are shown in the tree
Canis familiaris
Erinaceus europa
Suncus murinus
Myotis lucifugus
Echinops telfairi
Elephantulus myurus
Bos taurus
Macaca mulata
Homo sapiens
Pan troglodytes
Otolemur garnetti
Tupaia belangeri
Oryctolagus cuniculus
Mus musculus
Rattus norvegicus
Dicrostonyx groenlandicus
Mesocricetus auratus
Phodopus sungorus
1000
860
554
520
1000
875
957
999
970
0.1

Figure 3

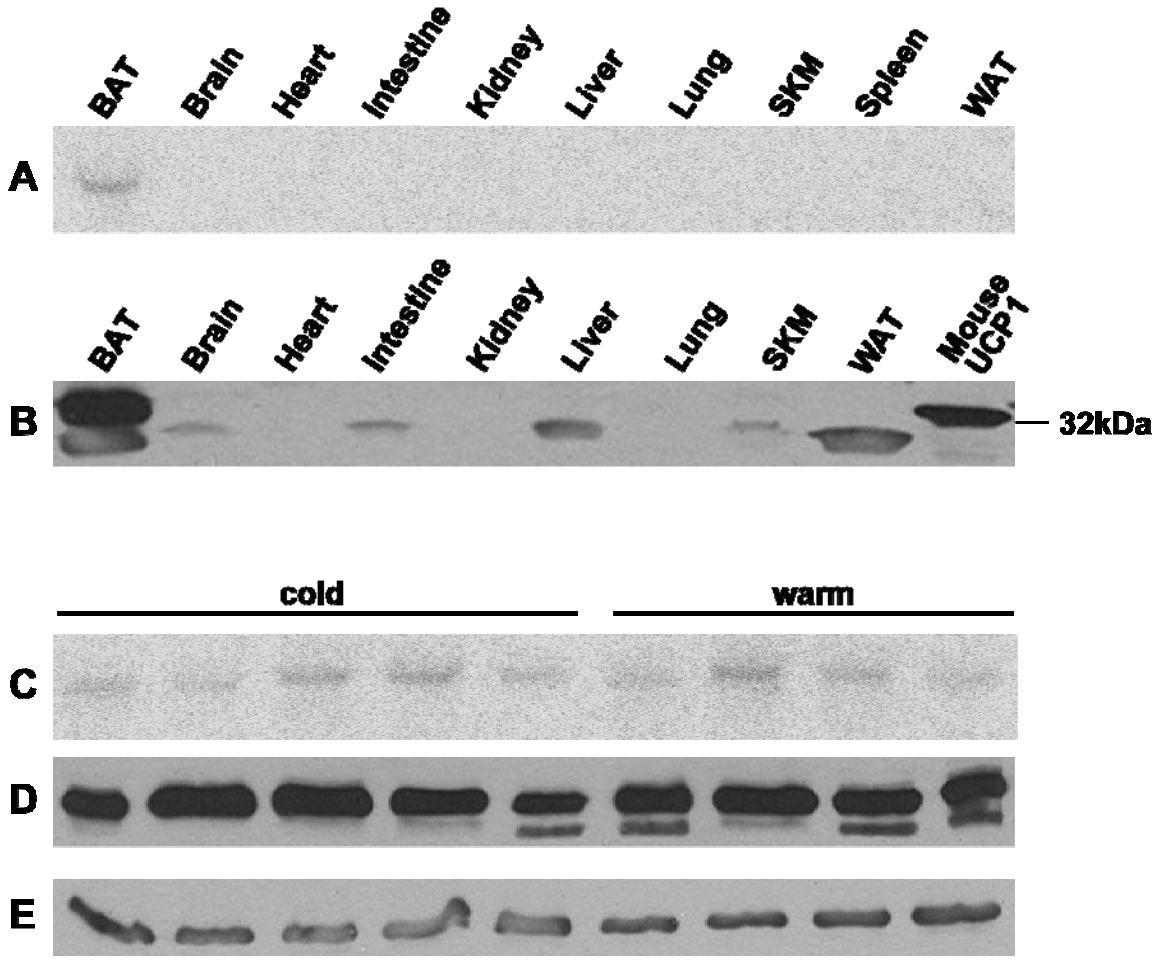
BAT
Brain
Heart
Intestine
Kidney
Liver
Lung
SKM
Spleen
WAT
A
BAT
Brain
Heart
Intestine
Kidney
Liver
Lung
SKM
WAT
Mouse UCP1
B
32kDa
cold
warm
C
D
E

Figure 4

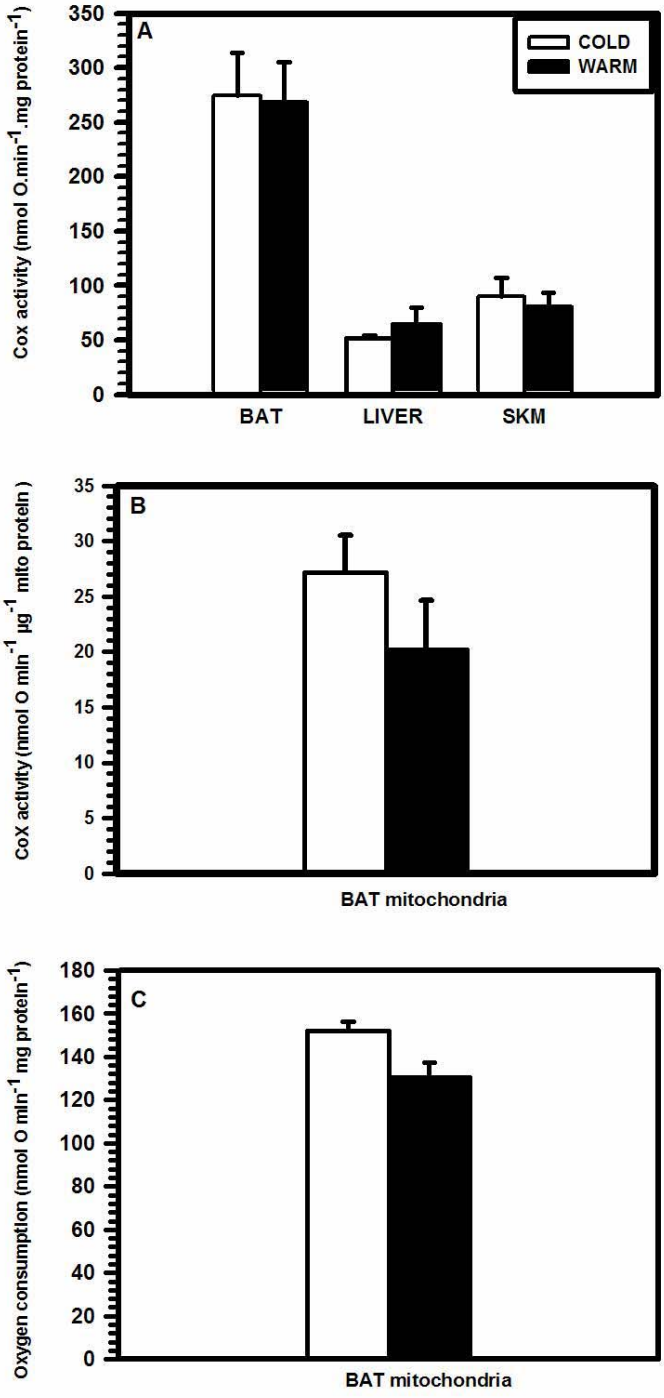
A
COLD
WARM
Cox activity (nmol O.min-1.mg protein-1)
350
300
250
200
150
100
50
0
BAT
LIVER
SKM
B
CoX activity (nmol O min-1 µg-1 mito protein)
35
30
25
20
15
10
5
0
BAT mitochondria
C
Oxygen consumption (nmol O min-1 mg protein-1)
180
160
140
120
100
80
60
40
20
0
BAT mitochondria

Figure 5

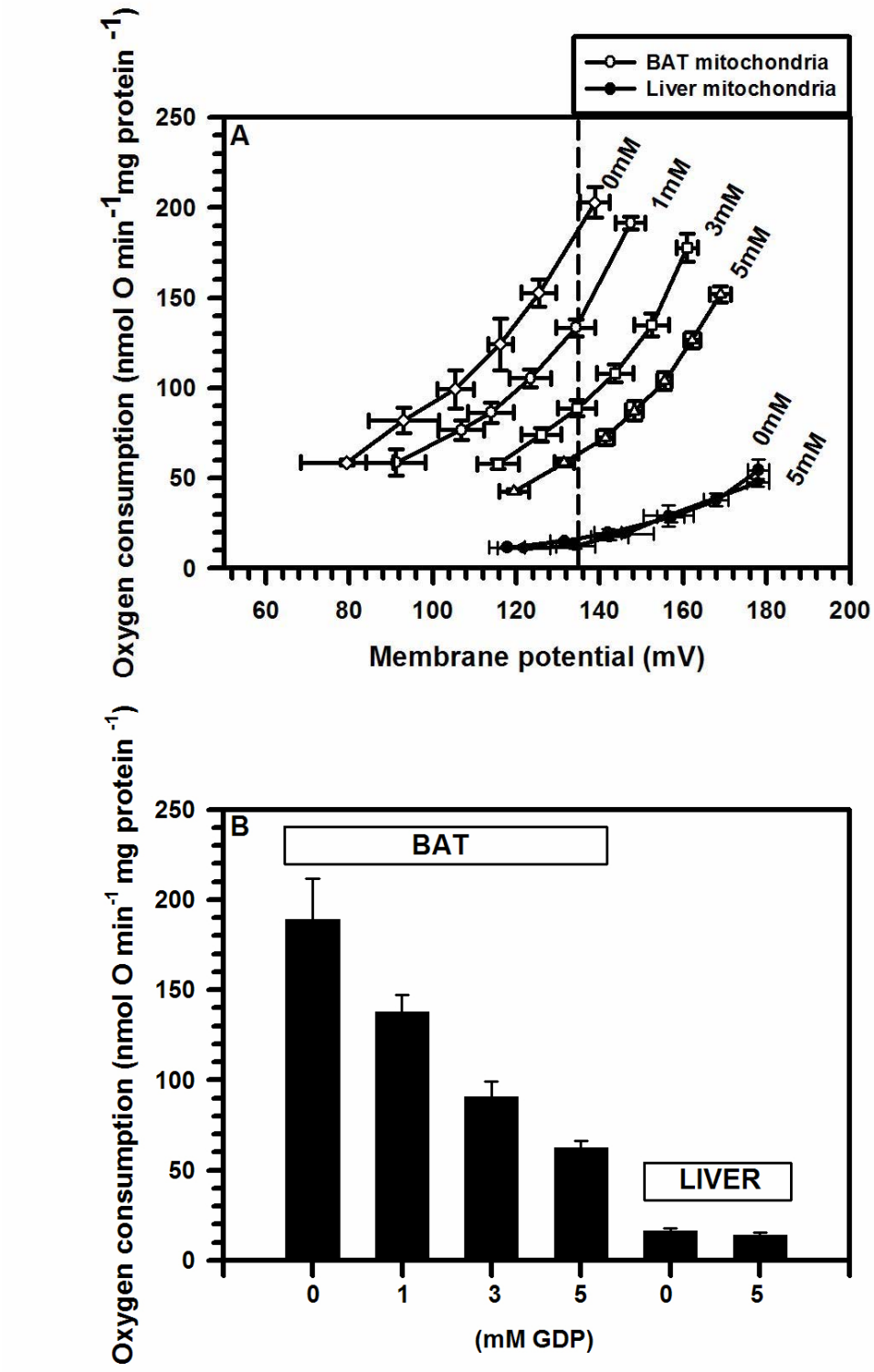
BAT mitochondria
Liver mitochondria
A
0mM
1mM
3mM
5mM
0mM
5mM
Oxygen consumption (nmol O min-1mg protein -1)
Membrane potential (mV)
B
BAT
LIVER
Oxygen consumption (nmol O min-1 mg protein -1)
(mM GDP)

Figure 6

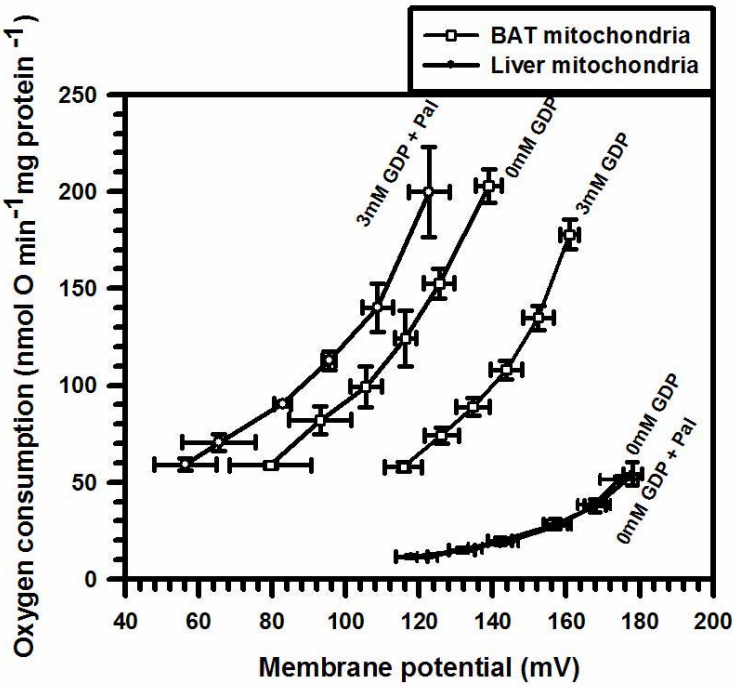
BAT mitochondria
Liver mitochondria
3mM GDP + Pal
0mM GDP
3mM GDP
0mM GDP
0mM GDP + Pal
Oxygen consumption (nmol O min-1mg protein -1)
Membrane potential (mV)
250
200
150
100
50
0
40
60
80
100
120
140
160
180
200

Figure 7

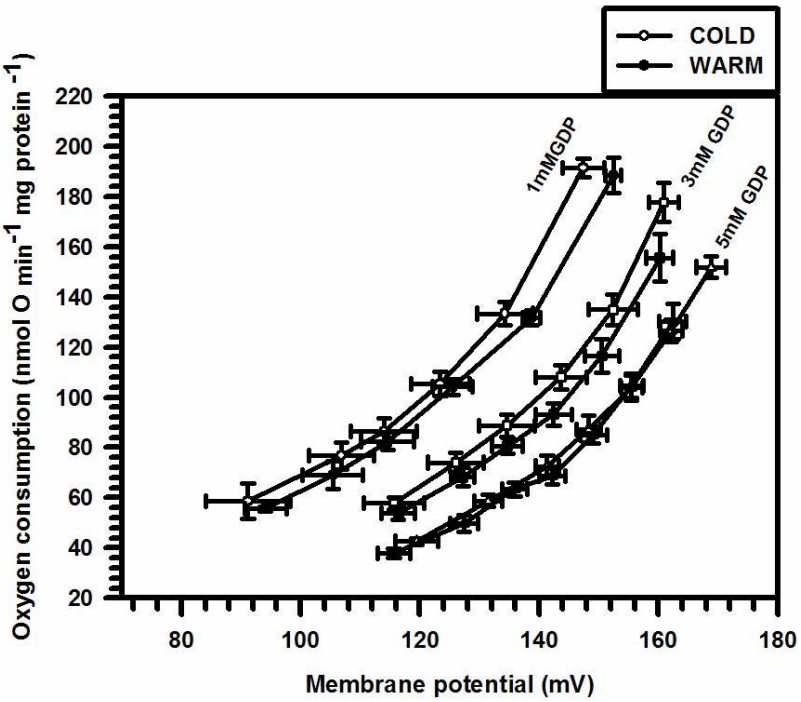
COLD
WARM
1mMGDP
3mM GDP
5mM GDP
Oxygen consumption (nmol O min-1 mg protein-1)
Membrane potential (mV)
20
40
60
80
100
120
140
160
180
200
220
80
100
120
140
160
180

Proton conductance in myotubular mitochondria of the cold-acclimated marsupial *Antechinus flavipes* has a role in mild uncoupling but not in thermogenesis

Jastroch M., Withers K. W., Stoehr S. and Klingenspor M.

[1]Department of Animal Physiology, Faculty of Biology, Philipps-Universität Marburg, Karl-von-Frisch-Str. 8, 35032 Marburg, Germany, [2]Department of Biological and Physical Sciences, University of Southern Queensland, Toowoomba, Qld, Australia

Running head: Mitochondrial proton conductance in skeletal muscle of marsupials

To whom correspondence should be addressed: Martin Jastroch, Philipps University Marburg, Department of Biology, Animal Physiology, Karl-von-Frisch-Str. 8, 35043 Marburg, Germany, Email: Jastroch@staff.uni-marburg.de,Phone: +49-6421-2823389, Fax: +49-6421-282893

Abstract

The organs and molecular mechanisms contributing to adaptive thermogenesis in marsupials are not understood as they apparently lack brown adipose tissue (BAT). Studies in the marsupial *Monodelphis domestica* demonstrate increased oxidative capacity and uncoupling protein 3 (UCP3) expression in skeletal muscle leading to speculations on uncoupled respiration to sustain endothermy in the cold as found for BAT.

Here, we investigated the role of mitochondrial proton conductance in the small Australian marsupial *Antechinus flavipes*. In accordance with studies in *M. domestica*, we found a tendency towards higher oxidative capacity in skeletal muscle indicating metabolic adjustments in cold-acclimated (CA) individuals. Despite elevated UCP3 expression in the cold, we observed no change in basal proton conductance of isolated myotubular mitochondria. Furthermore, proton conductance of liver mitochondria was also not affected by cold. In eutherians, 4-hydroxynonenal (HNE) is an activator of mild uncoupling mediated by UCP3 and ANT (adeninenucleotide transporter) to convey protection from lipid peroxidation and mitigating ROS production. In the marsupial *A. flavipes*, proton conductance in myotubular mitochondria was induced by HNE selectively in the CA group. Induced uncoupling activity could be attributed to the ANT as judged by inhibition with CAT (carboxyatractylate), while GDP, an inhibitor of rodent UCP3, had no effect on marsupial UCP3.

In contrast to previous expectations, we here exclude adaptive thermogenesis by increased mitochondrial proton conductance in the skeletal muscle of marsupials as it is found for eutherian BAT. Higher sensitivity of proton conductance to HNE indicates mechanisms mitigating reactive oxygen species by mild uncoupling during cold stress. The ANT is involved in mild uncoupling, whereas the physiological role of UCP3 remains unclear.

Introduction

In placental mammals, it has been well established that brown adipose tissue (BAT) contributes significantly to adaptive nonshivering thermogenesis (NST) (Cannon and Nedergaard 2004). Uncoupling protein 1 (UCP1), exclusively expressed in BAT, uncouples respiration from ATP production and dissipates proton motive force as heat (Nicholls and Locke 1984). In response to cold, UCP1 expression and mitochondrial biogenesis increase about 2-3 fold thereby providing higher NST capacity (Klingenspor et al. 1996).

Marsupials also thermoregulate well in the cold although the presence of BAT has not been unequivocally demonstrated (Hayward and Lisson 1992); (Kabat et al. 2003). It was suggested that shivering is the main source of heat production in marsupials but cold-acclimated kowari (*Dasyuroides byrney*) showed a decrease in shivering tremor of cold-acclimated (CA) individuals indicating some form of NST that replaced shivering thermogenesis (May 2003). Other studies pointed towards the presence of NST similar to observations in eutherians. For example, noradrenaline injections led to an increase of metabolic rate in macropods (Nicol 1978); (Nicol et al. 1997); (Ye et al. 1996); (Loudon et al. 1985) which was attributated to skeletal muscle by others (Ye et al. 1996). In other marsupials, small responses could not be unambiguously interpreted as NST (Reynolds W and Hulbert 1982); (Dawson and Olson 1988); (Smith B.K. and Dawson T.J. 1984); (Opazo et al. 1999). The controversy around marsupial adaptive thermogenesis led to the search for alternative thermogenic organs and mechanisms. In other endothermic vertebrates lacking BAT, NST in skeletal muscle was previously proposed in birds (Talbot et al. 2004); (Raimbault et al. 2001), pigs (Berthon et al. 1996) and UCP1-ablated mice (Monemdjou et al. 2000).

Studies in the Southamerican marsupial *M. domestica* suggested that skeletal muscle was responsible for nonshivering thermogenesis in the cold because CA individuals showed higher costs of transport indicating an increase in muscle energetics (Schaeffer et al. 2005). The

concordant upregulation of the muscle-specific UCP3 implied a molecular explanation for thermogenic processes in the *M. domestica*. In CA macropods, NST mediated by UCP3 was suggested without providing functional analysis (Kabat et al. 2003); (Schaeffer et al. 2005). Taken together, these observations suggested that in absence of UCP1 and BAT, marsupial UCP3 may have a thermogenic role in skeletal muscle.

In eutherians, there is minor evidence for UCP3-mediated heat production. UCP3 knockout mice have a diminished thermogenic response to the drug MDMA (3,4-methylenedioxymethamphetamine) in skeletal muscle (Mills et al. 2003) but the physiological significance under pharmacological conditions is questioned. The role of UCP3 is controversial and there is doubt of whether low protein concentration as compared to UCP1 in BAT can produce sufficient amounts of heat (Nedergaard and Cannon 2003). Furthermore, thermogenic uncoupled respiration is expected to be reduced in response to fasting but in contrast, UCP3 gene expression is increased (Boss et al. 1998); (Jastroch et al. 2004b). However, rodent UCP3 exhibits an uncoupling function that can be induced with superoxide and 4-hydroxynonenal in isolated mitochondria but these activators relate to protection from lipid peroxidation by mild uncoupling (Echtay et al. 2002); (Echtay et al. 2003).

Recently, UCP3 has been identified in muscle of *Antechinus flavipes* (Jastroch et al. 2004b) but the function of UCP3 in marsupials has not been investigated so far.

Our approach was to acclimate the small marsupial *A. flavipes* to the cold and confirm increases in oxidative capacity and UCP3 levels as found for *M. domestica*. With subsequent measurements of mitochondrial proton conductance, we aimed to substantiate previous speculations on uncoupling activity in myotubular mitochondria as found for thermogenic BAT

Materials and Methods

Animal Experiments

All experimental protocols were approved by the Animal Ethics Committee of the University of Southern Queensland, Queensland Environmental Protection Agency (permit number WISP02633304) and Environment Australia (export number WT2005-12380). Seven *Antechius flavipes* were captured with Elliott traps from several subtropical habitats in southeast Queensland (Australia) between January and March 2005 and housed individually for at least one week at 24°C (12:12 light/dark, lights on at 0700h) with free access to water and food (mealworms and cat food mix including calcium carbonate). To investigate the effect of cold exposure, four individuals were transferred to a climate chamber at 10°C for 17 – 22 days (cold-acclimated; CA) whereas three individuals remained at 24°C (warm-acclimated; WA). The body weight of the individuals ranged from 24.9 to 38.5 grams. The two acclimation groups were balanced for body weight.

Tissue dissection

A. flavipes were euthanased (carbon dioxide) and the bulk of skeletal muscle and liver was used to isolate mitochondria. Small samples of skeletal muscle for molecular analysis were immediately snap frozen in liquid nitrogen and shipped to Marburg, Germany.

Cytochrome c oxidase (COX) activity

COX activity was measured polarographically in a temperature-controlled chamber. 40 to 60 mg of frozen skeletal muscle tissue was homogenized in 500 µl ice-cold tissue buffer (33.9 mmol l^{-1} KH_2PO_4, 66.1 mmol l^{-1} K_2HPO_4, 2 mmol l^{-1} EDTA, 10 mmol l^{-1} glutathion, pH 7.5) with a Ultraturrax tissue homogenizer. Protein extracts from skeletal muscle were quantified using the Bradford method. The homogenate was diluted 1:2 with polyoxyethylenether W1 (Sigma),

1.5%. Oxygen consumption was measured using a Clark-type oxygen electrode (Rank Brothers Ltd., United Kingdom) maintained at 25°C and calibrated with air-saturated measuring buffer (79 mmol l^{-1} K_2HPO_4, 20.1 mmol l^{-1} KH_2PO_4, 5 mmol l^{-1} EDTA, 3 mmol l^{-1} horse cytochrome C (Sigma), 0.25 mol l^{-1} ascorbate; pH 7.4) which was assumed to contain 479 nmol O_2 ml^{-1} (Reynarfarje et al. 1985). 10, 20 or 30 µl of diluted homogenate were suspended in 1 ml medium.

50µg of skeletal muscle protein were loaded onto polyacrylamide gels and separated by electrophoresis, transferred to nitrocellulose membrane (Hybond C, Amersham). The Western blot was probed with a rat/mouse UCP3 antibody kindly provided by Lawrence Slieker (Eli Lilly) as shown previously (Jastroch et al. 2004a). .For the detection of ANT1, we probed the Western blots with an 1:50 diluted antibody raised in rabbit against a rodent ANT peptide (C-G-D-Q-A-L-S-F-L-K-D-F; Biogenesis, U.K.). Signals on the film were quantified densitometrically using Scion Image Software 4.0.2.

Isolation of skeletal muscle and liver mitochondria

Skeletal muscle tissue was immediately placed in ice-cold isolation CP1-medium containing 100 mmol l^{-1} KCl, 50 mmol l^{-1} Tris-HCl and 2 mmol l^{-1} EGTA, pH 7.4, at 4°C. Muscle tissue was cleaned from adipose tissue patches, minced with scissors, and repeatedly rinsed with CP-1 medium, stirred for 3 min in CP-2 medium (CP-1 plus 1 mmol l^{-1} ATP, 5 mmol l^{-1} MgCl2, 0.5% (w/v) bovine serum albumin (BSA), 2.1 U ml^{-1} protease (Subtilisin A), pH 7.4, at 4°C) and homogenised in CP-2 medium using a polytron tissue homogeniser (Kinetica). The homogenate was stirred in CP-2 for 3 min, then mitochondria were isolated using differential centrifugation and resuspended in CP-1 medium. The liver was placed in ice-cold STE medium (250mmol l^{-1} sucrose, 5mmol l^{-1} Tris, 2 mmol l^{-1} EGTA, pH 7.4, at 4°C) and minced with scissors and disrupted with a Dounce homogenizer with a medium-fitted pestle. Protein concentration was

determined using the biuret method with free fatty acid bovine serum albumine as standard (Sigma No. A3803).

Measurement of Mitochondrial Oxygen Consumption

Oxygen consumption was measured using a Clark-type oxygen electrode (Rank Brothers Ltd., United Kingdom) maintained at 35°C and calibrated with air-saturated medium (120 mmol l^{-1} KCl, 5 mmol l^{-1} KH_2PO_4, 3 mmol l^{-1} HEPES, 1 mmol l^{-1} EGTA, and 0.3% (w/v) defatted BSA, pH 7.2) which was assumed to contain 416 nmol O ml^{-1} (Reynarfarje et al. 1985). Mitochondria were suspended at 0.35 mg ml^{-1} to 0.5 mg ml^{-1} (for skeletal muscle) and 1.0 mg ml^{-1} (for liver) in 2.5 ml medium and incubated with 6 mmol l^{-1} succinate, 8 µmol l^{-1} rotenone, 4µg ml^{-1} oligomycin, and 110 ng ml^{-1} nigericin.

Measurement of Proton Conductance

The respiration rate of mitochondria, in the presence of oligomycin to inhibit ATP synthesis (State 4), is proportional to the rate at which protons leak across the inner membrane. The kinetic response of the proton conductance to its driving force (proton motive force) can therefore be measured as the relationship between respiration rate and membrane potential when the potential is varied by titration with electron transport chain inhibitors (Nicholls 1974); (Brand 1990). Respiration rate and membrane potential were determined simultaneously using electrodes sensitive to oxygen and to the potential-dependent probe $TPMP^+$ (Brand 1995). The $TPMP^+$ electrode was calibrated with sequential additions of up to 1.25µmol l^{-1} $TPMP^+$. Six mmol L^{-1} succinate was added to start the reaction. TPMP+ correction factor was assumed to be 0.4 for liver and 0.35 for liver as described previously (Rolfe et al. 1994).

Statistical Analysis

Values presented are means ± S.E.M. Unpaired Student's t tests and one-way ANOVA were performed with level of significance set to $p<0.05$.

Results

COX activity and UCP3 protein content

COX activity may be used to estimate oxidative capacity and is a marker for mitochondrial density in tissues. Measuring crude skeletal muscle tissue homogenates of *A. flavipes*, we found a tendency towards higher oxidative capacity in CA individuals (WA: 106.2 ± 7.3 vs. CA: 135.3 ± 13.3 µatoms O min^{-1} g^{-1} wet weight) (Fig. 1A). We then probed the protein homogenates with a rodent UCP3 antibody as described previously (Jastroch et al. 2004a). UCP3 protein levels were elevated two-fold in response to cold ($p<0.05$) (Fig. 1B).

State 4 respiration and basal proton conductance of liver and skeletal muscle mitochondria

We measured oxygen consumption of isolated mitochondria and compared the values of resting (state 4) respiration in isolated skeletal muscle and liver mitochondria of WA and CA *A. flavipes*. When respiring on succinate, state 4 respiration was not significantly different in liver (WA, 46.14 ± 5.40 nmol O min^{-1} mg^{-1}; CA, 48.80 ± 1.53 nmol O min^{-1} mg^{-1}) and skeletal muscle (WA, 69.78 ± 7.59 nmol O min^{-1} mg^{-1}; CA, 71.74 ± 2.34 nmol O min^{-1} mg^{-1}). At 35°C, we compared the full kinetic response of proton leak (monitored as oxygen consumption rate) to stepwise changes in its driving force, membrane potential, in skeletal and liver mitochondria from WA and CA *A. flavipes* (Fig. 2). In response to cold, the kinetic response of proton leak was slightly but not significantly increased in both tissues of CA animals. As known for placental mammals, liver basal proton conductance was lower than skeletal muscle proton conductance (about 50% when compared at the highest common potential).

Hydroxy-nonenal induced proton conductance of skeletal muscle mitochondria is sensitive to carboxy-atractylate but not guanosine-diphosphate

Proton conductance can be changed by activation and inhibition of mitochondrial carriers with an uncoupling function. Additional proton leakage is reflected in a shift of the basal proton leak curve to the left. In rodents, HNE increases proton conductance in isolated mitochondria of tissues that express UCPs or high levels of the ANT. Prevention of HNE activation by GDP indicates the involvement of a UCP whereas inhibition by CAT indicates the involvement of the ANT. In this study, we incubated isolated skeletal muscle mitochondria with 35µmol l^{-1} HNE to induce proton conductance (Fig. 3). HNE clearly shifted the proton leak curve of CA *A. flavipes* to the left, demonstrating higher conductance (Fig. 3A), while in WA skeletal mitochondria, HNE had only a minor effect (Fig. 3B). The administration of CAT prevented the induction by HNE. We next quantified the induced proportion of proton leak. As proton leak is a nonlinear function of membrane potential, to make comparisons between the two-acclimation temperatures we compared the oxygen consumption driving proton leak at a common membrane potential. At the common potential of 150 mV (Fig. 3C), HNE treatment in the CA group results in a 40% increase of proton leak (basal: 41.87± 2.28 nmol O min^{-1} mg^{-1} protein; HNE induced: 58.57± 3.18 nmol O min^{-1} mg^{-1} protein, $P < 0.05$) which could be fully prevented by the administration of CAT (43.25± 3.29 nmol O min^{-1} mg^{-1} of protein). This effect was not apparent in WA animals (basal: 38.29± 1.14 nmol O min^{-1} mg^{-1} protein, HNE induced: 46.86± 3.23 nmol O min^{-1} mg^{-1} protein, CAT + HNE: 46.38± 4.04 nmol O min^{-1} mg^{-1} protein). GDP (1mmol l^{-1}) had no inhibitory effect on HNE activation in neither the WA nor the CA group (Fig. 3C). Palmitate (100 µmol l^{-1}) had no additional effect on proton conductance on either basal conditions or HNE-induced conditions (data not shown).

Regulation of ANT gene expression in skeletal muscle of A. flavipes

The functional assay in isolated skeletal muscle mitochondria clearly showed a greater effect of the ANT in CA *A. flavipes*. These effects may be reflected in gene expression of UCP3. Western blot analysis using a commercially available anti-rodent ANT1 antibody did not cross-react with ANT1 as judged by comparing the expected size (deduced from the nucleotide sequence) with the band pattern. We found highest ANT1 mRNA expression in skeletal muscle (suppl. 1). Our Northern blot experiments revealed no difference in ANT1 mRNA between the CA and WA group but levels of mRNA may not reflect protein content. The best example for differences between transcriptional and translational regulation is UCP3 where protein levels are elevated in the cold (Fig. 1) but mRNA levels are unchanged (compare *A. flavipes* UCP3 mRNA expression (Jastroch et al. 2004b) with UCP3 protein levels (Jastroch et al. 2004a)).

Discussion

We investigated the role of proton conductance in myotubular mitochondria during cold stress in the small marsupial *A. flavipes*. Previously, the lack of BAT in marsupials led to suggestions on a thermogenic role for skeletal muscle (Schaeffer et al. 2003); (Schaeffer et al. 2005); (Kabat et al. 2003); (May 2003). The upregulation of UCP3 in *M. domestica* in response to cold coincided with the absence of UCP1 suggesting that UCP3 uncoupled myotubular mitochondria in a thermogenic manner thereby compensating the lack of BAT. We demonstrated that uncoupling of skeletal muscle mitochondria of *A. flavipes* plays no role in heat generation as found for BAT. Instead, the induction of mild uncoupling by HNE in CA *A. flavipes* suggested regulated increase of proton conductance to protect from lipid peroxidations during cold-exposure.

Most importantly, a tendency towards increased oxidative capacity and increased UCP3 levels in response to cold demonstrated adaptive metabolic changes in skeletal muscle of *A. flavipes* as

found for *M. domestica*. Although cold exposure triggered an increase in oxidative capacity of skeletal muscle in marsupials (*A. flavipes* and *M. domestica*), one could not distinguish between higher demand for ATP or inefficient mitochondrial coupling. A higher demand for ATP may be dependent on increased locomotion or shivering (May 2003); (Schaeffer et al. 2005), whereas uncoupling of the mitochondria would increase nonshivering heat dissipation directly.

We here demonstrated that basal proton conductance was unchanged between WA and CA *A. flavipes* despite elevated UCP3 levels and concluded that UCP3 did not increase basal proton conductance. A thermogenic role for marsupial UCP3 was unlikely when compared to the situation of BAT mitochondria in eutherians: a high UCP1 concentration (reaching up to 5% of mitochondrial protein, Ricquiers et al. 1984) leads to an elevation of basal leak respiration which can only be diminished by addition of UCP1-inhibiting purine nucleotides like GDP (Nicholls and Locke 1984). The high proportion of uncoupled respiration by UCP1 provides the basis for nonshivering thermogenesis. Notably, UCP1 uncoupling activity can be induced by addition of palmitate. Palmitate induction also points towards the thermogenic function as the cascade leading to dramatic free fatty acid release in BAT is triggered by cold (Lowell and Spiegelman 2000). In our experiments, the addition of 100µmol l^{-1} palmitate had no effect on basal proton conductance of the myotubular mitochondria.

Whilst a slight elevation of basal proton conductance was found in myotubular mitochondria of cold-acclimated, it could not be related directly to UCP3 protein levels as a similar elevation in found in liver mitochondria (containing no UCP3).

Basal mitochondrial proton conductance is however flexible. Static mitochondrial basal proton conductance causes problems in situations of high proton motive force as it increases the generation of superoxides that subsequently produce carbon centred radicals in the cellular system (Brand 2005). HNE is a carbon centred radical and a well-characterized metabolite of lipid peroxidation. Superoxides and HNE themselves mitigated de novo production in a feedback mechanism by lowering proton motive force (Echtay et al. 2002); (Echtay et al. 2003).

In isolated rodent mitochondria containing UCPs and high contents of the ANT, superoxide and HNE activated mild uncoupling activity. In *A. flavipes*, we demonstrated that HNE induced proton conductance selectively in the CA group. Considering that lipid metabolism in the muscle is enhanced during cold exposure promoting lipid peroxidations, the sensitivity to HNE-induced uncoupling can be explained by the proposed feedback mechanism. Under challenging physiological conditions, increased HNE induction could be provoked in rodents during fasting (Echtay et al. 2002). During fasting, the organism is forced to save energy instead of wasting energy by inefficient ATP production. Mild uncoupling occurs despite unfavourable energy dissipation demonstrating the importance of peroxide reduction in cells. The primary role of mild uncoupling is therefore prevention of superoxide production. A secondary role in heat production is questionable as mild uncoupling most likely does not produce sufficient heat under physiological concentrations of superoxide and HNE. The HNE concentration used by others and in this study was necessary to measure mild uncoupling activity of mitochondrial carriers in the proton leak assay.

We examined the molecular mechanism underlying mild uncoupling in *A. flavipes* and found prevention by CAT demonstrating the involvement of the ANT. The eponymous function of the ANT is the exchange of ADP/ATP between cytosol and the mitochondrial compartment. Further functions have been suggested like the involvement in the permeability transition pore but also in mild uncoupling (Echtay et al. 2003); (Halestrap et al. 1997). We showed that *A. flavipes* ANT1 (GenBank Acc. No. EF450126) was most prominent in skeletal muscle and likely to explain induced uncoupling in myotubular mitochondria. As found for UCP3, ANT1 mRNA levels did not differ between the WA and CA group. Immunological detection using the only commercial available ANT1 antibody failed in the marsupial *A. flavipes*. If higher HNE-sensitivity during cold exposure was caused by higher ANT protein concentration or allosteric changes will require further investigation. Considering that HNE also reacts with proteins and

lipids in mitochondria, different concentration of downstream metabolites between WA and CA mitochondria may be responsible for increased ANT uncoupling activity in the cold.

In contrast to rodents we found no evidence for an involvement of UCP3 in mild uncoupling as no inhibition in the presence of 1mM GDP was observed. These experiments suggested that marsupial UCP3 was not involved in HNE-induced uncoupling activity. This was somehow unexpected as all so far known UCPs possess a putative nucleotide binding site. Unphysiological concentrations of HNE, necessary to observe uncoupling in vitro, may have activated UCP3 constitutively and inhibited GDP-binding. However, studies in the UCP1-knockout mouse show that mitochondrial proton leak is GDP-insensitive despite elevated levels of UCP2 and UCP3 (Monemdjou et al. 1999).

Heat as a by-product may be of benefit but as suggested previously, induced proton conductance by superoxides (and HNE) relates to increased lipid peroxidation. One has to compare heat output of a nonshivering skeletal muscle to finalise a thermogenic role of this tissue. In our study, we examined isolated myotubular mitochondria and excluded the involvement of basal proton conductance in adaptive thermogenesis of the marsupial *A. flavipes*.

Acknowledgements

This research was supported by Deutsche Forschungsgemeinschaft DFG KL973/7 (to M. K.) and by a grant to *Centre for rural and environmental biology* fellowship (to K.W. and M.J.) from the Department of Biological and Physical Sciences, University of Southern Queensland. We thank Adele Jones for excellent technical assistance.

References

1. **Berthon, D., Herpin, P., Bertin, R., De Marco, F., and le Dividich, J.** (1996). Metabolic changes associated with sustained 48-hr shivering thermogenesis in the newborn pig. *Comp.Biochem.Physiol.B Biochem.Mol.Biol.*, **114**, 327-335.

2. **Boss, O., Samec, S., Kuhne, F., Bijlenga, P., Assimacopoulos-Jeannet, F., Seydoux, J., Giacobino, J. P., and Muzzin, P.** (1998). Uncoupling protein-3 expression in rodent skeletal muscle is modulated by food intake but not by changes in environmental temperature. *J Biol Chem*, **273**, 5-8.

3. **Brand, M. D.** (1990). The proton leak across the mitochondrial inner membrane. *Biochim.Biophys.Acta*, **1018**, 128-133.

4. **Brand, M. D.** (1995). Measurement of mitochondrial protonmotive force. In: *Bioenergetics - a practical approach* (ed. Brown, G. C.), pp. 39-62. Oxford: IRL Press.

5. **Brand, M. D.** (2005). The efficiency and plasticity of mitochondrial energy transduction. *Biochem Soc.Trans.*, **33**, 897-904.

6. **Cannon, B. and Nedergaard, J.** (2004). Brown adipose tissue: function and physiological significance. *Physiol Rev.*, **84**, 277-359.

7. **Dawson, T. J. and Olson, J. M.** (1988). Thermogenic capabilities of the opossum Monodelphis domestica when warm and cold acclimated: similarities between American and Australian marsupials. *Comp Biochem Physiol A*, **89**, 85-91.

8. **Echtay, K. S., Esteves, T. C., Pakay, J. L., Jekabsons, M. B., Lambert, A. J., Portero-Otin, M., Pamplona, R., Vidal-Puig, A. J., Wang, S., Roebuck, S. J., and Brand, M. D.** (2003). A signalling role for 4-hydroxy-2-nonenal in regulation of mitochondrial uncoupling. *EMBO J*, **22**, 4103-4110.

9. **Echtay, K. S., Roussel, D., St Pierre, J., Jekabsons, M. B., Cadenas, S., Stuart, J. A., Harper, J. A., Roebuck, S. J., Morrison, A., Pickering, S., Clapham, J. C., and Brand, M. D.** (2002). Superoxide activates mitochondrial uncoupling proteins. *Nature*, **415**, 96-99.

10. **Halestrap, A. P., Woodfield, K. Y., and Connern, C. P.** (1997). Oxidative stress, thiol reagents, and membrane potential modulate the mitochondrial permeability transition by affecting nucleotide binding to the adenine nucleotide translocase. *J Biol Chem*, **272**, 3346-3354.

11. **Hayward, J. S. and Lisson, P. A.** (1992). Evolution of brown fat: its absence in marsupials and monotremes. *Can J Zool*, **70**, 171-179.

12. **Jastroch, M. *et al.*** (2004a). A quest for the origin of mammalian uncoupling proteins. In: *Life in the Cold: Evolution, Mechanisms, Adaptation, and Application* (eds. Barnes, B. M. and Carey, H. V.), pp. 417-426. Fairbanks - Alaska: University of Alaska Fairbanks, Institute of Arctic Biology.

13. **Jastroch, M., Withers, K., and Klingenspor, M.** (2004b). Uncoupling protein 2 and 3 in marsupials: identification, phylogeny, and gene expression in response to cold and fasting in *Antechinus flavipes*. *Physiol Genomics*, **17**, 130-139.

14. **Kabat, A. P., Rose, R. W., Harris, J., and West, A. K.** (2003). Molecular identification of uncoupling proteins (UCP2 and UCP3) and absence of UCP1 in the marsupial Tasmanian bettong, Bettongia gaimardi. *Comp Biochem Physiol B Biochem Mol Biol*, **134**, 71-77.

15. **Klingenspor, M., Ivemeyer, M., Wiesinger, H., Haas, K., Heldmaier, G., and Wiesner, R. J.** (1996). Biogenesis of thermogenic mitochondria in brown adipose tissue of Djungarian hamsters during cold adaptation. *Biochem J*, **316**, 607-613.

16. **Loudon, A. S. I., Rothwell, N. J., and Stock, M. J.** (1985). Brown fat, thermogenesis and physiological birth in a marsupial. *Comp Biochem Physiol*, **81A**, 815-819.

17. **Lowell, B. B. and Spiegelman, B. M.** (2000). Towards a molecular understanding of adaptive thermogenesis. *Nature*, **404**, 652-660.

18. **May, E. L.** (2003). Effects of cold acclimation on shivering intensity in the kowari (Dasyuroides byrnei), a dasyurid marsupial. *Journal of Thermal Biology*, **28**, 477-487.

19. **Mills, E. M., Banks, M. L., Sprague, J. E., and Finkel, T.** (2003). Pharmacology: uncoupling the agony from ecstasy. *Nature*, **426**, 403-404.

20. **Monemdjou, S., Hofmann, W. E., Kozak, L. P., and Harper, M. E.** (2000). Increased mitochondrial proton leak in skeletal muscle mitochondria of UCP1-deficient mice. *Am.J.Physiol.Endocrinol.Metab.*, **279**, E941-E946.

21. **Monemdjou, S., Kozak, L. P., and Harper, M. E.** (1999). Mitochondrial proton leak in brown adipose tissue mitochondria of Ucp1-deficient mice is GDP insensitive. *Am.J Physiol*, **276**, E1073-E1082.

22. **Nedergaard, J. and Cannon, B.** (2003). The 'novel' 'uncoupling' proteins UCP2 and UCP3: what do they really do? Pros and cons for suggested functions. *Exp.Physiol*, **88**, 65-84.

23. **Nicholls, D. G.** (1974). The influence of respiration and ATP hydrolysis on the proton-electrochemical gradient across the inner membrane of rat-liver mitochondria as determined by ion distribution. *Eur.J.Biochem*, **50**, 305-315.

24. **Nicholls, D. G. and Locke, R. M.** (1984). Thermogenic mechanisms in brown fat. *Physiol Rev*, **64**, 1-64.

25. **Nicol, S. C.** (1978). Non-shivering thermogenesis in the potoroo, Potorous tridactylus (Kerr). *Comp Biochem Physiol*, **59**, 33-37.

26. **Nicol, S. C., Pavlides, D., and Andersen, N. A.** (1997). Nonshivering thermogenesis in marsupials: Absence of thermogenic response to beta 3-adrenergic agonists. *Comp Biochem Physiol A*, **117**, 399-405.

27. **Opazo, J. C., Nespolo, R. F., and Bozinovic, F.** (1999). Arousal from torpor in the chilean mouse-opposum (Thylamys elegans): does non-shivering thermogenesis play a role? *Comp Biochem Physiol A Mol Integr Physiol*, **123**, 393-397.

28. **Raimbault, S., Dridi, S., Denjean, F., Lachuer, J., Couplan, E., Bouillaud, F., Bordas, A., Duchamp, C., Taouis, M., and Ricquier, D.** (2001). An uncoupling protein homologue putatively involved in facultative muscle thermogenesis in birds. *Biochem J*, **353**, 441-444.

29. **Reynarfarje, B., Costa, L. E., and Leninger, A. L.** (1985). O2 solubility in aqueous media determined by kinetic methods. *Anal Biochem*, **145**, 406-418.

30. **Reynolds W and Hulbert, A. J.** (1982). Cold acclimation in a small dasyurid marsupial: Antechinus stuartii. (ed. Archer, M.), pp. 278-283. Mosman, N.S.W.: Royal Zoological Society of NSW.

31. **Rolfe, D. F. S., Hulbert, A. J., and Brand, M. D.** (1994). Characteristics of mitochondrial proton leak and control of oxidative phosphorylation in the major oxygen-consuming tissues of the rat. *Biochim Biophys Acta*, **1188**, 405-416.

32. **Schaeffer, P. J., Villarin, J. J., and Lindstedt, S. L.** (2003). Chronic cold exposure increases skeletal muscle oxidative structure and function in Monodelphis domestica, a marsupial lacking brown adipose tissue. *Physiol.Biochem Zool*, **76**, 877-887.

33. **Schaeffer, P. J., Villarin, J. J., Pierotti, D. J., Kelly, D. P., and Lindstedt, S. L.** (2005). Cost of transport is increased after cold exposure in Monodelphis domestica: training for inefficiency. *J Exp.Biol*, **208**, 3159-3167.

34. **Smith B.K. and Dawson T.J.** (1984). Changes in the thermal balance of a marsupial (Dasyuriodes byrnei) during cold and warm acclimation. *J therm Biol*, **9**, 199-204.

35. **Talbot, D. A., Duchamp, C., Rey, B., Hanuise, N., Rouanet, J. L., Sibille, B., and Brand, M. D.** (2004). Uncoupling protein and ATP/ADP carrier increase mitochondrial proton conductance after cold adaptation of king penguins. *J Physiol*, **558**, 123-135.

36. **Ye, J. M., Edwards, S. J., Rose, R. W., Steen, J. T., Clark, M. G., and Colquhoun, E. Q.** (1996). alpha-adrenergic stimulation of thermogenesis in a rat kangaroo (Marsupialia, Bettongia gaimardi). *American Journal of Physiology*, **40**, R586-R592.

Figure legends

Fig.1: A. COX activity in skeletal muscle. Black bars display 24°C, whereas white bars display 10°C exposed *A. flavipes*. B. UCP3 protein levels in skeletal muscle quantified by Western blot analysis; 50µg of skeletal muscle protein were hybridised with a UCP3 peptide antibody. The loading was controlled by Ponceau staining (supplemental material). Bars are means ± S.E.M of three (warm exposed) or four (cold exposed) independent experiments/individuals each performed in duplicate. Asterisk indicates significance ($P<0.05$; Student's t-test).

Fig. 2: Measurement of basal proton conductance. (A) This graph shows the full kinetic response of proton leak from mitochondria isolated from warm (filled symbols) and cold (white symbols) exposed *A. flavipes*. Upper curves display the proton leak of skeletal muscle (diamonds), lower curves display the proton leak of liver (squares). Data are means ± SEM of three (warm exposed) or four (cold exposed) independent experiments/individuals each performed in duplicate.

Fig. 3: Inducible proton conductance in skeletal muscle mitochondria of *A. flavipes*. A. Full kinetic response of proton leak under basal conditions (filled (24°C) and white (10°C) diamonds), after addition of HNE (filled (24°C) and white (10°C) squares), and after addition of HNE and CAT (crossed filled squares). C. The left panel shows the effect of HNE, HNE + CAT and HNE + GDP on mitochondria from 24°C exposed individuals, the right panel the effect on mitochondria from 10°C exposed individuals. The bar chart shows the comparison of oxygen consumption under different treatments at a common potential of 150 mV. Data are means ± SEM of three (warm exposed) or four (cold exposed) independent experiments/individuals each performed in duplicate. $*P<0.05$ HNE versus control/HNE + CAT.

Figure 1

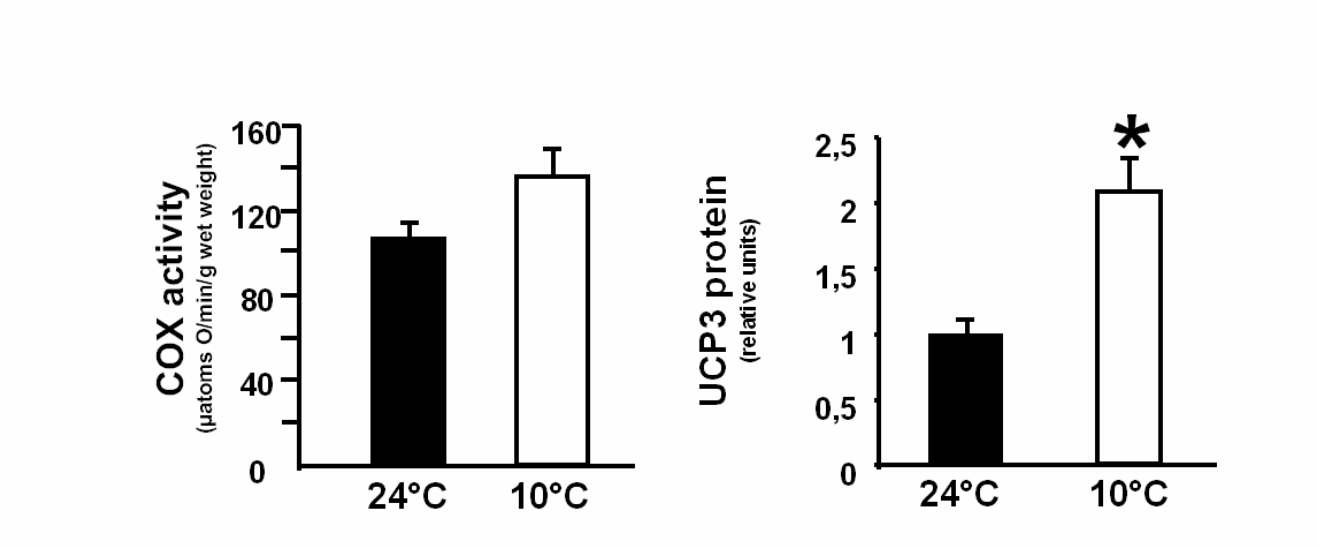
COX activity
(µatoms O/min/g wet weight)
160
120
80
40
0
24°C
10°C
UCP3 protein
(relative units)
2,5
2
1,5
1
0,5
0
*
24°C
10°C

Figure 2

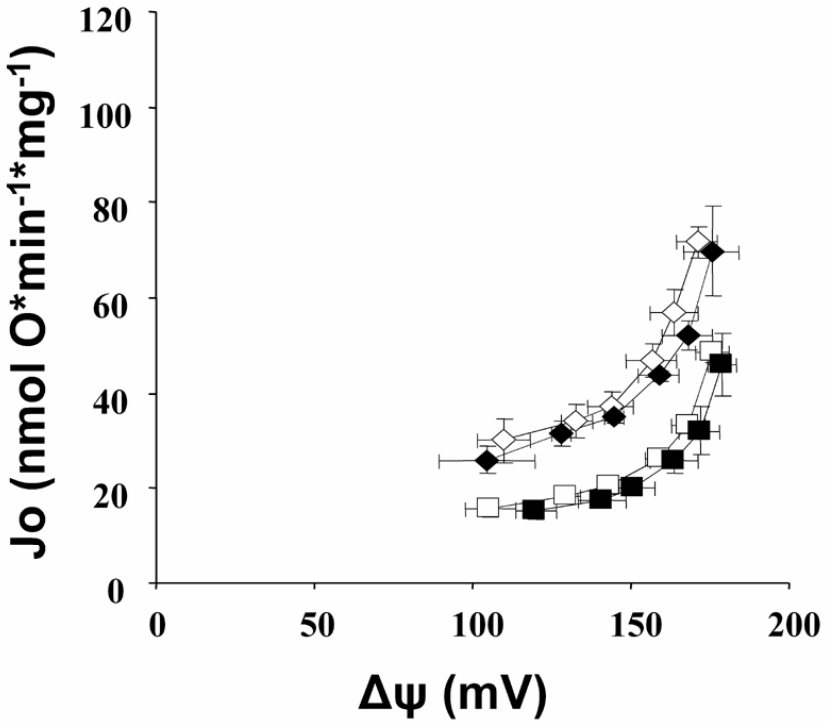

Figure 3

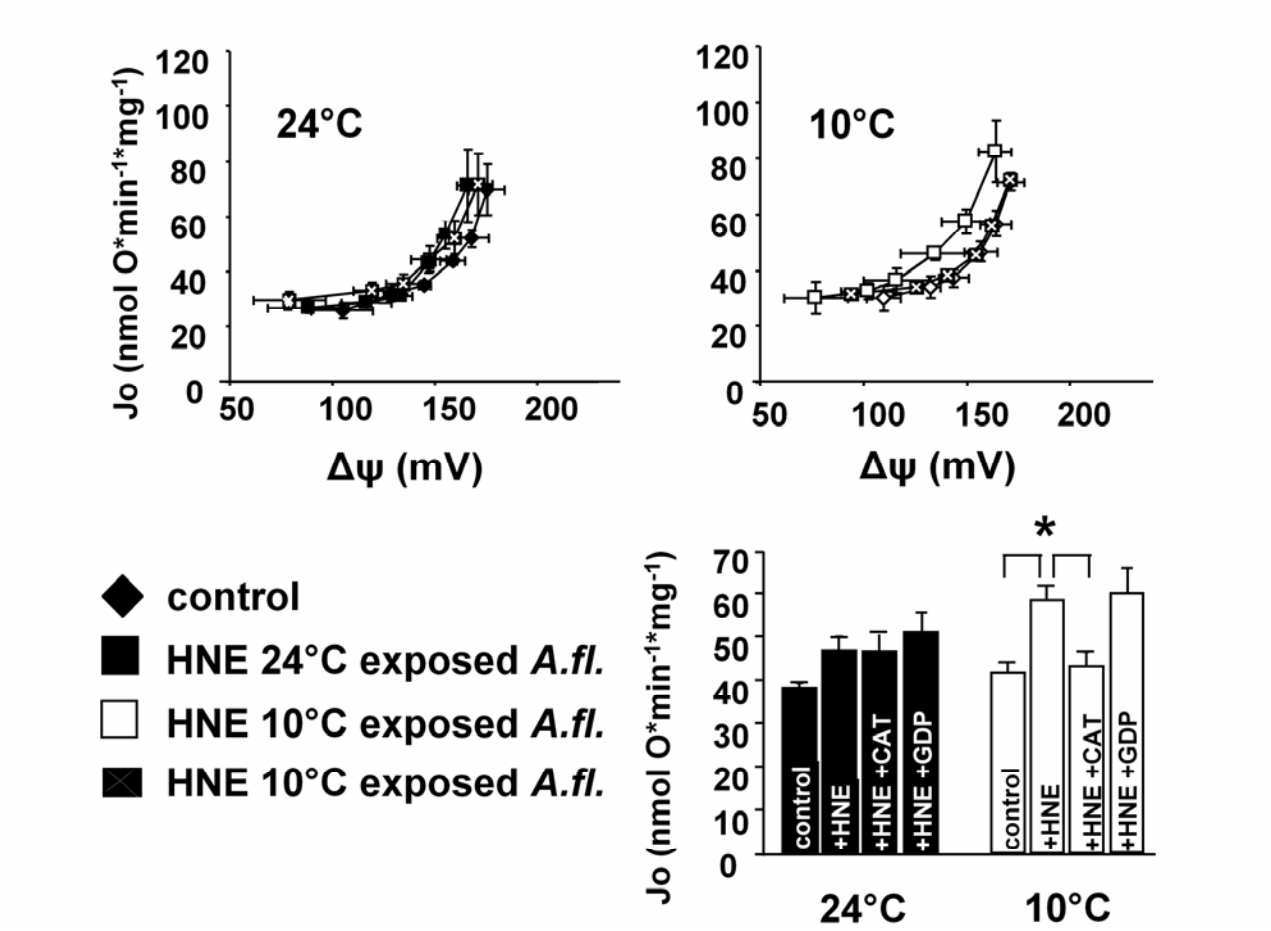
24°C
10°C
Jo (nmol O*min-1*mg-1)
Δψ (mV)
control
HNE 24°C exposed A.fl.
HNE 10°C exposed A.fl.
HNE 10°C exposed A.fl.
*
control
+HNE
+HNE +CAT
+HNE +GDP
24°C
10°C

Supplemental material

Supp1: Immunological detection of UCP3 in skeletal muscle of *A. flavipes*

Western blot analysis; 50µg of skeletal muscle protein were hybridised with a UCP3 peptide antibody. The loading was controlled by Ponceau staining.

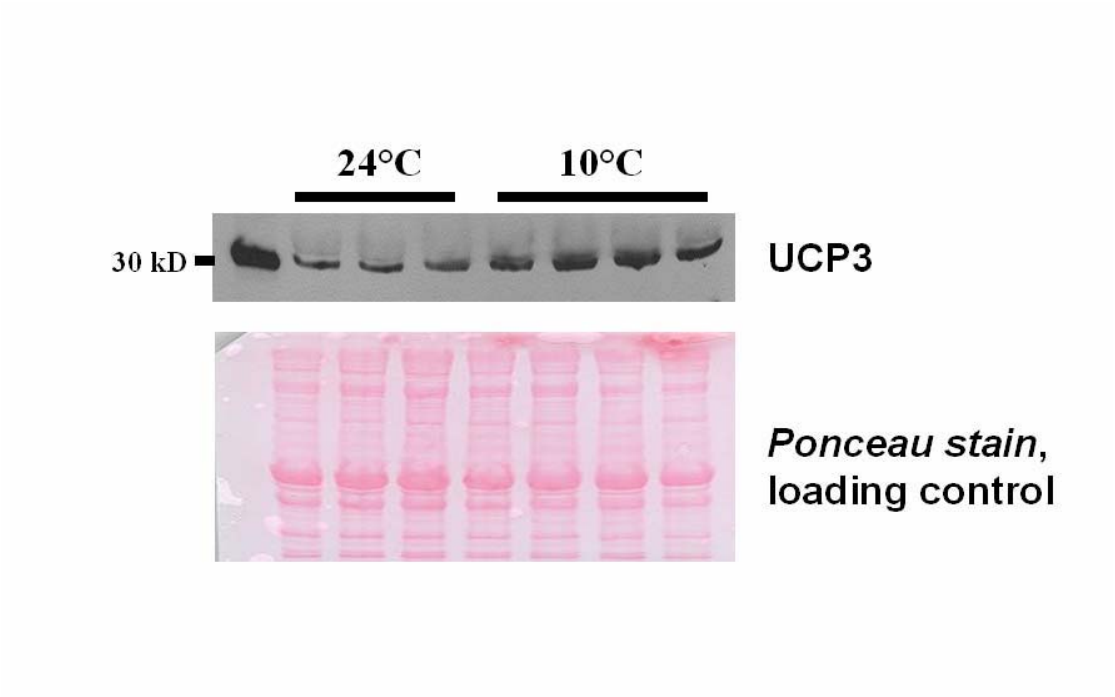

Suppl 2: *A. flavipes* ANT1 gene expression and phylogenetic classification

A. Northern blot analysis of ANT1 expression in multiple tissues of the *A. flavipes*. Total RNA (20µg) isolated from selected tissues was hybridised with a ANT1 700 bp cDNA fragment.

B. Phylogenetic inference of the ANT family including ANT1 using the neighbour joining approach. Bootstrap values are shown as internal edge labels and the oxalacetate malate carrier served as the outgroup.

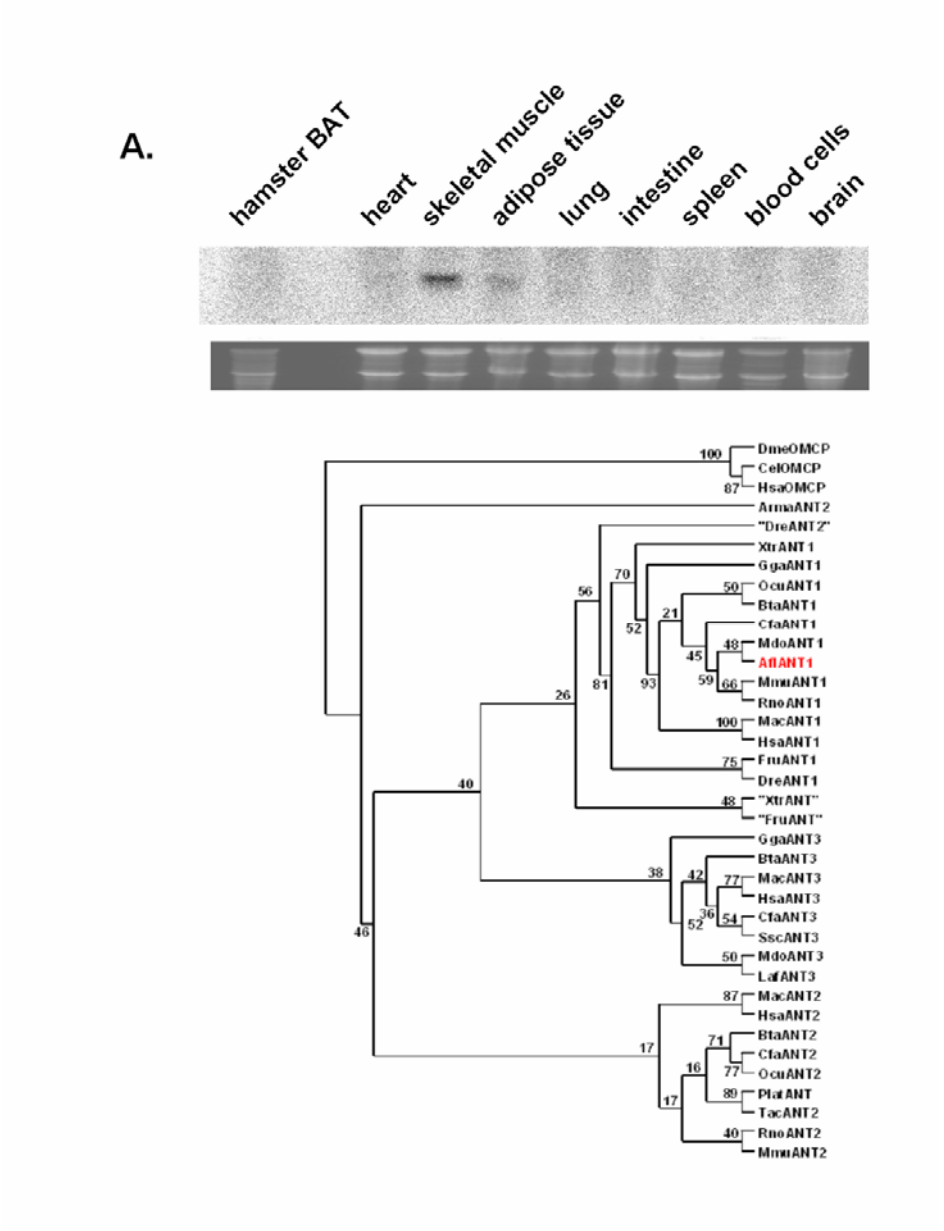

A. RNA isolation, reverse transcriptase - polymerase chain reaction and Northern blot analysis

Total RNA was isolated with TRIzol (GIBCO-BRL) according to the manufacturer's protocol. As an additional step, the RNA pellet was redissolved in a solution containing 6.3 mol L^{-1} guanidinium thiocyanate, 40 mmol L^{-1} sodium citrate pH 7, 0.8% sarcosyl, 8 mmol L^{-1} 2-mercaptoethanol, precipitated with 1 vol isopropanol, washed in 75% ethanol, and finally dissolved in DEPC-treated water. Total RNA was photometrically quantified at 260 nm and stored at –70°C.RNA was isolated from skeletal muscle of *A. flavipes* and used for first strand cDNA synthesis (SUPERSCRIPT II, GIBCO/BRL) according to the manufacturer's protocol. ANT1 primers were deduced from the genome of *Monodelphis domestica* (www.ensembl.org) and obtained from MWG Biotech, Ebersberg, Germany (Sense: 5'- GCT GCT GCA GGT CCA GCA TGC CAG CAA ACA; Antisense: 5'- TTC ATC TTT TGC AAT CTT CCT CCA GCA GTC). 40 cycles of denaturation at 94°C (1 min), annealing at 58°C (1 min) and extension at 72°C (1 min) were performed. A final extension at 72°C was applied for 10 minutes and followed by rapid cooling to 4°C. The PCR product was gel-purified and ligated into a pGEMT-easy vector (Promega). We also generated consensus primer for ANT2 (Sense: 5'- ATG ACA GAT GCC GCT GTG TCC TTC GCC AAG; Antisense: 5'- TGC CTG TGT ACA TGA TAT CAG TTC CTT TGC and ANT3 (Sense: 5'- TCC TTC TGG AGG GGC AAC CTG GCC AAT GTC; Antisense: 5'- CCG TCA CGG TCT GCG CGA TCA TCC AGC TCA).

Twenty micrograms of RNA was electrophoresed in a 1% denaturing agarose gel (5% formaldehyde, 0.02 mol l^{-1} MOPS, 5 mmol l^{-1} sodium acetate, 1 mmol l^{-1} disodium EDTA, pH 8), transferred overnight in 10x SSC to a nylon membrane (Hybond N, Amersham), and UV cross-linked. The UCP3 cDNA was random prime-labeled with [α-^{32}P]dCTP (Rediprime DNA labeling system, Amersham) and hybridised to the nylon membrane as described previously (Jastroch et al. 2004a); (Jastroch et al. 2004a). After hybridization, the blots were washed with 2x SSC/0.1% SDS for 20 min, 1x SSC/0.1% SDS for 10 min, and 0.5x SSC/0.1% SDS for 10 min at

room temperature. Signal intensities were then monitored by exposure to a PhosphorScreen (Molecular Dynamics). The hybridized probes were then detected by phosphor imaging (Storm 860, Molecular Dynamics), and signal intensities were quantified using ArrayVision 7.0 (Imaging Research). Ethidium bromide staining of total RNA served to normalize gel loading and was quantified densitometrically (Scion Image Software 4.0.2).

B. Phylogenetic inference

The search for ANT sequences of different vertebrates was performed in public databases (Ensembl genome browser, www.ensembl.org/ NCBI, www.ncbi.nlm.nih.gov). All ANT sequences were subjected to phylogenetic inference using the Neighbour joining method (Felsenstein J. *PHYLIP Phylogeny Inference Package version 3.6.* Distributed by the author. Seattle, WA: Univ. of Washington, 2004. http://evolution.genetics.washington.edu/phylip). Bootstrapping involved 100 replicates and the consensus tree was illustrated using TreeView (http://taxonomy.zoology.gla.ac.uk/rod/treeview.html). The oxaloacetate-malate carrier, considered as an "ancient" branch of the mitochondrial anion carrier family, was used as the outgroup.Phylogenetic relations of the ANT family in vertebrates including ANT1 of marsupials. The neighbor joining tree was derived from the amino acid alignment. Bootstrap values from 100 replications are given next to the internal branches. The oxaloacetate-malate carrier served as the outgroup. Afl, *A. flavipes*; Arma, Dasypus novemcinctus (Armadillo); Bta, *Bos Taurus*; Cel, Caenorhabditis elegans; Cfa, *Canis familiaris*; Dme, *Drosophila* melanogaster; Dre, *Danio rerio*; Fru, *Fugu rubripes;* Gga, *Gallus gallus*; Hmu, Hsa, *H. sapiens*; Laf, Loxodonta africana; Mac, *Macaca mulatto*; Mdo, *Monodelphis* domestica; Mmu, *M. musculus*; Ocu, *Oryctolagus cuniculus*; Plat, *Ornithorhynchus anatinus* (platypus); Rno, *Rattus norvegicus*; Ssc, *Sus scrofa*; Tac, *Tachyglossus* aculeatus; Xtr, *Xenopus tropicalis.*

INTRODUCING A MAMMALIAN CELL SYSTEM TO STUDY THE FUNCTION OF EVOLUTIONARY DISTANT UNCOUPLING PROTEINS

M. Jastroch[1], V. Hirschberg[1], M.D. Brand[2], M. Liebig[1], K. Weber[1], F. Bolze[1], M. Klingenspor[1]

1 - Animal Physiology, Department of Biology, Philipps University, Marburg, Germany

2 - Medical Research Council Dunn Human Nutrition Unit, Cambridge, United Kingdom

jastroch@staff.uni-marburg.de

In mammals, uncoupling protein 1 (UCP1) enables brown fat mitochondria to increase proton conductance and respire at maximal rates in the absence of ATP-synthesis thus resulting in nonshivering thermogenesis (NST). In contrast, the physiological roles of UCP2 and UCP3 have not been resolved yet but may be related to mitochondrial ROS production[1]. Our search for the evolutionary origin of thermogenic UCP1 by comparative genomics surprisingly revealed the presence of all three UCPs in fish[2], and recently in amphibians and marsupials (unpublished data). Isolated liver mitochondria of the Common Carp (*Cyprinus carpio*) expressing UCP1 displayed increased proton conductance by addition of palmitate or 4-hydroxynonenal (HNE). This inducible proton conductance was prevented by addition of GDP[3]. These properties strongly suggest that carp UCP1 is a functional uncoupling protein with broadly the same activatory and inhibitory characteristics as mammalian UCP1. Evolution and cross-species comparative studies of UCPs are of interest to elucidate their general physiological role(s) in vertebrates and to determine conserved structure-function relationships. However, comparative studies of UCP paralogues (UCP1, UCP2 and UCP3) and UCP orthologues (e.g. UCP1 of vertebrates) in native mitochondria are hampered by differential tissue specificity and different genetical backgrounds. We therefore established stable expression of UCPs at various levels in HEK293 (human embryonic kidney) cells allowing comparative measurements in the same cell system. Isolated HEK293 mitochondria expressing different levels of mouse UCP1 displayed GDP-sensitive uncoupling activity in response to palmitate. Fatty acid induced proton conductance strongly correlated with UCP1 content. In contrast, no change of proton conductance was observed in control mitochondria (-UCP1) in response to identical amounts of palmitate and GDP. For cell lines expressing mouse UCP3, the HNE-inducible uncoupling property correlated with protein content. These findings demonstrate the suitability of the HEK293 system to investigate native behaviour of ectopically expressed UCPs to directly evaluate uncoupling activity of mammalian UCP1 and UCP3 as well as their impact on ROS production and cellular damage. Comparing the uncoupling property of mammalian UCP1 and the novel vertebrate UCP1 orthologues casts light on the evolution of UCP1-mediated NST.

1. M. D. Brand and T. C. Esteves (2005) Cell Metab 2(2),85
2. M. Jastroch, S. Wuertz, W. Kloas, and M. Klingenspor (2005) Physiol Genomics 22, 150
3. M. Jastroch, J. A. Buckingham, M. Klingenspor, and M. D. Brand (2006) *submitted*

UNCOUPLING PROTEIN 1 IS EXPRESSED IN THE BRAIN OF ECTOTHERMIC VERTEBRATES

M. Klingenspor[1], M. Helwig[1], T. Fromme[1], M.D. Brand[2], W. Kloas[3], S. Taudien[4], M. Platzer[4], M. Jastroch[1]

1 - Faculty of Biology, Dept. of Animal Physiology, Philipps-Universitat Marburg, Germany

2 - Medical Research Council Dunn Human Nutrition Unit, Cambridge, UK

3 - Dept. of Inland Fisheries, Leibniz-Institute of Freshwater Ecology and Inland Fisheries, Berlin, Germany

4 - Leibniz Institute for Age Research Fritz-Lipmann-Institute, Genome Analysis, Jena, Germany

klingens@staff.uni-marburg.de

Uncoupling proteins (UCPs) regulate proton conductance of the mitochondrial inner membrane. Until recently the thermogenic uncoupling protein 1 (UCP1) was considered to be unique to brown adipose tissue mitochondria of placental mammals where it dissipates proton motive force as heat (non-shivering thermogenesis, NST). We identified the ortholog of mammalian UCP1, as well as the two paralogs UCP2 and UCP3 in ectothermic bony fishes suggesting that the members of the core UCP family already existed 420 million years ago and are present in all living vertebrates (1). Accordingly, we found all three UCPs in the genomes of the Clawed frog (*Amphibia*) and the Opossum (*Marsupialia*), whereas in the Chicken genome only UCP3 can be found so far.

The biological function of thermogenic UCP1 in ectothermic vertebrates is not understood.
In the Common Carp (*Cyprinus carpio*) UCP1 is strongly expressed in the liver. In isolated Carp liver mitochondria fatty acids increase proton conductance in a GDP-sensitive manner. Thus, UCP1 orthologs of fish and mammals share key functional characteristics. UCP1 expression is also detected in the brain, albeit at lower expression levels than in liver. We studied the effect of cold acclimation on UCP1 gene expression in the Carp. Whereas UCP1 mRNA levels sharply declined in the liver of cold exposed Carp, Northern blot analysis of whole brain RNA revealed a two-fold increase of UCP1 expression. We therefore performed In Situ Hybridisation (ISH) of coronal and sagittal sections of the Carp brain with a ^{35}S-labelled Carp UCP1 cRNA probe. This analysis revealed distinct localised expression of UCP1 in the forebrain (periventricular grey zone of the optic tectum) and the brain stem (solitary and trigeminal tract). We hypothesise that cold-induced UCP1 expression may increase the capacity for local non-shivering thermogenesis in selected brain regions in order to maintain critical neuronal functions in cold water.

1. Jastroch M, Wuertz S, Kloas W, Klingenspor M. Uncoupling protein 1 in fish uncovers an ancient evolutionary history of mammalian nonshivering thermogenesis. *Physiol Genomics* 22: 150-156, **2005**

Available online at www.sciencedirect.com
ScienceDirect
General and Comparative Endocrinology 150 (2007) 140–150
GENERAL AND COMPARATIVE ENDOCRINOLOGY
www.elsevier.com/locate/ygcen

Communication in Genomics and Proteomics

The role of the IGF-I system for vitellogenesis in maturing female sterlet, *Acipenser ruthenus* Linnaeus, 1758

S. Wuertz [a,*], A. Nitsche [b], M. Jastroch [c], J. Gessner [a], M. Klingenspor [c], F. Kirschbaum [a,d], W. Kloas [a,d]

[a] *Leibniz Institute of Freshwater Ecology and Inland Fisheries, Berlin, Germany*
[b] *Robert Koch Institut, Berlin, Germany*
[c] *Philipps University Marburg, Germany*
[d] *Humboldt University, Berlin, Germany*

Received 19 April 2006; revised 5 July 2006; accepted 11 July 2006
Available online 1 September 2006

Abstract

Transition from previtellogeneic to vitellogenic oocyte growth is a critical phase for folliculogenesis in sturgeon and may often be postponed for several years. Recent findings on the involvement of insulin-like growth factor I (IGF-I) in cell differentiation processes of oocyte follicle and ovarian steroidogenesis of teleosts *in vitro* led to the hypothesis that paracrine IGF-I could function as a potential trigger *in vivo*. For the first time, IGF-I and its corresponding receptor (IGF-IR) were identified in a non-teleostean fish. Real-time PCR assays for IGF-I and IGF-IR mRNA were established, normalising mRNA expression of the target genes to β-microglobulin (β2m). We clearly show that expression of IGF-I in the gonad is a substantial source for IGF-I-mediated effects in follicles compared to liver, brain, muscle and adipose tissue. Among these tissues, IGF-IR mRNA was highest in the gonad. With regard to different cohorts of coexisting follicles, highest expression of IGF-I and IGF-IR were met in developing follicles, indicating that IGF-I functions as an intraovarian modulator of follicle faith. Comparing previtellogenic follicles in females that matured within two years with non-maturing females f the same age, revealed an increases of 2.3-fold for IGF-I and 2.8-fold for IGF-IR mRNA expression in maturing females. These findings implicate an important role of paracrine IGF-I in early vitellogenesis and identify it as candidate vitellogenesis inducing factor (VIF), determining the faith of the follicle.

Keywords: Gonad maturation; IGF-I; IGF-IR; IGF-I receptor; Insulin-like growth factor; Cyclical reproduction; Folliculogenesis; Vitellogenesis; Puberty

1. Introduction

In view of declining sturgeon populations worldwide and a variety of national and international countermeasures implemented recently (Williot et al., 2002), a stagnation in follicle development often observed—at the previtellogenic stage—implicates the needs for a better understanding of the endocrine mechanisms underlying sturgeon vitellogenesis (Doroshov et al., 1997; Williot and Brun, 1998). In fish, vitellogenesis has been studied intensively, but the transition from previtellogenic to vitellogenic growth is still poorly understood, but seems to be the striking step in first-maturing females and will subsequently be termed puberty here.

Numerous studies in mammals and more recently in teleost fish described IGF-I as potent paracrine modulator in a variety of tissues, regulating tissue-specific cell differentiation (Patino and Kagawa, 1999; Weber and Sullivan, 2001) and proliferation (Kadakia et al., 2005). IGF-I-mediated effects *in vitro* characterise striking steps of the folliculogenesis such as steroidogenesis (Maestro et al., 1997b; Weber and Sullivan, 2000), follicle differentiation (Kagawa et al., 2003) and the accumulation of vitellogenin (Tyler et al., 1987) and seem to be highly conserved

* Corresponding author. Fax: +49 030 641 81 750.
E-mail address: sveno@igb-berlin.de (S. Wuertz).

0016-6480/$ - see front matter © 2006 Elsevier Inc. All rights reserved.
doi:10.1016/j.ygcen.2006.07.005

among vertebrates (Lavoie et al., 1999; Reinecke and Collet, 1998). Based on findings in mammals, Adashi (1995) has therefore proposed IGF-I as paracrine regulator of follicular faith initiating the maturation of a follicle as intraovarian regulator.

With regard to the initiation of puberty in fish, research focused mainly on plasma IGF-I (Dufour et al., 2000; Huang et al., 1998); the gonad as source for IGF-I-mediated action has been widely ignored and its IGF-I expression during the reproductive cycle has not received much attention so far. Recently, IGF-I has been identified in a variety of teleosts, particularly in species of commercial interest including chinook salmon (*Oncorhynchus tshawytscha*) (Wallis and Devlin, 1993), coho salmon (*Oncorhynchus kisutch*) (Duguay et al., 1992), catfish (*Clarias macrocephalus*) (Mc Rory and Sherwood, 1994), perch (*Perca fluviatilis*) (Jentoft et al., 2004), and channel catfish (*Ictalurus punctatus*) (Peterson et al., 2004). Surprisingly, no sequence has been identified in any basal actinopterygian species so far.

For IGF-I-mediated effects, target cells require the ability to respond, and thus the presence of specific receptors: there are two distinct receptors demonstrating IGF-I binding capacity, the insulin receptor and the IGF-IR; the latter is considered to be the main target for IGF-I (Maestro et al., 1997a; Steele-Perkins et al., 1988). Full-length coding sequences (CDS) IGF-IR have been reported from a limited number of teleosts, namely from *Cyprinus carpio* (AY144592, unpublished), *Danio rerio* (Maures et al., 2002), and *Paralichthys olivaceus* (Nakao et al., 2002).

In this study, IGF-I and IGF-IR CDS were identified in sturgeon. The expression of IGF-I and IGF-IR in the ovary over the reproductive cycle of first maturing sterlet was investigated by real-time PCR normalising the expression of the target genes to a commonly used housekeeping gene, β-microglobulin (β2m).

2. Materials and methods

2.1. Animals and sampling

Four-year-old sterlet *A. ruthenus* of both sexes were reared under a natural photoperiod and temperature cycle in four tanks, 1.2 m^3 each (max. 15 kg/m^3) in a partial recirculation system (water exchange rate 1.5 vol/h). They were fed commercial trout feed at approximately 0.6% of the body weight/d. PIT tagging (Trovan®, Germany) allowed individual sampling. Animal care and performance of experiments were approved by the LaGetSi (Landesamt für Gesundheit und technische Sicherheit, Berlin, Germany, G0095/01). For sampling, animals were either sacrificed (tissue samples) or biopsied under narcosis (70 ppm MS-222), allowing successive individual sampling. Over a period of two years, from spring 2002 to winter 2003/04, gonad tissue samples were taken from female sterlet in 3 month intervals. Histological samples were fixed in Bouin's and cut to 8 μm (hematoxylin–eosin staining). Maximum follicle diameters refers to the furthest developed cohort of coexisting follicles, determined as average of at least 10 follicles for each cohort under a dissecting microscope. For RNA extraction, samples were immediately shock frozen in 500 μL TRIZOL® (Invitrogen, Germany) and stored at −80 °C until further processing. Staging was performed according to Le Le Menn and Pelissero (1991).

2.2. RT-PCR amplification

RNA extraction was carried out with TRIZOL® according to Kloas et al. (1999). The RNA pellet was redissolved in SOL D solution containing 6.3 M guanidium thiocyanate, 40 mM sodium citrate and 0.8% sarcosyl, 8 mM 2-mercaptoethanol in order to improve the purity of the nucleic acid extraction and to prevent RNA degradation in fat micelles. Using AMV-RT (Finnzymes, Finland), conditions followed the protocol by Kloas et al. (1999). PCR primers used are listed in Table 1. Sequencing was carried out with a CEQ 8800 (Beckman Coulter, Germany) according to the manufacturer's protocol. Sequences were analysed by database homology search tool BLAST (Altschul, 1999) and by multiple alignment sequence comparison using BioEdit 7.0.0.

2.3. RACE-PCR

Utilising mRNA isolated from total RNA with the Micro-FastTrack 2.0 kit (Invitrogen), RACE-PCR was carried out with a SMART RACE™ kit (*Biosciences Clontech*, Germany) and gene-specific primers (Table 1) according to the user manual. A touchdown strategy with an initial denaturation at 94 °C (3 min), 5 cycles denaturation at 94 °C (40 s), annealing at 72 °C (40 s), polymerisation at 72 °C (1 min), 5 cycles with annealing at 70 °C (40 s) and 30 cycles with annealing at 68 °C, followed by a final polymerisation at 72 °C (10 min) was used for PCR amplification. Amplicons were subsequently cloned into the pDrive Cloning Vector (Qiagen), isolated (QIAprep miniprep kit, Qiagen), and sequenced. Clones were further on used as quantification standard for the real-time PCR.

2.4. Real-time quantification

Hybridisation probes and a hot start Platinum *Taq* polymerase (Invitrogen) were used for real-time detection with a LightCycler under the following conditions: 94 °C initial denaturation for 5 min, followed by 40 cycles of 94 °C denaturation for 20 s, 58 °C primer annealing for 20 s, and 72 °C polymerisation for 20 s. Expression was normalised to β-2-microglobulin (β2m) as described by Pfaffl (2001a). For each run, a standard from a juvenile liver sample was quantified in duplicate as calibrator, compensating for lot-to-lot and run-to-run variations. Efficiency and detection limit was determined using a dilution series of the plasmid, ligated with the gene-specific PCR amplicon. All samples were performed in duplicate.

2.5. Statistical analysis

Results are presented as the mean ± SD of n replicates. Data were analysed for normal distribution by Kolmogorov–Smirnov and equal variance by Kruskal–Wallis One Way Analysis of Variance (passed if $p < 0.05$) using SigmaStat 2.0 software (Jandel Scientific, San Rafael, USA). Multiple comparison was carried out by parametric Tukey's Test or non-parametric Dunn's Test. For pairwise comparison, non-parametric Mann–Whitney rank sum test or parametric t test were used.

3. Results

3.1. Identification of genes

After identification of partial IGF-I (132 bp) of the highly conserved B and C domain, and IGF-IR (94 bp) of the β-subunit, sequences were elongated by RACE PCR. For IGF-I (Fig. 5), an ORF of 483 bp was characterised (DQ329352). Sequence identities of selected species ranged between 57–78% (CDS) and 55–79% (protein) with highest similarities to teleost species. Domains are designated in the alignment, showing identities of 86–97% for the B domain, 41–75% for the C domain, 86–90% for the A

Table 1
List of primers and hybridisation probes used. T_a—annealing temperature, LC705, LC640—fluorophore LightCycler Red 705, 640, P—phosphorylated 3′-end

Target	Primer	Sequence	Specification	T_a (°C)
β2m				
	β2m cF	TTTCgTggCggCTCTTgTA	Consensus primer	58
	β2m cR	AgggTgCTgTgCTCCACTT	Consensus primer	58
	ACI β2m F	ggACgCCACTgAAgCCAT	Primer real-time PCR	58
	ACI β2m R	ATgTCAggAgTCCAggTgAAgC	Primer real-time PCR	58
	ACI β2m FL	ACCAgggCTggCACTTCCACCT—***FL***	Hybridisation probe	
	ACI β2m LC	***LC640***–ACCAAgAgCgTggCCTTCACCC—***P***	Hybridisation probe	
IGF-I				
	IGF cF	ggggAgAgAggCTTTTATTTCAgCAA	Consensus primer	60
	IGF cR	gCgCAgTACATCTCTAgCCgC	Consensus primer	60
	GSP IGF F1	AACCAACAgggCTATggAg	Gene-specific primer	60
	GSP IGF F2	gTgCTgCTTCCAgAgCTgTg	Gene-specific primer	60
	GSP IGF R1	AggTCACAgCTCTggAAgC	Gene-specific primer	60
	GSP IGF R2	CACAgCTCTggAAgCAgCAC	Gene-specific primer	60
	ACI IGF F	TgCTCCTgTgTgTTCTATgCCT	Primer real-time PCR	58
	ACI IGF R	ggAAgCAgCACTCATTCACg	Primer real-time PCR	58
	ACI IGF FL	TCTCTCCCCACACACAAACTgAAgAgTg—***FL***	Hybridisation probe	
	ACI IGF LC	***LC640***–CCACAAgCTCAgCTCCgCACA—***P***	Hybridisation probe	
IGF-IR				
	IR cF	gCCATCAAAgACggTCAACgAATC	Consensus primer	60
	IR cR	TggTgACAgTTgAACTCCTTCA	Consensus primer	60
	GSP IR F1	CCATCAAAgACggTCAACgA	Gene-specific primer	60
	GSP IR F2	gACggTCAACgAATCggC	Gene-specific primer	60
	GSP IR R1	ggACgCCTCgTTCAggAA	Gene-specific primer	60
	GSP IR R2	ACgCCTCgTTCAggAACTC	Gene-specific primer	60
	ACI IR F	CAACgAACTCTgACgTgTggTA	Primer real-time PCR	58
	ACI IR R	gCTCCAACCgAATACCTTTCTg	Primer real-time PCR	58
	ACI IR FL	gCTgCAAACgAgACATCgAgACAg—***FL***	Hybridisation probe	
	ACI IR LC	***LC705***—CgCATCCgTTCAgCTTCTCCC—***P***	Hybridisation probe	

domain, 50–62% for the D domain, and 44–77% for the E domain of the prohormone. Highest sequence identities were found with the short subtype IGF-IEa (NCBI nomenclature). RACE PCR revealed a 770 bp partial CDS of the IGF-IR β-subunit (DQ340767, Fig. 6). A binding site for insulin receptor substrate 1 (IRS-I) (N-P-E-Y) and a potential ATP binding site (G–X–G–X–X–G-21*X–K) was characterised by sequence comparison in the alignment. Sequence identities for the CDS ranged between 69 and 74%. For the subsequent use as reference gene, β2m was selected from all commonly used reference genes. PCR identified a 307 bp fragment of β2m from liver-derived cDNA (DQ329353), showing high similarities (97–99%) to β2m of *A. baerii* (Lundqvist et al., 1999); here two species-specific substitutions (position 96, 198) were found. Primers subsequently used for real-time quantification (ACI β2m F, ACI β2m R) were conserved with regard to the cDNA species of *A. ruthenus* and *A. baerii* and positioned on the exon–intron boundaries to provide cDNA specificity. Primers for real-time quantification are positioned in the highly conserved B- and slightly less conserved C-domain.

3.2. Quantification assay

Standard quantification curves of the plasmid dilution series revealed amplification efficiencies of 1.99 (IGF-I), 1.99 (IGF-IR) and 1.97 (β2m). Interspecific and intraspecific variation of the CP values were below 2% for all genes ($n = 6$). In this study, β2m expression was constant, revealed by multiple comparison (Dunn's method) of the CP of β2m. All CP-values were normalised to a standard derived from a juvenile liver to assure maximal reproducibility and to compensate for PCR-specific run-to-run variations. This standard was set to 100% and corresponds to $26.8 \pm 0.4 \times 10^3$ copies of IGF-I cDNA/μL, $1.5 \pm 0.1 \times 10^3$ copies of IGF-IR cDNA/μL, and $3.1 \pm 0.1 \times 10^6$ copies of β2m cDNA/μL.

3.3. Gene expression in selected tissues

Comparing tissue-specific gene expression in the gonad, liver, brain, muscle and adipose tissue (Fig. 1), IGF-I mRNA expression was highest in the liver ($179 \pm 19\%$) and in the ovary ($152 \pm 22\%$). In contrast, IGF-I expression in the brain ($32 \pm 20\%$), the muscles ($27 \pm 18\%$), and adipose tissue associated with the gonad ($44 \pm 20\%$) was significantly lower ($p < 0.001$, Tukey's Test) than in the gonad. IGF-IR expression was extremely elevated in the gonad ($2005 \pm 837\%$), when compared to all other tissues (liver $111 \pm 42\%$, $p < 0.05$; adipose tissue $219 \pm 109\%$, $p < 0.05$; brain $363 \pm 322\%$, muscle $389 \pm 172\%$). The low expression in the brain and the muscles were not significant due to their high standard deviations.

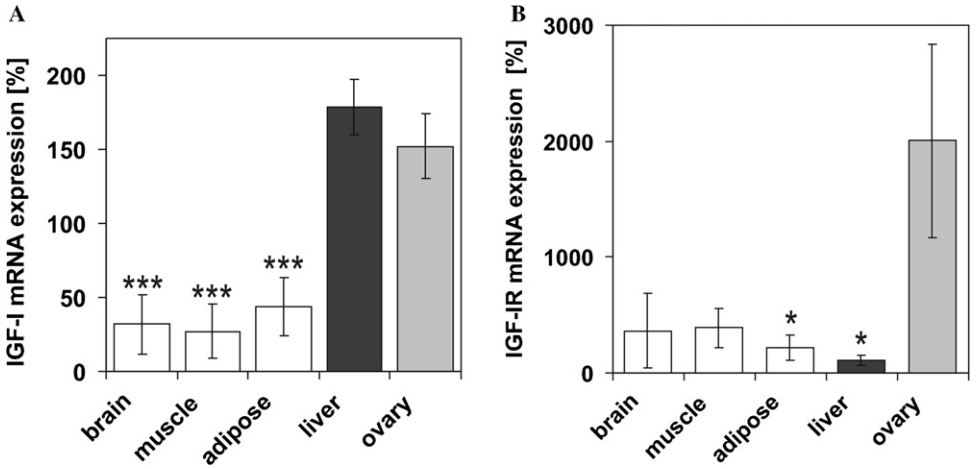

Fig. 1. IGF-I (A) and IGF-IR (B) mRNA expression in different tissues of female sterlet ($n = 5$), statistical analysis by pairwise multiple comparison (IGF-I Tukey, IGF-IR Dunn), significant values are marked by asterisks ($^{***}p < 0.001$, $^{**}p < 0.01$, $^{*}p < 0.05$).

3.4. Gene expression in different cohorts of follicles

Three cohorts of follicles deriving from the same ovary could be compared in maturing females and size-sorting revealed three groups, follicles 1 (∅ 160 ± 20 μm, $n = 141$), follicles 2 (∅ 420 ± 170 μm, $n = 155$), and follicles 3 (∅ 1590 ± 190 μm, $n = 148$). Follicles 1 already contained some lipid globules and corresponded to late stage II. In follicles 2, a vitelline envelope was visible, but less pronounced compared to follicles 3 and corresponded to stage III, while the moderately pigmented (greenish-gray) follicles 3 were assigned to stage IV. IGF-I increased from the smaller follicles (follicles 1) with 88 ± 18% to the further developed cohort of follicles 2 with 109 ± 26% ($n = 5$). The highest expression of IGF-I (165 ± 24%) was measured in the late vitellogenic follicles 3, close to maturation (Fig. 2). Differences in IGF-I expression between follicles 1 and 2 were not significant (Tukey's Test), due to high standard deviation. Correspondingly, IGF-IR increased from 1780 ± 270% in follicles 1 to 3740 ± 1370% ($p < 0.027$) in follicles 2. In late vitellogenic follicles, IGF-IR showed highest expression (5080 ± 1090%). No significant difference was revealed between follicles 2 and 3. Likewise IGF-I, IGF-IR increased throughout the course of development.

3.5. In vivo gene expression in maturing females

Within the female population, follicle diameter fluctuated within a broad range as seen in high standard deviations. Two groups of females were characterised by the progress of gonad development (Fig. 3); follicle diameter was used as parameter to classify maturing and non-maturing females: in maturing females, follicles grew to a size of at least 500 μm, in non-maturing females, this size was never reached within the two years surveyed. No significant difference in body size in terms of total body length and weight was observed between the two groups (confirmed by t test). Within the stock, 42.5% ($n = 17$) non-maturing and 57.5% ($n = 23$) maturing females were identified. In non-maturing females, follicle size increased only slightly

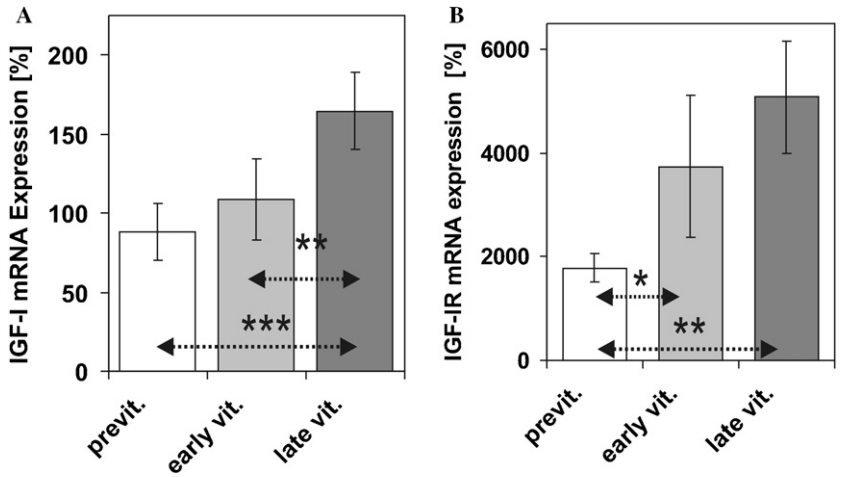

Fig. 2. IGF-I (A) and IGF-IR (B) mRNA expression in different cohorts of follicles of female sterlet ($n = 5$). Follicles 1 (∅ 160 ± 20 μm, $n = 141$, stage II), follicles 2 (∅ 420 ± 170 μm, $n = 155$, stage III), follicles 3 (∅ 1590 ± 190 μm, $n = 148$, stage III), statistical analysis by pairwise multiple comparison (Tukey), significant values are marked by asterisks ($^{***}p < 0.001$, $^{**}p < 0.01$, $^{*}p < 0.05$).

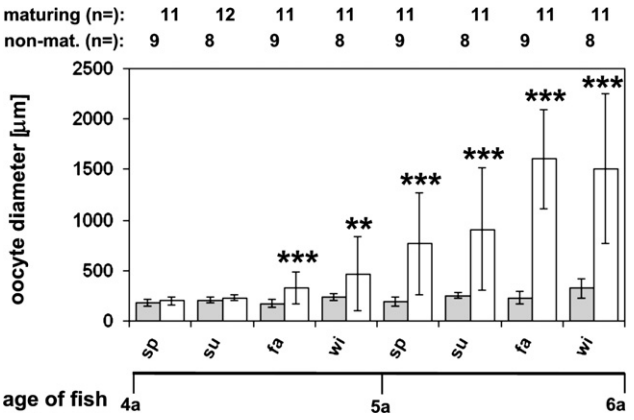

Fig. 3. Increase of the oocyte diameter in four year-old maturing and non-maturing female sterlet over a period of two years. Significant differences between maturing and non-maturing females are marked by asterisks ($^{***}p < 0.001$, $^{**}p < 0.01$, Mann–Whitney Rank Sum Test).

(spring '02: 180 ± 36 µm; winter '02/03: 231 ± 65 µm, winter '03/04: 323 ± 92 µm, $p < 0.05$). In contrast, maturing follicles grew from 198 ± 36 µm to 1508 ± 739 µm. A significant difference between maturing and non-maturing females was only detected since autumn '02 ($p < 0.001$) on. Comparing previtellogenic follicles (max. Ø < 240 µm) at the same sampling date (spring '02, summer '02), gene expression revealed a significant increase of IGF-I (2.78-fold) and IGF-IR (2-fold) in follicles of maturing females compared to equally sized (no significant difference by *t* test) follicles of non-maturing females (Fig. 4).

4. Discussion

Surprisingly, and in contrast to its significance for growth, nutrition, and reproduction, neither IGF-I nor IGF-IR has been in a basal actinopterygian species. In the present study, IGF-I and IGF-IR were identified in sturgeon for the first time. A partial IGF-I sequence submitted for *Acipenser gueldenstadtii* (DQ201138) shows 97% identity on the nucleotide sequence and 95% on the amino acid sequence. Mostly, 3′RACE results in successful amplification due to mRNA stabilisation of the polyA terminal (Maniatis et al., 1976) and was successfully applied here for the elongation of the IGF-I and IGF-IR sequence. Despite problems encountered in 5′-elongations (Lundqvist et al., 1999), complete CDS of IGF-I was characterised here. Highest similarity was observed for the B domain, whereas lowest similarity was scored for the E domain. This is a characteristic for IGF-I hormones since folding behaviour of IGF-I is mainly controlled by the B-domain as recently shown by means of protein engineering (Guo et al., 2002) and the E-domain is generally cleaved during posttranslational processing (Daughaday and Rotwein, 1989). The highly conserved cleavage motif (K–X–X–K–X–X–R) described by Duguay et al. (1995) was confirmed. The signal peptide predicted here shows low similarity with the signal peptides of teleosts, concordant with the taxonomic position of the Acipenseridae and the high sequence variability of this leader sequence among vertebrates. Although multiple mRNA species have been reported in vertebrates including teleosts (Shamblott and Chen, 1992; Wallis and Devlin, 1993), the one identified here most likely corresponded to the IGF-IEa splicing variant (according NCBI nomenclature). Primers used for the quantification were consequently positioned upstream for contributing to this variability in the E-domain.

IGF-I-mediated effects not only depend upon IGF-I but also on the ability of target cells to respond to IGF-I, and thus on the presence of specific receptors. In principle, two distinct receptors show IGF-I binding capacity, the insulin receptor and the IGF-IR. Since the insulin receptor is characterised by low IGF-I affinity, IGF-IR is considered the main target for mediating IGF-I effects (Maestro et al., 1997a; Steele-Perkins et al., 1988). Additionally, predominance of IGF-IR over insulin receptors in teleosts has been

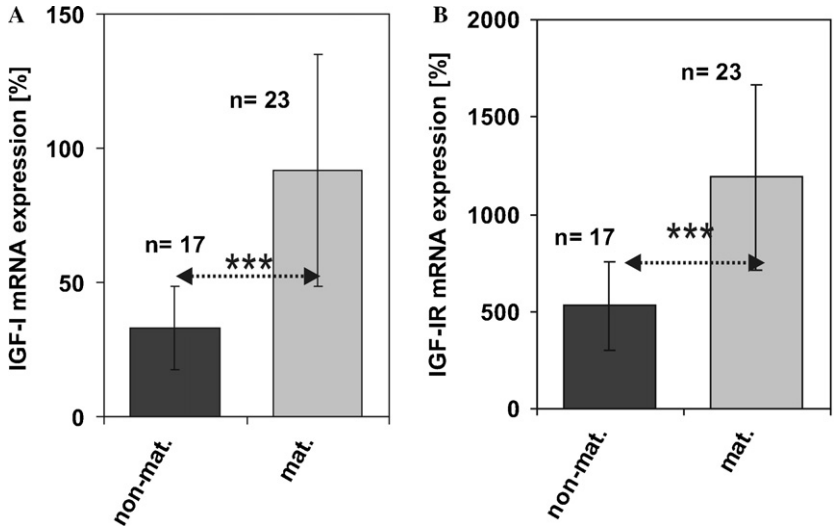

Fig. 4. IGF-I (A) and IGF-IR (B) mRNA expression in previtellogenic follicles of maturing and non-maturing female sterlet before the onset of puberty. Significant differences are marked by asterisks ($^{***}p < 0.001$, Mann–Whitney Rank Sum Test).

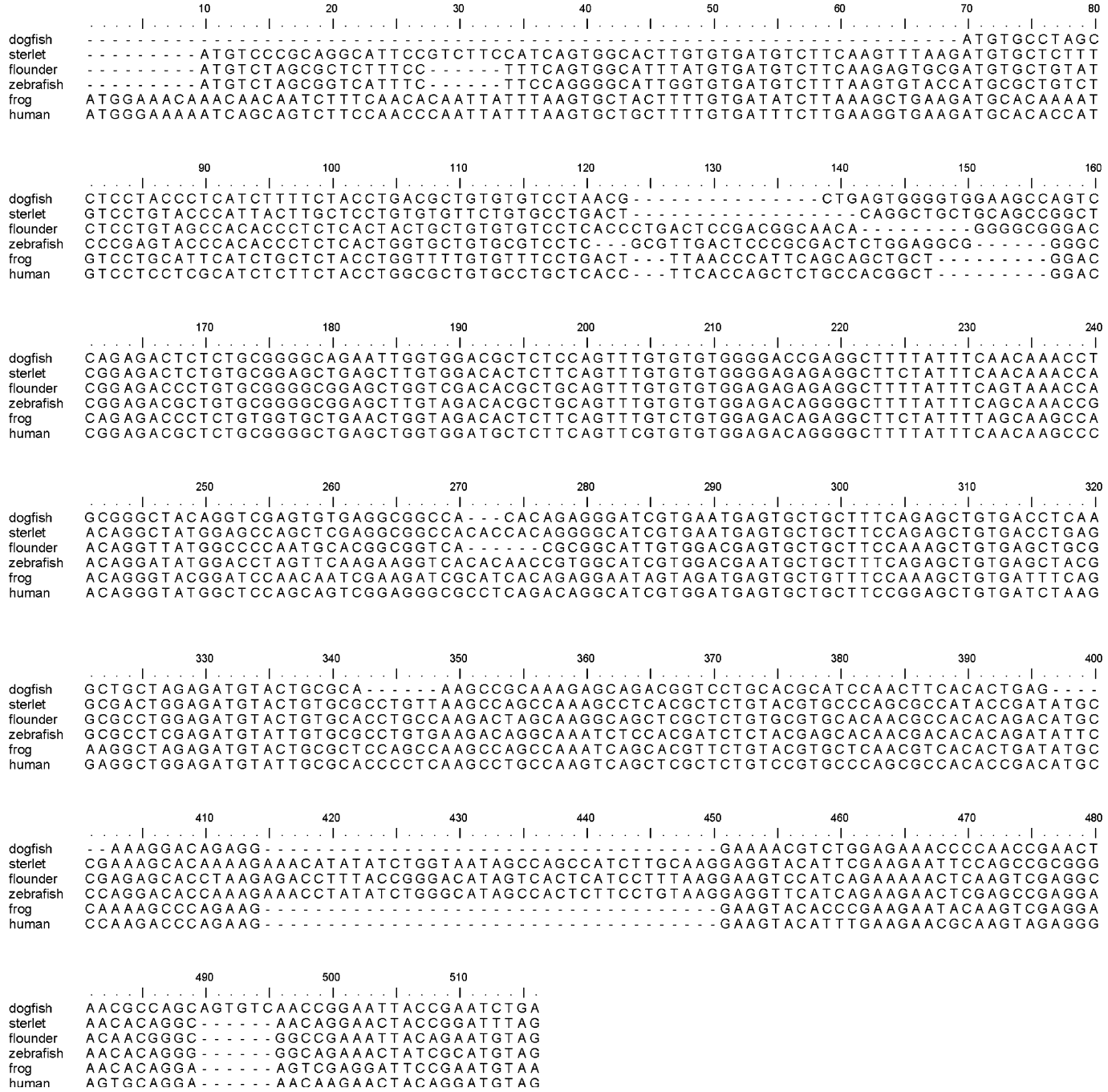

Fig. 5. Alignment of IGF-I coding sequences, accession code (NCBI) in parentheses, domains are designated above the alignment. Dogfish *Squalus acanthias* (Z50081), sterlet *Acipenser ruthenus* (DQ329352), flounder *Paralichthys japonica* (AJ010602), zebrafish *Danio rerio* (NM_131825), frog *Xenopus laevis* (M29857), human (NM_000618).

reported for most tissues (Maestro et al., 1997a; Mendez et al., 2001). Up to now, full-length IGF-IR CDS were only reported for *Cyprinus carpio* (AY144592, unpublished), *Danio rerio* (Maures et al., 2002), and *Paralichthys olivaceus* (Nakao et al., 2002), and partial CDS for *Carassius auratus* (AF216772, unpublished), *Epinephelus coioides* (AY772255, unpublished), some salmonids (Greene and Chen, 1999; Tao and Boulding, 2003), and *Oreochromis mossambicus* (AF463795, unpublished). Here partial CDS of *Acipenser ruthenus* was identified and important functional sites were characterised. In particular, conserved regions—known to be critical for the biological activity of IGF-IR—were identified in the amino acid alignment: (i) a binding site for IRS-I, where upon activation by phosphorylation the signalling pathway is initiated (Baserga et al., 1997), (ii) a potential ATP binding site in the tyrosine kinase domain, essential for the ATP-dependent phosphorylation of the insulin-receptor substrate 1 (IRS-I) (Favelyukis et al., 2001), and (iii) a transmembrane domain characterised by considerable sequence variation (Adams et al., 2000).

Selection of the reference gene was a critical factor, as most of the commonly used housekeeping genes vary considerably in a tissue-specific manner, with regard to the developmental stage or health status, and may fluctuate in a cyclic way (Warrington et al., 2000). In humans, systematic evaluation has been carried out on a large scale (Radonic et al., 2004; Warrington et al., 2000), but—despite the number of gene expression studies conducted in the last decade—not in lower vertebrates. In fish, most authors normalise to β-actin and GAPDH (Ikeuchi et al., 1999; Kajimura et al., 2004), despite the number of studies reporting variable gene expression (Lupberger et al., 2002; Schmittgen and Zakrajsek, 2000). For the present study, fluctuations in cellular metabolism had to be accounted for due to temperature changes throughout the annual cycle, turning metabolism-related genes (e.g., GAPDH) less suited. On the other hand, structure-related genes such as tubulin or β-actin were rejected due to the major changes in oocyte volume and reorganisation of the cytoskeleton during folliculogenesis. With regard to the variable rRNA:mRNA ratio and multiple 18S rRNA genes in sturgeon (Krieger and Fuerst, 2002), 18S rRNA was considered inappropriate. Here, β2m revealed an even expression, confirming the application as reference gene in studies on mammalian gonad tissues such as ovaries of different stages (Dong et al., 2001), ovarian cancer (Hata et al., 2002), and granulosa cell tumours (Fuller et al., 2002). The β2m sequence identified in sterlet shared an identity of >95% with all β2m coding sequences of *A. baerii* (Lundqvist et al., 1999). The primers used for real-time quantification (ACI β2m F, ACI β2m R) were cDNA-specific and conserved for all mRNA subtypes described in *A. baerii*, balancing out extreme fluctuations in the expression rates of a single subtype.

The quantification assays were particularly optimised with regard to low detection limits, contributing to the low IGF-I and IGF-IR mRNA levels in the gonad reported by Perrot et al. (2000) in seabream. Pfaffl (2001b) presented a SYBR Green based assay improving the detection limit from 10^5 to 10^9 cDNA copies by conventional RT-PCR to 10^2–10^9 RNA copies by real-time PCR. By the use of hybridisation probes and BSA supplementation, detection limit was 10 copies for both target genes and the housekeeping gene.

The IGF-I mRNA expression in the gonad did not differ significantly compared to the liver, but was higher in comparison to the brain, the muscles above the lateral line and the adipose tissue associated with the gonad. This is particularly surprising since the liver is considered to be the main organ for IGF-I synthesis and the principal source for circulating IGF-I, mediating the effect of growth hormone secretion from the pituitary (Daughaday and Rotwein, 1989). Therefore, highest IGF-I expression was expected for the liver, in conformity with the findings in tilapia, salmon or carp (Duguay et al., 1992; Schmid et al., 1999; Vong et al., 2003). The presence of the IGF-I peptide and mRNA in the ovary of fish has been documented (Maestro et al., 1997b; Negatu et al., 1998), but here, a very high local IGF-I mRNA expression—comparable to the expression in the liver—was detected in the ovary of maturing sterlet. Concordantly, Schmid et al. (1999) reported 80% IGF-I mRNA expression in the ovary compared to the liver. With regard to the brain, muscle and adipose tissue, low levels of IGF-I mRNA were reported here, congruently with Caelers et al., 2004 reporting 8.9 ± 0.7 pg/μg total RNA in the liver, 2.15 ± 0.7 pg/μg total RNA in testis, 0.14 ± 0.06 pg/μg total RNA in the muscle and 1.36 ± 0.41 pg/μg total RNA in the brain in tilapia; no data in the ovary were published. The high receptor expression in the ovary exceeded that of all other tissues. Therefore, high expression of IGF-IR in the ovary confirms the role of IGF-I-mediated actions: Compared to the liver, IGF-IR expression was 2-fold elevated in adipose tissue, more than 3-fold in the muscle, nearly 4-fold in the brain but 20-fold in the female gonad. A substantial role of the paracrine IGF-I system in gonad development is concluded with regard to other organs known for paracrine IGF-I regulation, confirming the cellular actions of IGF-I in follicle cell cultures that have been reported recently (see above). Obviously, there is a duality of the IGF-I system: Some tissues highly depend on plasma IGF-I, and therefore ultimately on the gene-expression in the liver, whereas others such as the ovary, show temporarily high expression rates. Paracrine growth factors might thus be involved in the differential regulation of growth, shifting energy resources from one organ to another, dependent on the developmental stage.

In the ovary of sterlet, only few follicles undergo vitellogenesis and achieve final maturation to subsequently ovulate, whereas others stagnate in their development and

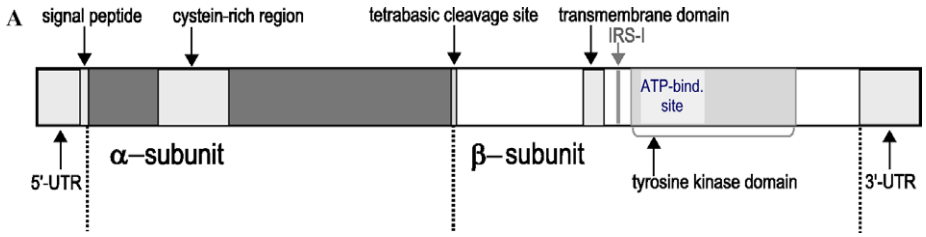

Fig. 6. (A) Scheme of IGF-IR and its functional domains. ATP-bind. site—ATP-binding site, IRS-1—insulin receptor substrate 1, UTR—untranslated region. (B) Alignment of the partial IGF-IR coding sequence identified in sterlet *Acipenser ruthenus* (DQ340767) and the non-allelic receptor subtypes a and b described in zebrafish *Danio rerio* (IGF-IRa—*NM_152968*; IGF-IRb—*NM_152969*) and flounder *Paralichthys japonica* (IGF-IRa—AB065098; IGF-IRb—*AB065099*). Functional regions (see, A) are designated above the alignment.

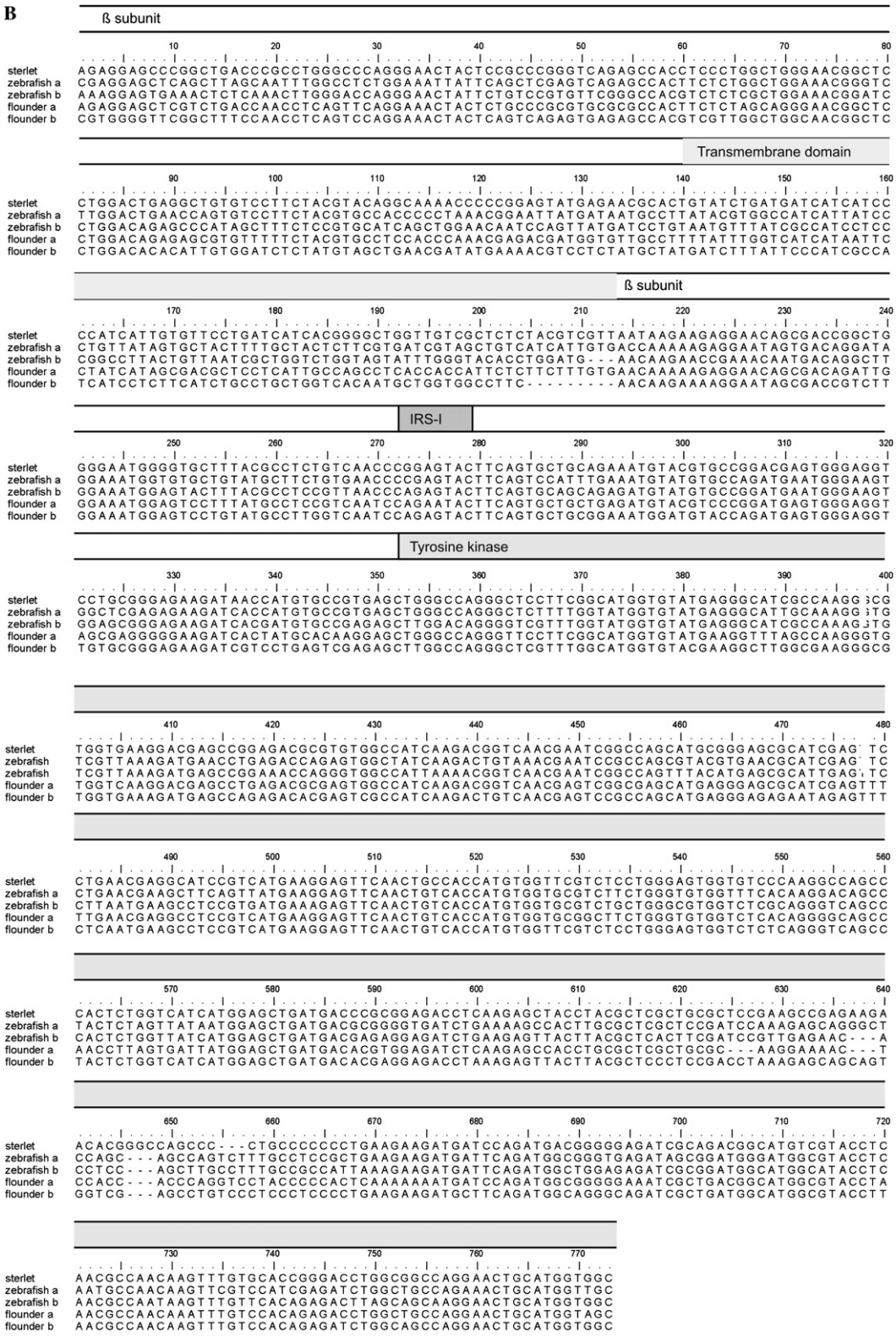

Fig. 6 (*continued*)

resume vitellogenesis at a later stage. This suggests the existence of an intraovarian modulator(s) determining the faith of follicles. Although Adashi (1995) formulated the hypothesis of IGF-I as intraovarian modulator a decade ago, convincing evidence is still lacking. Here, three cohorts of follicles revealed differential expression of IGF-I and IGF-IR. Lowest IGF-I expression was determined in arrested previtellogenic follicles, highest IGF-I expression was

detected in late vitellogenic follicles. Congruently, IGF-IR mRNA was elevated in vitellogenic follicles compared to developmentally arrested follicles. In *Acipenser transmontanus*, a drastic increase in granulosa cell number was restricted to the transition phase before the actual onset of vitellogenesis (Doroshov et al., 1991), and, in mammals, granulosa cell proliferation is regulated by IGF-I (Kadakia et al., 2005). Thus, IGF-I-mediated modulation of follicular faith might be a result of a mitotic differentiation of the granulosa layer by IGF-I. On the other hand, IGF-I is involved in steroid synthesis, particularly in estradiol synthesis at the onset of vitellogenesis. It has been shown that IGF-I up-regulates the transport of cholesterol into the mitochondria (rate-limiting step) by inducing StAR mRNA expression (Lavoie et al., 1999). Increased vitellogenin uptake (Tyler et al., 1987) and the underlying regulation by IGF-I are not understood so far. However, these findings support the concept that IGF-I is an intraovarian modulator of follicle development. Here, this is further strengthened by the differential IGF-I and IGF-IR expression observed in follicles of differential faith.

Within the female sterlets, two groups were characterised due to different gonad development: (i) maturing and (ii) non-maturing females. This arrested development at an early stage of gonad development has been described in different sturgeon species (Doroshov et al., 1997; Williot and Brun, 1998). Here, for the first time, this stagnation is observed in individuals and assigned to early vitellogenesis characterised by a follicle diameter of less than 300 μm. At this stage, a significant difference in IGF-I and IGF-IR expression was observed between maturing and non-maturing females: High levels of IGF-I and IGF-IR mRNA were found in follicles, which subsequently matured within two years. Kajimura et al. (2004) recently reported high IGF-I mRNA expression in the early phase of gonad development of tilapia and suggested an important function of paracrine IGF-I for this phase. Our findings further support the involvement of the paracrine IGF-I system in early vitellogeneic growth. In conclusion, an involvement of the IGF-I system in the induction of vitellogenic growth as indicated by several mechanisms reported in cell culture is further supported by this study. Here, substantial evidence is presented for an important role of paracrine IGF-I in the puberty of sterlet. In addition, due to size of the gonad which can reach 30% of the body weight (in sterlet, 16–18% in wild fish and up to 27% in captivity, Holcik, 1989), intraovarian IGF-I might even contribute to the plasmatic pool and, to a certain extent therefore contribute to the IGF-I feedback on the hypothalamus and the pituitary, increasing the secretion of stFSH and stLH: IGF-I has been reported to increase GnRH expression in the hypothalamus (Hiney et al., 1996), to enhance both, LH content and release (Huang et al., 1998) and FSH content (Baker et al., 2000) of pituitary cells, and to multiply the steroidogenic effects of gonadotropins in the gonad (Kagawa et al., 2003). The involvement of paracrine IGF-I in gonad maturation of sterlet provides new insights into the onset of puberty in fish and might even represent a promising approach for application in reproduction of sturgeon in aquaculture.

Acknowledgments

This study was supported in part by a grant from the German Federal Agency for Nature Conservation (BfN) as part of the project "Exemplary measures for the conservation and restoration of the almost extinct European Sturgeon (*Acipenser sturio* L.) in Germany".

References

Adams, T.E., Epa, V.C., Garrett, T.P.J., Ward, C.W., 2000. Structure and function of the type 1 insulin-like growth factor receptor. Cell. Mol. Life Sci. 57, 1050–1093.

Adashi, E.Y., 1995. With a little help from my friends—the evolving story of intraovarian regulation. Endocrinology 136, 4161–4162.

Altschul, S., 1999. Hot papers—Bioinformatics—Gapped BLAST and PSI-BLAST: a new generation of protein database search programs by S.F. Altschul, T.L. Madden, A.A. Schaffer, J.H. Zhang, Z. Zhang, W. Miller, D.J. Lipman—Comments. Scientist 13, 15.

Baker, D.M., Davies, B., Dickhoff, W.W., Swanson, P., 2000. Insulin-like growth factor I increases follicle-stimulating hormone (FSH) content and gonadotropin-releasing hormone-stimulated FSH release from coho salmon pituitary cells in vitro. Biol. Reprod. 63, 865–871.

Baserga, R., Hongo, A., Rubini, M., Prisco, M., Valentinis, B., 1997. The IGF-I receptor in cell growth, transformation and apoptosis. BBA-Rev. cancer 1332, F105–F126.

Caelers, A., Berishvili, G., Meli, M.L., Eppler, E., Reinecke, M., 2004. Establishment of a real-time RT-PCR for the determination of absolute amounts of IGF-I and IGF-II gene expression in liver and extrahepatic sites of the tilapia. Gen. Comp. Endocrinol. 137, 196–204.

Daughaday, W.H., Rotwein, P., 1989. Insulin-like growth factors I and II. Peptide, messenger, ribonucleic acid and gene structures, serum, and tissue concentrations. Endocr. Rev. 10, 68–91.

Dong, Y., Kaushal, A., Bui, L., Chu, S., Fuller, P.J., Nicklin, J., Samaratunga, H., Clements, J.A., 2001. Human kallikrein 4 (KLK4) is highly expressed in serous ovarian carcinomas. Clin. Cancer Res. 7, 2363–2371.

Doroshov, J.N., Eenennaam, J.P., Chapman, F.A., Doroshov, S.I., 1991. Histological study of the ovarian development in wild white sturgeon, *Acipenser transmontanus*. In: Williot, P. (Ed.), Proc. First Int. Symp. on Sturgeon. 3–6 October 1989, Bordeaux Gironde, France, pp. 129–135.

Doroshov, S.I., Moberg, G.P., Eenennaam, J.P.V., 1997. Observations on the reproductive cycle of cultured white sturgeon, *Acipenser transmontanus*. Environ. Biol. Fishes 48, 265–278.

Dufour, S., Huang, Y.S., Rousseau, K., Sbaihi, M., Le Belle, N., Vidal, B., Marchelidon, J., Querat, B., Burzawa-Gerard, E., Chang, C.F., Schmitz, M., 2000. Puberty in teleosts: New insights into the role of peripheral signals in the stimulation of pituitary gonadotropins. In: Norberg, B., Kjesbu, O.S., Taranger, G.L., Andersson, E., Stefansson, S.O. (Eds.), Reproductive Physiology of Fish, PO Box 7800, Bergen N 5020, University of Bergen, Norway, Dept. of Fish and Marine Biology 2000, pp. 455–461.

Duguay, S.J., Park, L.K., Samadpour, M., Dickhoff, W.W., 1992. Nucleotide sequence and tissue distribution of three insulin-like growth factor-I prohormones in salmon. Mol. Endocrinol. 6, 1202–1210.

Duguay, S.J., Jie, L.Z., Steiner, D.F., 1995. Mutational analysis of the insulin-like growth factor-I prohormone processing site. J. Biol. Chem. 270, 17566–17574.

Favelyukis, S., Till, J.H., Hubbard, S.R., Miller, W.T., 2001. Structure and autoregulation of the insulin-like growth factor 1 receptor kinase. Nat. Struct. Biol. 8, 1058–1063.

Fuller, P.J., Zumpe, E.T., Chu, S., Mamers, P., Burger, H.G., 2002. Inhibin-activin receptor subunit gene expression in ovarian tumors. J. Clin. Endocrinol. Metab. 87, 1395–1401.

Greene, M.W., Chen, T.T., 1999. Characterization of teleost insulin receptor family members—II. Developmental expression of insulin-like growth factor type I receptor messenger RNAs in rainbow trout. Gen. Comp. Endocrinol. 115, 270–281.

Guo, Z.Y., Shen, L., Feng, Y.M., 2002. The different folding behavior of insulin and insulin-like growth factor 1 is mainly controlled by their B-chain/domaint. Biochemistry 41, 1556–1567.

Hata, K., Udagawa, J., Fujiwaki, R., Nakayama, K., Otani, H., Miyazaki, K., 2002. Expression of angiopoietin-1, angiopoietin-2, and Tie2 genes in normal ovary with corpus luteum and in ovarian cancer. Oncology 62, 340–348.

Hiney, J.K., Srivastava, V., Nyberg, C.L., Ojeda, S.R., Dees, W.L., 1996. Insulin-like growth factor I of peripheral origin acts centrally to accelerate the initiation of female puberty. Endocrinology 137, 3717–3728.

Holcik, J. 1989. The freshwater fishes of Europe—general introduction to fishes Acipenseriformes. vol. 1, Part II.

Huang, Y.S., Rousseau, K., Belle, N.L., Vidal, B., Burzawa-Gerard, E., Marchelidon, J., Dufour, S., 1998. Insulin-like growth factor I (IGF-I) stimulates gonadotrophin production from eel pituitary cells- a possible metabolic signal for induction of puberty. J. Endocrinol. 159, 43–52.

Ikeuchi, T., Todo, T., Kobayashi, T., Nagahama, Y., 1999. cDNA cloning of a novel androgen receptor subtype. J. Biol. Chem. 274, 25205–25209.

Jentoft, S., Aastveit, A.H., Andersen, O., 2004. Molecular cloning and expression of insulin-like growth factor-I (IGF-I) in Eurasian perch (*Perca fluviatilis*): lack of responsiveness to growth hormone treatment. Fish Physiol. Biochem. 30, 67–76.

Kadakia, R., Arraztoa, J.A., Bondy, C., Zhou, J., 2005. Granulosa cell proliferation is impaired in the *igf1 null* ovary. Growth Horm. IGF Res. 11, 220–224.

Kagawa, H., Gen, K., Okuzawa, K., Tanaka, H., 2003. Effects of luteinizing hormone and follicle-stimulating hormone and insulin-like growth factor-I on aromatase activity and P450 aromatase gene expression in the ovarian follicles of red seabream, *Pagrus major*. Biol. Reprod. 68, 1562–1568.

Kajimura, S., Kawaguchi, N., Kaneko, T., Kawazoe, I., Hirano, T., Visitacion, N., Grau, E.G., Aida, K., 2004. Identification of the growth hormone receptor in an advanced teleost, the tilapia (*Oreochromis mossambicus*) with special reference to its distinct expression pattern in the ovary. J. Endocrinol. 181, 65–76.

Kloas, W., Lutz, I., Einspanier, R., 1999. Amphibians as a model to study endocrine disruptors: II. Estrogenic activity of environmental chemicals *in vitro* and *in vivo*. Sci. Total Environ. 225, 59–68.

Krieger, J., Fuerst, P.A., 2002. Evidence for a slowed rate of molecular evolution in the order Acipenseriformes. Mol. Biol. Evol. 19, 891–897.

Lavoie, H.A., Garmey, J.C., Veldhuis, J.D., 1999. Mechanisms of insulin-like growth factor I augmentation of follicle-stimulating hormone-induced porcine steroidogenic acute regulatory protein gene promoter activity in granulosa cells. Endocrinology 140, 146–153.

Le Menn, F., Pelissero, C., 1991. Histological and ultrastructural studies of oogenesis of the Siberian sturgeon *Acipenser baeri*. In: Williot, P. (Eds.), Proc. First Int. Symp. on Sturgeon, 3–6 October 1989, Bordeaux Gironde, France, pp. 113–127.

Lundqvist, M.L., Appelkvist, P., Hermsen, T., Pilstrom, L., Stet, R.J., 1999. Characterization of beta2-microglobulin in a primitive fish, the Siberian sturgeon (*Acipenser baeri*). Immunogenetics 50, 79–83.

Lupberger, J., Kreuzer, K.A., Baskaynak, G., Peters, U.R., le Coutre, P., Schmidt, C.A., 2002. Quantitative analysis of beta-actin, beta-2-microglobulin and porphobilinogen deaminase mRNA and their comparison as control transcripts for RT-PCR. Mol. Cell. Probes 16, 25–30.

Maestro, M.A., Mendez, E., Parrizas, M., Gutierrez, J., 1997a. Characterization of insulin and insulin-like growth factor-I ovarian receptors during the reproductive cycle of carp (*Cyprinus carpio*). Biol. Reprod. 56, 1126–1132.

Maestro, M.A., Planas, J.V., Moriyama, S., Gutierrez, J., Planas, J., Swanson, P., 1997b. Ovarian receptors for insulin and insulin-like growth factor I (IGF-I) and effects of IGF-I on steroid production by isolated follicular layers of the preovulatory coho salmon ovarian follicle. Gen. Comp. Endocrinol. 106, 189–201.

Maniatis, G.M., Ramirez, F., Cann, A., Marks, P.A., Bank, A., 1976. Translation and stability of human globin mRNA in *Xenopus* oocytes. J. Clin. Invest. 58, 1419–1427.

Maures, T., Chan, S.J., Xu, B., Sun, H., Ding, J., Duan, C.M., 2002. Structural, biochemical, and expression analysis of two distinct insulin-like growth factor I receptors and their ligands in zebrafish. Endocrinology 143, 1858–1871.

Mc Rory, J.E., Sherwood, N.M., 1994. Catfish express two forms of insulin-like growth factor-I (IGF-I) in the brain—ubiquitous IGF-I and brain-specific Igf-I. J. Biol. Chem. 269, 18588–18592.

Mendez, E., Smith, A., Figueiredo-Garutti, M.L., Planas, J.V., Navarro, I., Gutierrez, J., 2001. Receptors for insulin-like growth factor-I (IGF-I) predominate over insulin receptors in skeletal muscle throughout the life cycle of brown trout, *Salmo trutta*. Gen. Comp. Endocrinol. 122, 148–157.

Nakao, N., Tanaka, M., Higashimoto, Y., Nakashima, K., 2002. Molecular cloning, identification and characterization of four distinct receptor subtypes for insulin and IGF-I in Japanese flounder, *Paralichthys olivaceus*. J. Endocrinol. 173, 365–375.

Negatu, Z., Hsiao, S.M., Wallace, R.A., 1998. Effects of insulin-like growth factor-I on final oocyte maturation and steroid production in *Fundulus heteroclitus*. Fish Physiol. Biochem. 19, 13–21.

Patino, R., Kagawa, H., 1999. Regulation of gap junctions and oocyte maturational competence by gonadotropin and insulin-like growth factor-I in ovarian follicles of red seabream. Gen. Comp. Endocrinol. 115, 454–462.

Perrot, V., Moiseeva, E.B., Gozes, Y., Chan, S.J., Funkenstein, B., 2000. Insulin-like growth factor receptors and their ligands in gonads of a hermaphroditic species, the gilthead seabream (*Sparus aurata*): Expression and cellular localization. Biol. Reprod. 63, 229–241.

Peterson, B.C., Waldbieser, G.C., Bilodeau, L., 2004. IGF-I and IGF-II mRNA expression in slow and fast growing families of USDA 103 channel catfish (*Ictalurus punctatus*). Comp. Biochem. Physiol. A 139, 317–323.

Pfaffl, M.W., 2001a. Development and validation of an externally standardised quantitative insulin-like growth factor-1 RT-PCR using LightCycler SYBR Green technology. In: Meuer, S., Wittwer, C., Nakagawara, K. (Eds.), Rapid Cycle Real-time PCR—Methods and Applications. Springer, Germany, pp. 281–291.

Pfaffl, M.W., 2001b. A new mathematical model for relative quantification in real-time RT-PCR. Nucleic Acids Res., 29.

Radonic, A., Thulke, S., Mackay, I.M., Landt, O., Siegert, W., Nitsche, A., 2004. Guideline to reference gene selection for quantitative real-time PCR. Biochem. Biophys. Res. Commun. 313, 856–862.

Reinecke, M., Collet, C., 1998. The phylogeny of the insulin-like growth factors. Int. Rev. Cytol. 183, 1–94.

Schmid, A.C., Naf, E., Kloas, W., Reinecke, M., 1999. Insulin-like growth factor-I and -II in the ovary of a bony fish, *Oreochromis mossambicus*, the tilapia: *in situ* hybridisation, immunohistochemical localisation, Northern blot and cDNA sequences. Mol. Cell. Endocrinol. 156, 141–149.

Schmittgen, T.D., Zakrajsek, B.A., 2000. Effect of experimental treatment on housekeeping gene expression: validation by real-time, quantitative RT-PCR. J. Biochem. Biophys. Methods 46, 69–81.

Shamblott, M.J., Chen, T.T., 1992. Identification of a second insulin-like growth-factor in a fish species. Proc. Natl. Acad. Sci. USA 89, 8913–8917.

Steele-Perkins, G., Turner, J., Edman, J., Hari, J., Pierce, S.B., Stover, C., Rutter, W., Roth, R., 1988. Expression and characterization of a functional human insulin-like growth factor I receptor. J. Biol. Chem. 263, 11486–11492.

Tao, W.J., Boulding, E.G., 2003. Associations between single nucleotide polymorphisms in candidate genes and growth rate in Arctic charr (*Salvelinus alpinus* L.). Heredity 91, 60–69.

Tyler, C.R., Sumpter, J.P., Bromage, N.R., 1987. The hormonal control of vitellogenin uptake into cultured oocytes of the rainbow trout. In: Proceedings of the 3rd International Symposium of Reproductive Physiology of Fish, Memorial University Press, p. 142.

Vong, Q.P., Chan, K.M., Cheng, C.H.K., 2003. Quantification of common carp (*Cyprinus carpio*) IGF-I and IGF-II mRNA by real-time

PCR: differential regulation of expression by GH. J. Endocrinol. 178, 513–521.

Wallis, A.E., Devlin, R.H., 1993. Duplicate insulin-like growth factor-I genes in salmon display alternative splicing pathways. Mol. Endocrinol. 7, 409–422.

Warrington, J.A., Nair, A., Mahadevappa, M., Tsyganskaya, M., 2000. Comparison of human adult and fetal expression and identification of 535 housekeeping/maintenance genes. Physiol. Genomics 2, 143–147.

Weber, G.M., Sullivan, C.V., 2000. Effects of insulin-like growth factor-I on *in vitro* final oocyte maturation and ovarian steroidogenesis in striped bass, *Morone saxatilis*. Biol. Reprod. 63, 1049–1057.

Weber, G.M., Sullivan, C.V., 2001. *In vitro* hormone induction of final oocyte maturation in striped bass (*Morone saxatilis*) follicles is inhibited by blockers of phosphatidylinositol 3-kinase activity. Comp. Biochem. Physiol. B 129, 467–473.

Williot, P., Brun, R., 1998. Ovarian development and cycles in cultured Siberian sturgeon, *Acipenser baeri*. Aquat. Living Resour. 11, 111–118.

Williot, P., Arlat, G., Chebanov, M., Gulyas, T., Kasimov, R., Kirschbaum, F., Patriche, N., Pavlovskaya, L.P., Poliakova, L., Pourkazemi, M., Kim, Y., Zhuang, P., Zholdasova, I.M., 2002. Conservation and broodstock management. Int. Rev. Hydrobiol. 87, 483–506.

Zusammenfassung der Dissertation

Die vorliegende Arbeit befasst sich mit dem stammesgeschichtlichen Ursprung von Entkopplerproteinen (uncoupling proteins, UCPs). Ein besonderes Augenmerk liegt dabei auf UCP1, das eine Schlüsselrolle bei der zitterfreien Wärmebildung im braunen Fettgewebe von Kleinsäugern, Winterschläfern und Neugeborenen spielt. Dort entkoppelt es die oxidative Phosphorylierung von der ATP-Synthese und setzt die protonenmotorische Kraft als Wärme frei. Die Arbeitshypothese war, dass die Charakterisierung phylogenetisch entfernter UCP1 Orthologe von Vertretern verschiedener Wirbeltierklassen Aufschluss darüber geben könnte, wann die zitterfreie Wärmebildung entstanden ist, die für moderne Säuger einen entscheidenden Vorteil in der Kälte darstellt.

In dieser Arbeit wurde ein UCP1 Ortholog in ektothermen Fischen identifiziert, das bereits ähnliche biochemische Eigenschaften wie das Säugetier-UCP1 aufweist, jedoch nicht im Fettgewebe exprimiert wird. Dies widerlegte die gängige Meinung, dass UCP1 ein monophyletisches Merkmal der Säugetiere ist.

Durch genomische Analysen konnte UCP1 erstmals auch in Beuteltieren nachgewiesen werden, bei denen die Fähigkeit zur zitterfreien Wärmebildung bisher kontrovers diskutiert wurde. Auf dieser Stufe der Wirbeltierentwicklung ist das UCP1-Genprodukt in bestimmten Fettgewebedepots zu finden und seine Expression wird, wie in modernen Kleinsäugern, durch Kälte induziert.

Der Nachweis von UCP1 vermittelter Entkopplung im braunen Fettgewebe der Elefantenspitzmaus zeigte, dass nicht nur moderne sondern auch alte Eutheria schon diese Form der zitterfreien Wärmebildung besitzen.

Zusammenfassend wurde in dieser Arbeit die stammesgeschichtliche Entwicklung von UCP1 wie folgt aufgeklärt: Die biochemischen Eigenschaften von Säugetier-UCP1 sind schon in Fischen zu finden, während die Expression im Fettgewebe erst in Beuteltieren auftritt. Ob das Thermogeneseorgan bereits bei Beuteltieren oder erst bei alten Eutheria-Spezies funktionell ist kann nun in Studien gezeigt werden, die die Thermogenese-Eigenschaften des UCP1-exprimierenden Fettgewebes im Beuteltier und des braunen Fettgewebes von Eutheria direkt vergleichen.

Martin Matthias Jastroch

CONTACT INFORMATION

Martin Jastroch
Department of Animal Physiology/ Faculty of Biology
Philipps-Universität Marburg
Karl-von-Frisch-Strasse 8
35032 Marburg (Germany)
+49-6421-28-23389
Jastroch@staff.uni-marburg.de
http://cgi-host.uni-marburg.de/~omtierph/stoff/member.php?mrm=jastroch&lang=en

PERSONAL INFORMATION

Date/ place of Birth:	4th, April 1977/ Berlin (Germany)
Nationality:	German
Marital status:	single
Sex:	male

EDUCATION

8/1987 – 6/1996	Herzog-Ernst-Gymnasium (mathem.-scientific secondary school)	Uelzen, Germany
10/1997 – 10/1999	Undergraduate Student at the Philipps-Universität	Marburg, Germany
9/1999	Prediploma in Biology Grade point: "high distinction"	Marburg, Germany
2/2000 – 11/2000	Exchange Student. University of Southern Queensland	Toowoomba, QLD, Australia
2/2001 – 4/2001 and 5/2002 – 6/2002	Research Exchange Student at the University of Southern Queensland Collaboration with Dr. Kerry Withers, Animal Physiology, Faculty of Biological Sciences	Toowoomba, QLD, Australia
10/1999 – 3/2003	Diploma studies at the Department of Animal Physiology, Faculty of Biology, Philipps-Universität Major subjects: Animal Physiology, Biochemistry, Molecular Genetics and Zoology	Marburg, Germany
3/2003	Diploma in Biology (German equivalent to M.S.) Grade point: 1,1 (high distinction)	Marburg, Germany

DIPLOMA THESIS

12/5/2002 – 17/3/2003 Identification of Uncoupling Proteins in Marsupialia and Monotremata: Tissue-specific Expression and Physiological Regulation of uncoupling protein 2 (UCP2) in *Antechinus flavipes*. Supervision by HD Dr. Martin Klingenspor

PHD PROJECT

since 11/2003	Evolution and functional characterisation of uncoupling proteins in vertebrates
5/2004 – 10/2004	visiting PhD student at the MRC Dunn Human Nutrition Unit University of Cambridge, UK. (with Dr. Martin Brand)
1/2005 – 4/2005	Visiting Researcher Fellowship. Project: Physiological and molecular mechanisms of adaptive nonshivering thermogenesis in marsupials.

EMPLOYMENT HISTORY

7/1996 – 8/1997	Military Service at the Deutsche Bundesmarine
8/2002 – 1/2003; 5/2003 – 2/2004	Research Assistant. Department of Animal Physiology/ Faculty of Biology, Philipps-Universität Marburg, Germany. Employer: Dr. Martin Klingenspor.

SCHOLARSHIPS/ AWARDS/ GRANTS

- Study abroad fellowship from the Philipps-Universität Marburg. (February 2000)
- Travel award for scientific research from the Marburger Förderverein. (February 2001)
- Member of the International Max Planck Research School for Environmental, Cellular and Molecular Microbiology; PhD scholarship and reception of a research grant. (since March 2004)
- DAAD award to study at the MRC Dunn, Cambridge, U.K. (May 2004)
- Recipient of a travel allowance and student award for the Life in the cold conference, Seward Alaska from the Hibernation Society and the Max-Planck-Gesellschaft. (July 2004)
- Centre for Rural and Environmental Biology (CREB), University of Southern Queensland, Toowoomba, Queensland, Australia. Recipient of a Research Visiting Researcher Fellowship and Grant. Project: Physiological and molecular mechanisms of adaptive nonshivering thermogenesis in marsupials. (January - April 2005)
- Recipient of a travel award from the organizers and winner of the 1.poster prize at the Workshop “Uncoupling proteins: Current status and therapeutic aspects”. (April 2005)
- Winner of the young scientists competition award “Frontiers in Thermoregulation” and Comparative Physiology Award at the Second International Meeting on Physiology and Pharmacology of Temperature Regulation in Phoenix, Arizona, USA. (March 2006) (http://www.feverlab.net/meting/program.htm)
- CsBi (Center for Systems Biology) Research Grant at the University of Southern Queensland, Toowoomba, Queensland, Australia. “Proton leak in the amphibian *Bufo marinus* (cane toad)”. (February 2006)

INTERNATIONAL RESEARCH VISITS

- Oral presentation at the Biology seminar at Department of Biological and Physical Sciences, University of Southern Queensland, Queensland, Australia. (March 2005)
- Oral presentation at seminars at School of Life Sciences, University of Nevada, Las Vegas, Nevada, USA ; at the Division of Endocrinology, Department of Medicine, Beth Israel Deaconess Medical Center, Harvard Medical School, , Boston, MA, USA and at the MRC Dunn Human Nutrition Unit, Hills Road, Cambridge, UK. (March 2006)

PUBLICATIONS

- **Jastroch M.**
  Identification of Uncoupling Proteins in Marsupialia and Monotremata: Tissue-specific Expression and Physiological Regulation of uncoupling protein 2 (UCP2) in *Antechinus flavipes.* Diploma thesis, 2003.

Peer-reviewed

- **Jastroch M**., Withers K.W., and Klingenspor M. Uncoupling Protein 2 and 3 in Marsupials: Identification, Phylogeny and Gene Expression in Response to Cold and Fasting in *Antechinus flavipe*s. *Physiol Genomics* 17, 130-139, 2004.
- **Jastroch M.**, Stoehr S., Withers K.W., and Klingenspor M. 2004. A quest for the origin of three mammalian uncoupling proteins. In *Life in the cold: Evolution, Mechanisms, Adaptation, and Application,* edited by Brian M. Barnes and Hannah V. Carey, pp. 417 - 426.
- **Jastroch M**., Wuertz S., Kloas W., and Klingenspor, M.. Uncoupling protein 1 in fish uncovers an ancient evolutionary history of nonshivering thermogenesis. *Physiol Genomics* 22, 150 – 156, 2005.
- Wuertz S., Nitsche A., **Jastroch M**., Gessner J., Klingenspor M., Kirschbaum F., and Kloas W. The role of the IGF-I system for vitellogenesis in maturing female sterlet, *Acipenser ruthenus* Linnaeus, 1758. *Gen Comp Endocrinol*. 150(1), 140-50, 2007
- **Jastroch M**., Buckingham J., Helwig M., Klingenspor M, and Brand M.D. Functional characterisation of UCP1 in the common carp: Uncoupling activity in liver mitochondria and cold-induced expression in the brain. *Journal of Comparative Physiology B*, 2007.

Manuscripts submitted or in preparation

- Mzilikazi N., **Jastroch M.**, Meyer C., and Klingenspor M. The molecular and biochemical basis of nonshivering thermogenesis in a phylogenetically ancient eutherian mammal, the rock elephant shrew, *Elephantulus myurus*. Submitted to *American Journal of Physiology*
- **Jastroch M**., Withers K., Stöhr S., and Klingenspor M. Proton conductance in myotubular mitochondria of the cold-acclimated marsupial *Antechinus flavipes* has a role in mild uncoupling but not in thermogenesis. In preparation.
- **Jastroch M**., Withers K.W., Taudien S., Frappell P.B., Helwig M., Fromme T., Hirschberg V., Heldmaier G., McAllan B.M., Firth B.T., Burmester T., Platzer M., and Klingenspor M. The molecular identification of uncoupling protein 1 in marsupials sheds light on the evolution of brown adipose tissue in mammals. In preparation.

MEETINGS (CONTRIBUTIONS)

- Withers K.W., Billingsley J., **Jastroch M**., McConnell P., McKilligan N., and Lundie-Jenkins J. Consumption of Bunya Nuts in Bunya Mountains National Park. *2001 Annual Meeting of the Central Plains Society of Mammalogists.* Kansas, 2001. 6,4, E3,8. ***Poster***
- **Jastroch M**., Withers K.W., and Klingenspor M. Cloning, Tissue Specific Expression and Physiological Regulation of UCP2 in Two Marsupial Species. *Annual Meeting of the Deutsche Zoologische Gesellschaft*. Berlin, June 2003. ***Poster***
- Withers K.W., Marshall R., Billingsley J., Larsen K., Schiefelbein, **Jastroch M**., McConnell P., McKilligan N., and Lundie-Jenkins J. Whose been nibbling the Bunya's nuts? *XX Scientific Meeting, Australian and New Zealand Society for Comparative Physiology and Biochemistry*: Hobart, 2003. ***Poster***
- Withers K.W., Billingsley J., **Jastroch M**., McConnell P., McKilligan N., and Lundie-Jenkins J. Observations on the consumption of bunya nuts in Bunya Mountains National Park, Partners in Parks Collaborative Research Forum. Brisbane, 2003. pp. 17. ***Article***
- **Jastroch M**. The origin of three uncoupling proteins in vertebrates. *International Physiology Meeting 2004*. Greifswald, June 2004. ***Oral Presentation***
- **Jastroch M**. and Klingenpor M. Tracing the origin of uncoupling proteins. *International Hibernation Symposium 2004*. Vancouver, CAN – Seward, Alaska, 2004. ***Poster and Oral Presentation***
- **Jastroch M**., Kloas W., Brand M.D., and Klingenspor M. Uncoupling protein 1 in fish mediates fatty acid/GDP-sensitive proton conductance and uncovers an ancient evolutionary history of nonshivering thermogenesis. *Uncoupling proteins: Current Status and Therapeutic Prospects*. Madrid, 2005. ***Poster***
- **Jastroch M**., Withers K.W. and Klingenspor M. Skeletal muscle mitochondria as a source of nonshivering thermogenesis in the marsupial Antechinus flavipes. *22nd Annual Meeting – Australian & New Zealand Society for Comparative Physiology & Biochemistry*. Dunedin, 2005. ***Poster***
- **Jastroch M**., Brand M.D., Kloas W., Buckingham J.A., Helwig M., and Klingenspor M. Uncoupling protein 1 in fish uncovers an ancient evolutionary history of mammalian nonshivering thermogenesis, at the *Second International Meeting on Physiology and Pharmacology of Temperature Regulation* in Phoenix, Arizona, USA, March 3-6, 2006. ***Poster and Oral presentation***
- **Jastroch M**., Hirschberg V., Brand M.D., Liebig M. Weber K., Bolze F. and Klingenspor M. Introducing a mammalian cell system to study the function of evolutionary distant uncoupling proteins. *EBEC 2006.* Moscow, 2006. ***Poster***
- Klingenspor M., Helwig M., Fromme T., Brand M.D., Kloas W., Taudien S., Platzer M., and **Jastroch M**. Uncoupling protein 1 is expressed in the brain of ectothermic vertebrates. *EBEC 2006*, Moscow, 2006. ***Poster***
- Trzcionka M., Withers K.W., and **Jastroch M.** Proton flux and uncoupling proteins in mitochondria from the amphibian *Bufo marinus. 23rd Annual Meeting – Australian & New Zealand Society for Comparative Physiology & Biochemistry.* Brisbane, 2006. ***Poster***

Acknowledgements

I am grateful to Dr. Martin Klingenspor for an excellent supervision of this thesis. His efforts and enthusiasm led to the success of this project. Without hesitation, he supported and discussed the ideas and questions that arose during this thesis. He promoted my visits in other labs, conference attendances, and despite leading a large group, he took long-hours teaching me how to write scientifically.

I was delighted working with Kerry Withers and Martin Brand who put a lot of effort into my project and were always accessible when I needed help to discuss and proceed with my project. Kerry and his family took care of me during my visits in Australia. Martin inspired by interest for the biochemistry of UCPs.

I thank Michaela for everything since she stepped into my life. I deeply appreciate her presence and her patience in good and in bad times.

I thank Siggi for assistance, which was not only restricted to work. A thanks goes to the Klingenspor group, but also to the Brand group in Cambridge for a wonderful time during my PhD. A special thank you goes to the people who enriched my life during the thesis (and also to the ones that I forgot): my ex-flat-mates Rene, Sebastian and Jan, my office-mate Verena, my fishing mates Carola, Bernd and Ron, my Southafrican-mate Kwezi, my Portugesian-mate Telma, my pub-mates Nadeene and Charlie, my soccer-mates, my kicker-mates, my poker-mates, my toad-mate Magda, my Greek-mate Elias, my Luzie-mate, my Kansas-mates Nat and Lisa, my navy-mates, my sliding-mates, my Burgerking-mates, my Aussie-aussie-aussie mates, my Svensk-mate Christopher, my best-mate Henning, and my parents who made me.

I also like to thank further collaborators (S. Würtz, W. Kloas, S. Taudien, B. McAllen, P. Frappell, P. Elsworths, T. Burmester) and foundations (DAAD and the Max-Planck) for their terrific support.

ERKLÄRUNG

Ich versichere, dass ich meine Dissertation

Evolution and functional characterisation of uncoupling proteins in vertebrates

selbständig, ohne unerlaubte Hilfe angefertigt und mich dabei keinen anderen als der von mir ausdrücklich bezeichneten Quellen und Hilfen bedient habe.

Die Dissertation wurde in der jetzigen oder einer ähnlichen Form noch bei keiner anderen Hochschule eingereicht und hat noch keinen sonstigen Prüfungszwecken gedient.

Marburg, den _____ _____

(Martin Jastroch)